

主論文

**Molecular Design of Transition Metal Catalysts
toward Practical Hydrogenation of Carboxylic Acids**

(カルボン酸の実用的な水素化に向けた遷移金属触媒の分子設計に関する研究)

YOSHIOKA Shota

吉岡 頌太

461802104

Noyori Laboratory
Department of Chemistry, Graduate School of Science
Nagoya University

2021

Preface

This work was carried out at the Noyori laboratory in the Graduate School of Science, Nagoya University, from April 2016 to March 2021. This study is concerned with molecular design of transition metal catalysts toward practical hydrogenation of carboxylic acids.

The author wishes to express his sincerest gratitude to Professor Dr. Susumu Saito for his patient guidance, helpful discussions and continuous kind encouragement throughout this work. The author wishes to express his deepest gratitude to Assistant Professor Dr. Hiroshi Naka and Assistant Professor Dr. Jung Jieun for their constant and helpful guidance, precise suggestions and continuous encouragement. The author wishes to express his deepest gratitude to University Professor Dr. Ryoji Noyori for his precise guidance, valuable suggestions and encouragement with warm enthusiasm.

The author would like to express his appreciation to Professor Dr. Kenichiro Itami and Professor Dr. Shigehiro Yamaguchi for their valuable suggestions and kind encouragement.

The author wishes to express his deepest gratitude to Professor Dr. Masaya Sawamura and Lecturer Dr. Tomohiro Iwai for giving him the opportunity to work in their laboratory at division of chemistry, Hokkaido university. The author also appreciates to Ms. Yuko Kihara for kind assistance throughout this collaboration.

The author thanks Mr. Toshiaki Noda, Ms. Hideko Natsume and Mr. Hisakazu Okamoto for their excellent works of scientific glassware.

The author is grateful to Dr. Masayuki Naruto, Dr. Ke Wen, Ms. Laurie Neuman, Ms. Akari Saito, Mr. Takuya Okada, Mr. Bendik Brømer, Mr. Kazuki Teramoto, and Ms. Fangru Li for their great assistance and collaborations.

The author thanks the former and present members of the Noyori Laboratory for their kind considerations.

Ms. Yuriko Nakamura	Dr. Siong Wan Foo	Dr. Kaliyamoorthy Selvam
Dr. Dinesh Sawant	Dr. Dattatraya Bagal	Dr. Sujit Chavan
Dr. Seonghee Bae	Dr. Yuki Takada	Dr. Lyu-Ming Wang
Ms. Yuna Morioka	Mr. Yuya Akao	Mr. Takahiro Isogawa
Mr. Masaki Shibata	Mr. Taiki Shimomura	Mr. Kiyotaka Mori
Mr. Takahiro Aoki	Mr. Toshiki Iwatsuki	Mr. Atsushi Nakamura
Ms. Manami Muraki	Mr. Hiroyuki Okabe	Ms. Saeko Ogawa
Mr. Tomoya Kanda	Ms. Ryoko Nagata	Mr. Kenji Kamada
Ms. Tomomi Banno	Mr. Kensuke Kobayashi	Mr. Shogo Mori
Ms. Farzaneh Soleymani Movahed	Ms. Hiroko Okuwa	Mr. Hiroya Tada
Ms. Yumiko Mizuno	Ms. Tomoyo Tamura	Ms. Asuka Naraoka
Ms. Yumiko Mizuno	Ms. Ivven Huang	Mr. Masaki Nomura
Mr. Taku Wakabayashi	Mr. Hiroaki Shibayama	Mr. Toshiki Asai
Mr. Yuki Sakai	Mr. Riku Hashimoto	Mr. Alan K. Kimura
Ms. Buddhini Ranasinghe	Ms. Kellie Binder	Ms. Choi Hyosun
Ms. Lubov Kozinskaya	Ms. Taimeng Liang	Ms. Horne Ella Frances

The author also thanks Integrative Graduate Education and Research Program in Green Natural Sciences (IGER) program for the fellowship.

YOSHIOKA Shota

Noyori Laboratory
Department of Chemistry
Graduate School of Science
Nagoya University
2021

Contents

General Introduction **1**

Chapter 1. **15**

Development of Effective Bidentate Diphosphine Ligands of Ruthenium Catalysts toward Practical Hydrogenation of Carboxylic Acids

Chapter 2. **132**

Catalytic Hydrogenation of N-protected α -Amino Acids Using Ruthenium Complexes with Monodentate Phosphine Ligands

Chapter 3. **177**

Reaction of H₂ with Mitochondria-Relevant Metabolites Using a Multifunctional Molecular Catalyst

List of Publications **232**

List of Abbreviations

Ac	acetyl	L	ligand
acac	acetylacetonato	M	metal
AL	alcohol	Me	methyl
Ar	aryl	Me-allyl	2-methylallyl
BINAP	2,2'-bis(diphenylphosphino)-1,1'-binaphthyl	mol	mole
Boc	tertiary butoxycarbonyl	Ms	methanesulfonyl
Bu	butyl	MS	mass spectrometry
CA	carboxylic acid	<i>n</i> -Bu	normal butyl
cod	1,5-cyclooctadiene	NMR	nuclear magnetic resonance
conv.	conversion	OMe	methoxy
CPME	Methoxycyclopentane	<i>p</i>	para
Cy	cyclohexyl	Ph	phenyl
DFT	density functional theory	P_{H_2}	hydrogen pressure
DMAP	<i>N,N</i> -dimethyl-4-aminopyridine	r.t.	room temperature
DMSO	dimethyl sulfoxide	<i>T</i>	reaction temperature
DPPB	1,4-(diphenylphosphino)butane	<i>t</i>	reaction time
ES	ester	<i>t</i> -Bu	tertiary butyl
ESI	electrospray ionization	Tf	trifluoromethanesulfonyl
Et	ethyl	THF	tetrahydrofuran
GC	gas chromatography	tmm	trimethylenemethane
HRMS	High-resolution mass spectra	TON	turnover number
<i>i</i> -Pr	isopropyl	Triphos	1,1,1-tris(diphenylphosphinomethyl)ethane
<i>J</i>	coupling constant		

General Introduction

A rich variety of carboxylic acids (CAs) is abundantly available from fossil and other natural sources. The hydrogenation of CAs to alcohols, which can be used as alternative organic energy (H₂) carriers or as platform chemicals, remains as attractive as it is challenging.^[1] According to a 2004 report from the US Department of Energy (DOE), the vast majority of high-value-added chemicals from biomass at that time were CAs,^[2] although the order, nature, and number of the CAs should have changed since, given the technological advancements in that period.^[3] However, there should be hardly any doubt that CAs will remain on such lists, given that they represent a highly attractive biomass feedstock, and they are most likely also on other confidential lists that are usually not disclosed by industry.

Alternatively, CAs can be produced artificially, e.g. from CO₂, H₂, and olefins.^[4] More recently, it has been demonstrated that light-derived energy may offer great potential for the synthesis of CAs: for example, using a photosensitizer in a micro-channel allows to transform CO₂ and amines into α -amino CAs.^[5] Treating CO₂ with *ortho*-carbonyl-substituted toluene derivatives under exposure to LED light (365 nm)^[6] results in the formation of different CAs even though this reaction is thermodynamically unfavorable ($\Delta G > 0$). Furthermore, formic acid is obtained from the hydrogenation of CO₂^[7] or from the photo-reduction of CO₂ with H₂O using solar energy.^[8] Further improvements on the reduction methods for CO₂ may be beneficial for the “methanol economy”, i.e., the anthropogenic chemical carbon cycle.^[9] The identification of carbon-neutral alternatives to fossil fuels represents a major milestone on the way to sustainable development goals (SDGs). When CAs are sourced from biomass and/or produced from CO₂, they represent indeed a potential renewable resource.

Moreover, the hydrogenation of CAs is an ideal method for the bulk production of alcohols, given that water is the only byproduct of this reaction. Hydrogenation methods that are widely applicable to a broad spectrum of CAs and that selectively produce alcohols should therefore be highly desirable. Even though simple molecular hydrogenation catalysts that enable such conversions remain scarce, our systematic studies have disclosed a prototypical catalyst structure for the hydrogenation of CAs.^[10]

Similar to amides, CAs exhibit relatively unreactive electrophilic carbonyl carbon atoms (Figure 1) and α -C–H hydrogen atoms with very low acidity.^[11] So far, these features have significantly hampered the development of new approaches to the catalytic hydrogenation and carbon–carbon bond formation reaction at CH_{*n*}COOH moieties of R_{3-*n*}CH_{*n*}COOH (*n* = 1–3).

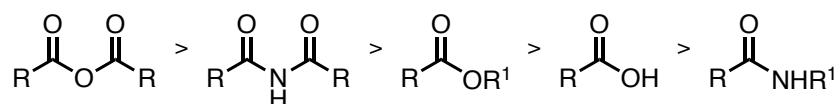
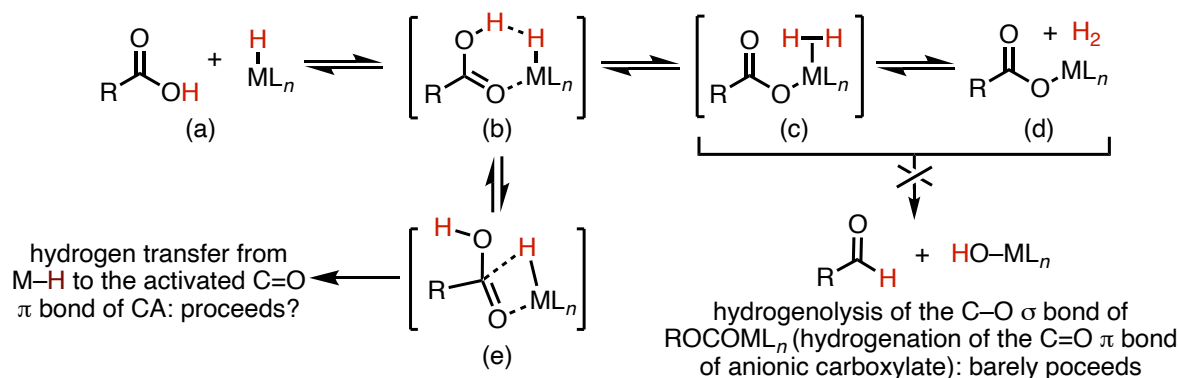


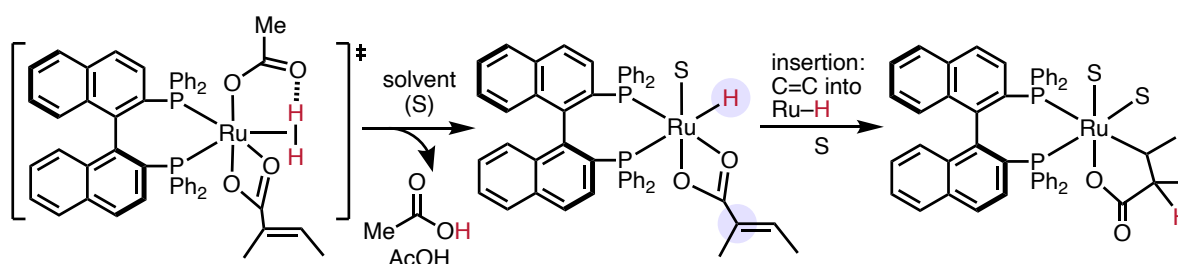
Figure 1 | CA derivatives, ordered according to their expected decreasing electrophilicity of the C=O group in their catalytic hydrogenation using molecular hydrogen (H₂).

The catalytic hydrogenation of CA derivatives such as esters^[12] and amides^[13] proceeds well under basic to neutral conditions, while investigations into similar hydrogenations using a CA as the acidic reaction medium are scarce, as they should not operate efficiently.^[12] Considering the *ex vi termini* acidity of CAs, it is understandable that the rational design of single-active-site catalysts that effectively hydrogenate the thermodynamically stable and kinetically inert COOH group is no mundane task. Compared to the hydrogenation of CAs, i.e., the addition of H₂ followed by elimination of H₂O, which has so far not been explored in detail, the dehydrative amidation and esterification of CAs with amines^[14] and alcohols,^[15] respectively, share a richer history of advanced research. Such stepwise reactions, which involve the addition of O–H or N–H bonds to the double bond of HOC=O, followed by the elimination of H₂O to form new C–O or C–N bonds, are frequently catalyzed by Brønsted or Lewis acids; this feature could offer an advantage for the inherently acidic CAs, and these reactions should thus be much more accessible than the hydrogenation of CAs. Conversely, in the CA hydrogenation, metal hydride intermediates (H–ML_n; L = ligand; n = 0–4) that are commonly generated in the presence of H₂ would be rapidly neutralized by the excess of CA under concomitant formation of H₂ and the corresponding metal carboxylates (ROCO–ML_n), which are not easily hydrogenated (Scheme 1).^[16]

Metal carboxylates could also recapture H₂ and regenerate H–ML_n, which would result in the major equilibrium [ROCO–ML_n + H₂ ↔ H–ML_n + RCO₂H] [(a) ↔ (b) ↔ (c) ↔ (d)]. It had indeed been proposed much earlier that the neutral Ru-acetate species [Ru^{II}(OAc)₂P₂] and [Ru^{II}(OAc)(OC(O)R)P₂] (OAc = CH₃CO₂⁻) could trap and activate H₂ to generate the H–Ru(OC(O)R)P₂ species in the asymmetric hydrogenation of internal olefins of α,β-unsaturated CAs such as tiglic acid (MeCH=C(Me)COOH: CA-1)^[17] (Scheme 2). During this reaction, acetic acid (AcOH) is expelled from the metal center;^[18] however, at the time, AcOH was considered merely an undesirable by-product and removed from the catalytic cycle. In addition, the COOH group of CA-1 remained un-hydrogenated, acting merely as an innocent directing group for the hydrogenation of the olefin. Nevertheless, we speculated that the hydrogenation of CA may potentially occur, given the possible process (b) → (e), which deviates from the major equilibria (a) ↔ (d).

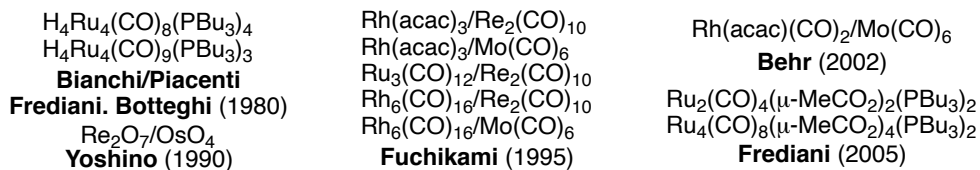


Scheme 1 | Major equilibria (a)→(b)→(c)→(d) and vice versa (d)→(c)→(b)→(a) involving CA, metal hydride, H_2 and metal carboxylate. (a) CA and metal hydride (H-ML_n) afford (b) a CA–metal coordination complex under subsequent formation of (c) a $\eta^2\text{-H}_2$ –metal complex that undergoes H–H bond cleavage, which generates (d) a metal carboxylate (ROCO-ML_n) and free H_2 . A deviated process from (b) to (e) would facilitate the hydrogenation of CA via a hydride transfer to the CA.

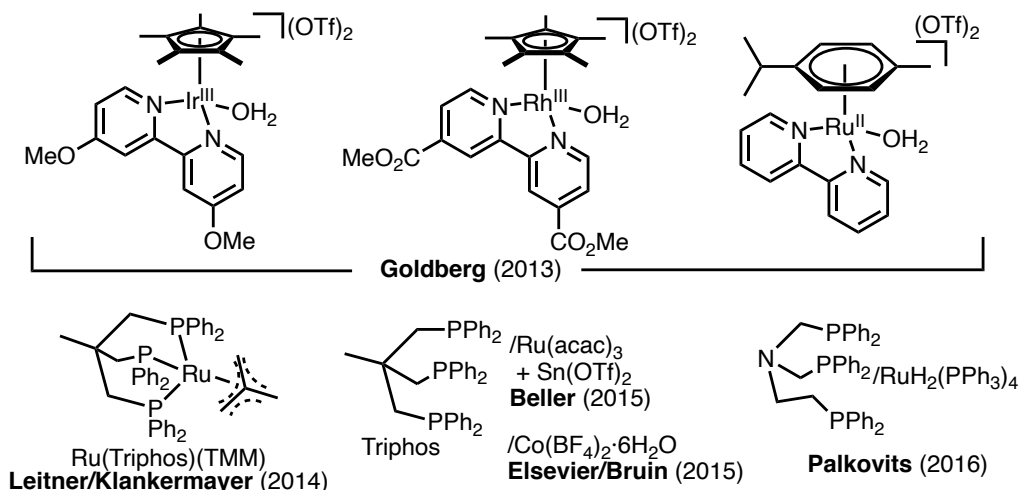


Scheme 2 | The insertion of C=O bonds of tiglic acid (CA-1) or AcOH into Ru–H bonds in asymmetric hydrogenations is not observed. Purple parts reacted.

(a) multi-nuclear transition metal complexes used for CA hydrogenation



(b) mono-nuclear transition metal complexes used for CA hydrogenation



(c) transition metal complexes mainly developed or used for CA hydrogenation in **our** group (2013–2017)

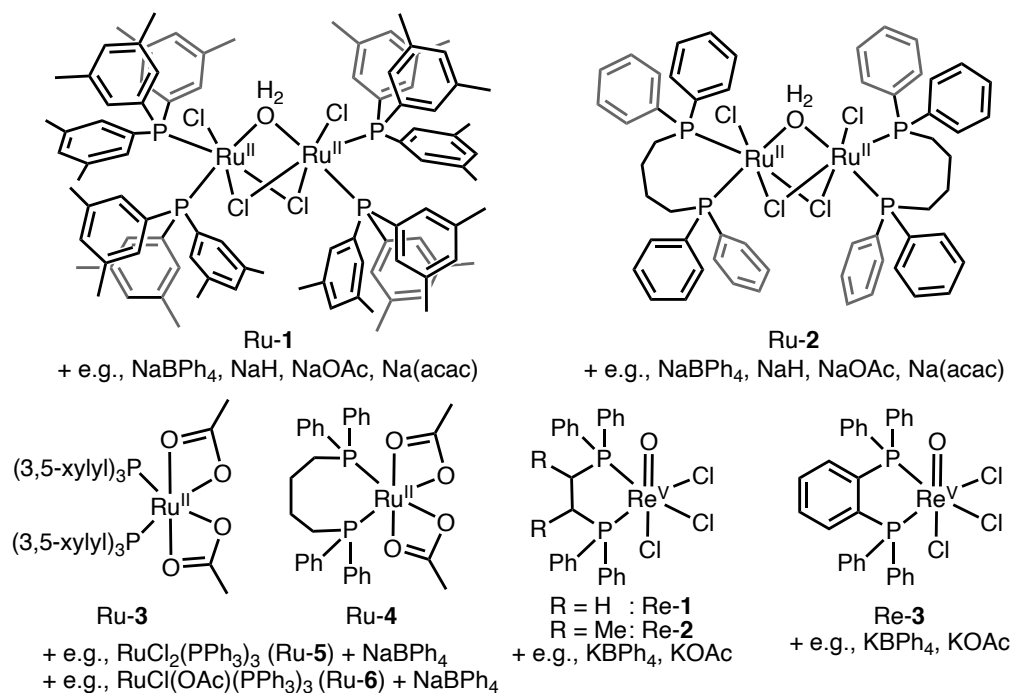


Figure 2 | Transition-metal complexes for the catalytic hydrogenation of CAs using H₂.

(a) Multi-nuclear transition metal complexes; (b) mono-nuclear transition metal complexes; (c) transition metal complexes in our group (2013–2017)^[10] mainly developed or used for CA hydrogenation.

Apart from the meticulous efforts dedicated to tackle the inherent obstacles of the “carboxylate-formation mechanism”, which is operative during the hydrogenation of the CAs, multinuclear metal (cluster) complexes were tested in earlier studies (Figure 2a). Heterobimetallic catalysts,^[19] which seem more intuitive or pragmatic, successfully reduce CAs to the corresponding alcohols, albeit at the expense of concomitant side reactions, which include dearomatic hydrogenations or overreductions under harsh conditions. A higher catalytic activity of binuclear Ru-carboxylato complexes^[20] relative to that of mononuclear derivatives and the importance of intermediary Ru(acyl)(alkoxy) complexes that are different from ours, were briefly noted, albeit that little evidence was provided.

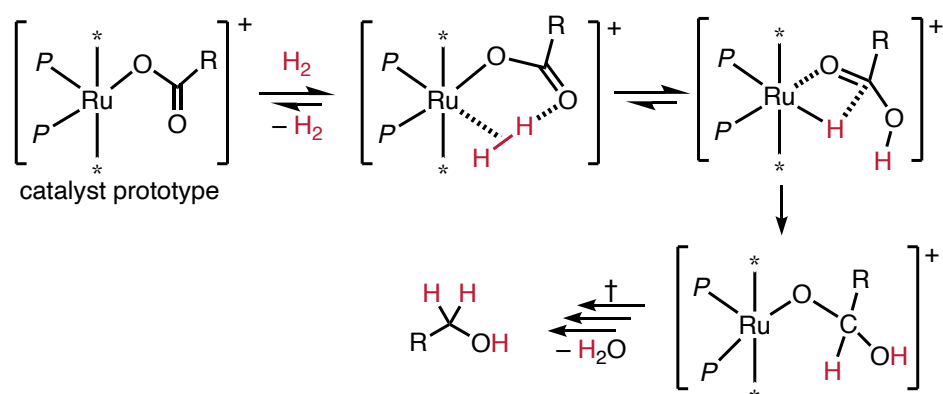
In contrast, mononuclear metal complexes have very rarely been examined (Figure 2b). One of the earliest attempts, using the Ru-acetato complex $\text{Ru}(\text{CO})_2(\text{OCOCH}_3)_2(\text{PBU}_3)_2$ ($\text{Bu} = \text{CH}_3(\text{CH}_2)_3$), did not lead to the hydrogenation of the COOH groups of CA-1 and its olefin-hydrogenated form, 2-methylbutanoic acid ($P_{\text{H}_2} = \text{ca. } 13 \text{ MPa}$, $T = 100 \text{ }^\circ\text{C}$).^[21] In contrast, the hydrogenation of acetic acid (AcOH) proceeded, but merely afforded the ester ethyl acetate (AcOEt), which was ascribed to “unknown catalytic species”. More recent studies by Goldberg *et al.* on functionalized bipyridine-coordinated Ru, Ir, and Rh catalysts^[22] showed that small aliphatic CAs such as AcOH can be hydrogenated under milder reaction conditions ($P_{\text{H}_2} = 0.3\text{--}5 \text{ MPa}$, $T = 120 \text{ }^\circ\text{C}$) with a rather high turnover number ($\text{TON} = \sim 800$; for comparison, an Ir complex with $\text{Sc}(\text{OTf})_3$ gives $\text{TON} \approx 1700$); however, the generated alcohol, e.g., ethanol (EtOH), likewise undergoes an *in situ* esterification with AcOH, which affords AcOEt as the major product. Moreover, the corresponding Ir catalyst, which is derived from its precatalyst (Figure 2b), decomposes into Ir black at temperatures $>120 \text{ }^\circ\text{C}$. Furthermore, it has been demonstrated experimentally^[22] that CAs with shorter aliphatic carbon chains such as AcOH react much more rapidly, which is consistent with previous investigations.^[20,21] With increasing size of the CA from C_1 to C_4 , the corresponding carboxylate carbon atom becomes more electron-rich and thus less susceptible to nucleophilic attacks from metal hydrides (H-ML_n).

In the development of CA hydrogenation methods based on molecular catalysts, the most critical issues to be addressed in order to ensure high reactivity and selectivity for the generation of alcohols should therefore be the discovery of rational ways: (i) to hydrogenate the carboxylic acid (COOH) before the metal carboxylate (COO^-) is formed; (ii) to prevent the *in situ* generation of esters; (iii) to subsequently convert the esters thus generated *in situ* to the parent CA in the presence of H_2O , i.e., to develop water-stable catalysts; and (iv) to hydrogenate not only CAs but also esters in a one-pot fashion using the same catalyst system. Meanwhile, (iii) and (iv) have partially but reasonably solved by Beller *et al.*^[23] and Leitner/Klankermayer *et al.*,^[24] respectively, using Ru-Triphos (Triphos = 1,1,1-

General Introduction

tris(diphenylphosphinomethyl)ethane) complexes (Figure 2b). The complexes were used with cooperative Lewis acids such as Sn(OTf)₂ under relatively strenuous hydrogenation conditions (typically: $P_{\text{H}_2} = 5\text{--}6$ MPa, $T = 160\text{--}220$ °C). In the context of (iv), more germinal studies by Elsevier *et al.* have demonstrated great potential for a Ru-Triphos system to effectively hydrogenate esters (typically: $P_{\text{H}_2} = 7.0\text{--}8.5$ MPa, $T = 100$ °C).^[25] Thorough subsequent studies by Leitner/Klankermayer *et al.* resulted in improved Ru-Triphos catalyst systems for the hydrogenation of esters,^[24] in which methyl benzoate and alkyl formates, formed *in situ* from the esterification of formic acid that is generated by the hydrogenation of CO₂ with the alcohol solvent, were hydrogenated under conditions that are simpler than those reported by Elsevier, and milder (typically: $P_{\text{H}_2} = 3\text{--}5$ MPa, $T = 140$ °C)^[24] than those for the hydrogenation of CAs (typically: $P_{\text{H}_2} = 5$ MPa, $T = 220$ °C).^[24] Thus, in many cases, the CA hydrogenation should in effect be the result of an *in situ*-generated ester (lactone), which serve as an intermediate and undergo hydrogenation more effectively.^[24a,24b,26] Cole-Hamilton *et al.* have used another Ru-Triphos system for the hydrogenation of relatively activated amides such as anilides, which engage in selective C=O bond cleavage in preference to C–N bond cleavage.^[27] Leitner/Klankermayer *et al.*^[24,26a,26b] and Frediani *et al.*^[26c] have used similar systems for hydrogenation of 4-keto-CAs and 1,4-dicarboxylic acids (C₄ constituting the main chain), which are essentially the hydrogenation of the ketone or the corresponding anhydrides of a five-membered ring system *in situ* formed from the 1,4-diCAs, respectively, followed by hydrogenation of the resulting γ -lactones in both cases. A nitrogen-centered Triphos variant has been introduced by Palkovits *et al.* for the hydrogenation of a similar series of bio-based dicarboxylic acids and small/medium size CAs including octanoic acid, even though the major products are frequently linear and cyclic esters, which the catalyst cannot hydrogenate further into the corresponding alcohols ($P_{\text{H}_2} = 7$ MPa, $T = 160\text{--}170$ °C).^[28] The Ru-Triphos system represents the current state-of-the-art and marked a milestone in the history of hydrogenation; however, the reason why Triphos is among the best ligands for the hydrogenation of many CA derivatives upon minor changes to the reaction conditions remains unclear. Moreover, since experimental proof for the underlying different catalytic mechanisms that underpin these hydrogenation systems remain elusive, some *ab initio* calculations on various mechanisms have been carried out.^[24a,26e,29]

Until 2015, our seminal studies had been the only ones that reported a molecular prototype obtained from the rational design of a single-active-site Ru catalyst for the hydrogenation of CAs (Figure 2c).^[10a] Four different precatalyst complexes (Ru-1–Ru-4) were mainly developed and used for the generation of single-active-site cationic Ru carboxylates. The CA-derived carboxylate coordinated to the Ru center initially functions as a proton acceptor for the heterolytic cleavage of a H–H bond, and subsequently also as an acceptor for a hydride from [Ru–H]⁺, which was generated in the first step (Scheme 3).



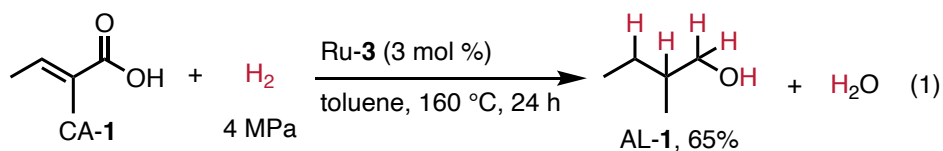
Scheme 3 | Carboxylic acid (CA) self-induced hydrogenation of CA; P: coordinating phosphine; †multiple steps for the regeneration of the catalyst. (i) Capture of a second molecule of H₂; (ii) hydrogenation of the aldehyde; (iii) exchange of the alkoxide on Ru with CA, which generates the cationic Ru-carboxylate “catalyst prototype”.

This catalytic cycle thus represents a “CA self-induced CA hydrogenation”. In the meantime, similar catalytic mechanisms involving “cationic metal mono-carboxylates” were proposed theoretically by *ab initio* calculations of catalytic cycles that involve a hydrogenation of CAs with a Co-Triphos complex^[29] and one for the hydrogenation of HCO₂H, *in situ* formed from the reduction of CO₂ using a Ru-Triphos complex.^[26e]

The catalysts developed in our group afford the corresponding alcohols selectively from a variety of CAs with longer and bulkier carbon chains, relative to smaller CAs mainly tested by other research groups so far. Our systems exhibit a higher functional-group tolerance than other state-of-the-art catalysts for CA hydrogenation, even though ours suffer from a selectivity that still remains unsatisfactory. For example, both the COOH and olefinic groups of CA-1 were hydrogenated using a catalytic amount of Ru-3 (eq 1). The corresponding esters were generated in 5±3% (average of three runs). Quite unlike the Ru-Triphos systems, the hydrogenation of esters is not promoted, clearly indicating that the CAs are more reactive than the esters under the applied conditions in the “CA self-induced CA hydrogenation” mechanism, which is quite

General Introduction

different from the catalytic cycle for the hydrogenation of esters. This catalyst system may thus constitute a milestone toward the development of catalytic hydrogenation methods for carbon feedstock derived from biomass or CO₂.



Homogeneous hydrogenation catalysts for CAs have been rapidly growing in recent years. However, low chemoselectivity and low catalytic activity of these catalysts limit their industrial applications in the practical points of view.

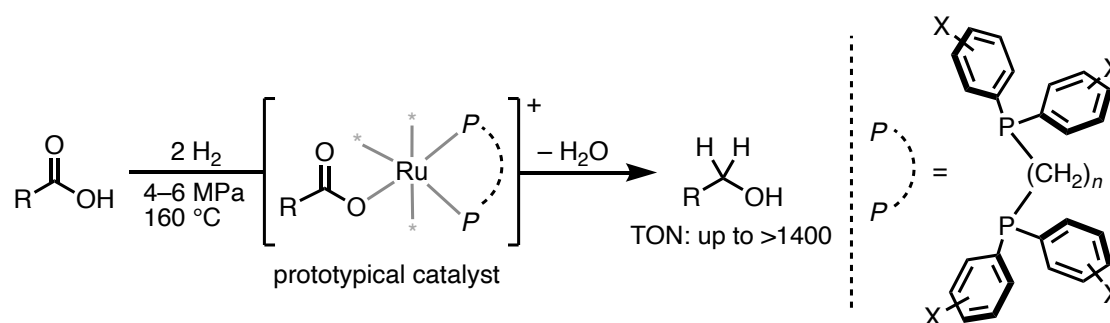
In addition, Noyori-type bifunctional catalyst, which often shows a quite high hydrogenation ability for carbonyl compounds such as ketones and esters,^[11,12b,30] have not been applied in CA hydrogenation. If Noyori-type bifunctional catalyst could work in CA hydrogenation, it opens the door to a new guideline of a rational design for hydrogenation catalysis.

Survey of this Thesis

In this thesis, the author conducted a research on molecular design of transition metal catalysts toward practical hydrogenation of carboxylic acids including α -amino acids and polycarboxylic acids.

In Chapter 1, the author developed an improvement in the catalytic activity of molecular Ru catalysts for the hydrogenation of carboxylic acids to alcohols by systematic studies on the induction of Ru catalysts from precatalysts that bear a variety of bidentate diphosphine (PP) ligands (Scheme 4).^[31]

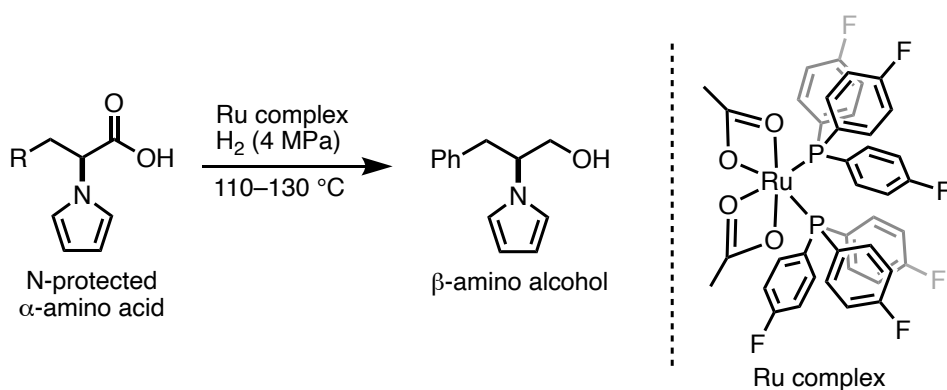
The author reports herein a rational design and development of highly active Ru catalysts by optimization of the structure of mono- and bidentate aryl phosphine ligands for the CA hydrogenation based on single-active-site Ru catalysts, in which the substrate (RCO₂H)-derived cationic Ru carboxylate [$P_2Ru(OCOR)^+$] (P denotes “one phosphorus coordination”), which was found to be the catalyst prototype for *CA self-induced CA hydrogenation*. After screening of aryl groups substituted on P atom(s), both a faster reaction rate and sustainable catalytic activity were achieved using bidentate ligands. The activity and durability of modified (PP)Ru catalysts were substantially higher (turnover number of >1400) than those of our original (PP)Ru catalysts.



Scheme 4 | Development of Effective Bidentate Diphosphine Ligands of Ruthenium Catalysts toward Practical Hydrogenation of Carboxylic Acids.

In Chapter 2, the author achieved catalytic hydrogenation of N-protected α -amino acids under essential retention of the configuration of their α -chiral centers using a Ru complex with a monodentate phosphine ligand, tris(*para*-fluorophenyl)phosphine (Scheme 5).^[32]

Optically active β -amino alcohols can serve as important chiral building blocks. Although hydrogenation of α -amino acids is one of the effective methods to obtain optically active β -amino alcohols, for which there are only a few reports of successful heterogeneous catalysts; however, those catalysts suffer from several drawbacks. For instance, excess strong Brønsted acids are required and aromatic ring reduction occurs. Our hydrogenation catalyst for carboxylic acids (CAs) based on “CA self-induced hydrogenation of CA” has potential to hydrogenate α -amino acids. However, epimerization of the α -carbon of the carbonyl group at a high reaction temperature has yet to be addressed. The author reports here that a new Ru complex was synthesized by modification of the ligand, thereby achieving hydrogenation of α -amino acids with negligible epimerization at 110–130 °C. Among the ligands tested for this hydrogenation, which proceeds at a relatively low temperature, tris(*para*-fluorophenyl)phosphine exhibited the best performance. In comparison, electron-rich monodentate, bidentate, and tridentate phosphines were far less effective. The precatalyst $\text{Ru}(\text{OAc})_2[(p\text{-FC}_6\text{H}_4)_3\text{P}]_2$ was synthesized and isolated, and its structure was determined by a single-crystal X-ray diffraction analysis. N-protected α -amino acids with neutral alkyl side chains, including polar functional groups such as sulfides, indoles, ethers, phenols, pyrroles, and arenes, are compatible with the applied hydrogenation conditions, affording the corresponding optically active 2-substituted-2-(1*H*-pyrrol-1-yl)ethan-1-ol (2-amino ethanol) derivatives in moderate to high yield.



Scheme 5 | Catalytic hydrogenation of N-protected α -amino acids using Ru complexes with monodentate phosphine ligands.

In Chapter 3, the author achieved a reaction of C₄-, C₅- and C₆-biobased polycarboxylic acids to di- and triol with H₂ catalyzed by iridium (Ir) complexes comprising sterically confined Ir-bipyridyl frameworks (Figure 3).^[33]

The Krebs cycle occurs in mitochondrial matrix in cells to produce and transfer electrons to generate energy-rich NADH, GTP and FADH₂, and conversely to produce not only C₄-dicarboxylic acids (succinic acid (SucA), fumaric acid (FumA), malic acid (MliA), oxaloacetic acid (OacA)), but also C₅- (2-oxoglutaric acid (OglA)) and C₆-polycarboxylic acid (aconitic acid (AcoA) and citric acid (CitA)) as metabolites. Those polycarboxylic acids are in highly oxidized or oxygenated states and thus energy-poor molecules, which are potential candidates as bio-renewable carbon feedstock if hydrogen atoms and electrons could be back into these molecules.

The author reports here that those C₄, C₅, and C₆ resources, in addition to mitochondria-relevant metabolites (aspartic acid (AspA), tartaric acid (TarA), itaconic acid (ItaA)) and sugar-derived artificial feedstock (levulinic acid (LevA)) are convergently reduced and dehydrated to corresponding diols or triols upon reaction with H₂ catalyzed by iridium (Ir) complexes comprising sterically confined Ir-bipyridyl frameworks. The single-metal-site Ir catalyst is spontaneously induced upon heating and self-hydrogenation of the Ir complex, rendering the catalytic method highly versatile and straightforward, and giving valuable molecular insights for paving a new avenue in the development of novel molecular technologies for reduction and dehydration of highly functionalized, bio-renewable resources.

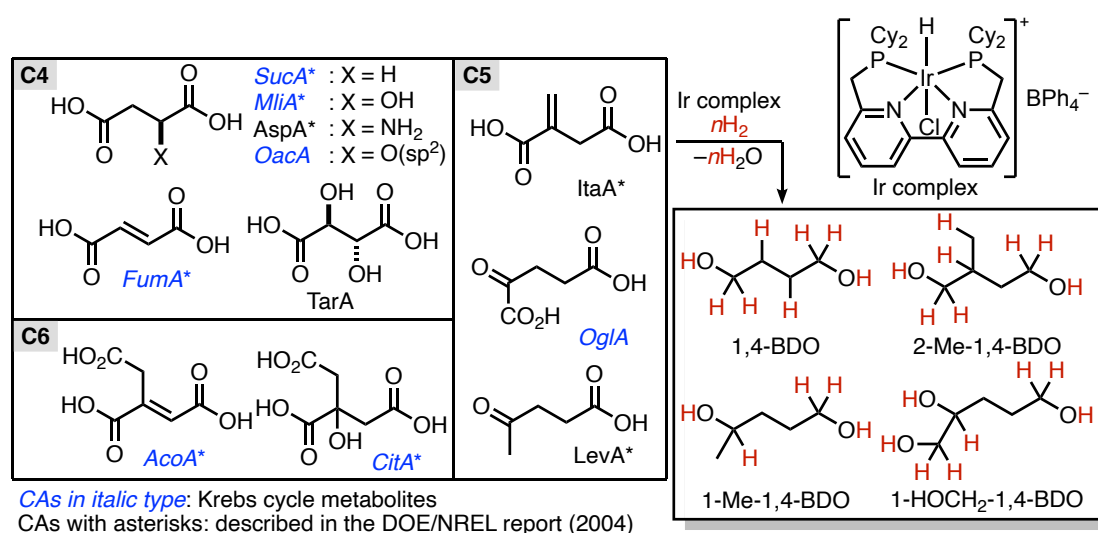


Figure 3 | Reaction of C₄-, C₅- and C₆-biobased carboxylic acids with H₂ using an Ir complex as pre-catalyst.

References

- [1] D. Teichmann, W. Arlt, P. Wasserscheid, R. Freymann, *Energy Environ. Sci.* **2011**, *4*, 2767–2773.
- [2] T. Werpy and G. Petersen, Top value added chemicals from biomass volume I—results of screening for potential candidates from sugars and synthesis gas, <https://www.nrel.gov/docs/fy04osti/35523.pdf>, (accessed May 2018).
- [3] J. J. Bozell, G. R. Petersen, *Green Chem.* **2010**, *12*, 539–554.
- [4] T. G. Ostapowicz, M. Schmitz, M. Krystof, J. Klankermayer, W. Leitner, *Angew. Chem. Int. Ed.* **2013**, *52*, 12119–12123.
- [5] H. Seo, M. H. Katcher, T. F. Jamison, *Nat. Chem.* **2016**, *9*, 453–456.
- [6] Y. Masuda, N. Ishida, M. Murakami, *J. Am. Chem. Soc.* **2015**, *137*, 14063–14066.
- [7] a) R. Tanaka, M. Yamashita, K. Nozaki, *J. Am. Chem. Soc.* **2009**, *131*, 14168–14169; b) W.-H. Wang, Y. Himeda, J. T. Muckerman, G. F. Manbeck, E. Fujita, *Chem. Rev.* **2015**, *115*, 12936–12973; c) Q. Liu, L. Wu, R. Jackstell, M. Beller, *Nat. Commun.* **2015**, *6*, 5933; d) P. G. Jessop, T. Ikariya, R. Noyori, *Nature* **1994**, *368*, 231–233; e) P. G. Jessop, T. Ikariya, R. Noyori, *Chem. Rev.* **1995**, *95*, 259–272.
- [8] a) S. Sato, T. Arai, T. Morikawa, K. Uemura, T. M. Suzuki, H. Tanaka, T. Kajino, *J. Am. Chem. Soc.* **2011**, *133*, 15240–15243; b) T. Arai, S. Sato, T. Morikawa, *Energy Environ. Sci.* **2015**, *8*, 1998–2002.
- [9] a) G. A. Olah, G. K. S. Prakash, A. Goepfert, *J. Am. Chem. Soc.* **2011**, *133*, 12881–12898; b) G. A. Olah, *Angew. Chem. Int. Ed.* **2013**, *52*, 104–107.
- [10] a) M. Naruto, S. Saito, *Nat. Commun.* **2015**, *6*, 8140; b) M. Naruto, S. Agrawal, K. Toda, S. Saito, *Sci. Rep.* **2017**, *7*, 3425.
- [11] P. A. Dub, T. Ikariya, *ACS Catal.* **2012**, *2*, 1718–1741.
- [12] a) M. L. Clarke, *Catal. Sci. Technol.* **2012**, *2*, 2418–2423; b) S. Werkmeister, K. Junge, M. Beller, *Org. Process Res. Dev.* **2014**, *18*, 289–302.
- [13] For reviews, see: a) A. M. Smith, R. Whyman, *Chem. Rev.* **2014**, *114*, 5477–5510; b) J. R. Cabrero-antonino, R. Adam, V. Papa, M. Beller, *Nat. Commun.* **2020**, *11*, 3893. For recent results from our group, see: c) T. Miura, I. E. Held, S. Oishi, M. Naruto, S. Saito, *Tetrahedron Lett.* **2013**, *54*, 2674–2678; d) T. Miura, M. Naruto, K. Toda, T. Shimomura, S. Saito, *Sci. Rep.* **2017**, *7*, 1586.
- [14] a) V. R. Pattabiraman, J. W. Bode, *Nature* **2011**, *480*, 471–479; b) R. M. de Figueiredo, J.-S. Suppo, J.-M. Campagne, *Chem. Rev.* **2016**, *116*, 12029–12122; Recent results: c) K. Wang, Y. Lu, K. Ishihara, *Chem. Commun.* **2018**, *54*, 5410–5413; from our group: d) D. N.

- Sawant, D. B. Bagal, S. Ogawa, K. Selvam, S. Saito, *Org. Lett.* **2018**, *20*, 4397–4400.
- [15] For reviews, see: a) J. Otera, in *Esterification; Methods, Reactions, and Applications*, Wiley-VCH, Weinheim, **2003**, ch. 1, pp. 5–145; b) K. Ishihara, *Tetrahedron* **2009**, *65*, 1085–1109.
- [16] R. H. Morris, in *The Handbook of Homogeneous Hydrogenation*, ed. J. G. de Fries and C. J. Elsevier, Wiley-VCH, Weinheim, **2007**, vol. 1, ch. 3, pp. 45–70.
- [17] M. T. Ashby, J. Halpern, *J. Am. Chem. Soc.* **1991**, *113*, 589–594.
- [18] a) A. B. Chaplin, P. J. Dyson, *Inorg. Chem.* **2008**, *47*, 381–390; b) M. Kitamura, M. Tsukamoto, Y. Bessho, M. Yoshimura, U. Kobs, M. Widhalm, R. Noyori, *J. Am. Chem. Soc.* **2002**, *124*, 6649–6667.
- [19] a) K. Yoshino, Y. Kajiwara, N. Takaishi, Y. Inamoto, J. Tsuji, *J. Am. Oil Chem. Soc.* **1990**, *67*, 21–24; b) D.-H. He, N. Wakasa, T. Fuchikami, *Tetrahedron Lett.* **1995**, *36*, 1059–1062.
- [20] a) M. Bianchi, G. Menchi, F. Francalanci, F. Piacenti, U. Matteoli, P. Frediani, C. Botteghi, *J. Organomet. Chem.* **1980**, *188*, 109–119; b) A. Salvini, P. Frediani, M. Bianchi, F. Piacenti, L. Pistolesi, L. Rosi, *J. Organomet. Chem.* **1999**, *582*, 218–228.
- [21] A. Salvini, P. Frediani, C. Giannelli, L. Rosi, *J. Organomet. Chem.* **2005**, *690*, 371–382.
- [22] T. P. Brewster, A. J. M. Miller, D. M. Heinekey, K. I. Goldberg, *J. Am. Chem. Soc.* **2013**, *135*, 16022–16025.
- [23] X. Cui, Y. Li, C. Topf, K. Junge, M. Beller, *Angew. Chem. Int. Ed.* **2015**, *54*, 10596–10599.
- [24] a) T. vom Stein, M. Meuresch, D. Limper, M. Schmitz, M. Ho, J. Coetzee, D. J. Cole-Hamilton, J. Klankermayer, W. Leitner, *J. Am. Chem. Soc.* **2014**, *136*, 13217–13225; b) S. Wesselbaum, T. vom Stein, J. Klankermayer, W. Leitner, *Angew. Chem. Int. Ed.* **2012**, *51*, 7499–7502.
- [25] a) H. T. Teunissen, C. J. Elsevier, *Chem. Commun.* **1997**, 667–668; b) H. T. Teunissen, C. J. Elsevier, *Chem. Commun.* **1998**, 1367–1368.
- [26] a) F. M. A. Geilen, B. Engendahl, A. Harwardt, W. Marquardt, J. Klankermayer, W. Leitner, *Angew. Chem. Int. Ed.* **2010**, *49*, 5510–5514; b) F. M. A. Geilen, B. Engendahl, M. Hölscher, J. Klankermayer, W. Leitner, *J. Am. Chem. Soc.* **2011**, *133*, 14349–14358; c) L. Rosi, M. Frediani, P. Frediani, *J. Organomet. Chem.* **2010**, *695*, 1314–1322; d) H. Mehdi, V. Fábos, R. Tuba, A. Bodor, L. T. Mika, I. T. Horváth, *Top. Catal.* **2008**, *48*, 49–54; e) S. Wesselbaum, V. Moha, M. Meuresch, S. Brosinski, K. M. Thenert, J. Kothe, T. vom Stein, U. Englert, M. Hölscher, J. Klankermayer, W. Leitner, *Chem. Sci.* **2015**, *6*, 693–704; f) C. A. Huff, M. S. Sanford, *J. Am. Chem. Soc.* **2011**, *133*, 18122–18125; g) C. Delhomme, D. Weuster-Botz, F. E. Kühn, *Green Chem.* **2009**, *11*, 13–26.
- [27] a) A. A. Núñez Magro, G. R. Eastham, D. J. Cole-Hamilton, *Chem. Commun.* **2007**, 3154–

General Introduction

- 3156; b) J. Coetzee, D. L. Dodds, J. Klankermayer, S. Brosinski, W. Leitner, A. M. Z. Slawin, D. J. Cole-Hamilton, *Chem. Eur. J.* **2013**, *19*, 11039–11050.
- [28] L. Deng, B. Kang, U. Englert, J. Klankermayers, R. Palkovits, *ChemSusChem* **2016**, *9*, 177–180.
- [29] T. J. Korstanje, J. I. van der Vlugt, C. J. Elsevier, B. de Bruin, *Science* **2015**, *350*, 298–302.
- [30] J. Pritchard, G. A. Filonenko, R. van Putten, E. J. M. Hensen, E. A. Pidko, *Chem. Soc. Rev.* **2015**, *44*, 3808–3833.
- [31] S. Yoshioka, K. Wen, S. Saito, *submitted*.
- [32] A. Saito, S. Yoshioka, M. Naruto, S. Saito, *Adv. Synth. Catal.* **2020**, *362*, 424–429.
- [33] S. Yoshioka, S. Nimura, M. Naruto, S. Saito, *Sci. Adv.* **2020**, *6*, eabc0274.

Chapter 1.

Development of Effective Bidentate Diphosphine Ligands of Ruthenium Catalysts toward Practical Hydrogenation of Carboxylic Acids

Abstract: Hydrogenation of carboxylic acids (CAs) to alcohols represents one of the most ideal reduction methods for utilizing abundant CAs as alternative carbon and energy sources. However, systematic studies on the effects of metal-to-ligand relationships on the catalytic activity of metal complex catalysts are scarce. We previously demonstrated a rational methodology for CA hydrogenation, in which CA-derived cationic metal carboxylate $[(PP)M(OCOR)]^+$ ($M = Ru$ and Re ; $P =$ one P coordination) served as the catalyst prototype for CA self-induced CA hydrogenation. Herein, we report systematic trial-and-error studies on how we could achieve higher catalytic activity by modifying the structure of bidentate diphosphine (PP) ligands of molecular Ru catalysts. Carbon chains connecting two P atoms as well as Ar groups substituted on the P atoms of PP ligands were intensively varied, and the induction of active Ru catalysts from precatalyst $Ru(acac)_3$ was surveyed extensively. As a result, the activity and durability of the (PP)Ru catalyst substantially increased compared to those of other molecular Ru catalyst systems, including our original Ru catalysts. The results validate our approach for improving the catalyst performance, which would benefit further advancement of CA self-induced CA hydrogenation.

1.1. Introduction

There are various sources of carboxylic acids (CAs), including petrochemical processes and biomass;^[1] in addition, intense efforts have been directed toward the synthesis of CAs by immobilization of CO₂ in organic frameworks via thermal^[2] and photo-induced processes.^[3] In 2004, the US Department of Energy identified and filed “the 30 Top Value Added Chemicals from Biomass” in which more than 20 different CAs as high-value-added chemicals from biomass are included.^[4] The four-electron-reduced form of CAs, alcohols, is more energy-rich, and thus more useful for energy storage and as building blocks for organic synthesis, in the material industry, and in the field of life science. A conventional method to produce alcohols from CAs is reduction by metal hydrides, including LiAlH₄^[5] and BH₃,^[6] in which more than the stoichiometric amount of salt waste is generated. A few hazardous techniques are handful for using such inflammable or hydroscopic reagents on a large scale; hence, such methods are mainly used in laboratories. On the other hand, hydrogenation utilizes hydrogen gas as a reductant and water is the only byproduct, which is generated via the sequence of hydrogen addition–water elimination (apparent hydrogenolysis of the OH group of CA). Therefore, this method can be used commercially.

Hydrogenation of CA (CA hydrogenation) including bio-based CAs is a sustainable alternative that complements conventional alcohol production from dwindling petrochemical resources. Hydrogenation of formic acid is significant in conjunction with “methanol economy”,^[7] as sustainable production routes of formic acid have been explored via photoreduction of CO₂ using H₂O as an electron donor.^[8] Despite the aforementioned utility of CAs for alcohol production, catalytic hydrogenation of CAs to their corresponding alcohols remains challenging in terms of low reactivity of CAs, low chemoselectivity, and low catalytic activity (Figure 1).^[9]

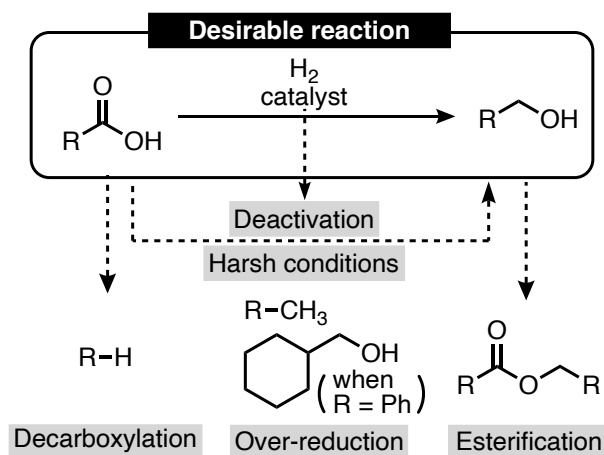


Figure 1 | Potential side reactions and drawbacks of the CA hydrogenation.

Heterogeneous catalysts have thus far been well studied from a practical point of view; they are more robust and easier to separate/reuse compared to homogeneous molecular catalysts. For this purpose, numerous heterogeneous catalysts based on precious metals such as Ru, Re, Rh, Pt, Pd, and their combinations have been reported.^[10] Recently, a common metal-based catalyst was used for the hydrogenation of stearic acid.^[11] However, many of those heterogeneous catalyst systems require strenuous reaction conditions ($P_{H_2} = \sim 35.5$ MPa, $T = \sim 275$ °C); others could work under milder conditions. For instance, Pt(–Re)/TiO₂, reported by Hardacre and co-workers, hydrogenates aliphatic CAs under relatively mild conditions ($P_{H_2} = 0.5$ – 2 MPa, $T = 60$ – 130 °C).^[12] However, product selectivity strongly depends on the substrate. For instance, when 3-cyclohexanepropionic acid was hydrogenated, hydrocarbons, which were obtained through decarboxylation of the substrate and hydrogenolysis of the corresponding alcohol, were the major products. Applicable substrate ranges remain limited in most heterogeneous systems. Thus, most studies have focused on the hydrogenation of simple aliphatic monocarboxylic and 1,4-dicarboxylic acids without the incorporation of special functional groups. Aromatic CAs are one of the most difficult substrates to be selectively hydrogenated because dearomatic hydrogenation of arene rings predominates in many cases. Selective hydrogenation of aromatic CAs to their corresponding aromatic alcohols using heterogeneous catalysts was recently reported by Tahara and co-workers (Ru/Sn/Al₂O₃),^[13] Shimizu and co-workers (Re/TiO₂),^[14] and Breit and co-workers (Pd/Re/C).^[15] In particular, Re/TiO₂ and Pd/Re/C can chemoselectively hydrogenate CAs bearing phenyl, chloro, and thienyl groups. Thus, the reaction conditions, product selectivity, and substrate scope of heterogeneous catalysts have steadily improved. Although various oxidation states of different metal centers and various morphologies of an active metallic site consisting of multiple transition metal atoms in nanoparticle forms have been proposed, there remains a need for a new approach to precisely control the property of heterogeneous catalysts.

In contrast to the practical advantages of heterogeneous catalysts, molecular catalysts are more suitable for gaining a solid molecular insight into an angstrom-scale active site and reaction mechanism in order to improve the competence of CA hydrogenation. The electronic and steric nature of the catalyst can readily be tweaked by precisely modifying the metal–ligand frameworks. However, successful examples of homogeneous systems to ensure both high catalytic activity and selective production of alcohols are scarce. After the benchmark achievements of homogeneous hydrogenation of dimethyl oxalate to ethylene glycol under mild conditions^[16] and the first successful example of hydrogenation of unactivated esters^[17] by Elsevier and Teunissen in late 1990s, the Ru(acac)₃ and Triphos (1,1,1-tris(diphenylphosphinomethyl)ethane) systems constitute the relatively rapid development of

homogeneous hydrogenation of inactive carboxyl compounds, including esters and activated amides.^[18] Since then, Ru and tridentate phosphines have been used by Leitner and co-workers^[19] and Beller and co-workers^[20] as precatalysts for CA hydrogenation. However, these complexes are effective hydrogenation catalysts for esters rather than for CAs. In addition, high catalyst loading (~4 mol %) with a lengthy reaction time (~48 h) are required to achieve high yields of the corresponding alcohols. In 2015, Elsevier and Bruin reported CA hydrogenation using a Co(BF₄)₂·6H₂O/Triphos system.^[21] This is the first example of a non-precious-metal-based single-metal-site catalyst for homogenous CA hydrogenation, in which not only CA but also esters were hydrogenated under a high H₂ pressure ($P_{\text{H}_2} = 8 \text{ MPa}$) at a low reaction temperature (internal $T = 100 \text{ }^\circ\text{C}$ set with an oil bath of $140 \text{ }^\circ\text{C}$). When small and considerably electrophilic, and thus inherently more reactive, CAs such as trifluoroacetic acid were hydrogenated, turnover number (TON) of the catalyst reached 8000. However, hydrogenation of a vault of CAs with longer alkyl chains requires a high catalyst loading (~10 mol %). In 2016, Palkovits and co-workers developed a Ru catalyst with a triphos-derived nitrogen-centered tridentate phosphine ligand for the hydrogenation of bio-based CAs.^[22] They succeeded in the hydrogenation of several hydroxyl aliphatic CAs including levulinic acid and lactic acid to obtain their corresponding alcohols under harsh conditions ($P_{\text{H}_2} = 7 \text{ MPa}$, $160\text{--}170 \text{ }^\circ\text{C}$) with low precatalyst loading (0.5–2 mol %). However, only 5%–39% of the corresponding alcohols were obtained after the hydrogenation of simple aliphatic CAs such as acetic acid, butyric acid, and octanoic acid owing to substantial esterification as an undesirable side process.

The TON of catalysts obtained so far has been low. Although there are theoretical investigations on successful CA hydrogenation with [(Triphos)RuH]⁺ by Leitner/Klankermayer and co-workers^[19,23] and Co-triphos by Elsevier and co-workers,^[21] the reason why triphos is considered one of the best ligands for the hydrogenation of many CA derivatives albeit with minor changes to the reaction parameters remains unclear.

Meanwhile, our group demonstrated in 2015 that mono- or bidentate phosphorus ligands are better than tridentate triphos for accelerating CA hydrogenation. The coordination of “two” P atoms to a Ru center was adequate. In addition, we clarified the catalyst prototype that benefits from the rational design of a single-active-site Ru catalyst for the hydrogenation of CAs.^[24] The CA (RCO₂H)-derived cationic Ru carboxylate [(PP)Ru(OCOR)]⁺ (**1**, P denotes “one phosphorus coordination”) was provided as a catalyst prototype for CA self-induced CA hydrogenation. This system requires milder reaction conditions and exhibits a wider substrate scope. As an infinite number of the structural modification of bidentate diphosphine (PP) ligands by their short-step synthesis that diversify (PP)Ru catalysts would virtually be possible,

further optimization of the bidentate PP ligand for better catalyst performance is essential for further improvement of molecular hydrogenation catalysts.

Here, as our continues endeavor to develop hydrogenation of CAs using molecular catalysts,^[25] we report a rational molecular design of a Ru catalyst by precisely tweaking the structure of bidentate PP ligand, which enabled a substantial improvement of TON from the current ~30 to ~1500. A combination of different ligands and Ru sources (precatalysts) affected the induction of the catalyst from the precatalyst and the durability of the resulting molecular catalyst.

1.2. Results and discussion

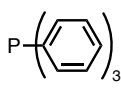
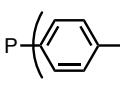
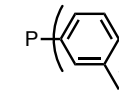
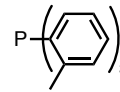
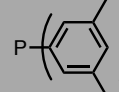
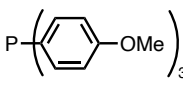
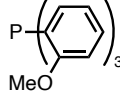
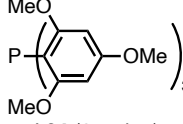
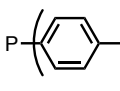
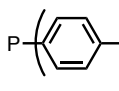
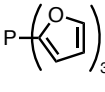
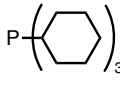
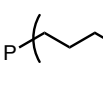
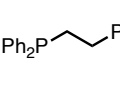
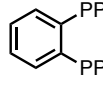
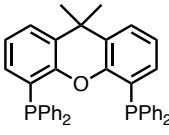
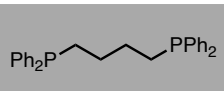
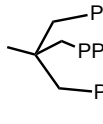
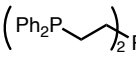
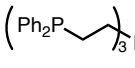
1.2.1. Design and synthesis of bidentate PP ligands.

In our primary screening of various mono- and multidentate phosphine (P_n ; $n = 1, 2, 3,$ or 4) ligands L18–L35 for the $(P_n)Ru$ complex-catalyzed hydrogenation of 3-phenylpropionic acid (CA-1) to 3-phenyl-1-propanol (AL-1), *cis*- $Ru^{II}Cl_2(dmsO)_4$ (2 mol %; *dmsO* = dimethylsulfoxide) was used as the Ru source in the presence of NaBPh₄ (10 mol %) under a H₂ pressure (P_{H_2}) of 8 MPa at a reaction temperature (T) of 160 °C for 24 h (Table 1). In this screening experiment, both $P(3,5\text{-xylyl})_3$ (AL-1, 49% yield) and 1,4-(diphenylphosphino)butane (DPPB; AL-1, 52% yield) were found to be among the most promising ligands (Table 1).^[24] A small amount of 3-phenylpropyl-3-phenylpropionate (ES-1) was coproduced (~14%) in both cases by in situ esterification between CA-1 and the resulting product AL-1. We have previously synthesized mono- or dinuclear Ru complexes bearing $P(3,5\text{-xylyl})_3$ or DPPB and demonstrated the effectiveness of these ligands for smooth CA hydrogenation.^[24] Later on, the Ru complex coordinated with two $P(4\text{-F}(C_6H_4))_3$ (L25) showed the best catalytic performance for the hydrogenation of N-protected α -amino acids at a low T (100–130 °C).^[30] Overall, a wide substrate scope and high AL selectivity were achieved under mild reaction conditions ($P_{H_2} = 1\text{--}6$ MPa, $T = 100\text{--}160$ °C). However, TON did not reach more than ~33 using 3 mol % (PP)Ru complexes in use of many different CAs.

Finally, we proposed a plausible catalytic cycle involving cationic $[(PP)Ru(OCOR)]^+$ species “catalyst prototype” **1** (Figure 2A). Starting CAs should act not only as integral carboxylates for the catalysts to cleave the H–H bond but also as protonated carboxylates that are simultaneously activated and reduced by the resulting $[Ru\text{--}H]^+$, which is generated in the first step (we call this CA self-induced CA hydrogenation). The importance of the Ru-carboxylate, (PP)Ru(OCOR) structure, was also supported theoretically by Li and co-workers, who coined the term “Saito catalyst”; they suggested that a possible mechanistic scenario for

the catalytic cycle involves neutral Ru dicarboxylate complexes, which is in contrast with the cationic Ru monocarboxylate that we proposed.^[31] In contrast, we investigated hydrogenation of CA-1 using kinetic studies and mass analyses to help explain the mechanistic aspects of the catalysis (Figure 2B). Electrospray ionization-mass spectrometry (ESI-MS) measurements after hydrogenation of CA-1 for 3 h using Ru-DPPB revealed a plausible resting state of catalyst $I_a(\text{DPPB})$ with seemingly deactivated species $I_b(\text{DPPB})$, where $I_b(\text{DPPB})$ is likely to be generated by the insertion of the *ortho*-C–H bond of the phenyl group to the Ru center. To improve the catalytic activity, further optimization of the phosphine ligands to suppress catalyst deactivation would be highly demanding. Based on our results encompassing the initial survey of phosphine ligands (Table 1),^[24] we designed and synthesized a series of new bidentate PP ligands comprising a partial structure of P(3,5-xylyl)₃ and/or DPPB (Figure 3). Various electron-donating or electron-withdrawing groups were introduced at the 3-, 4-, or 5-position of the phenyl ring (gray- and black-filled circles, L1–L6). Additionally, the conformational bias of the linear butyl chain connecting the two P atoms was precisely adjusted by fusing the cyclic ring in C2 and C3 of the butyl group (dashed circle, L7–L17). These ligands were synthesized in 3–7 steps and isolated, and all their synthetic procedures and spectroscopic data are summarized in the supporting information section.

Table 1 | Phosphine ligands screening (P(3,5-xylyl)₃, DPPB, and L18–L35) with *cis*-RuCl₂(dmsO)₄ (2 mol %).^[24]

$\text{Ph-CH}_2\text{-CH}_2\text{-COOH} \xrightarrow[\text{toluene (3 mL), 160 }^\circ\text{C, 24 h}]{\begin{array}{l} \textit{cis}\text{-RuCl}_2(\text{dmsO})_4 \text{ (2 mol \%)} \\ \text{NaBPh}_4 \text{ (10 mol \%)} \\ \text{ligand} \\ \text{H}_2 \text{ (8 MPa)} \end{array}} \text{Ph-CH}_2\text{-CH}_2\text{-OH} + \text{Ph-CH}_2\text{-CH}_2\text{-CO-O-CH}_2\text{-CH}_2\text{-Ph}$				
CA-1, 1 mmol	AL-1 ES-1			
ligand (AL-1 yield/ES-1 yield)				
 <p>L18 (6 mol %) (33%/14%, TON: 24)</p>	 <p>L19 (6 mol %) (27%/13%, TON: 20)</p>	 <p>L20 (6 mol %) (39%/15%, TON: 27)</p>	 <p>L21 (6 mol %) (0%/4%, TON: 2)</p>	 <p>P(3,5-xylyl)₃ (6 mol %) (49%/14%, TON: 32)</p>
 <p>L22 (6 mol %) (34%/20%, TON: 27)</p>	 <p>L23 (6 mol %) (5%/9%, TON: 7)</p>	 <p>L24 (6 mol %) (3%/6%, TON: 5)</p>	 <p>L25 (6 mol %) (5%/7%, TON: 6)</p>	 <p>L26 (6 mol %) (3%/7%, TON: 5)</p>
 <p>L27 (6 mol %) (4%/7%, TON: 6)</p>	 <p>L28 (6 mol %)^a (<1%/3%, TON: 2)</p>	 <p>L29 (6 mol %) (1%/7%, TON: 4)</p>	 <p>L30 (2 mol %) (4%/7%, TON: 6)</p>	 <p>L31 (2 mol %) (5%/7%, TON: 6)</p>
 <p>L32 (2 mol %) (20%/15%, TON: 18)</p>	 <p>DPPB (2 mol %) (52%/14%, TON: 33)</p>	 <p>L33 (2 mol %) (22%/13%, TON: 18)</p>	 <p>L34 (2 mol %) (48%/18%, TON: 33)</p>	 <p>L35 (2 mol %) (21%/13%, TON: 17)</p>

Unless otherwise specified, the reactions were carried out with *cis*-RuCl₂(dmsO)₄:NaBPh₄:CA-1 (mol %) = 2:10:100, P_{H_2} = 8 MPa, T = 160 °C, and t = 24 h ($[\text{Ru}]_0$ = 6.7 mM; $[\text{CA-1}]_0$ = 0.33 M; in toluene). ¹H NMR yields were determined based on the integral ratio of the signals of products and internal standard (mesitylene). TON is defined as mol (AL + ES)/mol Ru on the assumption that ES generates from a condensation of CA and the product AL.

^a1 M toluene solution of L28 was used.

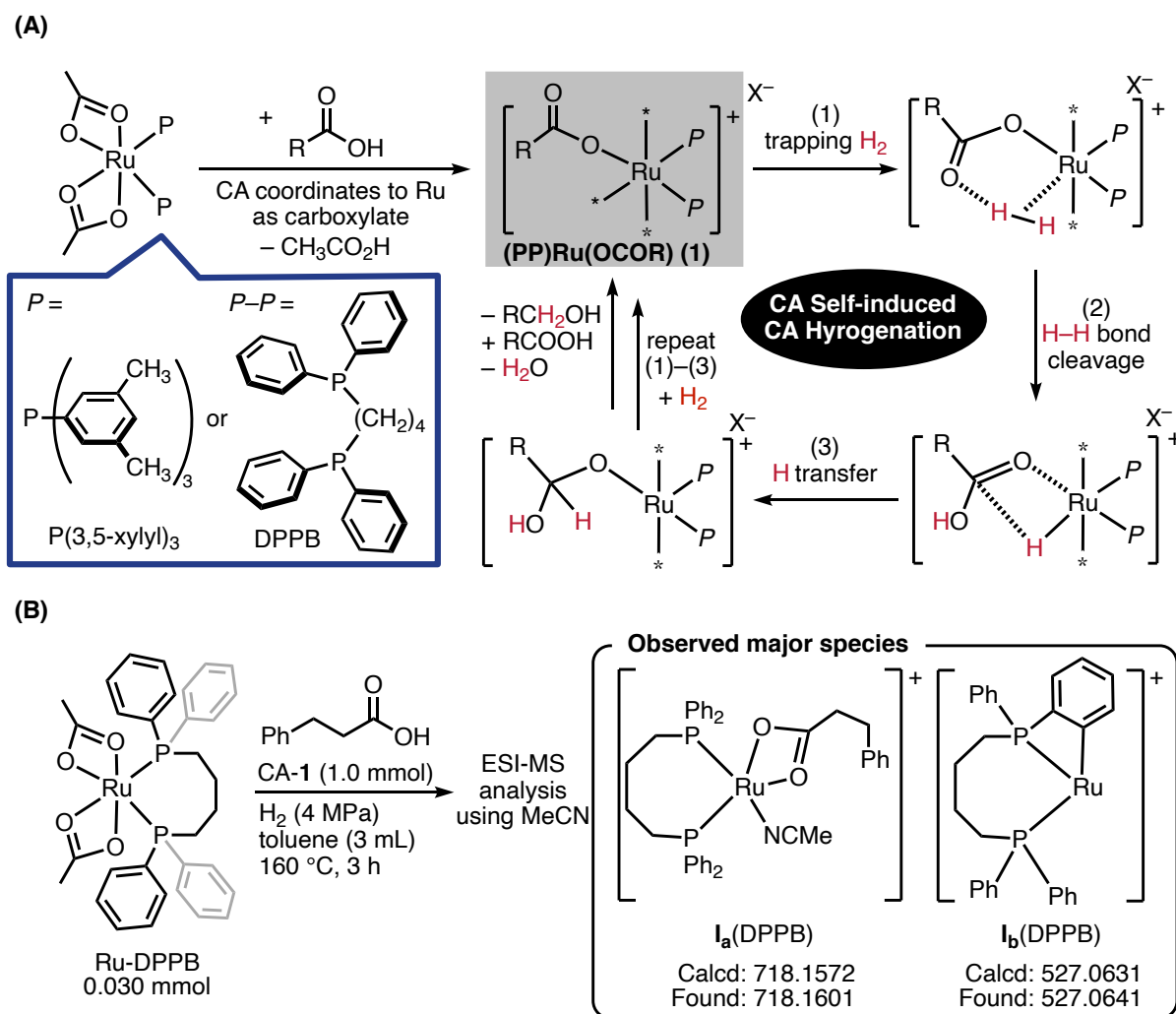


Figure 2 | Plausible mechanism of our proposed CA self-induced CA hydrogenation partially supported by ESI-MS analysis.^[24] (A) Overall mechanism of the catalytic cycle for the CA self-induced CA hydrogenation. X = RCO₂⁻ or MeCO₂⁻. (B) ESI-MS analysis of the reaction mixture using Ru-DPPB. I_a(DPPB) is corresponding to the catalyst prototype 1 and I_b(DPPB) is corresponding to catalytically inactive species.

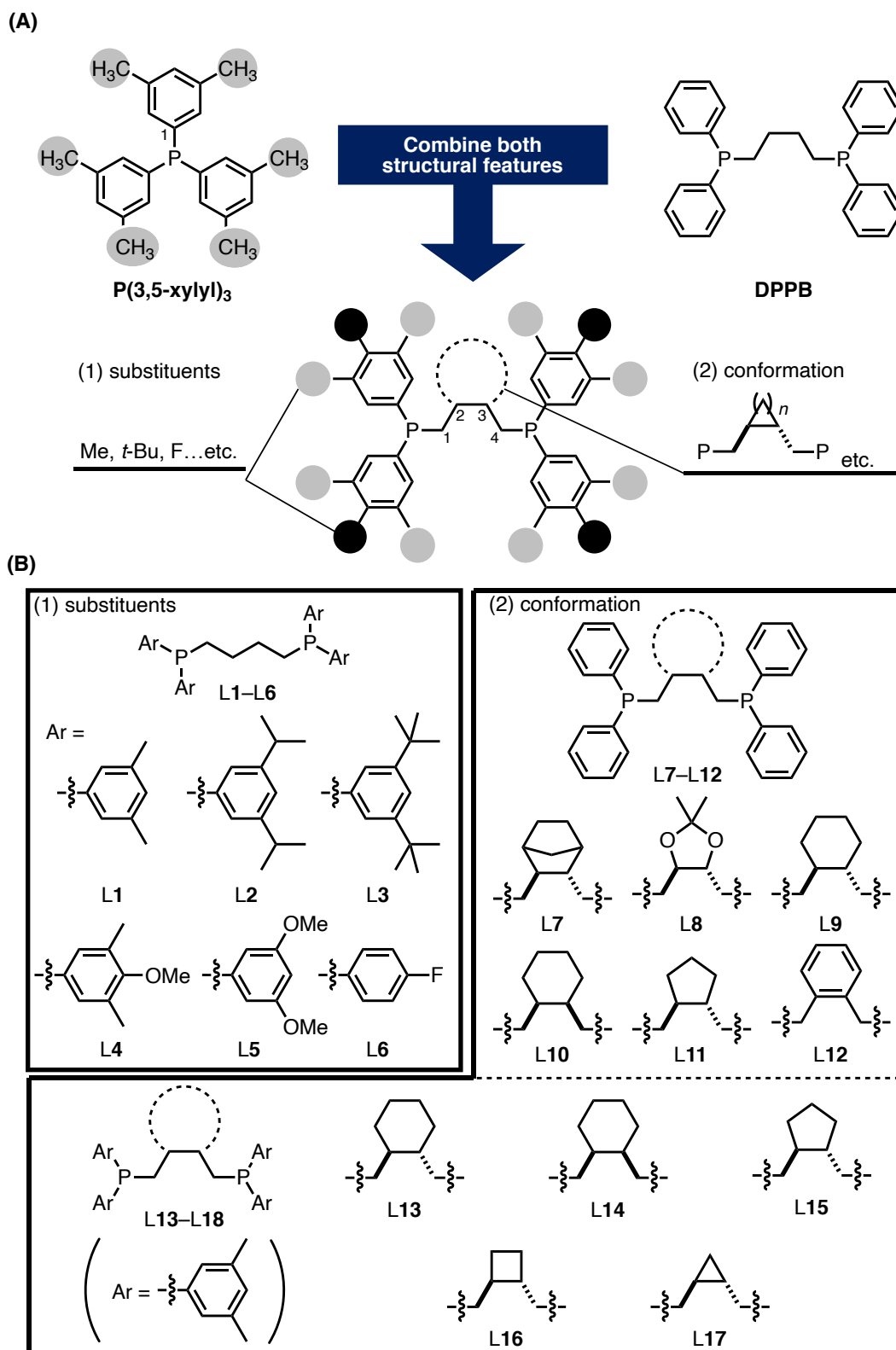


Figure 3 | A series of promising bidentate diphosphine ligands. (A) Basic concept for designing bidentate diphosphine ligands comprising structural features of both $P(3,5\text{-xylyl})_3$ and/or DPPB. (B) (1) Substituents introduced to the Ar group. Gray- and black-filled circles denote the substituents (L1–L6). (2) Controlling parameters of conformational changes in the butyl chain connecting between the two P atoms (L7–L17).

1.2.2. Screening of bidentate PP ligands using Ru(acac)₃ as Ru source.

Although we started using *cis*-Ru^{II}Cl₂(dms_o)₄ as the Ru source in our initial screening of ligands L18–L35, AL-1 was generally produced in low yields even with 2 mol % of the Ru source under harsh conditions. Hence, we switched the Ru source to Ru(acac)₃ (10,000 JPY/g, supplied from FUJIFILM Wako Pure Chemical Corporation, as of September 3, 2020), which is cheaper than others (*cis*-Ru^{II}Cl₂(dms_o)₄: 17,400 JPY/g; Ru(cod)(Me-allyl)₂: 47,500 JPY/g; Ru acetate: 65,200 JPY/g) and has frequently been used as a hydrogenation precatalyst by many researchers, including Elsevier, Leitner/Klankermayer, and Beller. Figure 4 shows the initial results of the effect of varying the steric bulk and electronic properties of the phosphine ligands L1–L6 on the hydrogenation of CA-1 with a low amount of Ru(acac)₃ (0.25 mol %, acac = acetylacetonato) at a reaction time of 18–36 h ($P_{\text{H}_2} = 4$ MPa, $T = 160$ °C). For comparison, the original P(3,5-xylyl)₃ and DPPB ligands were also investigated (Figure 4). Among the ligands tested, hydrogenation with L1 provided the highest TON of 216 (corresponding to the sum of the yields of AL-1 + ES-1) over a reaction time (t) of 36 h (Figure 4C), but with a significant amount of the corresponding ester ES-1 (AL-1/ES-1 = 0.8). The initial reaction rate observed when using P(3,5-xylyl)₃ was comparable to that obtained using L1, although the catalyst derived from P(3,5-xylyl)₃ was deactivated within 18 h (Figure 4A). A bidentate ligand DPPB provided a more sustainable catalytic activity, while the apparent hydrogenation rate was lower than that obtained using P(3,5-xylyl)₃ (Figure 4B). Overall, L1 provided a high reaction rate and exhibited sustainable catalytic activity by taking advantage of the combined features of P(3,5-xylyl)₃ and DPPB (Figure 4C). Ligands bearing more sterically bulky substituents exhibited apparent low catalytic activity owing to a lengthy induction period of the catalyst when used with Ru(acac)₃ (Figures 4D–4H). Although we recently reported a new Ru complex coordinated with two monodentate P(4-F(C₆H₄))₃ (L25), which is effective for the hydrogenation of N-protected α -amino acids at a low temperature (~110 °C),^[30] L6 was not suitable under the present harsh conditions (Figure 4H). Varying the substituents at the 2- and 3-positions of the phenyl ring (L2–L6) led to TONs lower than that obtained using L1. However, when using 0.25 mol % each of Ru(acac)₃ and a PP ligand, a side reaction, namely, in situ esterification, remained a significant obstacle.

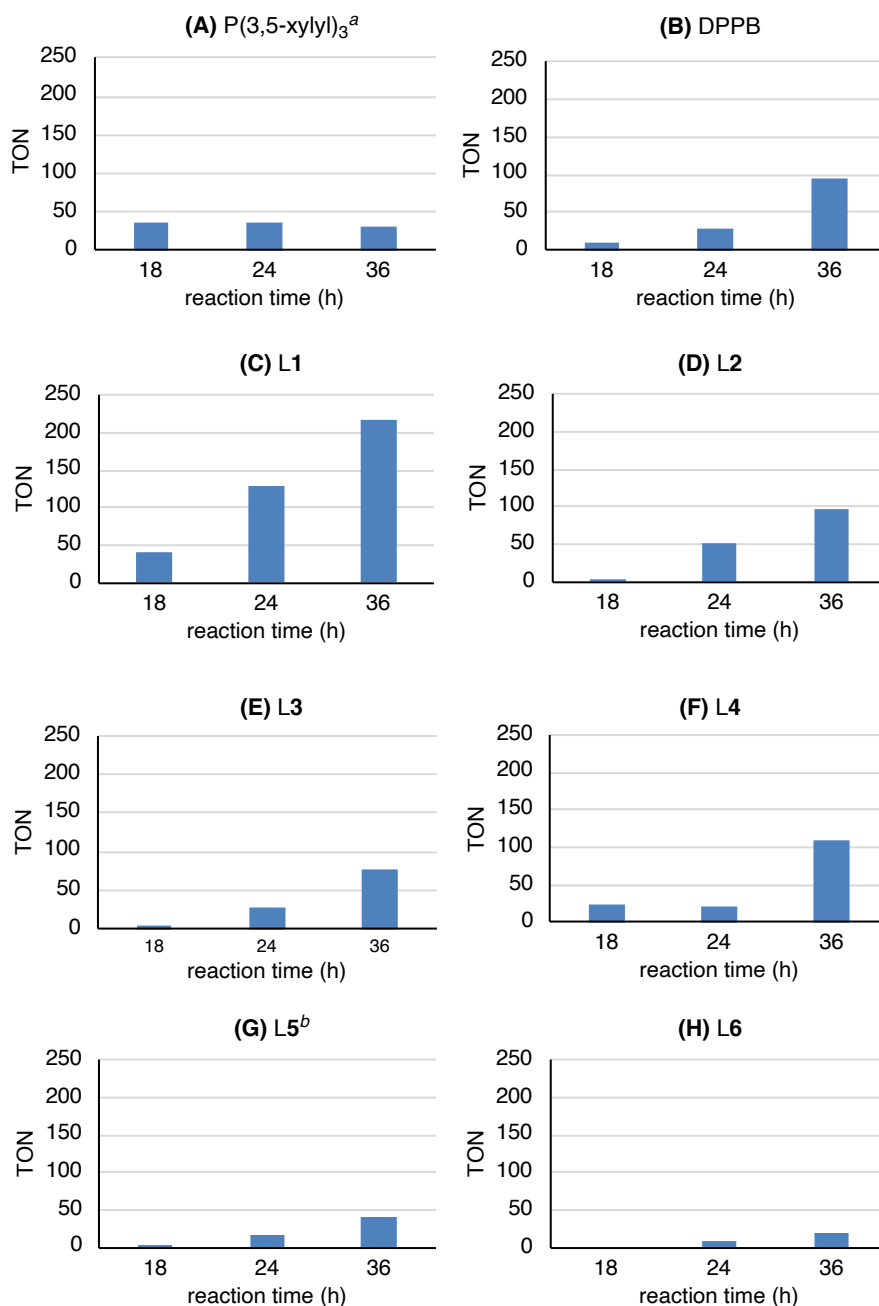
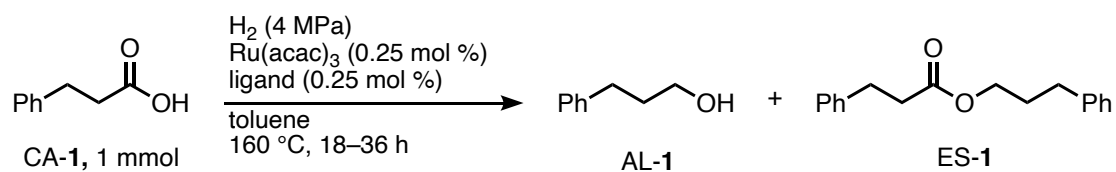


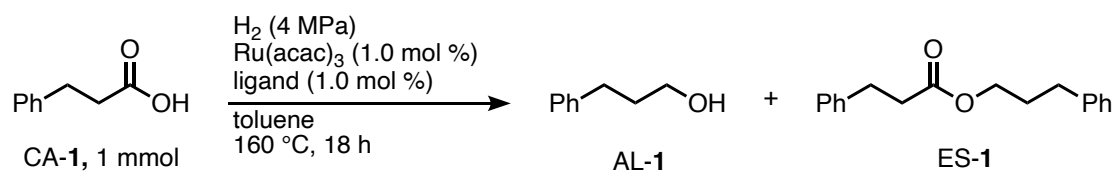
Figure 4 | Screening of different substituents of the Ar groups of ligands. Reactions were carried out over a period of 18–36 h ($[\text{CA-1}]_0 = 333 \text{ mM}$; $[\text{Ru}]_0 = 0.8 \text{ mM}$ in toluene). Yields were determined by ^1H NMR analysis using mesitylene as an internal standard. TON is defined as $(\text{mol AL} + \text{ES})/(\text{mol Ru})$ on the assumption that ES generates by condensation of CA with the AL. ^a0.5 mol % was added. ^bAverage of 2 runs.

entry	ligand	<i>t</i> (h)	Yield (%)		TON
			AL-1	ES-1	
1	P(xylyl) ₃ ^a	18	6	3	36
2		24	5	4	36
3		36	2	6	32
4	DPPB	18	2	<1	8
5		24	4	3	28
6		36	11	13	96
7	L1	18	6	4	40
8		24	21	11	128
9		36	24	30	216
10	L2	18	1	<1	4
11		24	7	6	52
12		36	3	21	96
13	L3	18	1	<1	4
14		24	3	4	28
15		36	11	8	76
16	L4	18	1	5	24
17		24	3	2	20
18		36	14	13	108
19	L5	18	1	<1	4
20 ^b		24	3	1	16
21 ^b		36	4	6	40
22	L6	18	0	0	0
23		24	<1	2	8
24		36	3	2	20

Figure 4 (continued). ^a0.5 mol % was added. ^bAverage of 2 runs.

A concentration of 0.25 mol % each of Ru(acac)₃ and a ligand seems too small to maintain competent hydrogenation catalysis and to deflect hydrogenation from esterification. The rate of esterification promoted by the acidic nature of the reaction system seems to surpass that of hydrogenation. It is also speculated that the catalyst is degraded in parallel with the induction of the catalyst from the precatalyst when the amount of Ru source was decreased to less than 1.0 mol %. Hence, we used 1.0 mol % bidentate phosphine ligand in which cyclic rings are fused into the butyl linkage to identify the most competent ligand (Table 2). The conformational bias of the butyl chain connecting the two P atoms had a significant influence on the catalytic activity (entries 1–4). However, Ph₂P-type ligands (L9, L11, and DPPB) showed lower TON than those of (*m*-xylyl)₂P variants (L13 and L15, and L1) with increasing ligand size (entries 5, 7, and 9 vs. 6, 8, and 10 respectively). The apparently slow hydrogenation catalyzed by a combination of Ru(acac)₃ and a set of (*m*-xylyl)₂P-incorporated ligands might be due to a long induction period of the catalyst before starting CA hydrogenation (the duration might also be accompanied by decay of the resulting catalyst). Different procedures to mix the PP ligand, Ru source, and CA-1 also significantly affected the apparent hydrogenation rate (entry 8). Ligands L9, L10, L11, and L15 are viscous oil and thus might be in direct contact and interact/coordinate effectively with Ru(acac)₃ before adding toluene. Indeed, these relatively hydrophobic oily ligands consistently gave better TONs, albeit with their steric bulkiness (entries 3, 5, 7, and 8). Further evaluation of extensive phosphine ligands (L36–L91) under similar conditions is summarized in Tables 3–6, which shows no further improvement in the overall reaction rate. Thus, first, optimization of the reaction conditions to shorten the induction period of the catalyst seemed to be of paramount importance.

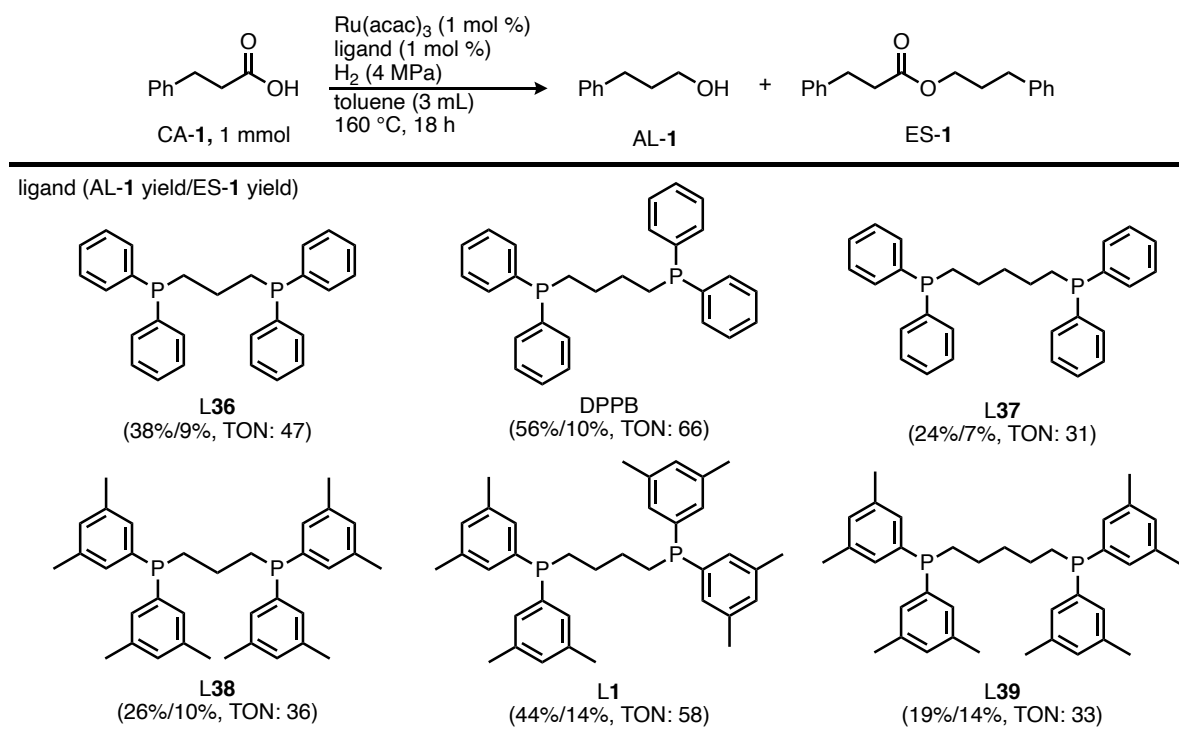
Table 2 | Hydrogenation using DPPB and ligands with cyclic rings fused in bidentate ligands (L7–L15 and L1).^a



entry	ligand	Yield (%)		TON
		AL-1	ES-1	
1	L7	30	8	38
2	L8	32	12	44
3	L10 ^b	55	8	63
4	L12	53	10	63
5	L9 ^b	41	29	70
6	L13	52	7	59
7	L11 ^b	74	13	87
8	L15 ^b	70±2 ^c (20 ^{c,d})	9±1 ^c (7 ^{c,d})	<82 (26 ^{c,d})
9	DPPB	56	10	66
10	L1	61	8	69

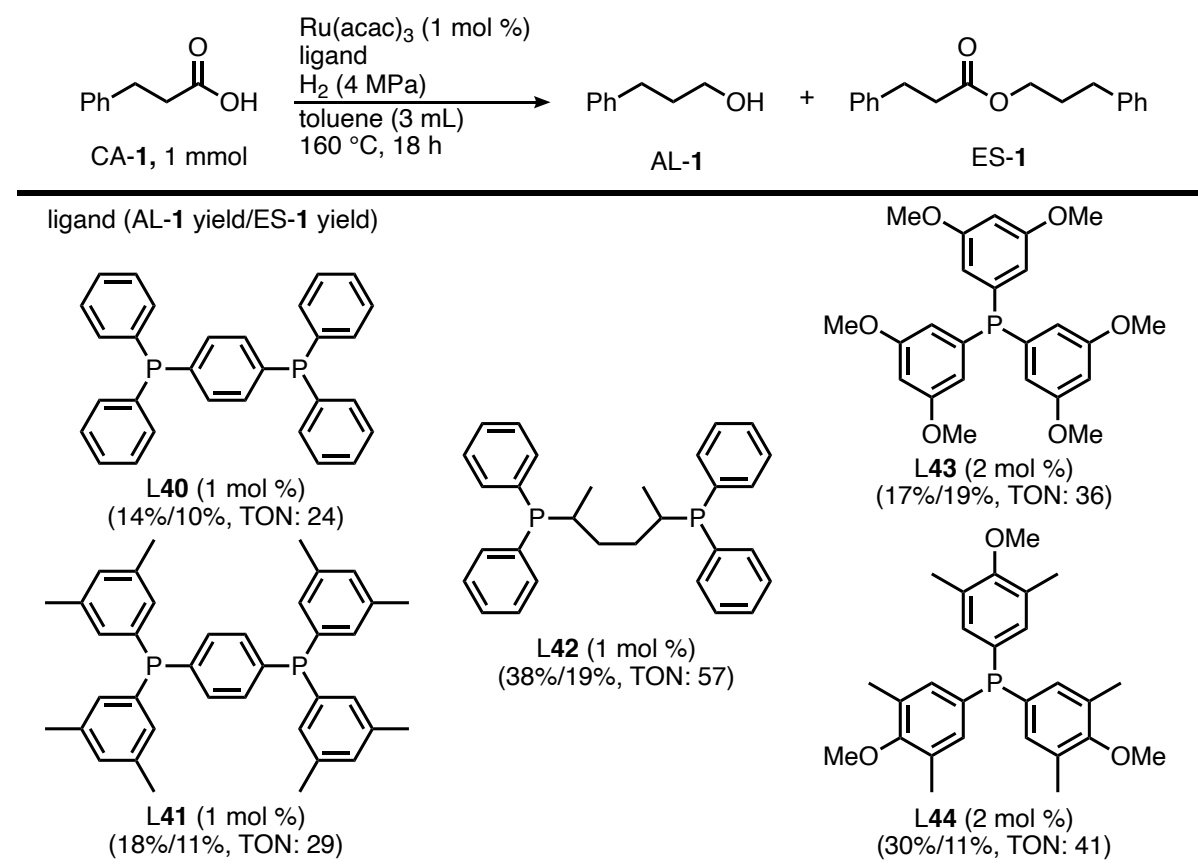
^aBefore starting hydrogenation in an autoclave, Ru(acac)₃, ligand, and CA-1 were added in a test tube, to which toluene was subsequently added. Reactions were carried out over a period of 18 h ([CA-1]₀ = 333 mM, [Ru]₀ = 3.3 mM in toluene). Yields were determined by ¹H NMR analysis using mesitylene as an internal standard. TON is defined as (AL + ES mol)/(Ru mol) on the assumption that ES generates by condensation of CA with the AL. ^bOily liquid. ^cAverage of 3 runs. ^dA stock solution of L15 in toluene was used.

Table 3 | Phosphine ligands screening bearing different carbon chain between the two phosphine atoms (DPPB, L1, and L36–L39) with Ru(acac)₃ in the hydrogenation of CA-1.



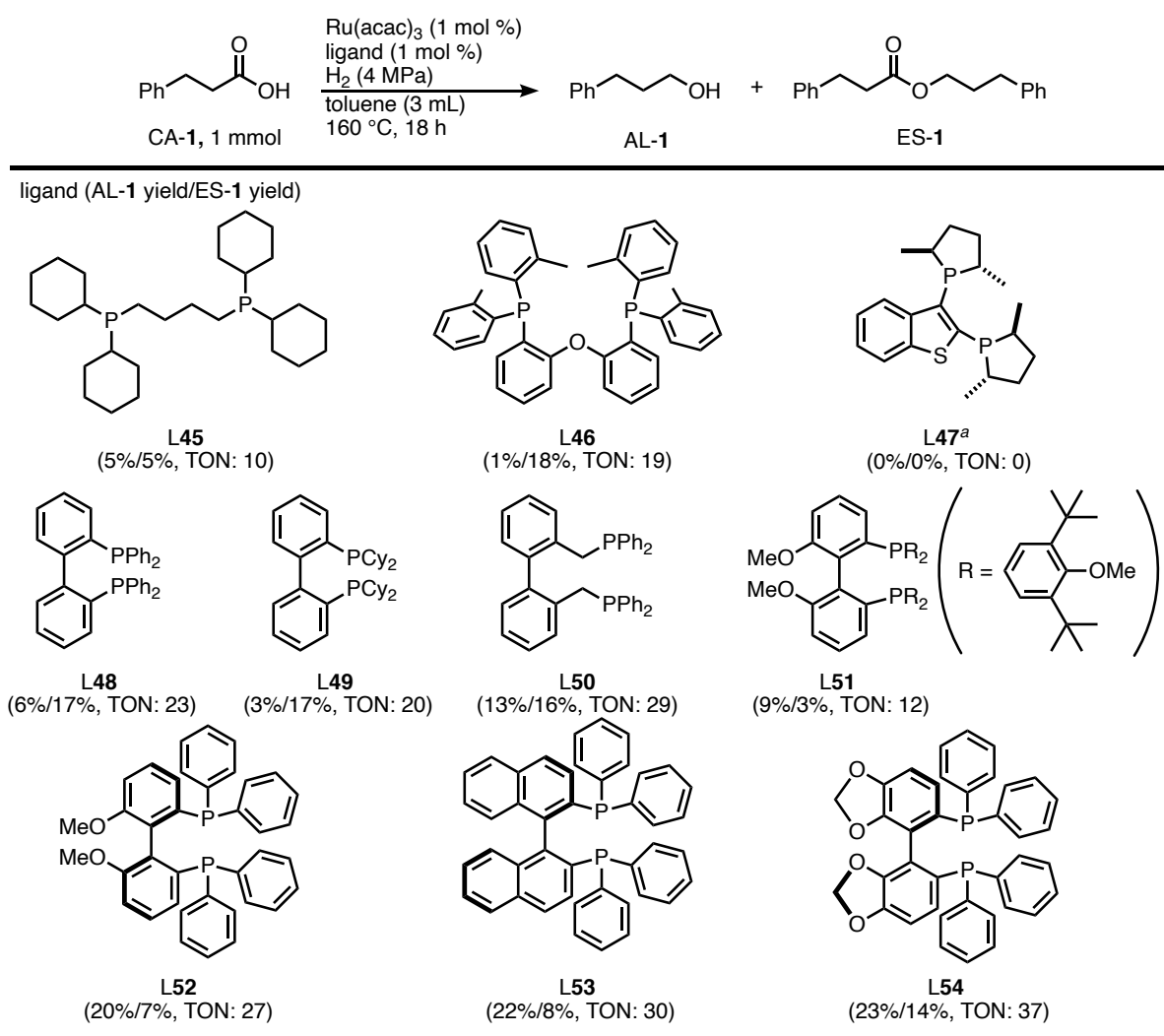
Unless otherwise specified, the reactions were carried out with Ru(acac)₃:ligand:CA-1 (mol %) = 1:1:100, P_{H_2} = 4 MPa, T = 160 °C, and t = 18 h ($[Ru]_0$ = 3.3 mM; $[CA-1]_0$ = 0.33 M; in toluene). ¹H NMR yields were determined based on the integral ratio of the signals of products and internal standard (mesitylene). TON is defined as mol (AL + ES)/mol Ru on the assumption that ES generates from a condensation of CA and the product AL.

Table 4 | Synthesized phosphine ligands screening (L40–L44) with a combination of Ru(acac)₃ in the hydrogenation of CA-1.



Unless otherwise specified, the reactions were carried out with Ru(acac)₃:ligand:CA-1 (mol %) = 1:1:100, P_{H_2} = 4 MPa, T = 160 °C, and t = 18 h ($[Ru]_0$ = 3.3 mM; $[CA-1]_0$ = 0.33 M; in toluene). ¹H NMR yields were determined based on the integral ratio of the signals of products and internal standard (mesitylene). TON is defined as mol (AL + ES)/mol Ru on the assumption that ES generates from a condensation of CA and the product AL.

Table 5 | Screening of commercially available diphosphine ligands (L45–L54) with a combination of Ru(acac)₃ in the hydrogenation of CA-1.



Unless otherwise specified, the reactions were carried out with Ru(acac)₃:ligand:CA-1 (mol %) = 1:1:100, P_{H_2} = 4 MPa, T = 160 °C, and t = 18 h ($[Ru]_0$ = 3.3 mM; $[CA-1]_0$ = 0.33 M; in toluene). ¹H NMR yields were determined based on the integral ratio of the signals of products and internal standard (mesitylene). ^aRh(cod)(BF₄) complex.

Table 6 | Phosphine ligands screening of the Solvias® Chiral Ligands Kit (L55–L91) with a combination of Ru(acac)₃ in the hydrogenation of CA-1.

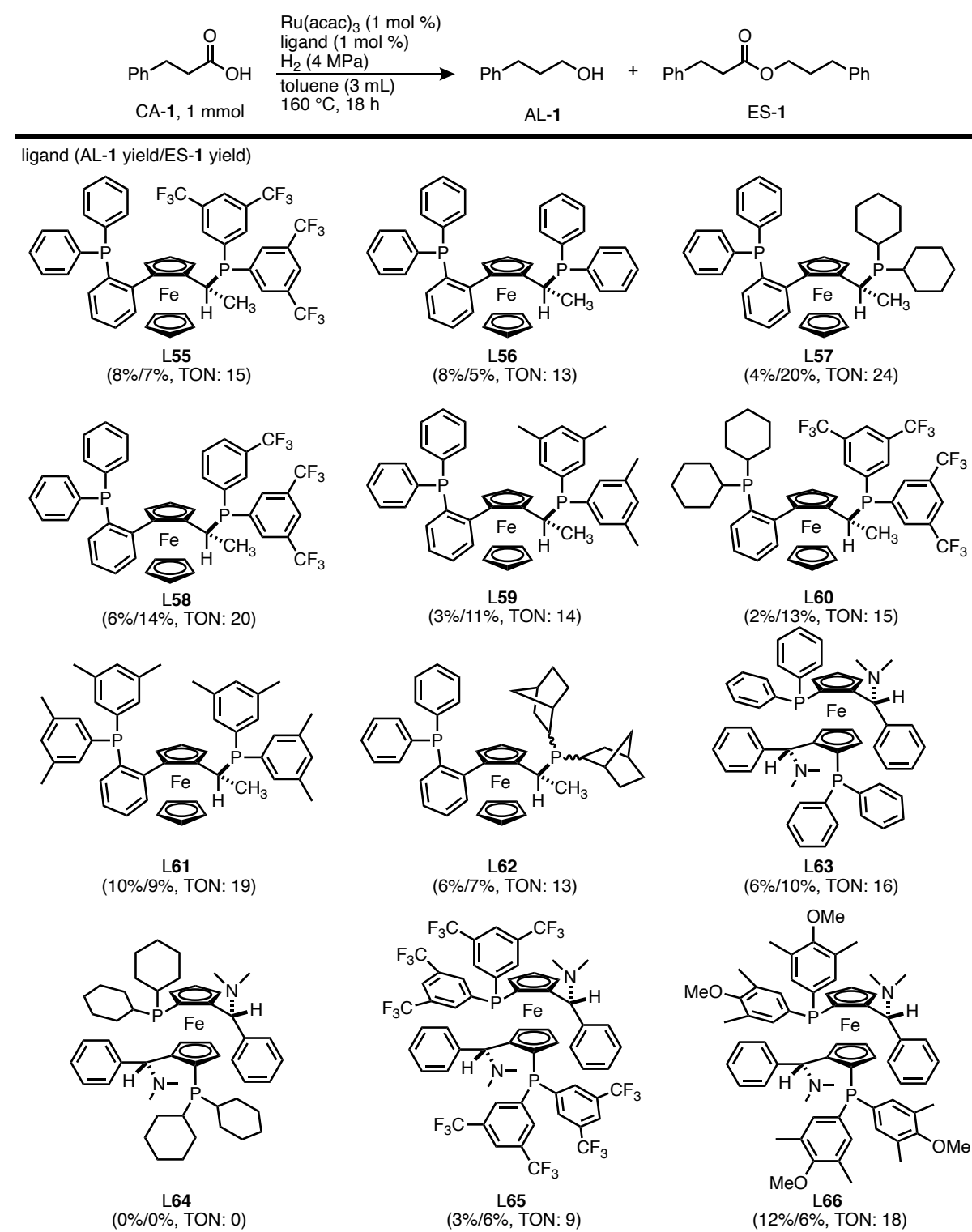
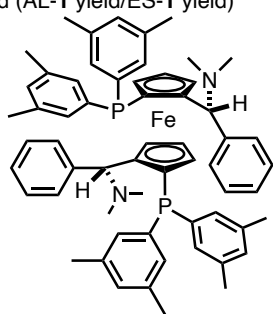
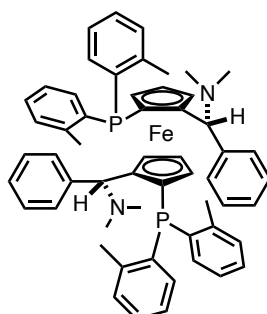


Table 6 (continued, L67–L78)

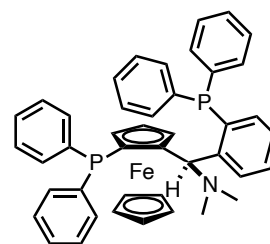
ligand (AL-1 yield/ES-1 yield)



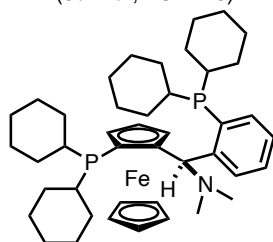
L67
(8%/7%, TON: 15)



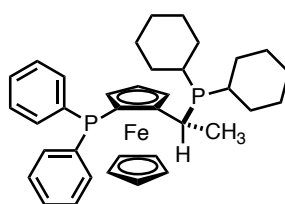
L68
(5%/4%, TON: 9)



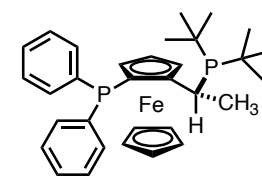
L69
(9%/5%, TON: 13)



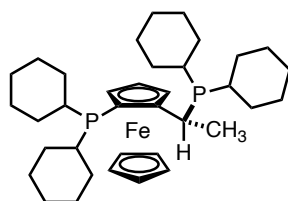
L70
(0%/1%, TON: 1)



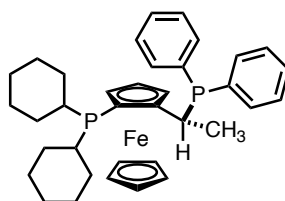
L71
(7%/4%, TON: 11)



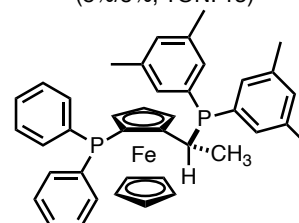
L72
(8%/5%, TON: 13)



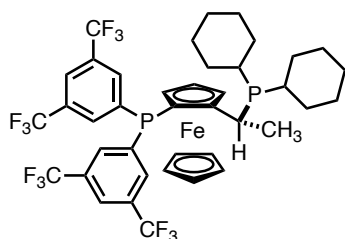
L73
(0%/4%, TON: 4)



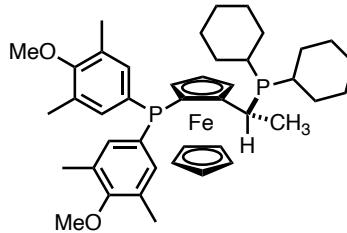
L74
(8%/6%, TON: 14)



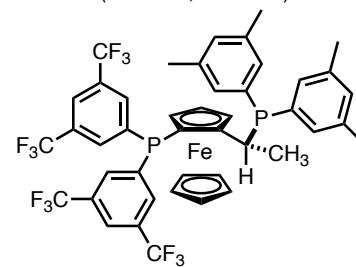
L75
(22%/8%, TON: 30)



L76
(12%/5%, TON: 17)

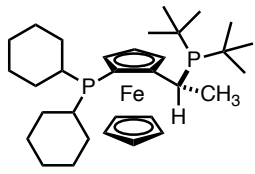
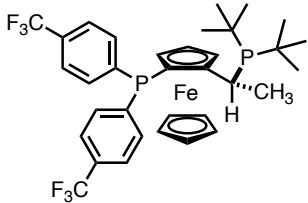
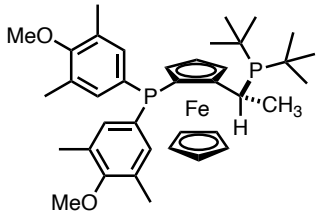
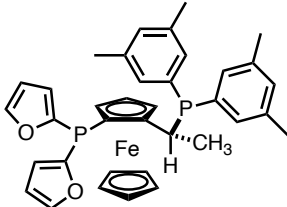
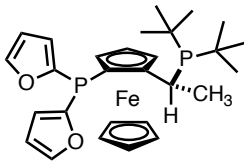
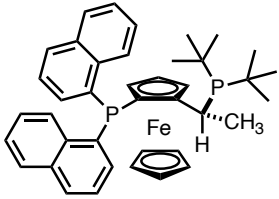
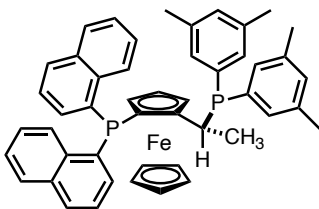
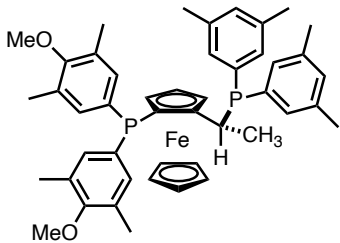
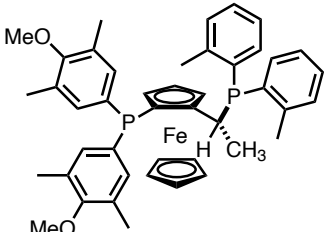
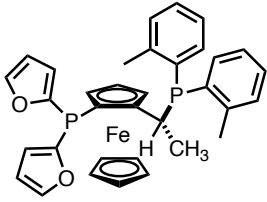
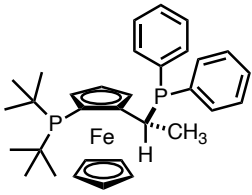
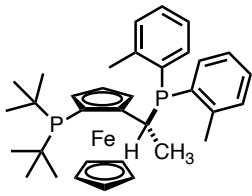
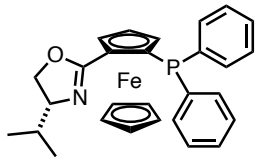


L77
(4%/7%, TON: 11)



L78
(9%/20%, TON: 29)

Table 6 (continued, L79–L91).

ligand (AL-1 yield/ES-1 yield)			
			
L79 (5%/3%, TON: 8)	L80 (12%/13%, TON: 23)	L81 (9%/10%, TON: 19)	
			
L82 (11%/22%, TON: 33)	L83 (12%/11%, TON: 23)	L84 (5%/4%, TON: 9)	
			
L85 (3%/2%, TON: 5)	L86 (22%/20%, TON: 42)	L87 (10%/6%, TON: 16)	
			
L88 (6%/24%, TON: 30)	L89 (0%/3%, TON: 3)	L90 (0%/2%, TON: 2)	L91 (Ru(PPh ₂) ₃ Cl ₂ complex) ^a (0%/0%, TON: 0)

Unless otherwise specified, the reactions were carried out with Ru(acac)₃:ligand:CA-1 (mol %) = 1:1:100, P_{H2} = 4 MPa, T = 160 °C, and t = 18 h ([Ru]₀ = 3.3 mM; [CA-1]₀ = 0.33 M; in toluene). ¹H NMR yields were determined based on the integral ratio of the signals of products and internal standard (mesitylene). ^aRu(acac)₃ was not added.

1.2.3. Optimization to shorten the induction period of the catalyst.

Our previous results suggested that an initial Ru^{III} species subjected to hydrogenation of N-protected phenylalanine was reduced by H₂ to (PP)Ru^{II} carboxylate species, [(PP)Ru^{II}(OCOR)]⁺ during a lengthy preactivation step at a low temperature (110–130 °C).^[30] To shorten the preactivation step at a high temperature, three different approaches were examined: (1) use of alternative Ru precatalysts such as Ru^{II}(cod)(Me-allyl)₂ and Ru^{III} acetate with PP ligands (Figure 5A); (2) pretreatment of a Ru^{III} starting complex with PP ligands under H₂ before starting CA hydrogenation (Figure 5B); and (3) synthesis, isolation, and use of PP ligand-coordinated Ru diacetate complexes ((PP)Ru(OAc)₂) as precatalysts for CA hydrogenation (Figure 5C).

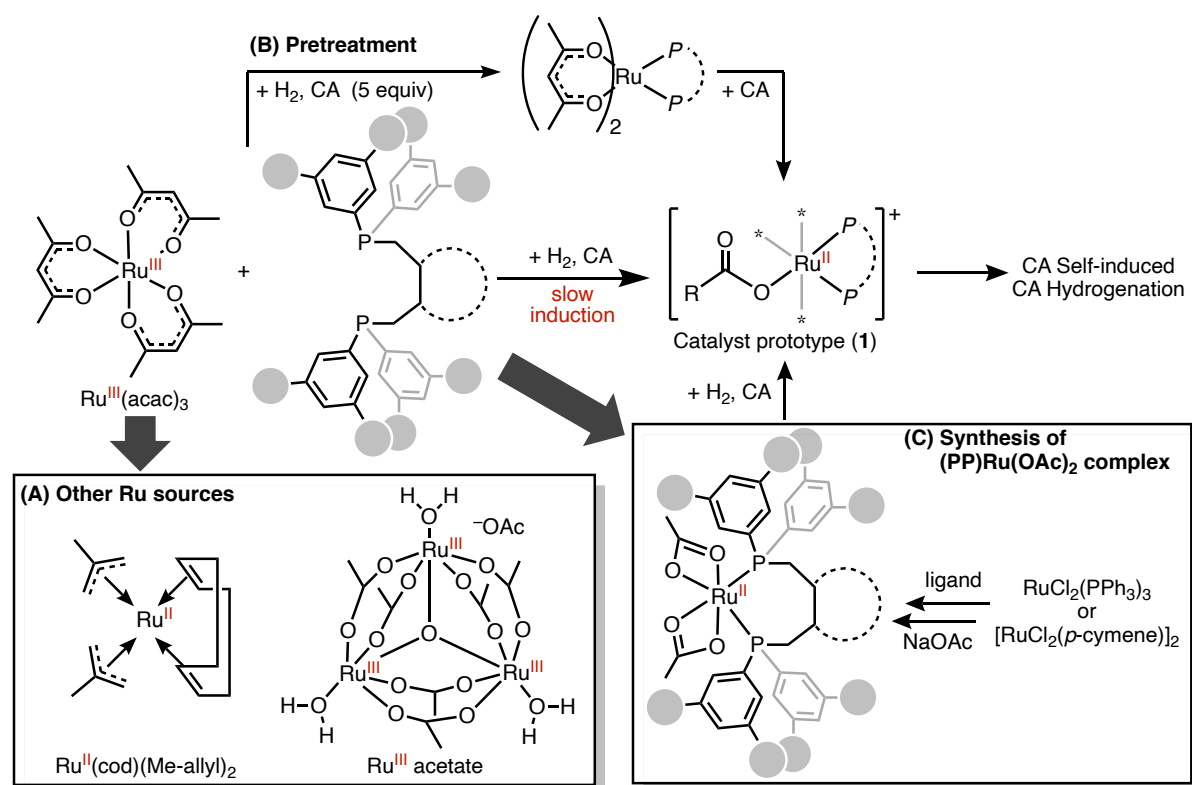
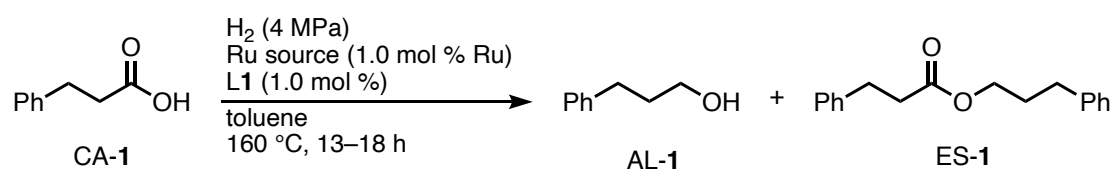


Figure 5 | Three approaches to induce catalytically active species. (A) Other Ru sources examined. The real structure of Ru^{III} acetate remains unknown. (B) Pretreatment of Ru^{III}(acac)₃ with PP ligands in the presence of CA under a high pressure H₂. (C) Synthesis of the corresponding Ru-diacetate complex bearing several optimized ligands.

1.2.4. Evaluation of Ru precatalysts.

One of the cheapest Ru sources, Ru^{III}(acac)₃, has thus far been chosen as a pivotal Ru precursor. However, a long period for inducing active Ru^{II} carboxylate species is an obstacle. By replacing Ru^{III}(acac)₃ with Ru^{II}(cod)(Me-allyl)₂ or Ru^{III} acetate, the apparent hydrogenation rate observed was higher than that obtained using Ru^{III}(acac)₃ (Table 7). This result suggests that the valency of Ru^{II} and the acetate coordination to Ru, inherent to each Ru precatalyst, would facilitate the rapid induction of (PP)Ru^{II}(OCOR) species prior to the initiation of CA self-induced CA hydrogenation. In contrast, a smooth uptake of H₂ was achieved when using [Ru^{II}Cl₂(*p*-cymene)]₂, resulting in considerable hydrogenation of toluene to methylcyclohexane upon generation of Ru⁰ species (entry 5), which was clearly observed as fine black precipitate after hydrogenation.

Table 7 | Comparison among Ru sources used with L1.^a

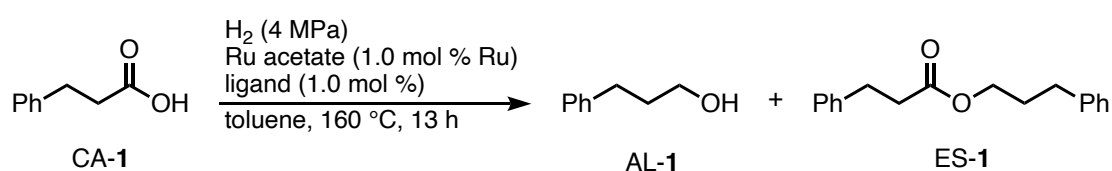


entry	Ru source	<i>t</i> (h)	Yield (%)		TON
			AL-1	ES-1	
1 ^b	Ru ^{III} (acac) ₃	18	61	8	69
2	Ru ^{II} (cod)(Me-allyl) ₂	18	86	7	93
3	Ru ^{III} (acetate) ^c	13	62	8	70
4 ^b		18	58	13	71
5 ^{d,e}	[Ru ^{II} Cl ₂ (<i>p</i> -cymene)] ₂	18	0	0	0

^aReactions were carried out over a period of 13–18 h ([CA-1]₀ = 333 mM, [Ru]₀ = 3.3 mM in toluene). Yields were determined by ¹H NMR analysis using mesitylene as an internal standard. TON is defined as (AL + ES mol)/(Ru mol) on the assumption that ES generates by condensation of CA with the AL. ^bAverage of two runs. ^cRu acetate contains 38.75 wt% of Ru. ^dNaOAc (5 mol %) was added. ^eDearomatic hydrogenation of toluene to methylcyclohexane significantly occurred. After the reaction, P_{H₂} was ~0.1 MPa.

Further survey of the combination of Ru^{III} acetate (1 mol % each) with L1–L3 or L5, which gave superior results in the initial screening (Figure 4), revealed that L1 was again the best ligand (entry 2, Table 8). However, decreasing the catalyst loading of Ru^{III} acetate to 0.25 mol % resulted in a very low conversion of CA within 36 h (Table 9), in contrast to that observed using Ru(acac)₃ (0.25 mol %), which provided a higher TON under similar conditions (Figure 4). The reason for this anomalous behavior at a low catalyst loading of Ru^{III} acetate is unclear.

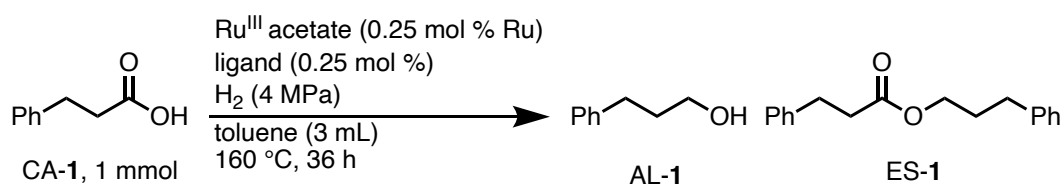
Table 8 | Effects of 3,5-disubstituted Ar group of phosphine ligands on hydrogenation with Ru acetate (1.0 mol %).^a



entry	ligand	Yield (%)		TON
		AL-1	ES-1	
1	DPPB	26	5	31
2	L1	62	8	70
3	L2	34	6	40
4	L3	24	5	29
5	L5	42	6	48

^aReactions were carried out over a period of 13 h ([CA-1]₀ = 333 mM, [Ru]₀ = 3.3 mM in toluene). Yields were determined by ¹H NMR analysis using mesitylene as an internal standard. TON is defined as (AL + ES mol)/(Ru mol) on the assumption that ES generates by condensation of CA with the AL.

Table 9 | Hydrogenation of CA-1 using 0.25 mol % Ru^{III} acetate.



entry	ligand	Yield (%)		TON
		AL-1	ES-1	
1	DPPB	1	2	12
2	L1	2	3	20
3	L2	2	2	16
4	L3	2	2	16
5	L4	2	1	12
6	L5	1	1	8

Unless otherwise specified, the reactions were carried out with Ru^{III} acetate:ligand:CA-1 (mol %) = 0.25:0.25:100, P_{H_2} = 4 MPa, T = 160 °C, and t = 36 h ($[\text{Ru}]_0$ = 0.83 mM; $[\text{CA-1}]_0$ = 0.33 M; in toluene). ¹H NMR yields were determined based on the integral ratio of the signals of products and internal standard (mesitylene). Ru^{III} acetate contains 38.75 wt% of Ru. TON is defined as mol (AL + ES)/mol Ru on the assumption that ES generates from a condensation of CA and the product AL.

1.2.5. Pretreatment of Ru^{III}(acac)₃ with PP ligands under a high H₂ pressure.

We have encountered in some cases with irreproducible results in obtained yields of AL-1 after the hydrogenation of CA-1 with Ru(acac)₃ and a PP ligand (1.0 mol % each). By careful assessment of the iterative control reactions before hydrogenation starts, the yields of AL-1 gradually increased, as the time for leaving a reaction vessel of a toluene mixture of CA-1, Ru(acac)₃, and L1 to stand statically was increased by 60 min at 25 °C “without stirring” (Table 10, Procedure A, entries 1–3). In contrast, “stirring” a similar toluene solution for 60 min at room temperature led to an increase in the amount of ES-1 (Table 10, Procedure B, entry 4). These results imply that a proper adjustment of the starting concentration of CA (the amount of CA-1 partially dissolved) for the preparation of catalytic species before starting hydrogenation was critical for both high TON and alcohol selectivity.

Table 10 | Hydrogenation following two different Procedures A and B.^a

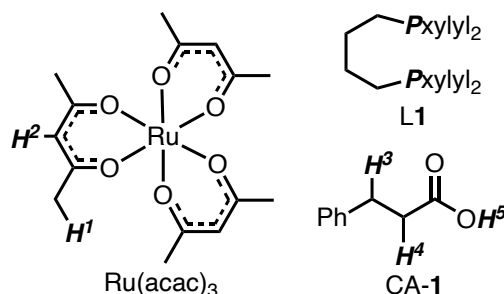
entry	Procedure	Yield (%)		TON
		AL-1	ES-1	
1 ^c	A (1–5 min)	61	8	69
2	A (20 min)	73	7	80
3 ^c	A (60 min)	82	8	90
4 ^c	B (60 min)	59	19	78

^aReactions were carried out over a period of 18 h ([CA-1]₀ = 333 mM, [Ru]₀ = 3.3 mM, [L1]₀ = 3.3 mM in toluene). Yields were determined by ¹H NMR analysis using mesitylene as an internal standard. TON is defined as (AL + ES mol)/(Ru mol) on the assumption that ES generates by condensation of CA with the AL. ^bH₂ (4 MPa), room temperature; 160 °C, 18 h.

^cAverage of 2 runs.

To gain further insight into the hidden effects of Procedure **A** on inducing catalysts, ^1H and $^{31}\text{P}\{^1\text{H}\}$ NMR studies on a toluene- d_8 mixture of CA-1, $\text{Ru}(\text{acac})_3$, and L1 in different amounts were carried out (Table 11). The addition of $\text{Ru}(\text{acac})_3$ and CA-1 to a toluene- d_8 solution of L1 resulted in no change in the $^{31}\text{P}\{^1\text{H}\}$ NMR spectrum of L1 (entries 2, 4, and 6), which suggests that L1 interacts with neither one of them. The ^1H NMR spectrum of a mixture of $\text{Ru}(\text{acac})_3$ and CA-1 led to a downfield shift of typical signals (H^3 and H^4) of CA-1, suggesting slight interactions between CA-1 and $\text{Ru}(\text{acac})_3$ upon their simple mixing at 25 °C (entry 1 vs. 3 vs. 5).

Table 11 | NMR study on chemical shift changes with various combinations of CA-1, $\text{Ru}(\text{acac})_3$, and L1.^a

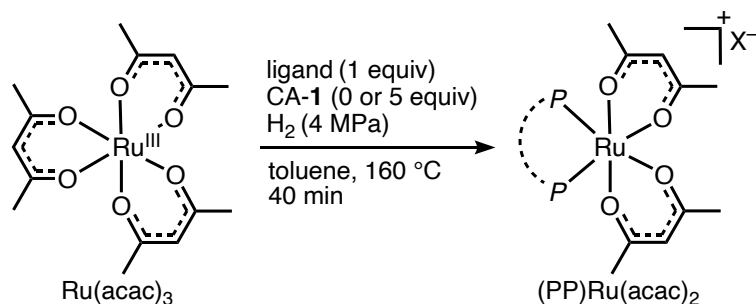


entry	Sample	Chemical shift (ppm)					
		Ru(acac) ₃		L1	CA-1		
		<i>H</i> ¹	<i>H</i> ²	<i>P</i>	<i>H</i> ³	<i>H</i> ⁴	<i>H</i> ⁵
1	Ru(acac) ₃	-5.3	-27.6	-	-	-	-
2	L1	-	-	-16.2	-	-	-
3	CA-1	-	-	-	2.29	2.67	11.8
4	Ru(acac) ₃ + L1 (1:1)	-5.3	-27.6	-16.2	-	-	-
5	Ru(acac) ₃ + CA-1 (1:5)	-5.3	-27.6	-	2.34	2.70	11.7
6	Ru(acac) ₃ + L1 + CA-1 (1:1:1)	-5.3	-27.6	-16.2	2.34	2.72	ND ^b

^aNMR conditions: ^1H NMR (500 MHz), $^{31}\text{P}\{^1\text{H}\}$ NMR (179 MHz, 50 scans), toluene- d_8 (0.5 mL) under Ar atmosphere. Multiplicity of each peak is omitted. ^bNot detected.

Transformation of $\text{Ru}^{\text{III}}(\text{acac})_3$ to $(\text{PP})\text{Ru}(\text{acac})_2$ species proceeded in the presence of 2 equiv of P' at P_{H_2} (0.1–5.0 MPa) (P' denotes a monodentate trialkyl phosphine), where reduction of the Ru^{III} to Ru^{II} was not clearly proved.^[32] Similarly, $^{31}\text{P}\{^1\text{H}\}$ NMR studies were carried out under various conditions to detect products obtained upon the reaction of $\text{Ru}^{\text{III}}(\text{acac})_3$ with DPPB, **L1**, or **L15** instead of P' (Table 12). However, the desired PP-coordinated $\text{Ru}(\text{acac})_2$ structures were barely formed under otherwise identical conditions previously used^[32] (entries 1, 3, and 5). By contrast, the addition of a small amount of **CA-1** (5 equiv relative to Ru) increased the relative intensity of the desirable PP-coordinated $\text{Ru}(\text{acac})_2$ species, but resulted in negligible coordination of **L15** to the Ru center in its diluted solution (entries 2 and 4 vs. 6). In marked contrast, the reaction of **L15** (a neat oil) with $\text{Ru}(\text{acac})_3$ without solvent toluene furnished effective complexation and even reduction of Ru^{III} to Ru^{II} (entry 7), giving **I_a(L15)**, **I_c(L15)**, and **I_d(L15)** within 40 min. In summary, a small amount of CA (RCO_2H) would facilitate the coordination of PP with Ru^{III} species in the presence of H_2 , followed by either rapid or gradual generation of $(\text{PP})\text{Ru}^{\text{II}}(\text{OCOR})$ species as catalyst prototype **1**, depending on steric bulkiness and the concentration of PP.

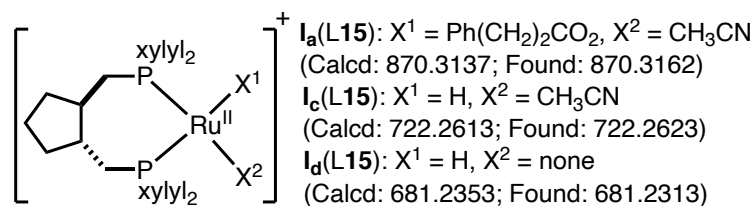
Table 12 | $^{31}\text{P}\{^1\text{H}\}$ NMR study on the pretreatment of $\text{Ru}(\text{acac})_3$ with DPPB, L1, or L15 under various conditions.^a



entry	ligand	CA-1 (5 equiv)	$^{31}\text{P}\{^1\text{H}\}$ NMR (relative intensity) ^{b,c}	
			Free ligand -19 to -15 ppm	$(\text{PP})\text{Ru}(\text{acac})_2$ 49–54 ppm
1	DPPB	–	99%	1%
2		+	89%	4%
3	L1	–	92%	3%
4		+	60%	20%
5	L15	–	96%	1%
6		+	98%	2%
7 ^{d,e}		+	trace	trace

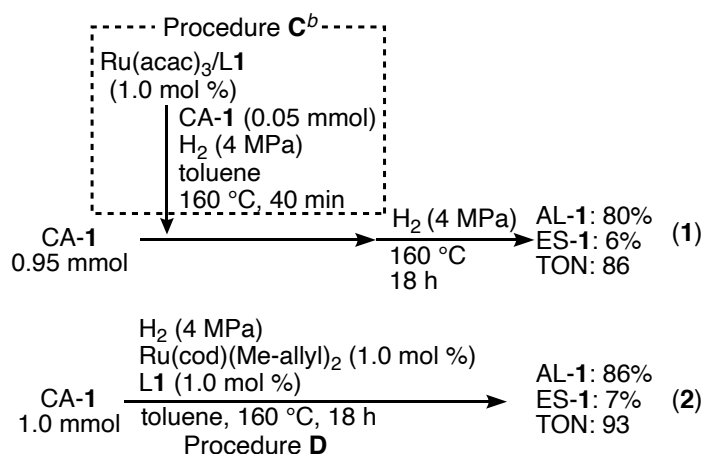
^aReactions were carried out over a period of 40 min ($[\text{CA-1}]_0 = 0\text{--}50$ mM, $[\text{ligand}]_0 = 10$ mM, $[\text{Ru}]_0 = 10$ mM in toluene). NMR conditions: $^{31}\text{P}\{^1\text{H}\}$ NMR (243 MHz), CDCl_3 , under Ar.

^bThe relative intensity of each peak was calculated based on the sum of all peak integrals (100%). ^cSome oxidized or unidentified species were detected not more than ~15% relative intensity. ^dNo toluene was used. ^e Ru^{II} species (**I_a**(L15), **I_c**(L15), and **I_d**(L15)) were detected using CH_3CN by ESI-MS analysis.



As most PP ligands we tested are solid, the following standard conditions were adopted for further studies on the induction period of the catalyst. The complexation of Ru(acac)₃ with L1 ([Ru]₀ = [L1] = 3.3 mM in toluene) was performed in the presence of 5 equiv of CA-1 under P_{H₂} = 4 MPa for 40 min (Scheme 1, Eq. 1, Procedure C), and subsequent hydrogenation of CA-1 started in an autoclave. As a result, this protocol for generating Ru catalyst from Ru(acac)₃ gave fairly good TON and product selectivity in favor of AL-1 over ES-1, comparable to that obtained using a more expensive Ru^{II}(cod)(Me-allyl)₂, which did not mandate such a separate step for precatalyst activation (Eq. 1, Procedure C vs. Eq. 2, Procedure D).

Scheme 1 | Hydrogenation with L1 using Ru(acac)₃ or Ru(cod)(Me-allyl)₂ following two different Procedures C (Eq. 1) and D (Eq. 2).^a



^aReactions were carried out over a period of 18 h with CA-1 (1.0 mmol, 333 mM), Ru(acac)₃ or Ru(cod)(Me-allyl)₂ (1.0 mol %, 3.3 mM), and L1 (1.0 mol %, 3.3 mM) in toluene. Yields were determined by ¹H NMR analysis using mesitylene as an internal standard. TON is defined as (AL + ES mol)/(Ru mol) on the assumption that ES generates by condensation of CA with the AL. ^b[Ru]₀ = 10 mM, [L1]₀ = 10 mM, [CA-1]₀ = 50 mM in toluene.

Next, synthesized ligands (**L1** and **L13–L17**), in which different cyclic rings are fused in the butyl chain connecting the two P atoms, were tested using Procedure C, which involves a pretreatment of a less amount of Ru(acac)₃ (0.5 mol %) with PP ligands using a 2.0 mmol of CA-1 (Table 13). The results showed that **L1** and **L13**, in addition to DPPB, were the most promising (entries 2 and 3). In all entries, except entry 7, the formation of ES-1 was fairly prevented within the reaction time of 18 h, even with a 0.5 mol % Ru source (AL-1/ES-1 = 3–5). The density functional theory (DFT) calculations (B3LYP/LANL2DZ) of the geometries of a series of (PP)Ru^{II}(OAc)₂ complexes, which are potential precatalysts, were also carried out to correlate the catalytic activity with the bite angles (P–Ru–P) and ligand dihedral angles (PC–C–CP). The correlation roughly indicated that an increase in the bite angles or the dihedral angles led to a decrease in the apparent TONs at a reaction time of 18 h with $P_{H_2} = 4$ MPa. It is speculated that the bidentate PP ligand of wider angles when coordinated to Ru showed a smaller coordination rate when complying with Procedure C, in which a diluted solution of PP and Ru(acac)₃ was used.

Table 13 | Ligand assessment by Procedure C.^a

Procedure C^b
 Ru(acac)₃/ligand (0.5 mol %)
 CA-1 (0.05 mmol)
 H₂ (4 MPa)
 toluene
 160 °C, 40 min

CA-1 (1.95 mmol) + H₂ (4 MPa) → AL-1 + ES-1
 160 °C, 18 h

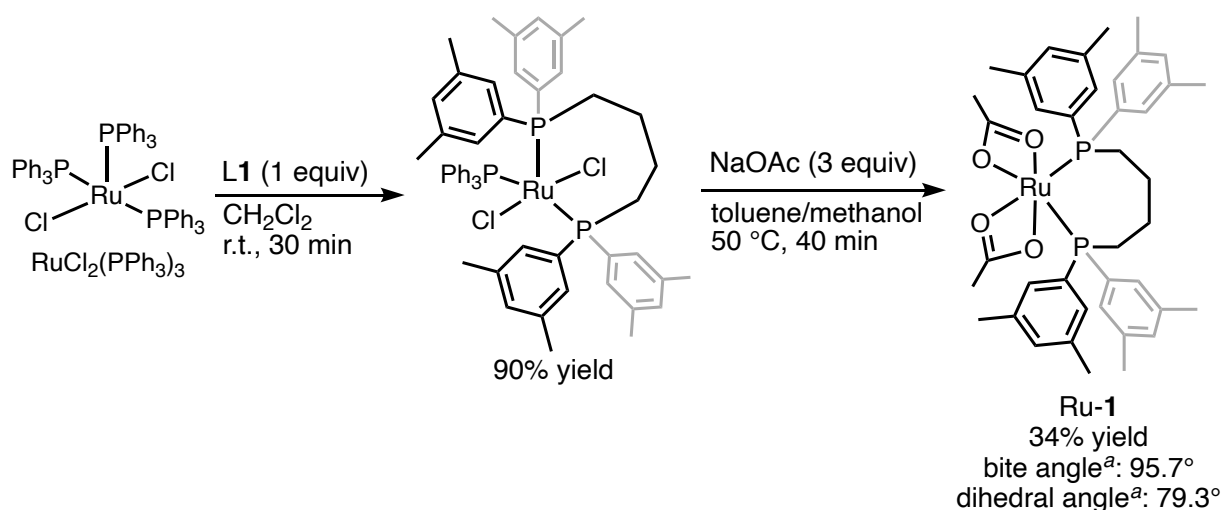
entry	ligand	Yield (%)		TON
		AL-1	ES-1	
1	DPPB	29	6	70
2	L1	30	6	72
3	L13	27	6	66
4	L14	22	6	56
5	L15	14	5	38
6	L16	18	5	46
7	L17	3	2	10

^aReactions were carried out over a period of 18 h with CA-1 (2.0 mmol, 333 mM), Ru(acac)₃ (0.5 mol %, 1.7 mM), and ligand (0.5 mol %, 1.7 mM) in toluene. Yields were determined by ¹H NMR analysis using mesitylene as an internal standard. TON is defined as (AL + ES mol)/(Ru mol) on the assumption that ES generates by condensation of CA with the AL. ^b[Ru]₀ = 10 mM, [L1]₀ = 10 mM, [CA-1]₀ = 50 mM in toluene.

1.2.6. Synthesis, isolation, and use of (PP)Ru^{II}(diacetate) complexes as precatalysts.

As demonstrated in previous discussions, when sterically bulky bidentate ligands (L13–L17) were combined with Ru^{III}(acac)₃ and subjected to reaction conditions for CA hydrogenation, slow and/or incompetent induction of catalytic Ru^{II} species apparently caused lower TONs, making it difficult to assess ligands that are truly viable for hydrogenation steps. To prevent the induction period of the catalyst from being unpredictable and lengthy, Ru^{II} diacetate complexes coordinated with PP bidentate ligands were separately synthesized and used directly as precatalysts for CA hydrogenation. Two different synthetic routes were established for the synthesis of different (PP)Ru(OAc)₂ complexes (Scheme 2 and Figure 6). Complex (L1)Ru(OAc)₂ (Ru-1) was synthesized in two steps (Scheme 2). After the first step, in which an exchange of L1 with the two PPh₃ molecules of Wilkinson-type Ru complex RuCl₂(PPh₃)₃ in a CH₂Cl₂ solution was carried out, an excess amount of NaOAc was added in the second step. The desirable Ru-1 was obtained in 34% yield after recrystallization in *n*-hexane. Ru complexes Ru-2 and Ru-3 were synthesized by treatment of [RuCl₂(*p*-cymene)]₂ with PP ligands L13 and L15, respectively, through a one-step procedure (Figure 6).^[33]

Scheme 2 | Synthetic routes to Ru-1 in two steps.^a



^aThe P–Ru–P bite angle and the PC–C–C–CP dihedral angle were estimated by the DFT calculation (B3LYP/LANL2DZ) of the optimized geometry of Ru-1 complex.

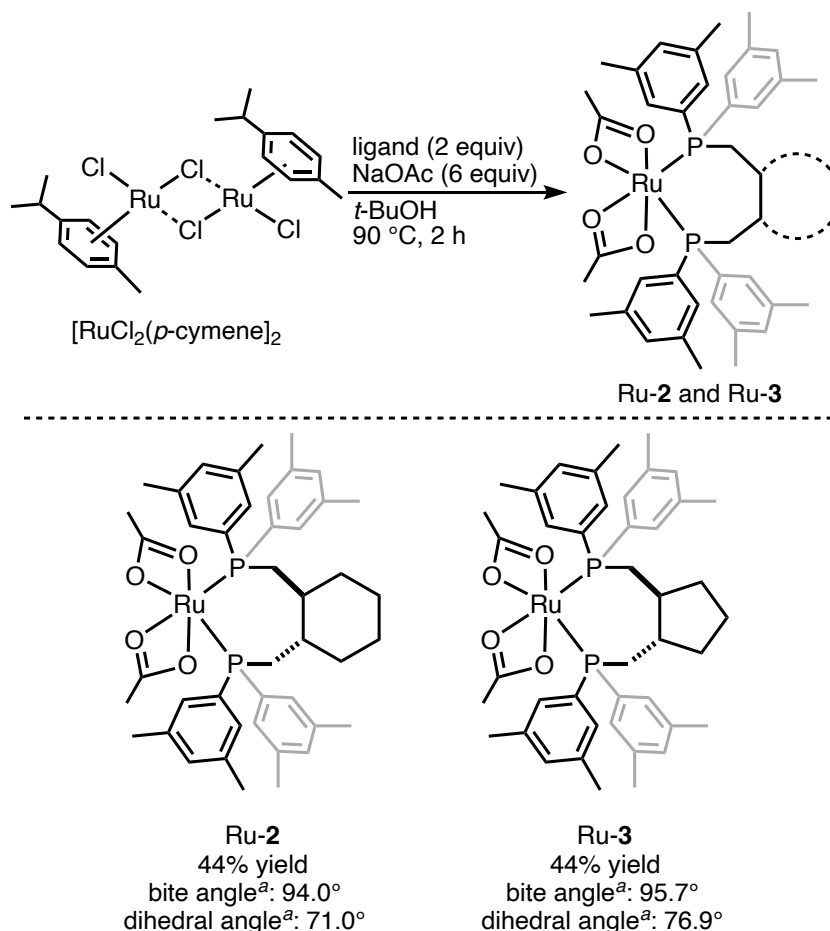


Figure 6 | Synthesis of Ru-diacetate complexes in one step. ^aThe P–Ru–P bite angles and the PC–C–C–CP dihedral angles were estimated by the DFT calculations (B3LYP/LANL2DZ) of the optimized geometries of Ru-2 and Ru-3 complexes.

The catalytic performance of the synthesized Ru complexes Ru-1–Ru-3 (1.0 mol %) in the hydrogenation of CA-1 by varying P_{H_2} pressure (P_{H_2}) was investigated (Table 14). The use of Ru-1 ((L1)Ru(OAc)₂) provided superior TON and AL selectivity (entry 1) comparable to those obtained using a combination of Ru(acac)₃ and L1 (Scheme 1, Eq. 1). Complexes Ru-2 and Ru-3 required a higher P_{H_2} (6–8 MPa) to afford saturated TON (~90) and AL selectivity (entries 2–7). The results suggest that the velocity of H₂ uptake (for inducing catalyst and CA hydrogenation) by (PP)Ru(OAc)₂ complexes depends on both bite angles and dihedral angles of (PP)Ru complexes. The smaller the dihedral angles, the slower the overall sequence involving the uptake of H₂ by the Ru catalyst and subsequent hydrogen transfer to CA from the Ru–H species (dihedral angle: Ru-1 (79.3°) > Ru-3 (76.9°) > Ru-2 (71.0°)). Assuming that the rate difference for inducing catalysts from precatalysts Ru-1–Ru-3 is almost identical or negligible, it can be concluded that the larger or smaller the bite angles than that of Ru-1, the slower the CA hydrogenation (bite angle: Ru-2 (94.0°) < Ru-1 (95.7°) = Ru-3 (95.7°)).

Indeed, Ru-1 and Ru-3, which showed the highest catalytic activities at $P_{H_2} = 4$ MPa (entries 1 and 5), have similar bite and dihedral angles. By also considering the argument that arises when Ru(acac)₃ and different PP bidentate ligands were used, the velocity of catalyst induction from Ru(acac)₃ may offset that of CA hydrogenation, given that the dihedral and bite angles of (PP)Ru are smaller than those of Ru-1. The overall reaction rate would be significantly attenuated by the worst mismatching of the both angles larger than those of Ru-1.

Table 14 | Hydrogenation with synthesized Ru diacetates ($t = 18$ h, $P_{H_2} = 4-8$ MPa).^a

Reaction scheme: CA-1 (3-phenylpropanoic acid) reacts with H₂ (4–8 MPa) and Ru complex (1.0 mol %) in toluene at 160 °C for 18 h to produce AL-1 (3-phenylpropan-1-ol) and ES-1 (3-phenylpropanoic acid ethyl ester).

entry	Ru complex	P_{H_2} (MPa)	Yield (%)		TON
			AL-1	ES-1	
1	Ru-1	4	74	10	84
2		4	35	20	55
3	Ru-2	6	74	9	83
4		8	74	11	85
5		4	58	13	71
6	Ru-3	6	61	19	80
7		8	72	10	82

^aReactions were carried out over a period of 18 h with CA-1 (333 mM) and Ru complex (1.0 mol % Ru, 3.3 mM) in toluene. Yields were determined by ¹H NMR analysis using mesitylene as an internal standard. TON is defined as (AL + ES mol)/(Ru mol) on the assumption that ES generates by condensation of CA with the AL.

Having established the reaction conditions for CA hydrogenation, we examined the substrate scope of the hydrogenation with three Ru complexes, Ru-1–Ru-3, at a low catalyst loading (0.25 mol % Ru) and at a reaction time of 36 h (Table 15). Unfortunately, hydrogenation of CA-1 to AL-1 using these Ru complexes required higher P_{H_2} (6 MPa) for having a relatively high TON (>100) (entries 1–6). In contrast, the hydrogenation of α -phenoxyacetic acid (CA-2) to AL-2 with Ru-1 proceeded with a higher TON (284), albeit with the formation of a considerable amount of ES-2 as a drawback (entry 7). This defect was partially solved by adding THF (250 mol %), which coordinated to a cationic Ru center and was in effect on detracting Lewis acidity of the Ru, which is the most responsible aspect for esterification (entry 8). To our delight, the TON of CA hydrogenation was apparently improved by compensating for the loss of esterification, which eventually increased the concentration of

CA to be hydrogenated. A trade-off between the two different reaction rates for the hydrogenation of CA to AL and *in situ* esterification of CA with AL was likely to be made. Reversible THF occupation of vacant *d* orbitals of Ru^{II} would also be beneficial for deflecting extra CAs from undergoing relatively irreversible bidentate coordination to the Ru center, by which H₂ uptake with Ru would be suppressed. Exceptionally, a Ru-3-catalyzed hydrogenation afforded both high TON and AL selectivity in the absence of THF (entry 10). Hydrogenation of 2-phenoxypropionic acid (CA-3) to AL-3 with Ru-1 resulted in more favorable ES-3 formation, where the addition of THF similarly improved both the product selectivity and TON (entries 11 and 12). 2-Naphthoxyacetic acid (CA-4), α -methoxyacetic acid (CA-5), and 2-tetrahydrofuroic acid (CA-6) were successfully hydrogenated to AL-4, AL-5, and AL-6, respectively, with fairly good TON and AL selectivity without the addition of THF, where intramolecular oxygen coordination might act as a surrogate for the function of THF (entries 13–16). N-pyrrole-protected glycine (CA-7) was also hydrogenated smoothly to AL-7, and THF improved the AL yield and TON (entries 17 and 18). Both Ru-1- and Ru-2-catalyzed hydrogenation of benzoic acid (CA-8), which is one of the least reactive CAs, occurred sluggishly (entries 19 and 20). Although the catalytic activity derived from Ru-2 was sustained over 115 h, ES-9 was produced in 18% yield with AL-8 in 28% yield (entry 21). Hydrogenation of the most demanding substrate sterically, 1-adamantanecarboxylic acid, CA-9 to AL-9 proceeded most sluggishly among the CAs tested, even with 1 mol % of Ru-1 or Ru-2 giving low TONs (entries 22 and 23), probably due to the significant steric interactions of this CA with Ru catalysts. Monodentate P(3,5-xylyl)₃ is a considerably better ligand than is DPPB for the hydrogenation of this specifically bulky CA-9. One of the best homogeneous catalysts for CA hydrogenation, the Ru(acac)₃/Sn(OTf)₂/Triphos system,^[20] was also tested for the hydrogenation of CA-2 under similar conditions (Ru = 0.25 mol %; P_{H₂} = 4–6 MPa, T = 160 °C, t = 36 h) for comparison; however, the crude yields were significantly lower (AL-2, 4–6%; ES-2, 3%; TON, 28–36; Table 16) than that of our present system.

To further substantiate the scalability and the catalyst competence of this method, we performed the hydrogenation of CA-2 using a 5 mmol of CA-2 with 0.05 mol % Ru-1 or a combined use of Ru(acac)₃ and L1 (Table 17). The reaction using Ru-1 in the presence of THF provided the highest TON of 1420, but unfortunately alcohol selectivity was low (entry 1). The reaction using Ru(acac)₃ and L1 provided a TON of 1100, but the reaction in favor of ES-2 over AL-2 remained a significant drawback (entry 2).

Finally, ESI-MS analysis of an aliquot prepared by sampling a reaction mixture obtained upon hydrogenation of CA-1 by Ru-1 was performed. The results showed the mass peak of the seemingly deactivated Ru species I_b(L1) ([ruthenacycle with L1]⁺, where the α -C–H bond of

the xylyl group is inserted into the Ru center), the intensity of which was much smaller than that of a resting catalyst $\mathbf{I}_a(\mathbf{L1})$ ($[(\mathbf{L1})\text{Ru}(\text{OCOR})(\text{MeCN})]^{+}$) (Figure 7). The relative intensity $\mathbf{I}_b(\mathbf{L1})/\mathbf{I}_a(\mathbf{L1})$ was also much smaller than that of $\mathbf{I}_b(\text{DPPB})/\mathbf{I}_a(\text{DPPB})$, which was derived from the Ru-DPPB complex. This result suggests that the Me groups of the xylyl groups incorporated in $\mathbf{L1}$ and $\mathbf{L13-L15}$ effectively suppressed the decay of catalytically active species, thus further justifying the current strategy for designing molecular catalyst bearing bidentate PP ligands.

Table 15 | Hydrogenation of various CAs with 0.25–1.0 mol % catalysts.^a

entry	CA	Ru complex	Yield (%)		TON
			AL	ES	
1		Ru-1	20	11	124
2		Ru-1 ^b	17	29	184
3		Ru-2	10	10	80
4		Ru-2 ^b	14	21	140
5		Ru-3	12	9	84
6		Ru-3 ^b	17	23	160
7		Ru-1	44	27	284
8		Ru-1 ^c	70	15	340
9		Ru-2	33	17	200
10		Ru-3	65	19	336
11		Ru-1	20	34	216
12		Ru-1 ^c	50	20	280
13		Ru-1	60	20	320
14		Ru-1	51	19	280
15		Ru-1	62	16	312
16		Ru-3	44	21	260
17		Ru-1	15	32	188
18		Ru-1 ^c	55	20	300
19		Ru-1 ^d	7	0	28
20		Ru-2 ^d	8	0	32
21		Ru-2 ^e	28	18	184
22		Ru-1 ^f	25	0	25
23		Ru-2 ^f	21	0	21

^aReactions were carried out over a period of 36 h with CA (333 mM), and Ru-1, Ru-2, or Ru-3 (0.25 mol % Ru, 0.83 mM) in toluene. Yields were determined by ¹H NMR analysis using mesitylene as an internal standard. TON is defined as (AL + ES mol)/(Ru mol) on the assumption that ES generates by condensation of CA with the AL. ^b*P*_{H₂} = 6 MPa. ^cTHF (250 mol % with respect to CA) was added. ^d48 h. ^e115 h. ^fRu-1 or Ru-2 (1.0 mol % Ru, 3.3 mM), 18 h.

Table 15 (continued) | Hydrogenation of various CAs with 0.25–1.0 mol % catalysts.^a

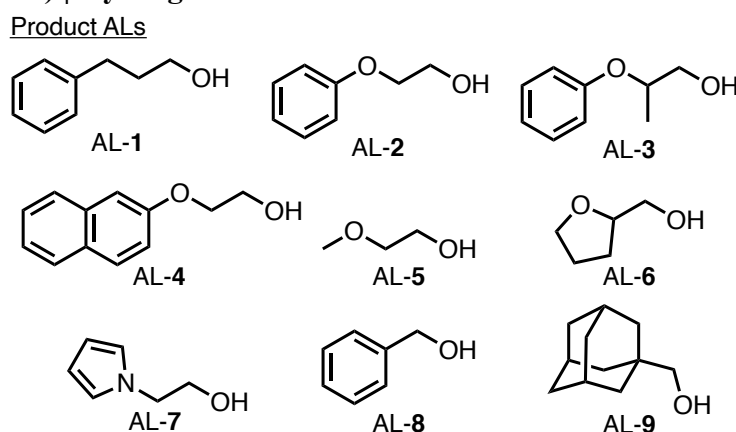
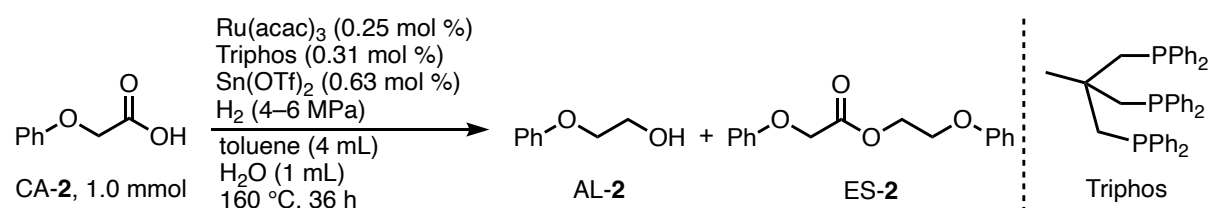


Table 16 | Hydrogenation of CA-2 with 0.25 mol % Ru of the Ru(acac)₃/Triphos/ Sn(OTf)₂ system.^[20]



entry	P_{H_2} (MPa)	Yield (%)		TON
		AL-2	ES-2	
1	4	4	3	28
2	6	6	3	36

Unless otherwise specified, the reactions were carried out with Ru(acac)₃:Triphos:Sn(OTf)₂:CA-1 (mol %) = 0.25:0.31:0.63:100, P_{H_2} = 4–6 MPa, T = 160 °C, and t = 36 h in toluene and H₂O. ¹H NMR yields were determined based on the integral ratio of the signals of products and internal standard (mesitylene). TON is defined as mol (AL + ES)/mol Ru on the assumption that ES generates from a condensation of CA and the product AL.

Table 17 | Scaled-up hydrogenation of CA-2 (5 mmol) using 0.05 mol % Ru (substrate/catalyst (S/C) = 2,000).^a

entry	Precatalyst	Yield (%)		TON
		AL-2	ES-2	
1	Ru-1 (0.05 mol %)	43	28	1420
2	Ru(acac) ₃ (0.05 mol %) L1 (0.05 mol %)	17	38	1100

^aReactions were carried out over a period of 96 h with CA-2 (333 mM), and Ru-1 (0.05 mol % Ru, 0.83 mM), or Ru(acac)₃ (0.05 mol %, 0.83 mM) and L1 (0.05 mol %, 0.83 mM) in toluene. Yields were determined by ¹H NMR analysis using mesitylene as an internal standard. TON is defined as (AL + ES mol)/(Ru mol) on the assumption that ES generates by condensation of CA with the AL.

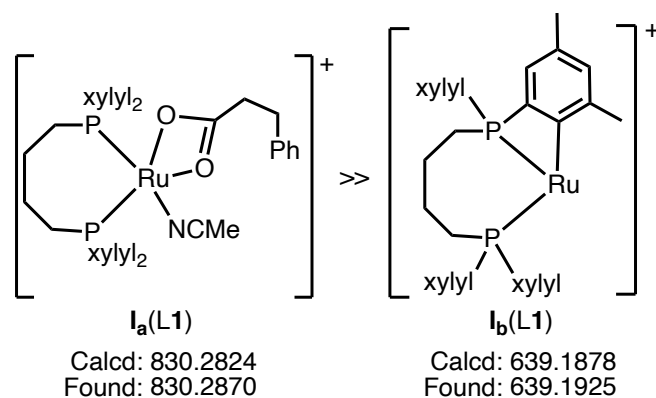


Figure 7 | ESI-MS analysis of an aliquot prepared by sampling a reaction mixture of Ru-1. I_a(L1): catalyst prototype; I_b(L1): deteriorated catalyst.

1.3. Conclusion

Here, we report a possible solution to a long-standing concern on how to achieve a high TON of CA hydrogenation by precisely tweaking the structure of bidentate PP ligands based on the structures of P(3,5-xylyl)₃ and DPPB, which were previously found to be the most promising ligands. The Ar groups substituted on P atoms and conformational control of the alkyl chain connecting the two P atoms were important for achieving high catalytic activity. Optimization of the reaction conditions to shorten the induction period of the catalyst from one of the cheapest Ru sources, Ru(acac)₃, has also been intensively investigated. Separate synthesis of (PP)Ru(OAc)₂, followed by its direct use seems to be among the most promising and straightforward ways to shorten the induction period of the catalyst. These results eventually validated our strategy for ligand improvement, which would benefit the practical application of this efficient hydrogenation system involving CA self-induced CA hydrogenation. Further development of an ingenious method for suppressing the *in situ* esterification, which remains a significant obstacle in this work, is underway in our laboratory.

1.4. Experimental section

1.4.1. Material.

1,4-Dibromobutane, 1,4-dicyanobenzene, diphenyl(trimethylsilyl)phosphane, *trans*-1,2-cyclopentanedicarboxylic acid, and Solvias® Chiral Ligands Kit (L47, L51, L52, and L55–L91) were purchased from Aldrich Chemical Co. 1-Bromo-3,5-dimethylbenzene, 1-bromo-3,5-di-*tert*-butylbenzene, 1-bromo-3,5-dimethoxybenzene, 4-bromo-2,6-dimethylanisole, 1,5-dibromopentane, 2,6-diisopropylaniline, bromine, 3-phenylpropionic acid, 1,4-dibromobenzene, zinc powder, dichloridobis(triphenylphosphane)nickel(II), 2,5-hexanediol, *N,N*-dimethyl-4-aminopyridine (DMAP), diphenylphosphine, 2,3-norbornedicarboxylic acid, *trans*-1,2-cyclohexanedicarboxylic acid, *cis*-1,2-cyclohexanedicarboxylic acid, 2,2'-bis(diphenylphosphino)biphenyl (L48), (*R*)-2,2'-Bis(diphenylphosphino)-1,1'-binaphthyl (BINAP, L53), 3-phenylpropionic acid (CA-1), α -phenoxyacetic acid (CA-2), 2-phenoxypropionic acid (CA-3), 2-naphthoxyacetic acid (CA-4), 2-tetrahydrofuroic acid (CA-6), and 1-adamantanecarboxylic acid (CA-9) were purchased from Tokyo Chemical Industry CO., Ltd. Hydrochloric acid, THF (anhydrous), toluene (anhydrous), dichloromethane, ethanol, chloroform, mesitylene, Na₂SO₄, NaOH, diethyl ether, Celite® 545, Sodium hydride (dispersion in paraffin liquid, 55% purity), lithium aluminum hydride, sodium nitrite, *n*-butyllithium (1.6 M *n*-hexane solution), and α -methoxyacetic acid (CA-5) were purchased from Kanto Chemicals, Ltd. Diethyl phosphite, iodine, 1,3-dibromopropane, 50% phosphinic acid solution, cerium(III) chloride heptahydrate, ruthenium(III) acetylacetonate, nickel(II) chloride hexahydrate, 2,2'-bipyridyl, potassium *tert*-butoxide, phosphorus trichloride, acetic acid, ethyl acetate, hexane, (2*S*,3*S*)-(+)-1,4-bis(diphenylphosphino)-2,3-*o*-isopropylidene-2,3-butanediol (DIOP, L8), and 1,4-bis(dicyclohexylphosphino)butane (L45) were purchased from FUJIFILM Wako Pure Chemical Corporation. Magnesium (turnings) and phosphorus tribromide were purchased from Across Organics, Ltd. 1,2-Bis(diphenylphosphinomethyl)benzene (L12) was purchased from Alfa Aesar. 2,2'-(Di-*o*-tolylphosphino)diphenylether (L46), 2,2'-bis(dicyclohexylphosphino)-1,1'-biphenyl (L49), 2,2'-bis(diphenylphosphinomethyl)-1,1'-biphenyl (L50), and (*R*)-5,5'-bis(diphenylphosphino)-4,4'-bi-1,3-benzodioxole (SEGPPOS, L54) were purchased from Strem Chemicals Inc. Benzoic acid (CA-8) was purchased from Nacalai tesque. CDCl₃ and DMSO-*d*₆ were purchased from Cambridge Isotope Laboratories, Inc. Hydrogen gas (H₂, 99.99%) was purchased from Alpha system. These chemicals were used without further purification.

Bis(3,5-dimethylphenyl)phosphine oxide (1a),^[26] 1,4-bis[bis(3,5-dimethylphenyl)phosphino]butane (L1), 4-bromo-2,6-diisopropylaniline (2a),^[35] 1-bromo-3,5-

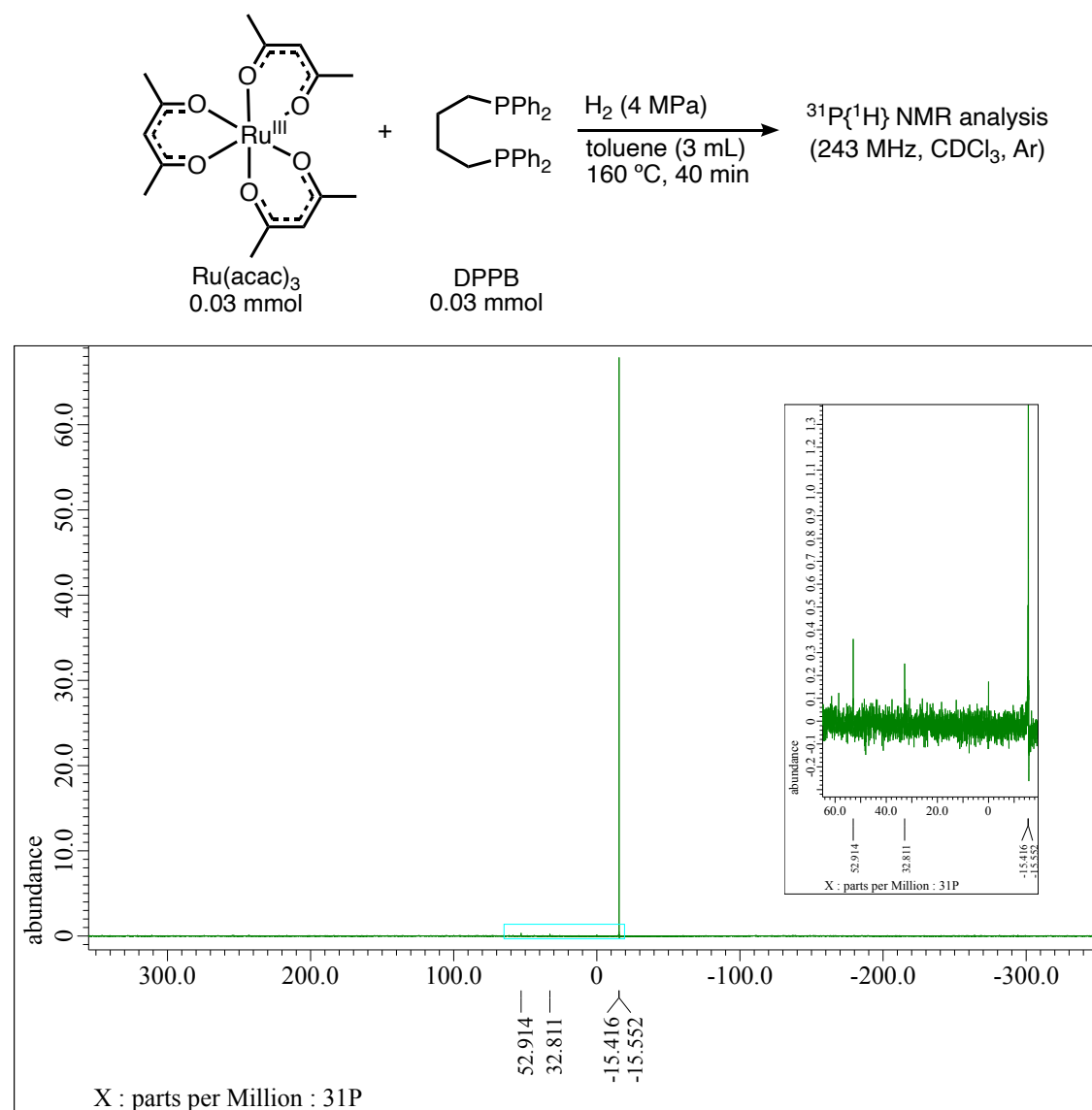
diisopropylbenzene (**2b**),^[36] bis(3,5-di(*tert*-butyl)phenyl)phosphine oxide (**3a**),^[37] bis(3,5-dimethyl-4-methoxyphenyl)phosphine oxide (**4a**),^[37] bis(3,5-dimethoxyphenyl)phosphine oxide (**5a**),^[38] bis(4-fluorophenyl)phosphine oxide (**6a**),^[37] bicyclo[2.2.1]heptane-2,3-dimethanol (**7a**),^[39] 1,4-bis(diphenylphosphino)benzene (**L40**),^[40] 1,4-phenylenebis[bis(3,5-dimethylphenyl)phosphine oxide] (**41a**),^[41] 1,4-bis(methylsulfonyloxy)-1,4-dimethylbutane (**42a**),^[42] 2,5-bis(diphenylphosphino)hexane (**L42**),^[42] tris(3,5-dimethoxyphenyl)phosphine (**L43**),^[43] tris(3,5-dimethyl-4-methoxyphenyl)phosphine (**L44**),^[43] are all known compounds. N-pyrrole-protected glycine (CA-7) was prepared by the literature.^[44]

1.4.2. General methods.

All experiments were performed under an argon (Ar) atmosphere unless otherwise noted. ¹H NMR spectra were measured on JEOL ECA-600 (600 MHz), JEOL ECA-500 (500 MHz), or JEOL ECS-400 (400 MHz) at ambient temperature unless otherwise noted. Data were recorded as follows: chemical shift in ppm from internal tetramethylsilane (0 ppm), multiplicity (br = broad, s = singlet, d = doublet, t = triplet, m = multiplet, dd = double doublet, ddd = double double doublet, dt = double triplet), coupling constant (Hz), integration, and assignment. ¹³C{¹H} NMR spectra were measured on JEOL ECA-600 (150 MHz), JEOL ECA-500 (126 MHz), or JEOL ECS-400 (100 MHz) at ambient temperature unless otherwise noted. Chemical shifts were recorded in ppm from the solvent resonance employed as the internal standard (chloroform-*d* at 77.06 ppm). ³¹P{¹H} NMR spectra were measured on JEOL ECA-600 (243 MHz) or JEOL ECA-500 (202 MHz) at ambient temperature unless otherwise noted. Chemical shifts were recorded in ppm from the solvent resonance employed as the external standard (phosphoric acid (85 wt% in H₂O) at 0.0 ppm). High-resolution mass spectra (HRMS) were obtained from BRUKER micrOTOF-QII (ESI). For thin-layer chromatography (TLC) analysis through this work, Merck precoated TLC plates (silica gel 60 GF254 0.25 mm) were used. The products were purified by preparative column chromatography on silica gel 60 (spherical, neutral, 230–400 mesh; Merck), Florisil[®] (75–150 μm; Wako), or alumina (activated; Wako).

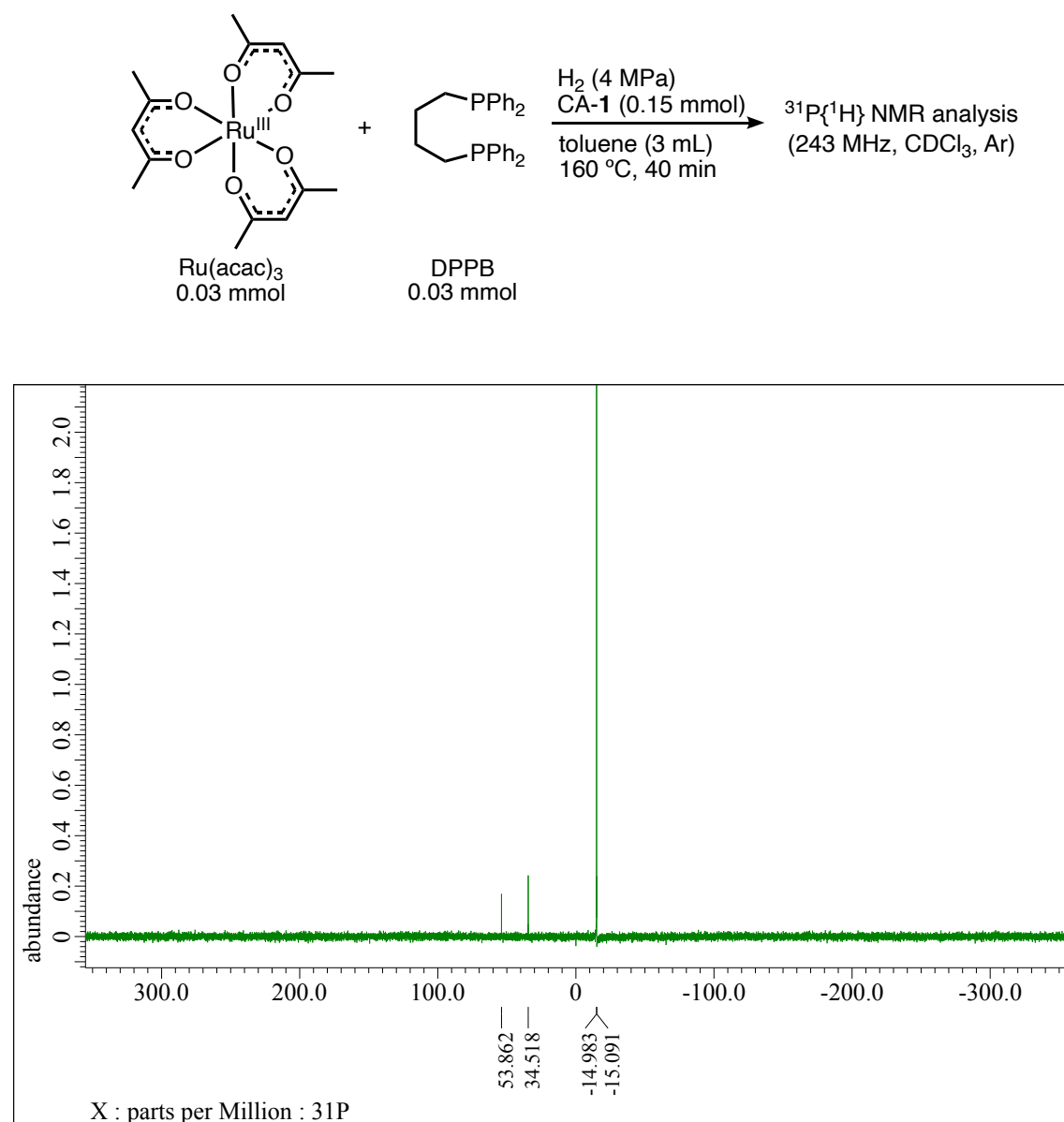
Density functional theory (DFT) calculations were carried out using Gaussian 09 Rev. B 01.^[34] The molecular structure was obtained at the B3LYP level with LANL2DZ with f-type pseudopotentials for Ru; 6–31G** for the other atoms.

1.4.3. Supplementary figures



Peak No.	ppm	intensity	relative intensity
1 (free ligand)	-15.6	67.8997	99.1%
2 ((PP)Ru(acac) ₂)	52.9	0.36274	0.5%
3 (oxidized species)	32.8	0.25504	0.4%
total		68.51748	100%

Figure S1 | $^{31}\text{P}\{^1\text{H}\}$ NMR study (243 MHz, CDCl_3 , Ar) on the pretreatment of $\text{Ru}(\text{acac})_3$ with DPPB (Table 12, entry 1).



Peak No.	ppm	intensity	relative intensity
1 (free ligand)	-15.0	2.7898	88.8%
2 ((PP)Ru(acac) ₂)	53.9	0.11978	3.8%
3 (oxidized species)	34.5	0.23112	7.4%
total		3.1407	100%

Figure S2 | $^{31}\text{P}\{^1\text{H}\}$ NMR study (243 MHz, CDCl_3 , Ar) on the pretreatment of $\text{Ru}(\text{acac})_3$ with DPPB in the presence of CA-1 (Table 12, entry 2).

Chapter 1. Development of Effective Bidentate Diphosphine Ligands of Ruthenium Catalysts toward Practical Hydrogenation of Carboxylic Acids

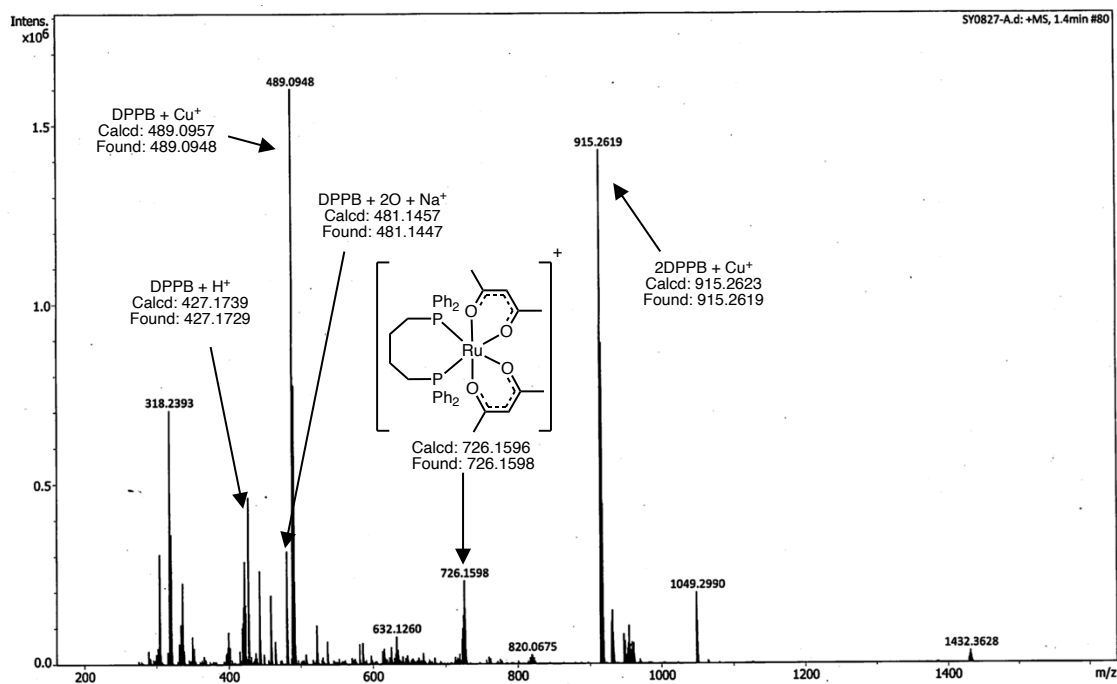
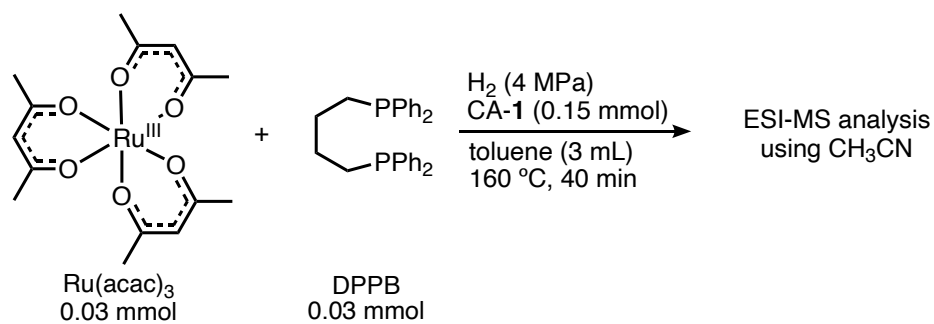
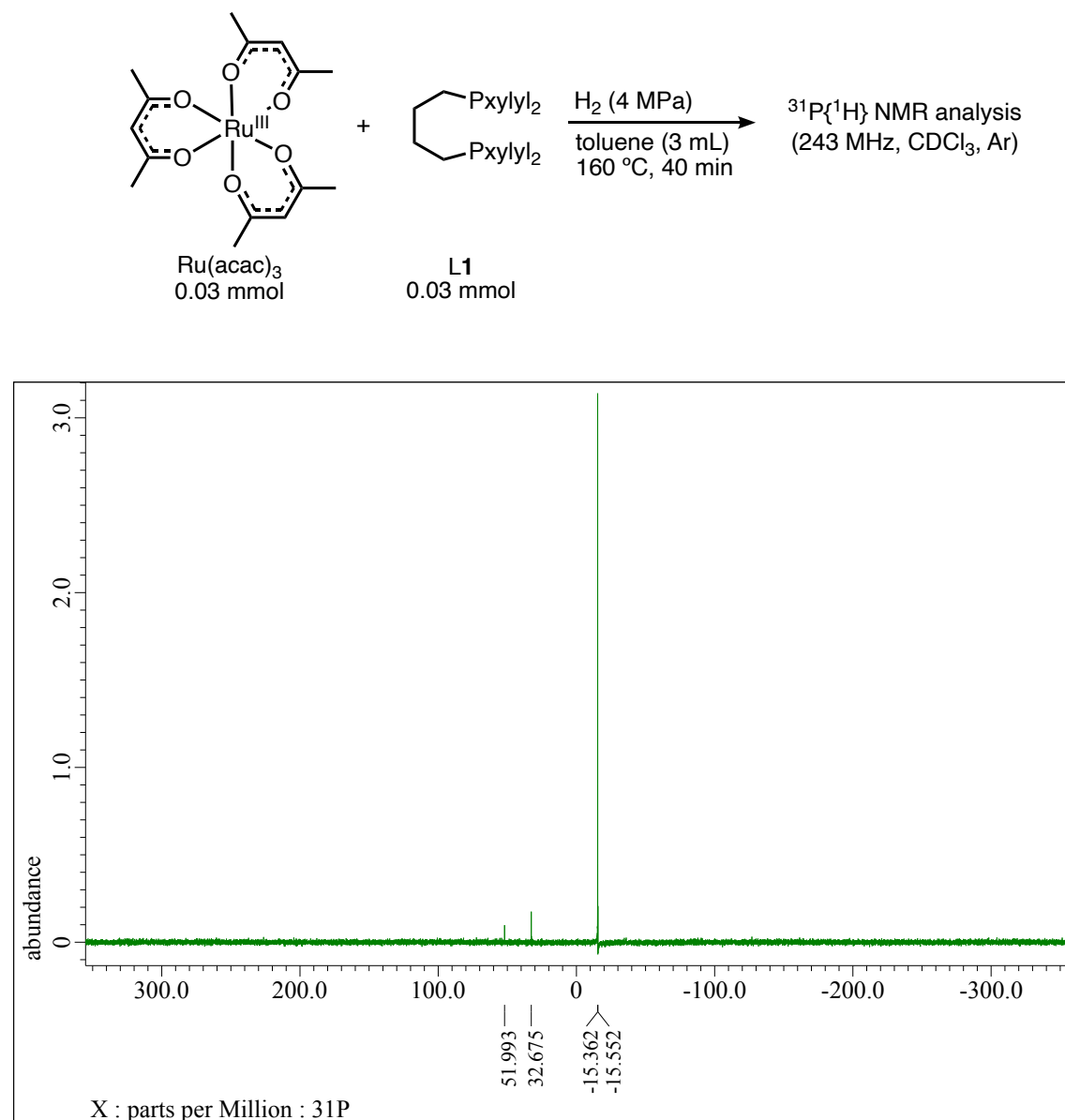


Figure S3 | ESI-MS study using CH₃CN on the pretreatment of Ru(acac)₃ with DPPB in the presence of CA-1 (Table 12, entry 2).



Peak No.	ppm	intensity	relative intensity
1 (free ligand)	-15.4	3.1403	92.0%
2 ((PP)Ru(acac) ₂)	52.0	0.097962	2.9%
3 (oxidized species)	32.7	0.17532	5.1%
total		3.413582	100%

Figure S4 | $^{31}\text{P}\{^1\text{H}\}$ NMR study (243 MHz, CDCl_3 , Ar) on the pretreatment of $\text{Ru}(\text{acac})_3$ with L1 (Table 12, entry 3).

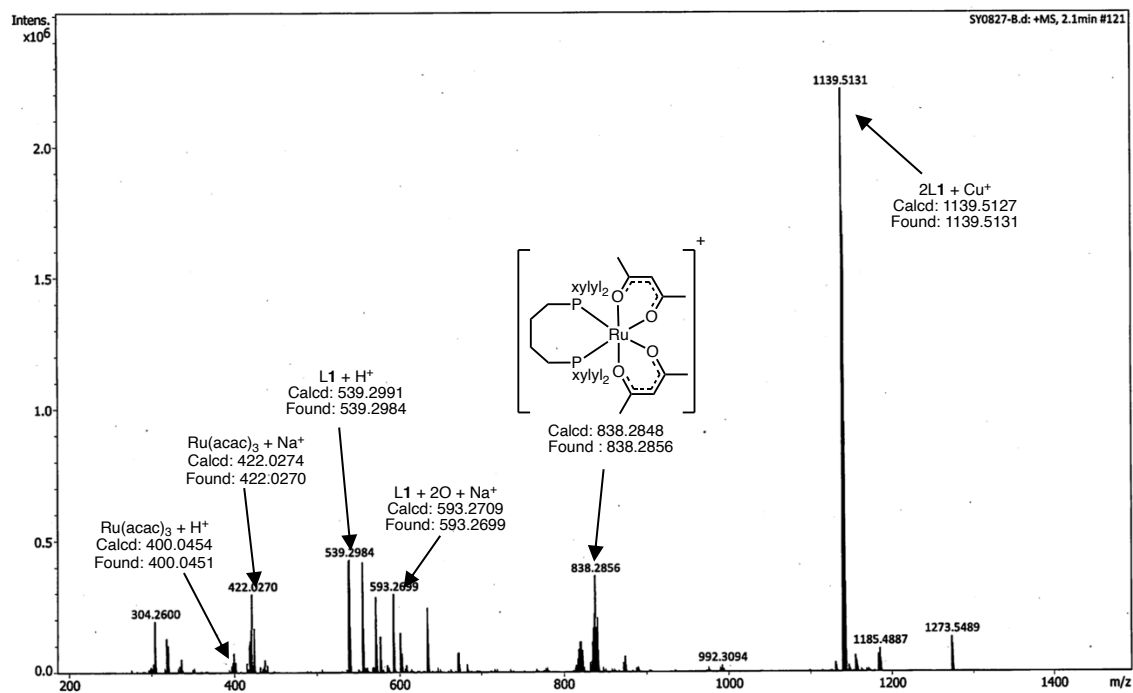
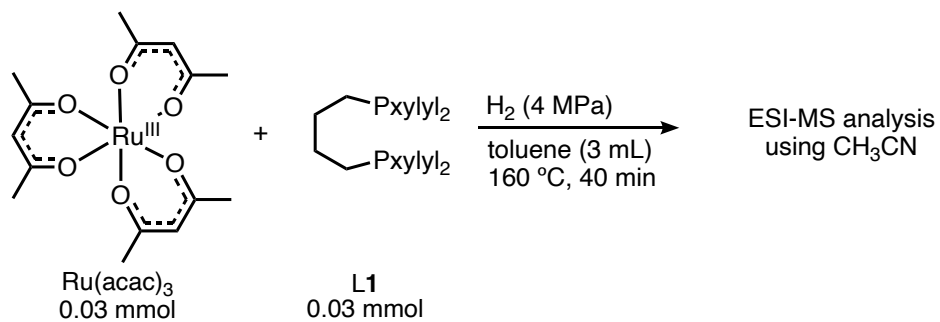
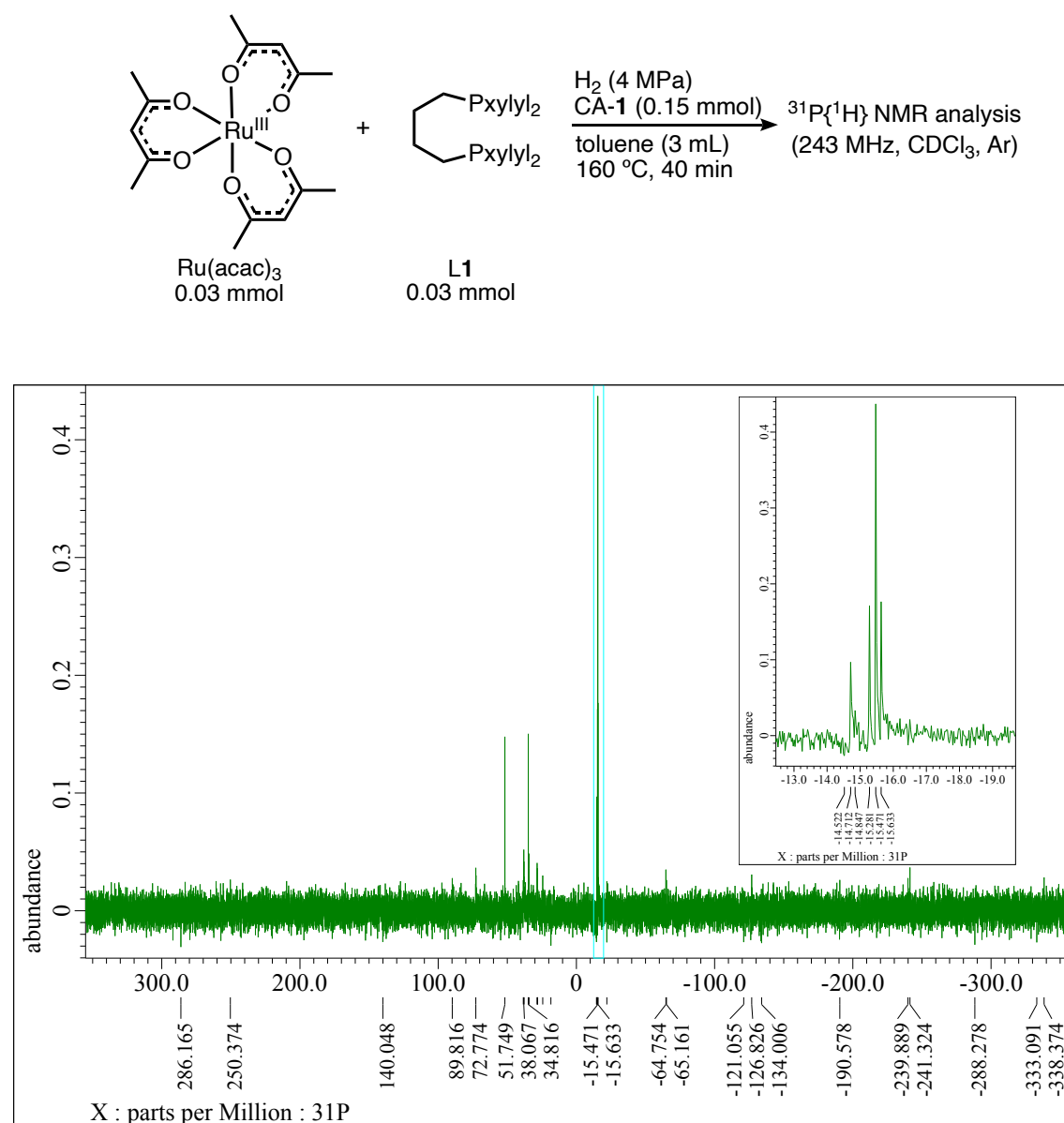


Figure S5 | ESI-MS study using CH₃CN on the pretreatment of Ru(acac)₃ with L1 (Table 12, entry 3).



Peak No.	ppm	intensity	relative intensity
1 (free ligand)	-15.5	437.1696	59.5%
2 ((PP)Ru(acac) ₂)	51.7	147.8262	20.1%
3 (oxidized species)	34.8	150.2725	20.4%
total		735.2683	100%

Figure S6 | $^{31}\text{P}\{^1\text{H}\}$ NMR study (243 MHz, CDCl_3 , Ar) on the pretreatment of $\text{Ru}(\text{acac})_3$ with **L1** in the presence of CA-1 (Table 12, entry 4).

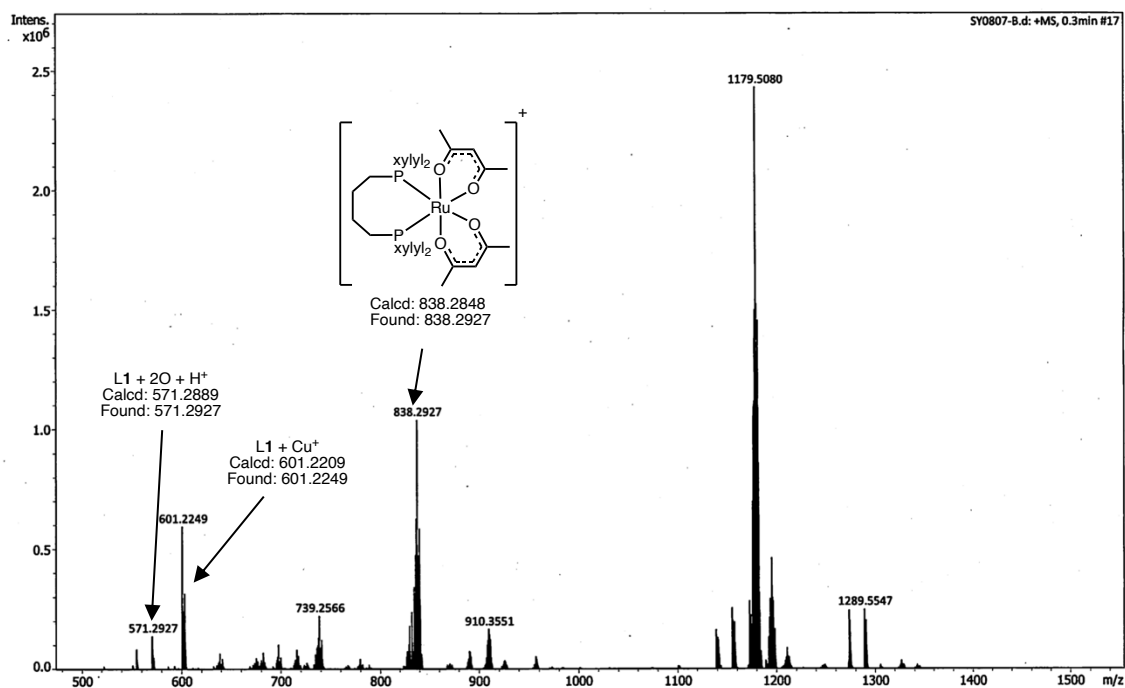
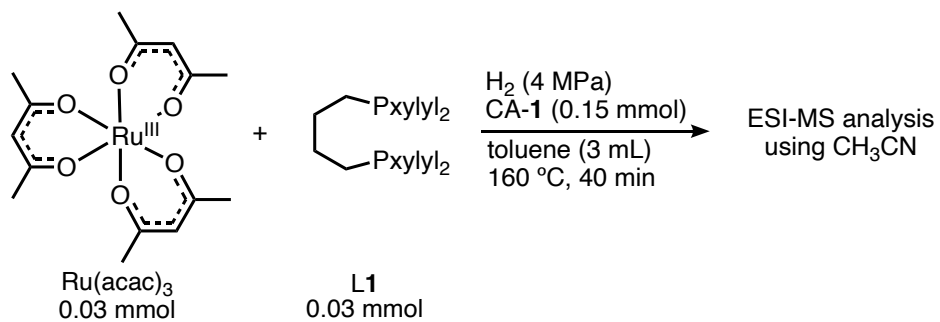
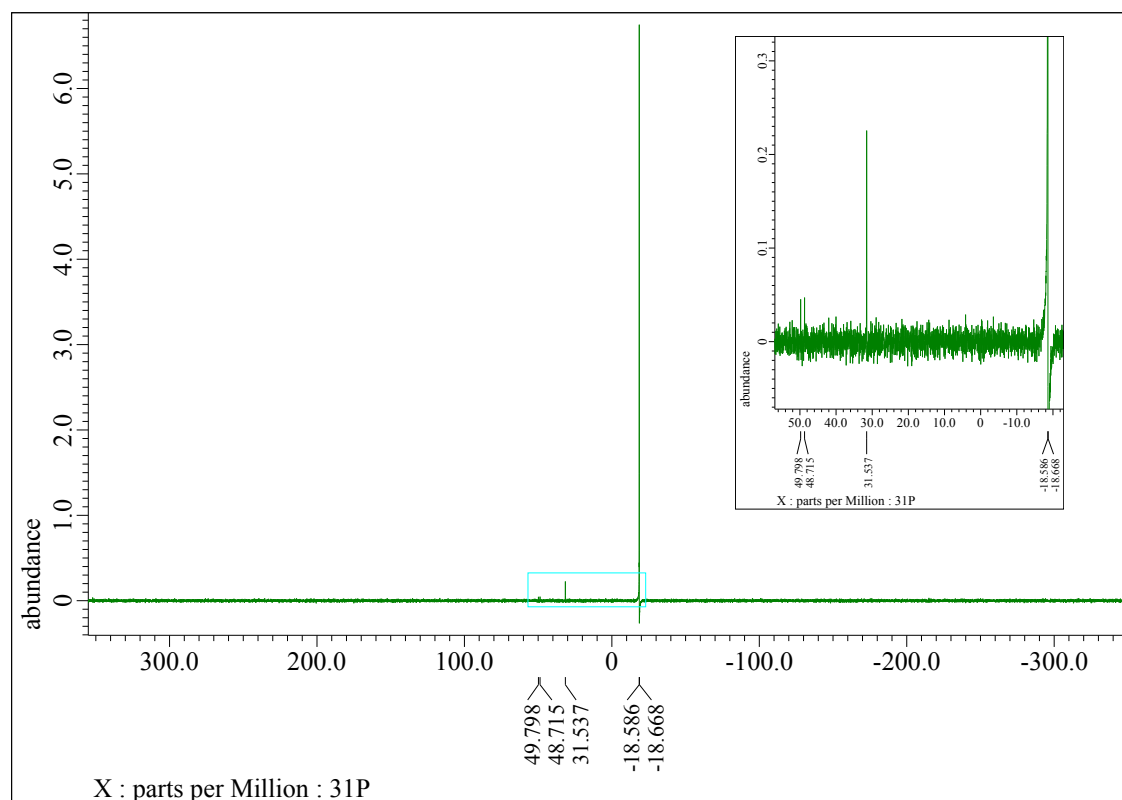
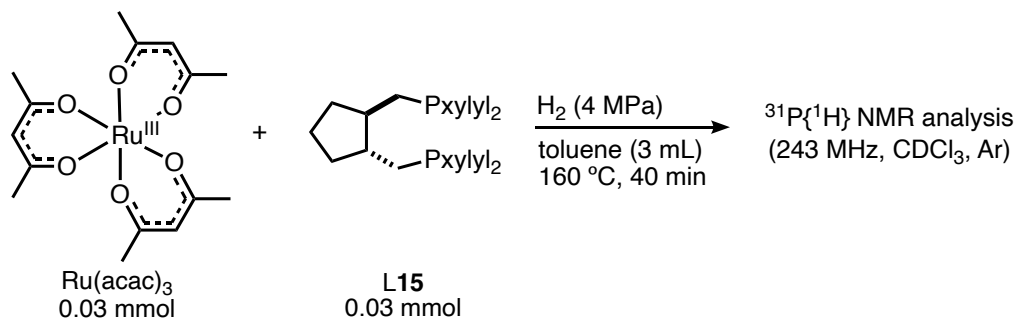


Figure S7 | ESI-MS study using CH₃CN on the pretreatment of Ru(acac)₃ with L1 in the presence of CA-1 (Table 12, entry 4).



Peak No.	ppm	intensity	relative intensity
1 (free ligand)	-18.6	6740.6	96.0%
2 ((PP)Ru(acac) ₂)	48.7	47.1012	0.7%
3 (oxidized species)	31.5	229.5239	3.3%
total		7017.2251	100%

Figure S8 | $^{31}\text{P}\{^1\text{H}\}$ NMR study (243 MHz, CDCl_3 , Ar) on the pretreatment of $\text{Ru}(\text{acac})_3$ with **L15** (Table 12, entry 5).

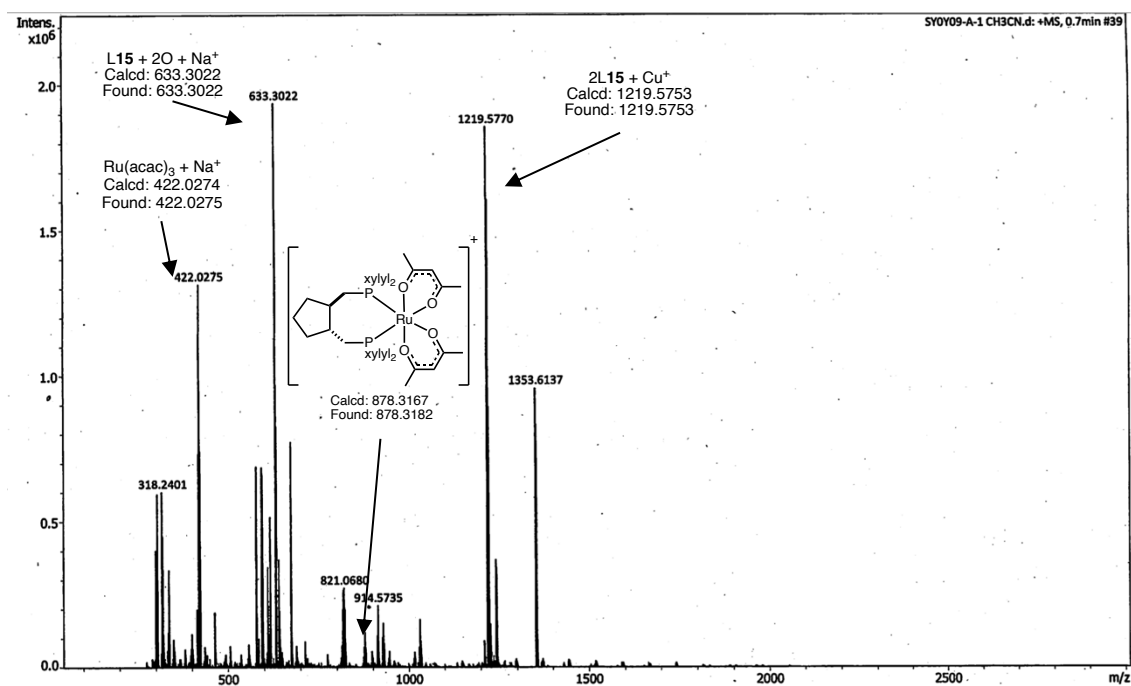
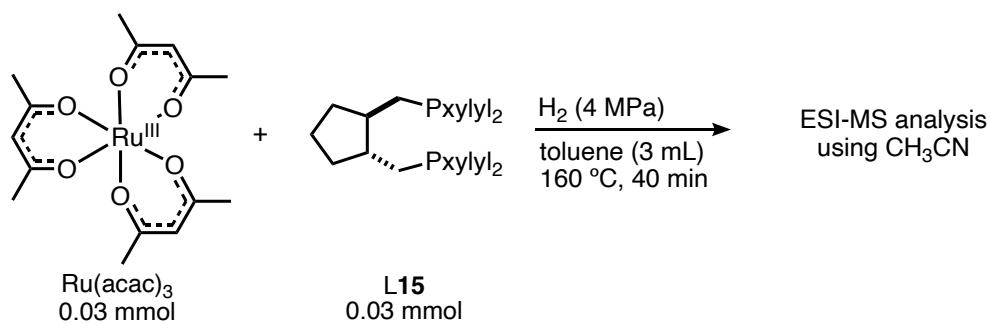
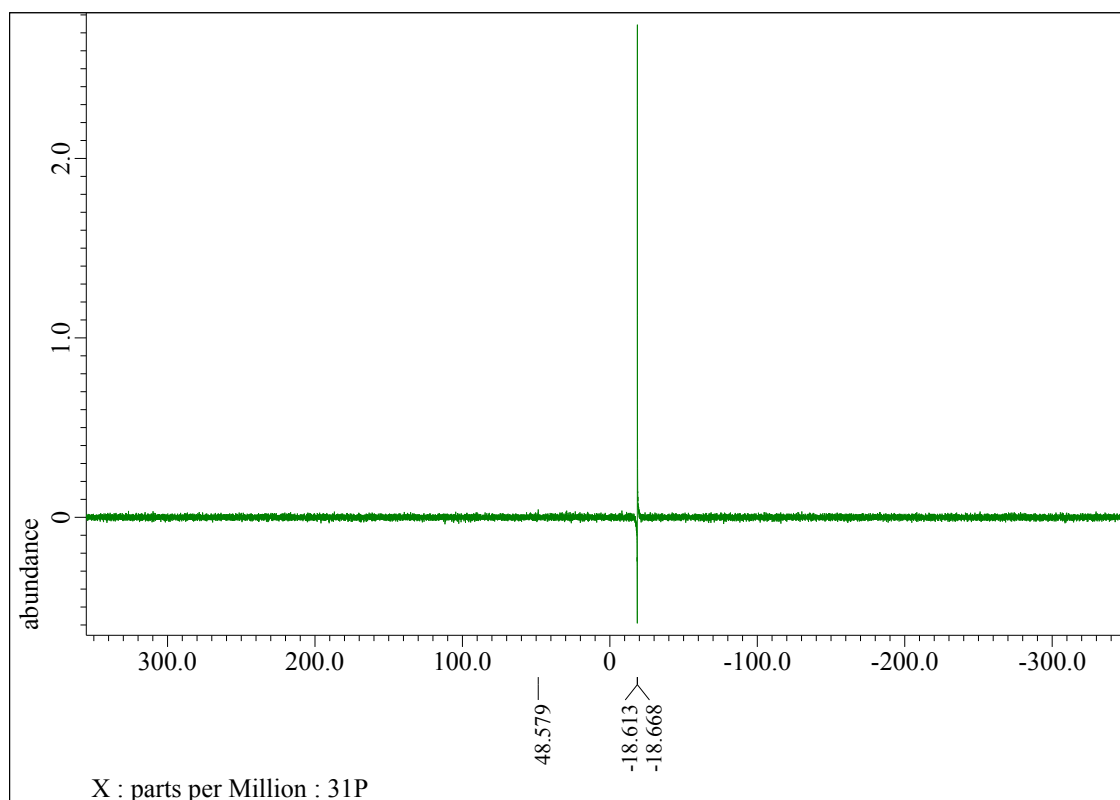
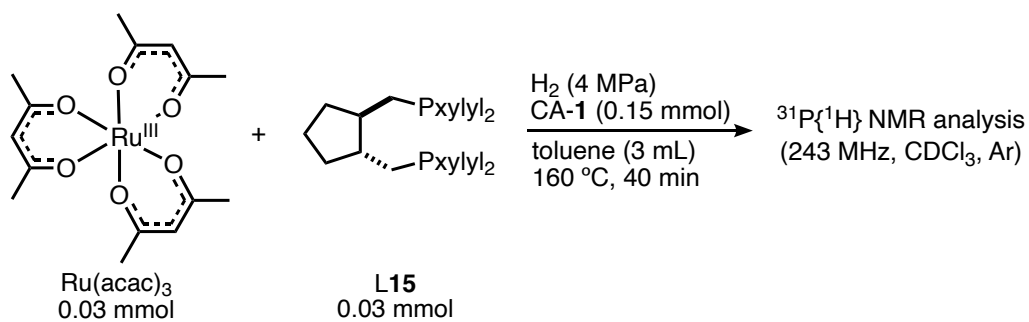


Figure S9 | ESI-MS study using CH_3CN on the pretreatment of $\text{Ru}(\text{acac})_3$ with **L15** (Table 12, entry 5).



Peak No.	ppm	intensity	relative intensity
1 (free ligand)	-18.7	2.7449	98.4%
2 ((PP)Ru(acac) ₂)	48.6	0.043621	1.6%
total		2.788521	100%

Figure S10 | $^{31}\text{P}\{^1\text{H}\}$ NMR study (243 MHz, CDCl_3 , Ar) on the pretreatment of $\text{Ru}(\text{acac})_3$ with **L15** in the presence of **CA-1** (Table 12, entry 6).

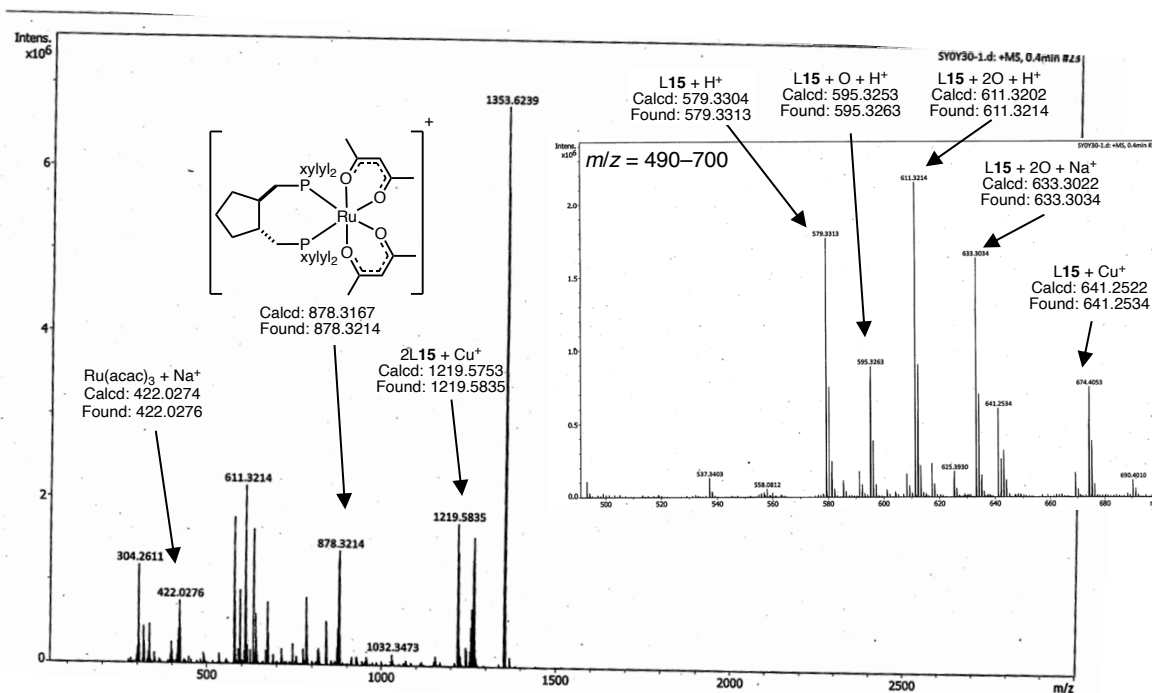
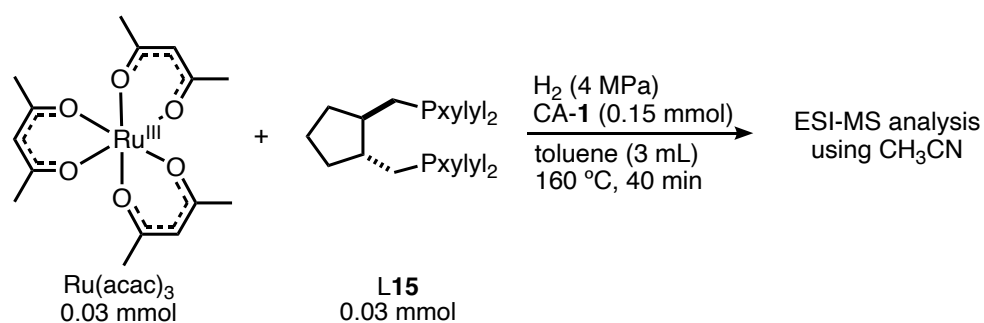


Figure S11 | ESI-MS study using CH_3CN on the pretreatment of $\text{Ru}(\text{acac})_3$ with **L15** in the presence of **CA-1** (Table 12, entry 6).

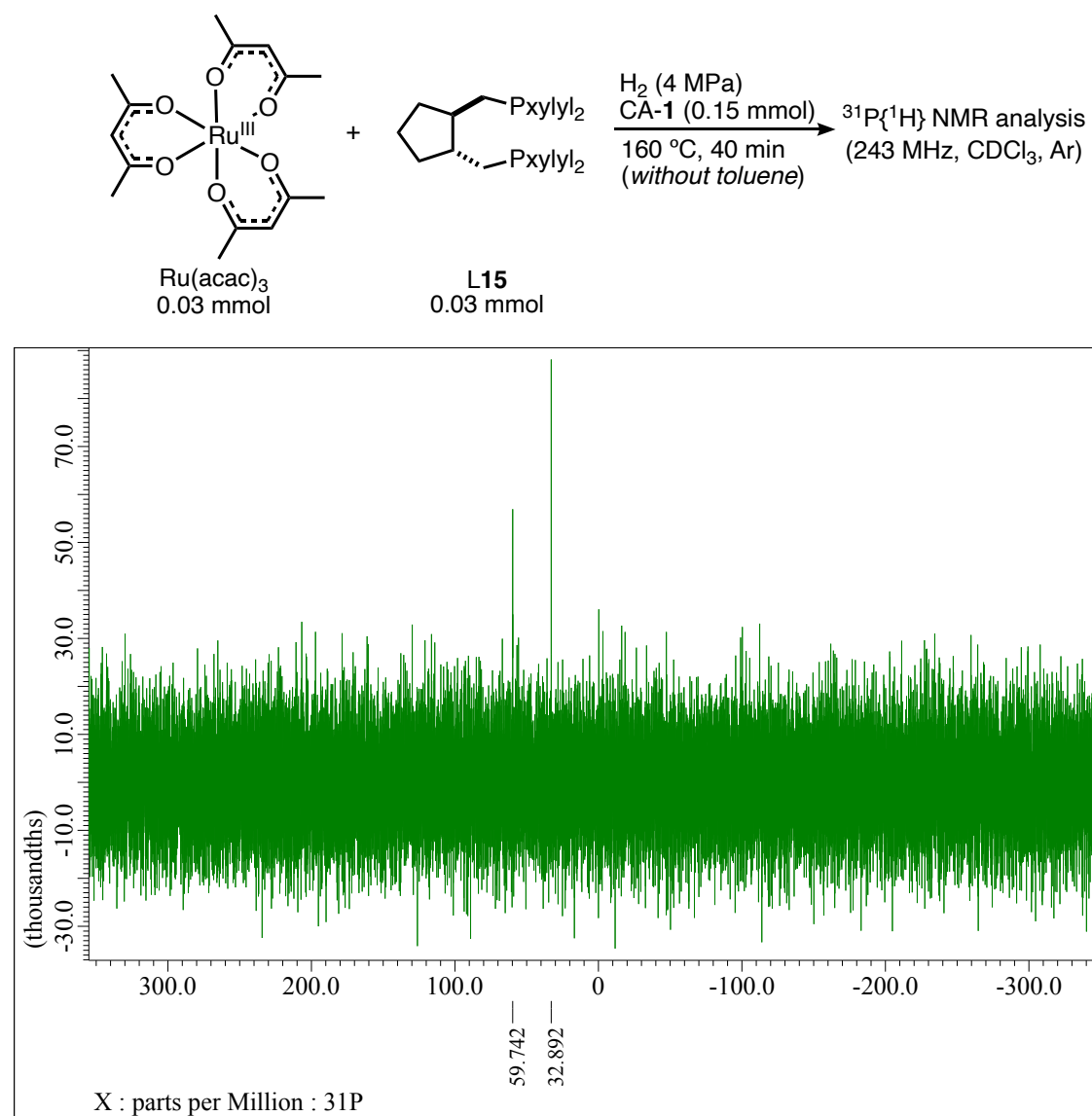


Figure S12 | $^{31}\text{P}\{^1\text{H}\}$ NMR study (243 MHz, CDCl_3 , Ar) on the pretreatment of $\text{Ru}(\text{acac})_3$ with **L15** in the presence of **CA-1** without toluene (Table 12, entry 7).

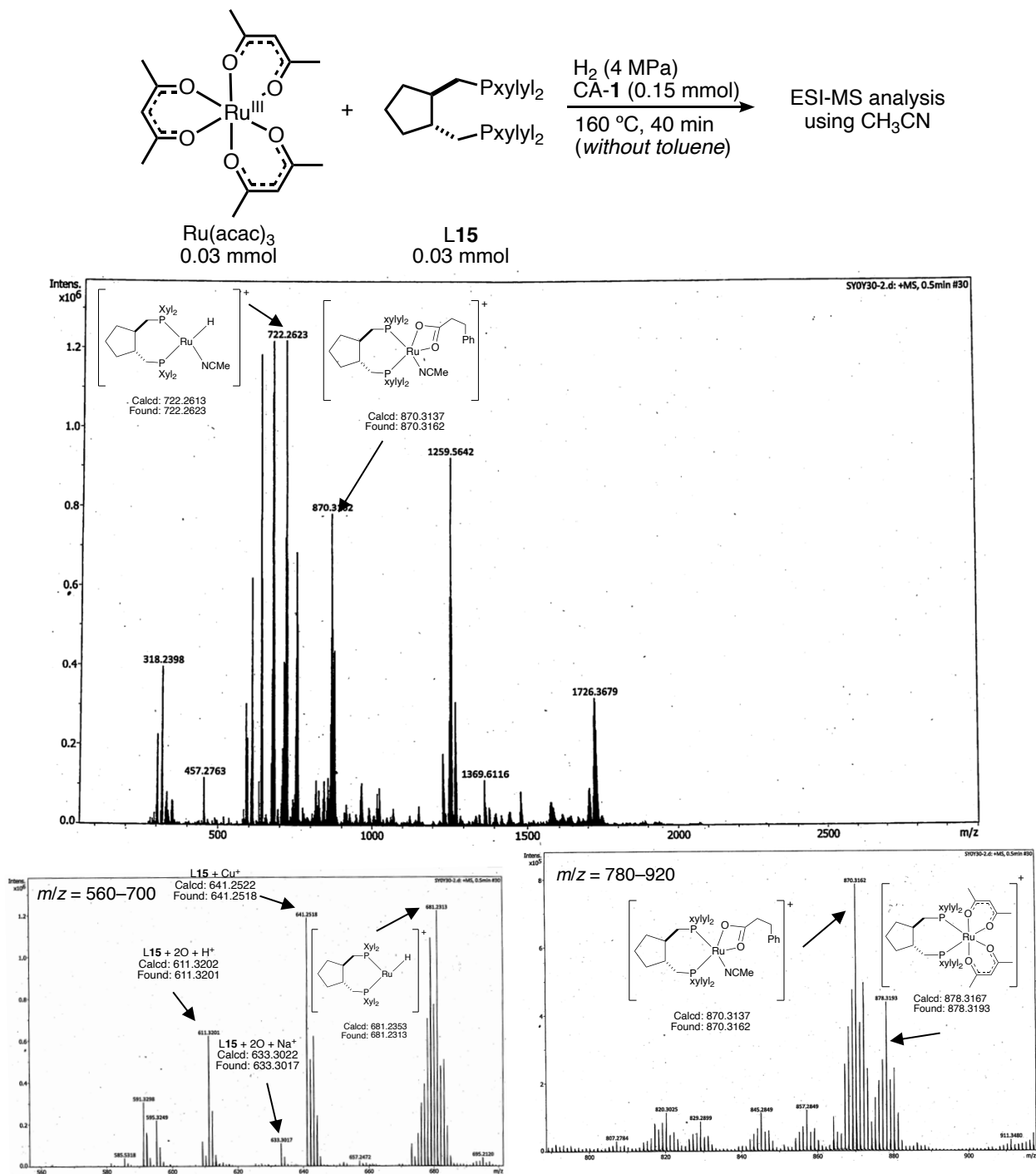


Figure S13 | ESI-MS study using CH₃CN on the pretreatment of Ru(acac)₃ with L15 in the presence of CA-1 without toluene (Table 12, entry 7).

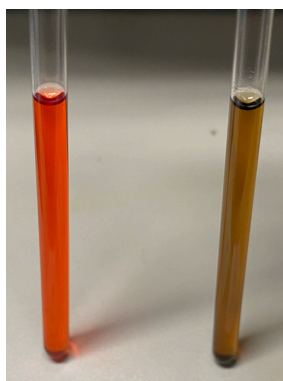


Table 6, Entry 6 Table 6, Entry 7

Figure S14 | NMR samples of entries 6 and 7 in Table 12.

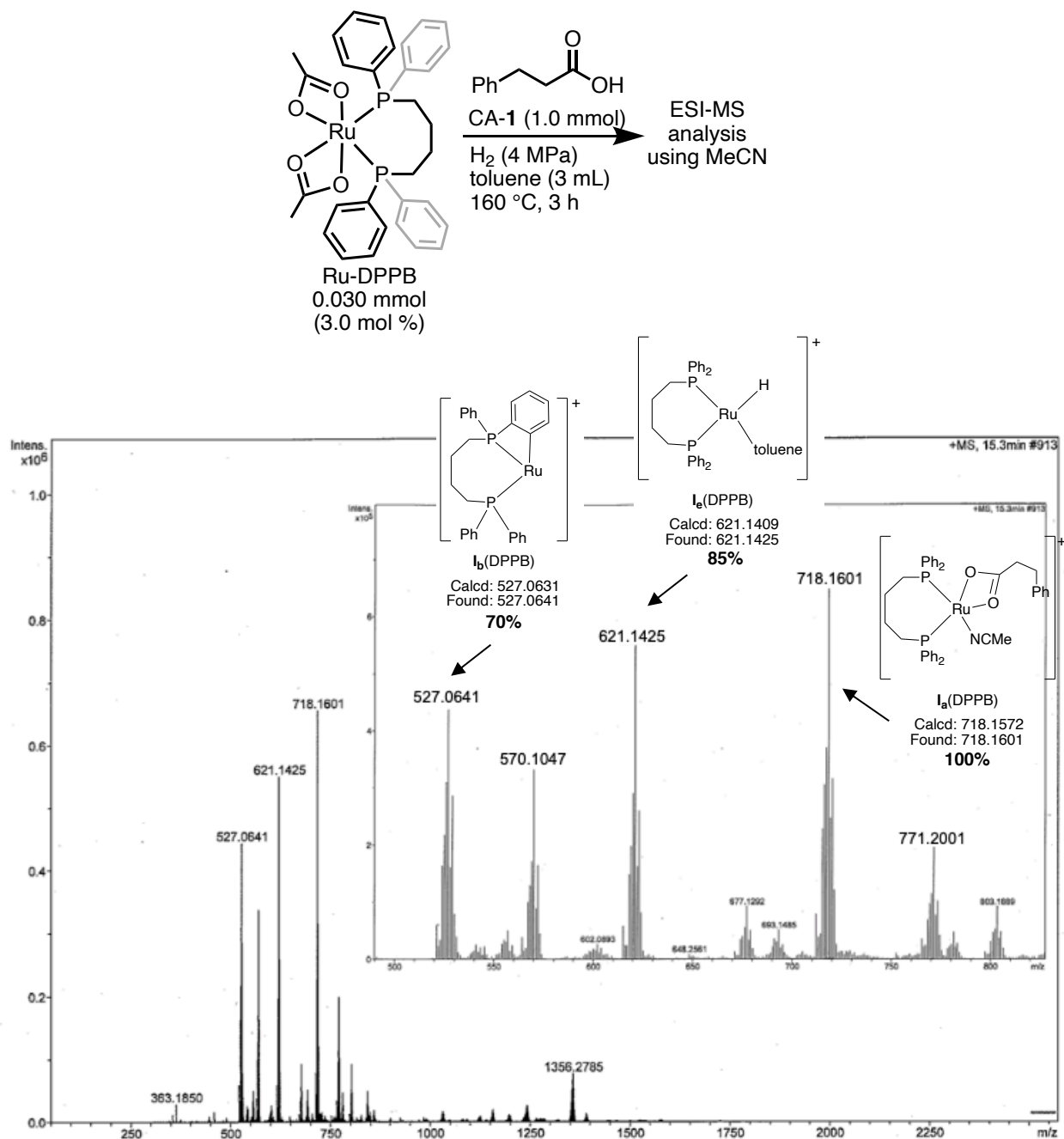


Figure S15 | ESI-MS analysis of an aliquot prepared by sampling a reaction mixture of Ru-DPPB (Figure 2B).^[24]

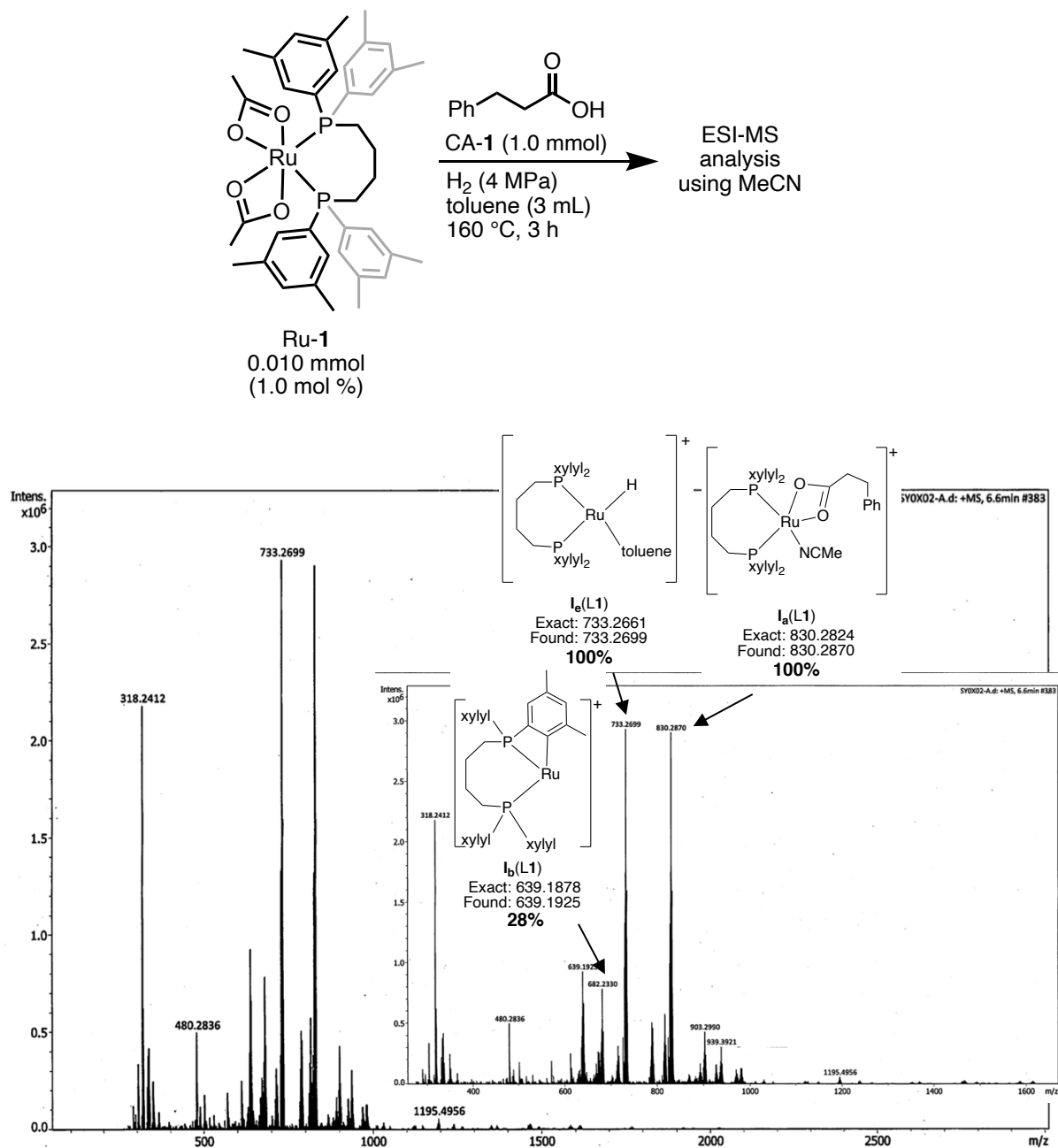


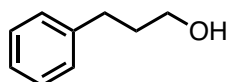
Figure S16 | ESI-MS analysis of an aliquot prepared by sampling a reaction mixture of Ru-1 (Figure 7).

1.4.4. Hydrogenation experiments

For isolation of the products, the reaction mixture was evaporated to dryness. To the resulting mixture CHCl_3 was added to dissolve all. Purification was performed using column chromatography (SiO_2 , hexane/EtOAc). For the isolation of the reaction of CA-1 and CA-9, the unreacted CAs were removed by extraction with 2 M NaOH aq before column chromatography.

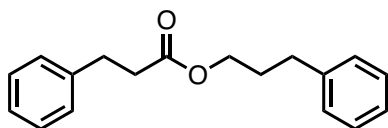
The structure of known AL-8^[50] and ES-8^[51] were determined using ^1H NMR or GC-MS analyses, which were matched with reported data. Commercially available authentic samples of AL-5, AL-8, and ES-8 were also used to confirm the structure of our products.

3-phenyl-1-propanol (AL-1)^[45]



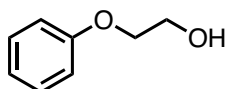
^1H NMR (600 MHz, CDCl_3): δ 7.29 (t, $J = 7.6$ Hz, 2H), 7.20 (d, $J = 8.3$ Hz, 3H), 3.68 (t, $J = 6.5$ Hz, 2H), 2.71 (t, $J = 7.9$ Hz, 2H), 1.92–1.87 (m, 2H), 1.39 (bs, 1H); $^{13}\text{C}\{^1\text{H}\}$ NMR (151 MHz, CDCl_3): δ 141.8, 128.4, 128.4, 125.9, 62.3, 34.2, 32.1.

3-phenylpropyl 3-phenylpropanoate (ES-1)^[46]



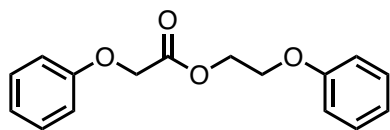
^1H NMR (600 MHz, CDCl_3): δ 7.30–7.27 (m, 4H), 7.22–7.18 (m, 4H), 7.15 (d, $J = 6.9$ Hz, 2H), 4.09 (t, $J = 6.8$ Hz, 2H), 2.95 (t, $J = 7.7$ Hz, 2H), 2.64 (t, $J = 7.1$ Hz, 2H), 1.95–1.91 (m, 2H). $^{13}\text{C}\{^1\text{H}\}$ NMR (151 MHz, CDCl_3): δ 172.9, 141.2, 140.5, 128.5, 128.4, 128.4, 128.3, 126.3, 126.0, 63.8, 35.9, 32.1, 31.0, 30.2.

2-phenoxyethanol (AL-2)^[47]



^1H NMR (600 MHz, CDCl_3): δ 7.29 (t, $J = 7.9$ Hz, 2H), 6.96 (t, $J = 7.2$ Hz, 1H), 6.91 (d, $J = 8.9$ Hz, 2H), 4.06 (t, $J = 4.5$ Hz, 2H), 3.94 (t, $J = 4.5$ Hz, 2H), 2.43 (bs, 1H). $^{13}\text{C}\{^1\text{H}\}$ NMR (151 MHz, CDCl_3): δ 158.6, 129.5, 121.1, 114.5, 69.1, 61.4.

2-phenoxyethyl 2-phenoxyacetate (ES-2)^[48]

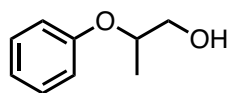


¹H NMR (600 MHz, CDCl₃): δ 7.31–7.25 (m, 4H), 7.00–6.97 (m, 2H), 6.91–6.90 (m, 4H), 4.68 (s, 2H), 4.57 (t, *J* = 4.8 Hz, 2H), 4.20 (t, *J* = 4.8 Hz, 2H).

¹³C{¹H} NMR (151 MHz, CDCl₃): δ 169.0, 158.3, 157.7, 129.6, 121.8, 121.3, 114.7, 114.6, 65.6, 65.2, 63.5.

HRMS (ESI) (*m/z*): [M+Na]⁺ calcd. for C₁₆H₁₆O₄Na⁺, 295.0941; found, 295.1003.

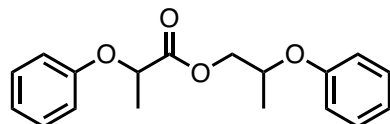
2-phenoxy-propan-1-ol (AL-3)^[14]



¹H NMR (600 MHz, CDCl₃): δ 7.30–7.25 (m, 2H), 6.97–6.92 (m, 3H). 4.52–4.47 (m, 1H), 3.77–3.69 (m, 2H), 2.14 (t, *J* = 6.2 Hz, 1H), 1.27 (d, *J* = 6.2 Hz, 3H).

¹³C{¹H} NMR (151 MHz, CDCl₃): δ 157.7, 129.6, 121.2, 116.1, 74.7, 66.3, 15.8.

2-phenoxypropyl 2-phenoxypropanoate (ES-3)

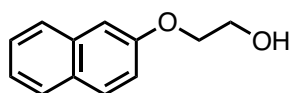


¹H NMR (600 MHz, CDCl₃): δ 7.27 (t, *J* = 7.6 Hz, 2H), 7.22 (dd, *J* = 8.9, 7.6 Hz, 1H), 7.18 (dd, *J* = 8.9, 7.6 Hz, 1H), 6.97–6.91 (m, 2H), 6.88 (d, *J* = 8.9 Hz, 2H), 6.84 (dd, *J* = 11.7, 8.9 Hz, 2H), 4.76 (qd, *J* = 7.2, 1.5 Hz, 1H), 4.61–4.54 (m, 1H), 4.38–4.34 (m, 1H), 4.23 (ddd, *J* = 11.4, 4.2, 1.2 Hz, 1H), 1.59 (dd, *J* = 8.3, 6.9 Hz, 3H), 1.27 (dd, *J* = 6.0, 3.6 Hz, 3H).

¹³C{¹H} NMR (151 MHz, CDCl₃): δ 172.1, 172.1 (diastereomer), 157.6, 157.5, 157.4 (diastereomer), 129.6, 129.5, 121.6, 121.5 (diastereomer), 121.3, 121.3 (diastereomer), 116.1, 116.0 (diastereomer), 115.0, 115.0 (diastereomer), 72.3, 72.3 (diastereomer), 71.6, 71.5 (diastereomer), 67.3, 18.6, 16.6, 16.6 (diastereomer).

HRMS (ESI) (*m/z*): [M+Na]⁺ calcd. for C₁₈H₂₀O₄Na⁺, 323.1254; found, 323.1330.

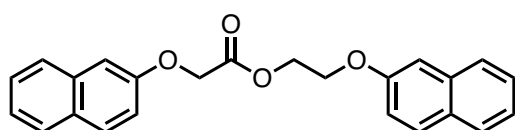
2-(naphthalene-2-yloxy)-ethanol (AL-4)^[14]



¹H NMR (600 MHz, CDCl₃): δ 7.78–7.72 (m, 3H), 7.45 (t, *J* = 7.6 Hz, 1H), 7.35 (t, *J* = 7.6 Hz, 1H), 7.18–7.17 (m, 1H), 7.16–7.15 (m, 1H), 4.21 (t, *J* = 4.5 Hz, 2H), 4.05–4.02 (m, 2H), 2.08 (t, *J* = 6.2 Hz, 1H).

¹³C{¹H} NMR (151 MHz, CDCl₃): δ 156.5, 134.4, 129.5, 129.1, 127.7, 126.8, 126.5, 123.8, 118.7, 106.8, 69.2, 61.5.

2-(naphthalen-2-yloxy)ethyl 2-(naphthalen-2-yloxy)acetate (ES-4)

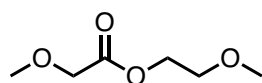


¹H NMR (600 MHz, CDCl₃): δ 7.78 (d, *J* = 8.3 Hz, 1H), 7.74 (d, *J* = 8.9 Hz, 3H), 7.71 (d, *J* = 8.2 Hz, 1H), 7.62 (d, *J* = 7.6 Hz, 1H), 7.45 (t, *J* = 7.6 Hz, 2H), 7.38–7.32 (m, 3H), 7.23 (dd, *J* = 8.9, 2.8 Hz, 1H), 7.14–7.10 (m, 2H), 7.07 (d, *J* = 2.8 Hz, 1H), 4.82 (s, 2H), 4.67 (t, *J* = 4.8 Hz, 2H), 4.32 (t, *J* = 4.5 Hz, 2H).

¹³C{¹H} NMR (151 MHz, CDCl₃): δ 168.9, 156.3, 155.7, 134.4, 134.2, 129.8, 129.6, 129.4, 129.2, 127.7, 127.6, 126.9, 126.8, 126.5, 124.1, 123.9, 118.7, 118.6, 107.1, 106.8, 65.7, 65.3, 63.5, one carbon atom was not found probably due to overlapping.

HRMS (ESI) (*m/z*): [M+Na]⁺ calcd. for C₂₄H₂₀O₄Na⁺, 395.1254; found, 395.1245.

2-methoxyethyl 2-methoxyacetate (ES-5)

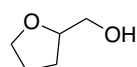


¹H NMR (400 MHz, CDCl₃): δ 4.33 (t, *J* = 4.4 Hz, 2H), 4.09 (s, 2H), 3.62 (t, *J* = 4.4 Hz, 2H), 3.46 (s, 3H), 3.39 (s, 3H).

¹³C{¹H} NMR (100 MHz, CDCl₃): δ 170.3, 70.3, 69.7, 63.7, 59.4, 59.0.

HRMS (FAB) (*m/z*): [M+H]⁺ calcd. for C₆H₁₃O₄⁺, 149.0808; found, 149.0874.

(tetrahydrofuran-2-yl)methanol (AL-6)^[14]

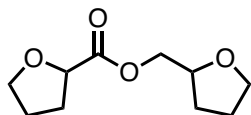


¹H NMR (600 MHz, CDCl₃): δ 4.04–4.00 (m, 1H), 3.89–3.85 (m, 1H), 3.81–3.78 (m, 1H), 3.69–3.66 (m, 1H), 3.52–3.48 (m, 1H), 2.30 (t, *J* = 6.2 Hz, 1H), 1.96–1.88 (m, 3H), 1.70–1.61

(m, 1H).

$^{13}\text{C}\{^1\text{H}\}$ NMR (151 MHz, CDCl_3): δ 79.4, 68.3, 64.9, 27.1, 26.1.

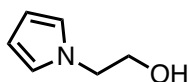
(tetrahydrofuran-2-yl)methyl tetrahydrofuran-2-carboxylate (ES-6)^[48]



^1H NMR (600 MHz, CDCl_3): δ 4.52–4.50 (m, 1H), 4.24–4.4.20 (m, 1H), 4.16–4.12 (m, 1H), 4.10–4.07 (m, 1H), 4.06–4.01 (m, 1H), 3.94–3.91 (m, 1H), 3.90–3.86 (m, 1H), 3.82–3.78 (m, 1H), 2.30–2.24 (m, 1H), 2.07–1.87 (m, 6H), 1.65–1.58 (m, 1H).

$^{13}\text{C}\{^1\text{H}\}$ NMR (141 MHz, CDCl_3): δ 170.3, 70.3, 69.7, 63.7, 59.4, 59.0.

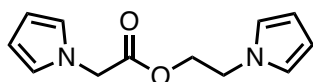
2-pyrrol-1-yl-ethanol (AL-7)^[49]



^1H NMR (600 MHz, CDCl_3): δ 6.71 (t, $J = 2.1$ Hz, 2H), 6.18 (t, $J = 1.8$ Hz, 2H), 4.02 (t, $J = 5.2$ Hz, 2H), 3.85 (dd, $J = 10.3, 5.5$ Hz, 2H), 1.67 (t, $J = 6.2$ Hz, 1H).

$^{13}\text{C}\{^1\text{H}\}$ NMR (151 MHz, CDCl_3): δ 120.9, 108.6, 63.0, 52.0.

2-(1H-pyrrol-1-yl)ethyl 2-(1H-pyrrol-1-yl)acetate (ES-7)

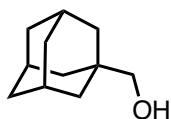


^1H NMR (600 MHz, CDCl_3): δ 6.63 (t, $J = 2.0$ Hz, 2H), 6.60 (t, $J = 2.4$ Hz, 2H), 6.21 (t, $J = 2.1$ Hz, 2H), 6.16 (t, $J = 2.1$ Hz, 2H), 4.62 (s, 2H), 4.38 (t, $J = 5.5$ Hz, 2H), 4.11 (t, $J = 5.2$ Hz, 2H).

$^{13}\text{C}\{^1\text{H}\}$ NMR (151 MHz, CDCl_3): δ 168.4, 121.8, 120.9, 109.2, 108.8, 65.0, 50.7, 47.9.

HRMS (ESI) (m/z): $[\text{M}+\text{Na}]^+$ calcd. for $\text{C}_{12}\text{H}_{14}\text{O}_2\text{N}_2\text{Na}^+$, 241.0947; found, 241.0989.

1-adamantanemethanol (AL-9)^[50]



^1H NMR (400 MHz, CDCl_3): δ 3.19 (s, 2H), 2.01–1.95 (m, 3H), 1.76–1.72 (m, 1H), 1.72–1.68 (m, 2H), 1.67–1.64 (m, 2H), 1.63–1.60 (m, 1H), 1.51–1.48 (m, 6H), 1.25 (bs, 1H).

$^{13}\text{C}\{^1\text{H}\}$ NMR (151 MHz, CDCl_3): δ 73.9, 39.0, 37.2, 34.5, 28.2.

General procedure for hydrogenation of 3-phenylpropionic acid with Ru(acac)₃ and phosphine ligand.

3-phenylpropionic acid (CA-1, 150.2 mg, 1.0 mmol), Ru(acac)₃, phosphine ligand, and a magnetic stirring bar were placed in a glass tube (21 mL capacity). The glass tube was inserted into an autoclave, which was closed tightly, and refilled with Ar. To the mixture was added anhydrous toluene (3 mL) under a continuous flow of Ar atmosphere. The autoclave was purged 10 times with H₂ gas (ca. 1 MPa). The autoclave was pressurized with 4 MPa of H₂ gas at room temperature and heated at 160 °C for desired reaction time under stirring (500 rpm). The autoclave was cooled to room temperature in an ice–water (0 °C) bath. The reaction mixture was transferred into a 100 mL round bottom flask with CHCl₃ and concentrated under a reduced pressure (ca. 35 mmHg, 40 °C). The residue was dissolved in CDCl₃ and analyzed by ¹H NMR. The yields of AL-1 and ES-1 were calculated based on the integral ratio among the signals of these compounds with respected to an internal standard (mesitylene).

Representative procedure for the pretreatment of Ru(acac)₃ (Scheme 1).

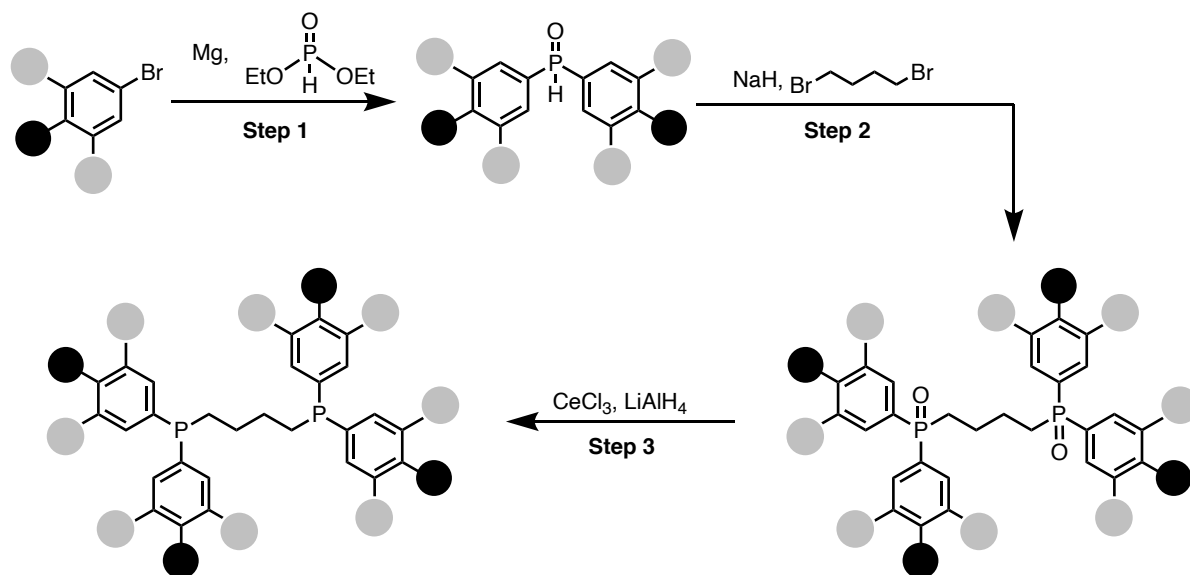
Ru(acac)₃ (4.0 mg, 0.01 mmol), L1 (5.4 mg, 0.01 mmol), CA-1 (7.5 mg, 0.05 mmol), and a magnetic stirring bar were placed in a glass tube (21 mL capacity). The glass tube was inserted into an autoclave, which was closed tightly, and refilled with Ar. To the mixture was added anhydrous toluene (1 mL) under a continuous flow of Ar atmosphere. The autoclave was purged 10 times with H₂ gas (ca. 1 MPa) and pressurized with 4 MPa of H₂ gas at room temperature and heated at 160 °C for 40 min under stirring (500 rpm). After the autoclave was cooled to room temperature in a water bath, hydrogen was blown away under an Ar stream using a three-way cock. To the resulting autoclave was added 475 mM toluene solution of CA-1 (2 mL, 0.95 mmol) under the continuous Ar flow. The autoclave, which was closed tightly, was pressurized with 4 MPa of H₂ gas at room temperature and heated at 160 °C for 18 h time under stirring (500 rpm). The autoclave was cooled to room temperature in an ice–water (0 °C) bath. The reaction mixture was transferred into a 100 mL round bottom flask with CHCl₃ and concentrated under a reduced pressure (ca. 35 mmHg, 40 °C). The residue was dissolved in CDCl₃ and analyzed by ¹H NMR. The yields of AL-1 (80%) and ES-1 (6%) were calculated based on the integral ratio among the signals of these compounds with respected to an internal standard (mesitylene).

Representative procedure for NMR study on hydrogenation of Ru(acac)₃.

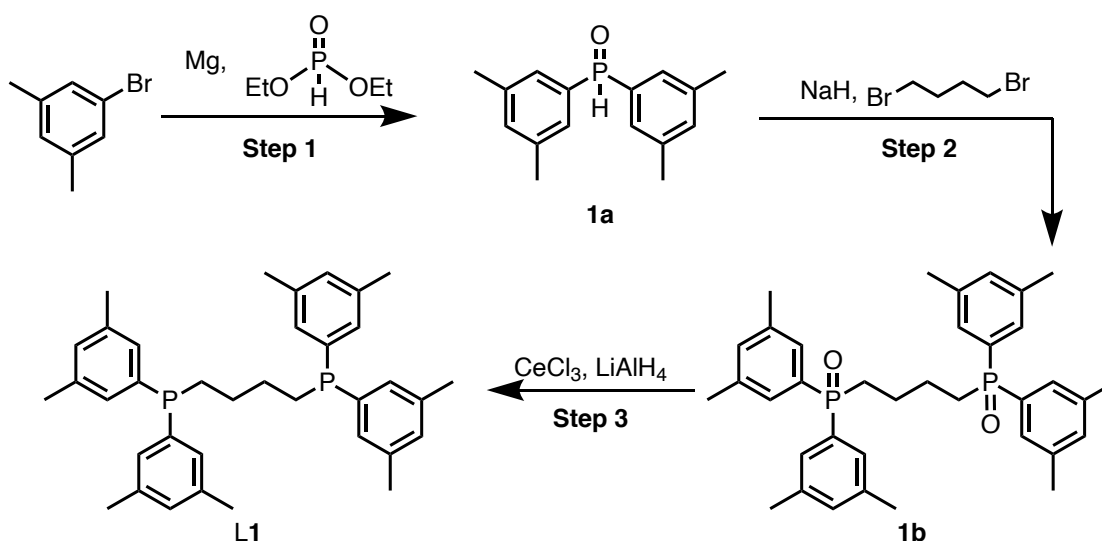
Ru(acac)₃ (12.0 mg, 0.03 mmol), DPPB (12.8 mg, 0.03 mmol), CA-1 (22.5 mg, 0.15 mmol), and a magnetic stirring bar were placed in a glass tube (21 mL capacity). The glass tube was inserted into an autoclave, which was closed tightly, and refilled with Ar. To the mixture was added anhydrous toluene (3 mL) under a continuous flow of Ar atmosphere. The autoclave was purged 10 times with H₂ gas (ca. 1 MPa). The autoclave was pressurized with 4 MPa of H₂ gas at room temperature and heated at 160 °C for 40 min under stirring (500 rpm). The autoclave was cooled to room temperature in an ice–water (0 °C) bath. The reaction mixture was diluted with CDCl₃ and analyzed by ³¹P{¹H} NMR (243 MHz) under Ar atmosphere. The relative intensity of unreacted DPPB, (dppb)Ru^{II}(acac)₂, and oxidized dppb was calculated based on the integral ratio among the signals of these compounds.

1.4.5. Ligand preparation (L1–L6)

General synthetic scheme



Synthesis of 1,4-bis[bis(3,5-dimethylphenyl)phosphino]butane (L1).



(Step 1) Bis(3,5-dimethylphenyl)phosphine oxide^[26]

Mg turnings (658.2 mg, 27 mmol) and a magnetic stirrer bar were placed in a 100 mL three-necked flask under Ar flow. THF (5 mL) and a small amount of I_2 (one bead) were added in and the mixture was stirred for 30 min at ambient temperature. A THF solution (20 mL) of 5-bromo-*m*-xylene (3.7 mL, 27 mmol) was added dropwise into the flask at 25 °C (water bath) for 1.5 h. Then, the solution was stirred at 40 °C (oil bath) for 30 min. After that, THF solution (5 mL) of diethyl phosphite (1.16 mL, 9 mmol) was added dropwise over ca. 30 min. at 25 °C (water bath) and stirred at room temperature for 15 h. The reaction was quenched with 5.9 M

aq. of K_2CO_3 (5 mL) at 0 °C, and stirred at room temperature for 30 min. Then, the mixture was filtrated through a pad of celite using ethanol as eluent. The solvent was removed under reduced pressure, then CHCl_3 (ca. 30 mL) and activated molecular sieves 4A were added to the residue, stirred for 2 h at room temperature and filtered through celite using CHCl_3 as eluent. Removing the solvent under reduced pressure yielded the product as a white solid (1.49 g, 64% yield). ^1H NMR (600 MHz, CDCl_3) δ 7.32 (s, 4H), 7.30 (s, 4H), 7.18 (s, 4H), 2.35 (s, 12H); $^{31}\text{P}\{^1\text{H}\}$ NMR (243 MHz, CDCl_3) δ 23.4.

(Step 2) Butane-1,4-diylbis[bis(3,5-dimethylphenyl)phosphine oxide]

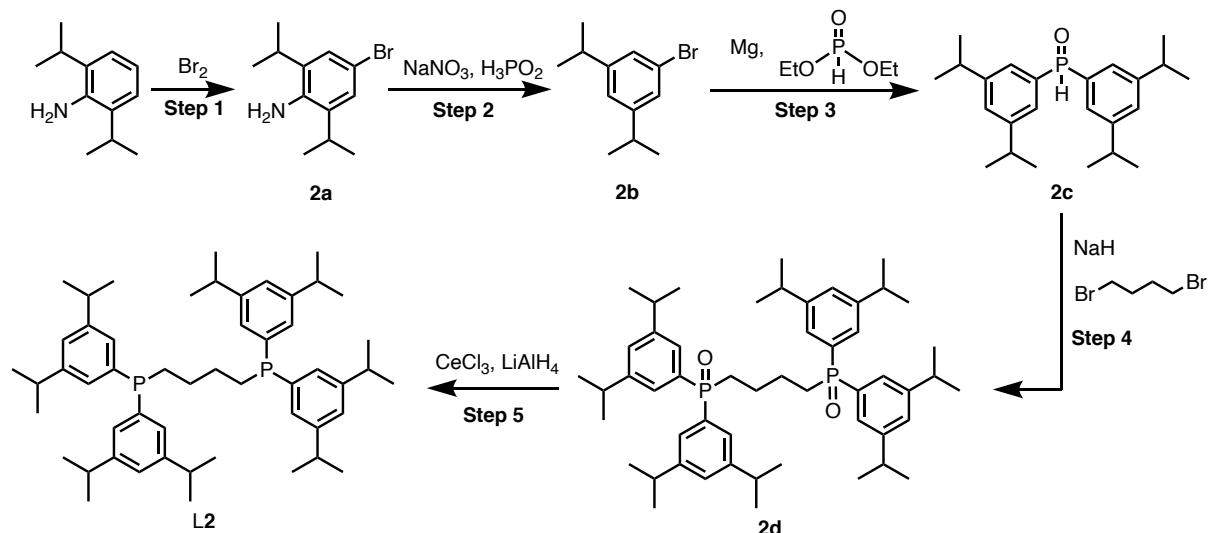
To a 200 mL two-necked flask were added bis(3,5-dimethylphenyl)phosphine oxide (1.29 g, 5.0 mmol), THF (50 mL), and a magnetic stirrer bar. NaH (0.22 g, 5.0 mmol) was added to the solution under Ar flow at room temperature and stirred for 1 h. Then, 1,4-dibromobutane (267 μL , 2.2 mmol) was added to the mixture dropwise. After stirring for 17 h, the crude product was collected by filtration, washed with water. After purification with recrystallization (methanol), the pure product was obtained as white solid (0.68 g, 57% yield). ^1H NMR (600 MHz, CDCl_3) δ 7.30 (s, 4H), 7.28 (s, 4H), 7.11 (s, 4H), 2.32 (s, 24H), 2.19 (dd, 4H, $J = 15.8$, 11.7 Hz), 1.69 (m, 4H); $^{31}\text{P}\{^1\text{H}\}$ NMR (243 MHz, CDCl_3) δ 32.9; $^{13}\text{C}\{^1\text{H}\}$ NMR (151 MHz, CDCl_3): δ 138.3 (d, $J = 13.0$ Hz), 133.3 (d, $J = 7.23$ Hz), 130.4, 130.3 (d, $J = 8.7$ Hz), 27.8 (d, $J = 15.9$ Hz), 27.6 (d, $J = 11.6$ Hz), 21.3.

(Step 3) 1,4-Bis[bis(3,5-dimethylphenyl)phosphino]butane (L1)

Smashed $\text{CeCl}_3 \cdot 7\text{H}_2\text{O}$ (1.5 mmol, 559 mg) and a magnetic stirrer bar were added to a 30 mL two-necked flask and dried *in vacuo* at 140 °C for 2 h. After cooling to ambient temperature, THF (5 mL) and butane-1,4-diylbis[bis(3,5-dimethylphenyl)phosphine oxide] (0.5 mmol, 270 mg) were added to the flask at once and the resulting mixture was stirred for 30 min. Then, the mixture was cooled to 0 °C, before LiAlH_4 (3 mmol, 113 mg) was added portionwise. The resulting mixture was stirred at room temperature for 1 h, then at 40 °C for 24 h. At 0 °C, 35% HCl aq. (1.0 mL) and H_2O (5 mL) were added in this order to the mixture to quench the reaction. The mixture was extracted with toluene (25 mL). The organic layer was collected and dried over Na_2SO_4 , and concentrated under reduced pressure. The crude product was purified with chromatography (eluent; AcOEt/hexane = 1/10), and recrystallized with CH_3OH to give L1 as white solid (47% yield, 119 mg). ^1H NMR (600 MHz, CDCl_3) δ 7.01 (s, 4H), 7.00 (s, 4H), 6.93 (s, 4H), 2.27 (s, 24H), 1.98 (t, 4H, $J = 7.2$ Hz), 1.54 (m, 4H); $^{31}\text{P}\{^1\text{H}\}$ NMR (243 MHz, CDCl_3) δ -15.8; $^{13}\text{C}\{^1\text{H}\}$ NMR (151 MHz, CDCl_3): δ 133.6 (d, $^3J_{\text{PC}} = 13.0$ Hz), 137.7 (d, $^1J_{\text{PC}} = 7.2$ Hz), 130.4, 130.3 (d, $^2J_{\text{PC}} = 8.7$ Hz), 27.7 (dd, $^{2,3}J_{\text{PC}} = 15.9$ Hz), 27.6 (d, $^1J_{\text{PC}} = 11.6$ Hz), 21.3.

HRMS (ESI, (M+H)⁺) Calcd for C₃₆H₄₅P₂⁺: 539.2991, Found *m/z* = 529.2974.

Synthesis of 1,4-bis[bis(3,5-diisopropylphenyl)phosphino]butane (L2).



(Step 1) 4-Bromo-2,6-diisopropylaniline (2a)

4-Bromo-2,6-diisopropylaniline was synthesized using typical procedure.^[35] Under air, a solution of 2,6-diisopropylaniline (12 mL, 66 mmol) in methanol (250 mL) was treated dropwise with bromine (3.6 mL, 70 mmol). The solution was stirred at room temperature for 30 min. Chloroform (150 mL) and 0.1 N NaOH (200 mL) were added and the organic layer was dried (Na₂SO₄), filtered and concentrated to a brack liquid. Column chromatography on silica gel (eluent; AcOEt/hexane = 1/10) afforded a colorless liquid **2a** (7.61 g, 43%). The spectral data were consistent with the literature.^[35]

(Step 2) 1-Bromo-3,5-diisopropylbenzene (2b)

1-Bromo-3,5-diisopropylbenzene was synthesized using typical procedure.^[36] In 300 mL a round bottom flask, **2a** (6.41 g, 25 mmol) was dispersed in 2 M HCl aq (100 mL) and cooled to 5 °C. NaNO₂ (4.35 g, 63 mmol) was added in small portions. After stirring for 10 minutes at this temperature, 50 % H₃PO₂ aq (30 mL, 250 mmol) was added. The reaction was then stirred for overnight at 0 °C and one day at room temperature. The biphasic mixture was extracted three times with AcOEt (50 mL) and the organic layer was dried over MgSO₄. Removing the solvent in vacuum yielded **2b** as yellow oil (1.206 g, 4.1 mmol, 82 %). The spectral data were consistent with the literature.^[36]

(Step 3) Bis(3,5-diisopropylphenyl)phosphine oxide (2c)

Mg turnings (535 mg, 24 mmol) and a magnetic stirrer bar were placed in a 200 mL three-

necked flask under Ar flow. THF (4 mL) and a small amount of I₂ (one bead) were added in and the mixture was stirred for 30 min at ambient temperature. A THF solution (18 mL) of **2b** (4.8 g, 20 mmol) was added dropwise into the flask at 25 °C (water bath) for 1.5 h. Then, the solution was stirred at 40 °C (oil bath) for 40 min. After that, THF solution (8 mL) of diethyl phosphite (1.12 g, 8 mmol) was added dropwise over ca. 30 min. at 25 °C (water bath) and stirred at r.t. for 15 h. The reaction was quenched with 5.9 M aq. of K₂CO₃ (4 mL) at 0 °C, and stirred at r.t. for 30 min. Then, the mixture was filtrated through Celite[®] using ethanol (ca. 300 mL) as eluent. The solvent was removed under reduced pressure, then CHCl₃ (70 mL) and activated molecular sieves 4A were added to the residue, stirred for 2 h at r.t. and filtered through Celite[®] using CHCl₃ as eluent. Removing the solvent under reduced pressure yielded **2c** as white solid (1.77 g, 60 % yield). ³¹P{¹H} NMR (243 MHz, CDCl₃) δ 23.2 (s).

(Step 4) Butane-1,4-diylbis[bis(3,5-diisopropylphenyl)phosphine oxide] (**2d**)

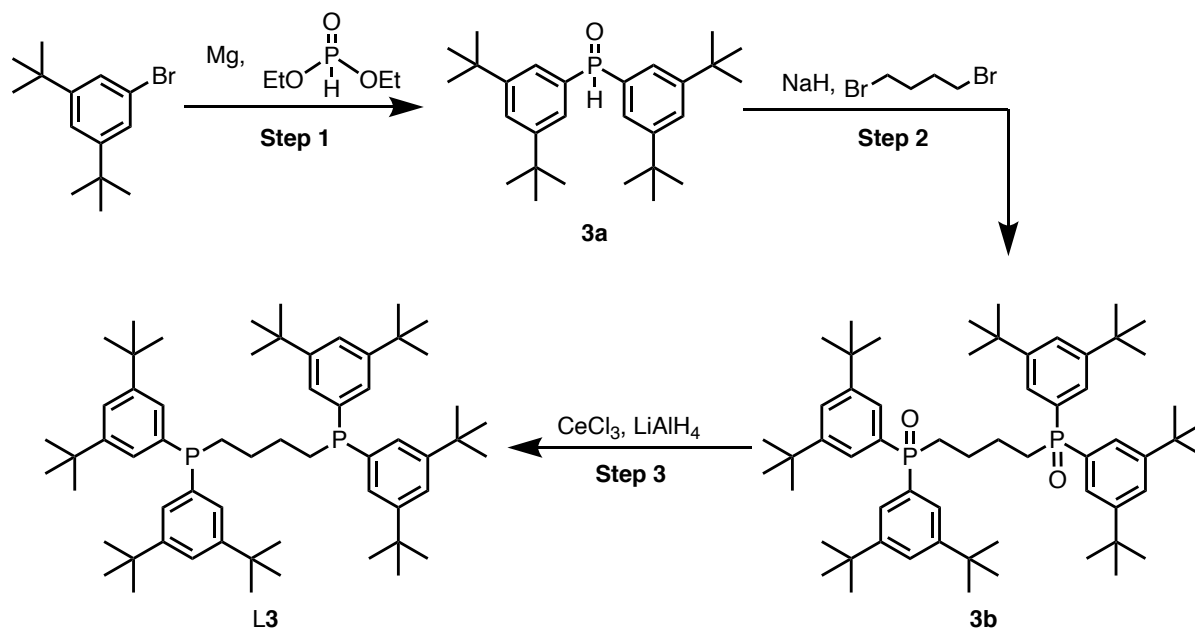
To a 100 mL two-necked flask were added **2c** (1.39 g, 3.8 mmol), THF (20 mL), and a magnetic stirrer bar. NaH (199 mg, 4.5 mmol) was added to the solution under Ar flow at r.t. and stirred for 1 h. Then, 1,4-dibromobutane (239 μL, 2 mmol) was added to the mixture dropwise. After stirring for 12 h, THF was removed under reduced pressure, the resulting white solid was dissolved in water (50 mL) and extracted with CH₂Cl₂ (30 × 4 mL). The organic layer was collected and dried over Na₂SO₄, and concentrated under reduced pressure. The crude product was purified by chromatography (AcOEt/hexane = 10/1) to give **2d** as a white solid (72% yield, 1.15 g). ³¹P{¹H} NMR (202 MHz, CDCl₃) δ 35.6.

(Step 5) 1,4-Bis[bis(3,5-diisopropylphenyl)phosphino]butane (**L2**)

Grinded CeCl₃·7H₂O (9.0 mmol, 3.37 g) and a magnetic stirrer bar were added to a 100 mL two-necked flask and dried *in vacuo* at 140 °C for 2 h. After cooling to ambient temperature, THF (13 mL) and **2d** (0.96 g, 2.0 mmol) were added to the flask at once and the resulting mixture was stirred for 30 min. Then, the mixture was cooled to 0 °C, before LiAlH₄ (0.68 g, 18 mmol) was added portionwise. The resulting mixture was stirred at r.t. overnight. At 0 °C, H₂O (0.7 mL), 2 M NaOH aq (1.4 mL), and H₂O (3.5 mL) were added in this order to the mixture to quench the reaction. The resulting mixture was filtered through Celite[®] using CHCl₃ as eluent. The filtrate was concentrated under reduced pressure. The resulting product was extracted with CH₂Cl₂ and the organic layer as dried over Na₂SO₄, and concentrated under reduced pressure. The crude product was purified with Florisil chromatography using hexane as eluent to give **L2** as white solid (28% yield, 0.26 g). ¹H NMR (600 MHz, CDCl₃) δ 7.1 (d, 4H, *J* = 2.0 Hz), 7.07 (d, 4H, *J* = 1.4 Hz), 7.00 (s, 4H), 2.84 (m, 8H, *CH*), 2.03 (t, 4H, *J* = 7.2

Hz, CCH_2C), 1.60 (m, 4H, PCH_2), 1.20 (d, 48H $J = 6.8$ Hz, CH_3); $^{31}\text{P}\{^1\text{H}\}$ NMR (243 MHz, CDCl_3) $\delta -14.3$; $^{13}\text{C}\{^1\text{H}\}$ NMR (151 MHz, CDCl_3): δ 148.6 (d, $^3J_{\text{PC}} = 5.8$ Hz), 138.2 (d, $^1J_{\text{PC}} = 13.0$ Hz), 128.2 (d, $^2J_{\text{PC}} = 18.8$ Hz), 125.0, 34.2, 28.2 (d, $^1J_{\text{PC}} = 11.6$ Hz), 28.0 (dd, $^{2,3}J_{\text{PC}} = 15.2$ Hz), 24.0, 24.0; HRMS (ESI, $(\text{M}+\text{H})^+$) Calcd for $\text{C}_{52}\text{H}_{77}\text{P}_2^+$: 763.5495, Found $m/z = 763.5506$.

Synthesis of 1,4-bis[bis(3,5-di(*tert*-butyl)phenyl)phosphino]butane (L3).



(Step 1) Bis(3,5-di(*tert*-butyl)phenyl)phosphine oxide (3a)

Mg turnings (1.10 g, 45 mmol) and a magnetic stirrer bar were placed in a 300 mL three-necked flask under Ar flow. THF (9 mL) and a small amount of I_2 (one bead) were added in and the mixture was stirred for 30 min at ambient temperature. A THF solution (30 mL) of 1-bromo-3,5-di-*tert*-butylbenzene (11.3 g, 42 mmol) was added dropwise into the flask at 25 °C (water bath) for 1.5 h. Then, the solution was stirred at 40 °C (oil bath) for 30 min. After that, THF solution (30 mL) of diethyl phosphite (1.93 mL, 15 mmol) was added dropwise over ca. 30 min. at 25 °C (water bath) and stirred at r.t. for 15 h. The reaction was quenched with 5.9 M aq. of K_2CO_3 (7.8 mL) at 0 °C, and stirred at r.t. for 30 min. Then, the mixture was filtrated through Celite[®] using ethanol as eluent. The solvent was removed under reduced pressure, then CHCl_3 (150 mL) and activated molecular sieves 4A were added to the residue, stirred for 2 h at r.t. and filtered through Celite[®] using CHCl_3 as eluent. Removing the solvent under reduced pressure yielded **3a** as white solid (5.81 g, 91% yield). ^1H NMR (600 MHz, CDCl_3) δ 8.08 (d, 1H, $J = 475$ Hz), 7.61 (d, 2H, $J = 2.1$ Hz), 7.55 (d, 2H, $J = 1.4$ Hz), 7.53 (d, 2H, $J = 1.4$ Hz),

1.31 (s, 36H, CH₃); ³¹P{¹H} NMR (243 MHz, CDCl₃) δ 24.4.

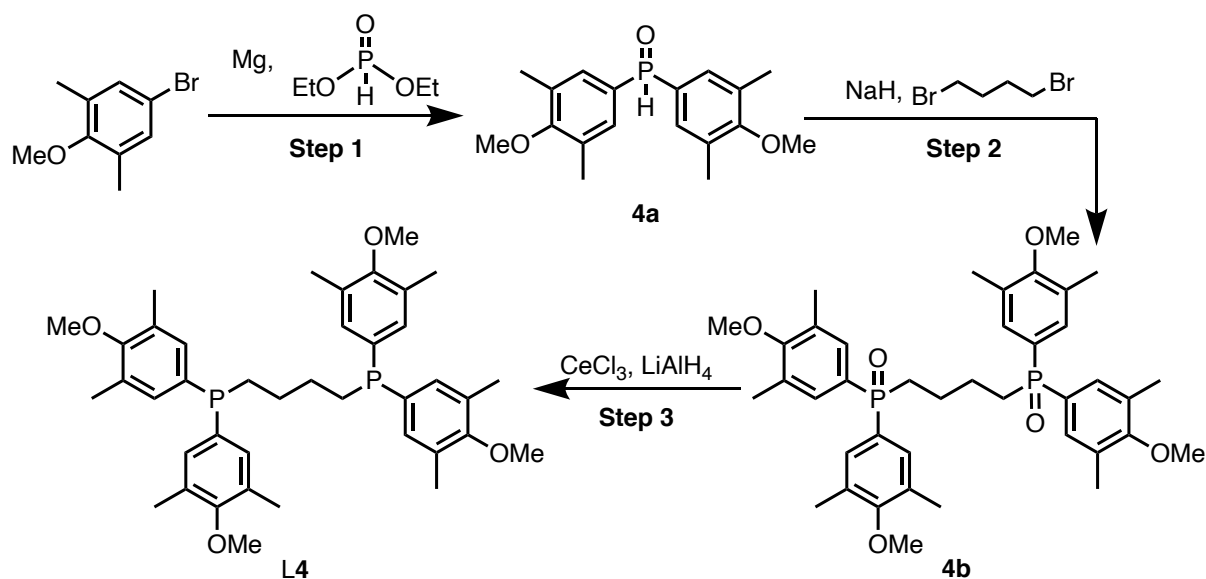
(Step 2) Butane-1,4-diylbis[bis(3,5-di(*tert*-butyl)phenyl)phosphine oxide] (**3b**)

To a 300 mL two-necked flask were added **3a** (8.5 g, 20 mmol), THF (50 mL), and a magnetic stirrer bar. NaH (1.1 g, 24 mmol) was added to the solution under Ar flow at r.t. and stirred for 0.5 h. Then, 1,4-dibromobutane (2.16 g, 10 mmol) was added to the mixture dropwise. After stirring for 16 h, THF was removed under reduced pressure, the resulting white solid was dissolved in water (70 mL) and extracted with CH₂Cl₂ (150 mL). The organic layer was collected and dried over Na₂SO₄, and concentrated under reduced pressure. The crude product was purified by chromatography (AcOEt:hexane = 10:1) to give **3b** as a white solid (35% yield, 3.16 g). ¹H NMR (600 MHz, CDCl₃) δ 7.55 (s, 4H, C₆H₃), 7.53 (s, 4H, C₆H₃), 7.51 (d, 4H, *J* = 1.4 Hz, C₆H₃), 2.21 (m, 4H, CH₂), 1.74 (br, 4H, PCH₂), 1.29 (s, 72H, CH₃); ³¹P{¹H} NMR (243 MHz, CDCl₃) δ 34.7; ¹³C{¹H} NMR (151 MHz, CDCl₃): δ 151.0 (d, *J* = 11.6 Hz), 150.6, 132.3, 131.7, 127.6, 126.4 (d, *J* = 10.1 Hz), 125.8, 124.9 (d, *J* = 10.1 Hz), 122.4, 122.2, 35.0, 31.5, 31.4, 30.5, 30.1, 29.7, 23.2 (d, *J* = 14.5 Hz).

(Step 3) 1,4-Bis[bis(3,5-di(*tert*-butyl)phenyl)phosphino]butane (**L3**)

Grinded CeCl₃·7H₂O (22.5 mmol, 8.4 g) and a magnetic stirrer bar were added to a 300 mL two-necked flask and dried *in vacuo* at 140 °C for 2 h. After cooling to ambient temperature, THF (35 mL) and **3b** (3.0 mmol, 2.7 g) were added to the flask at once and the resulting mixture was stirred for 30 min. Then, the mixture was cooled to 0 °C, before LiAlH₄ (54 mmol, 2.1 g) was added portionwise. The resulting mixture was stirred at r.t. for 16 h. At 0 °C, H₂O (2.1 mL), 2 M NaOH aq (4.2 mL), and H₂O (6.3 mL) were added in this order to the mixture to quench the reaction. The resulting mixture was filtered through Celite[®] using CHCl₃ as eluent. The filtrate was concentrated under reduced pressure. The resulting product was extracted with CH₂Cl₂ and the organic layer as dried over Na₂SO₄, and concentrated under reduced pressure. The crude product was purified with Florisil chromatography (AcOEt : hexane, 1:100) to give **L3** as white solid (62% yield, 1.69 g). ¹H NMR (600 MHz, CDCl₃) δ 7.35 (t, 4H, *J* = 2.4 Hz, C₆H₃), 7.24 (d, 4H, *J* = 2.0 Hz, C₆H₃), 7.22 (d, 4H, *J* = 1.4 Hz, C₆H₃), 2.05 (t, 4H, *J* = 7.6 Hz, CH₂), 1.65 (m, 4H, CH₂), 1.26 (s, 72H, CH₃); ³¹P{¹H} NMR (243 MHz, CDCl₃) δ -13.2; ¹³C{¹H} NMR (151 MHz, CDCl₃): δ 150.4 (d, ³*J*_{PC} = 7.2 Hz), 137.3 (d, ¹*J*_{PC} = 13.6 Hz), 126.8 (d, ²*J*_{PC} = 18.8 Hz), 122.5, 34.9, 31.4, 28.4 (d, ¹*J*_{PC} = 11.5 Hz), 28.2 (dd, ^{2,3}*J*_{PC} = 14.5 Hz); HRMS (ESI, (M+H)⁺) Calcd for C₆₀H₉₃P₂⁺: 875.6747, Found *m/z* = 875.6716.

Synthesis of 1,4-bis[bis(3,5-dimethyl-4-methoxyphenyl)phosphino]butane (L4).



(Step 1) Bis(3,5-dimethyl-4-methoxyphenyl)phosphine oxide (4a)

Mg turnings (0.93 mg, 38 mmol) and a magnetic stirrer bar were placed in a 200 mL three-necked flask under Ar flow. THF (6 mL) and a small amount of I₂ (one bead) were added in and the mixture was stirred for 30 min at ambient temperature. A THF solution (25 mL) of 4-bromo-2,6-dimethylanisole (5.54 mL, 35 mmol) was added dropwise into the flask at 25 °C (water bath) for 1.5 h. Then, the solution was stirred at 40 °C (oil bath) for 1 h. After that, THF solution (6 mL) of diethyl phosphite (1.55 mL, 12 mmol) was added dropwise over ca. 30 min. at 25 °C (water bath) and stirred at r.t. for 15 h. The reaction was quenched with 5.9 M aq. of K₂CO₃ (6.5 mL) at 0 °C, and stirred at r.t. for 30 min. Then, the mixture was filtrated through Celite[®] using ethanol as eluent. The solvent was removed under reduced pressure, then CHCl₃ (ca. 70 mL) and activated molecular sieves 4A were added to the residue, stirred for 2 h at r.t. and filtered through Celite[®] using CHCl₃ as eluent. Removing the solvent under reduced pressure and chromatography (AcOEt/hexane = 5/2) to give **4a** as white solid (82% yield, 3.13 g). ¹H NMR (600 MHz, CDCl₃) δ 7.92 (d, 1H, *J* = 477 Hz), 7.36 (s, 2H), 7.34 (s, 2H), 3.75 (s, 6H, OCH₃), 2.31 (s, 12H, CH₃); ³¹P{¹H} NMR (243 MHz, CDCl₃) δ 22.0.

(Step 2) Butane-1,4-diylbis[bis(3,5-dimethyl-4-methoxyphenyl)phosphine oxide] (4b)

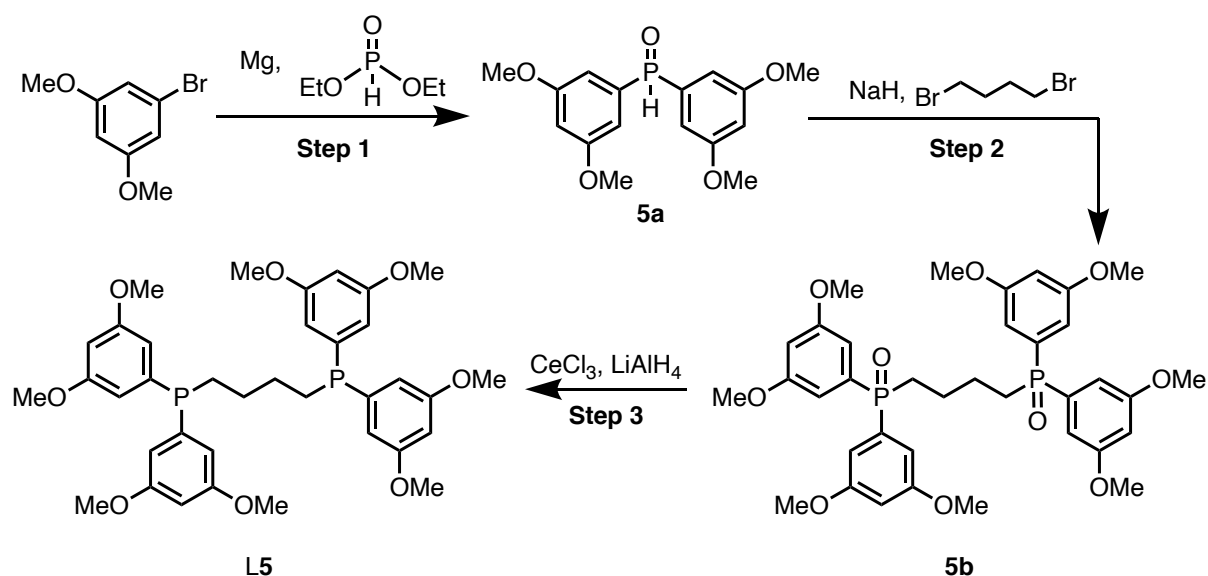
To a 100 mL two-necked flask were added **4a** (9 mmol, 2.64 g), THF (40 mL), and a magnetic stirrer bar. NaH (10 mmol, 436 mg) was added to the solution under Ar flow at r.t. and stirred for 1 h. Then, 1,4-dibromobutane (538 μL, 4.5 mmol) was added to the mixture dropwise. After stirring for 16 h, THF was removed under reduced pressure, the resulting white solid was dissolved in water and extracted with CH₂Cl₂. The organic layer was collected and dried over

Na₂SO₄, and concentrated under reduced pressure. The crude product was purified by chromatography (AcOEt/hexane = 10/1) to give **4b** as a white solid (87% yield, 2.58 g). ¹H NMR (600 MHz, CDCl₃) δ 7.33 (s, 4H, C₆H₃), 7.31 (s, 4H, C₆H₃), 3.73 (s, 12H, OCH₃), 2.28 (s, 24H, CH₃), 2.14–2.19 (m, 4H), 1.68 (t, 4H, *J* = 3.4 Hz, CH₂); ³¹P{¹H} NMR (243 MHz, CDCl₃) δ 32.4; ¹³C{¹H} NMR (151 MHz, CDCl₃): δ 159.9 (d, *J* = 2.9 Hz), 131.6 (d, *J* = 13.0 Hz), 131.3 (d, *J* = 10.1 Hz), 128.1, 127.4, 59.6, 29.8, 29.4, 23.0, 22.9 (d, *J* = 2.9 Hz), 16.2.

(Step 3) 1,4-Bis[bis(3,5-dimethyl-4-methoxyphenyl)phosphino]butane (L4)

Grinded CeCl₃·7H₂O (22.5 mmol, 8.39 g) and a magnetic stirrer bar were added to a 100 mL two-necked flask and dried *in vacuo* at 140 °C for 2 h. After cooling to ambient temperature, THF (20 mL) and **4b** (3.0 mmol, 1.96 g) were added to the flask at once and the resulting mixture was stirred for 30 min. Then, the mixture was cooled to 0 °C, before LiAlH₄ (54 mmol, 2.0 g) was added portionwise. The resulting mixture was stirred at r.t. for 16 h. At 0 °C, H₂O (2.1 mL), 2 M NaOH aq (4.2 mL), and H₂O (6.3 mL) were added in this order to the mixture to quench the reaction. The resulting mixture was filtered through Celite[®] using CHCl₃ as eluent. The filtrate was concentrated under reduced pressure. The resulting product was extracted with CH₂Cl₂ and the organic layer as dried over Na₂SO₄, and concentrated under reduced pressure. The crude product was purified with Florisil chromatography (AcOEt/hexane = 1/10) to give L4 as a white solid (28% yield, 0.55 g). ¹H NMR (600 MHz, CDCl₃) δ 7.04 (s, 4H, C₆H₃), 7.03 (s, 4H, C₆H₃), 3.71 (s, 12H, OCH₃), 2.24 (s, 24H, CH₃), 1.94 (t, 4H, *J* = 7.2 Hz, CH₂), 1.52 (m, 4H, CH₂); ³¹P{¹H} NMR (243 MHz, CDCl₃) δ -18.2; ¹³C{¹H} NMR (151 MHz, CDCl₃): δ 157.4, 133.4 (d, ¹J_{PC} = 11.6 Hz), 133.2 (d, ²J_{PC} = 18.8 Hz), 130.8 (d, ³J_{PC} = 7.2 Hz), 59.6, 28.0 (d, ¹J_{PC} = 10.1 Hz), 27.7 (dd, ^{2,3}J_{PC} = 15.2 Hz), 16.2; HRMS (ESI, (M+H)⁺) Calcd for C₄₀H₅₃O₄P₂⁺: 659.3414, Found *m/z* = 659.3381.

Synthesis of 1,4-bis[bis(3,5-dimethoxyphenyl)phosphino]butane (L5).



(Step 1) Bis(3,5-dimethoxyphenyl)phosphine oxide (5a)

Mg turnings (730 mg, 30 mmol) and a magnetic stirrer bar were placed in a 200 mL three-necked flask under Ar flow. THF (5 mL) and a small amount of I₂ (one bead) were added in and the mixture was stirred for 30 min at ambient temperature. A THF solution (10 mL) of 1-bromo-3,5-di-methoxybenzene (5.86 g, 27 mmol) was added dropwise into the flask at 25 °C (water bath) for 1.5 h. Then, the solution was stirred at 40 °C (oil bath) for 30 min. After that, THF solution (5 mL) of diethyl phosphite (1.24 g, 9 mmol) was added dropwise over ca. 30 min. at 25 °C (water bath) and stirred at r.t. for 15 h. The reaction was quenched with 5.9 M aq. of K₂CO₃ (30 mL) at 0 °C, and stirred at r.t. for 30 min. Then, the mixture was filtrated through Celite[®] using ethanol (ca. 150 mL) as eluent. The solvent was removed under reduced pressure, then CHCl₃ (50 mL) and activated molecular sieves 4A were added to the residue, stirred for 2 h at r.t. and filtered through Celite[®] using CHCl₃ as eluent. Removing the solvent under reduced pressure yielded **5a** as white solid (80% yield, 2.33 g). ¹H NMR (600 MHz, CDCl₃) δ 7.95 (d, 1H, *J* = 484.8 Hz), 6.84 (d, 2H, *J* = 2.0 Hz), 6.82 (d, 2H, *J* = 2.1 Hz), 6.61 (t, 2H, *J* = 2.1 Hz), 3.81 (s, 12H, CH₃); ³¹P{¹H} NMR (243 MHz, CDCl₃) δ 23.1.

(Step 2) Butane-1,4-diylbis[bis(3,5-dimethoxyphenyl)phosphine oxide] (5b)

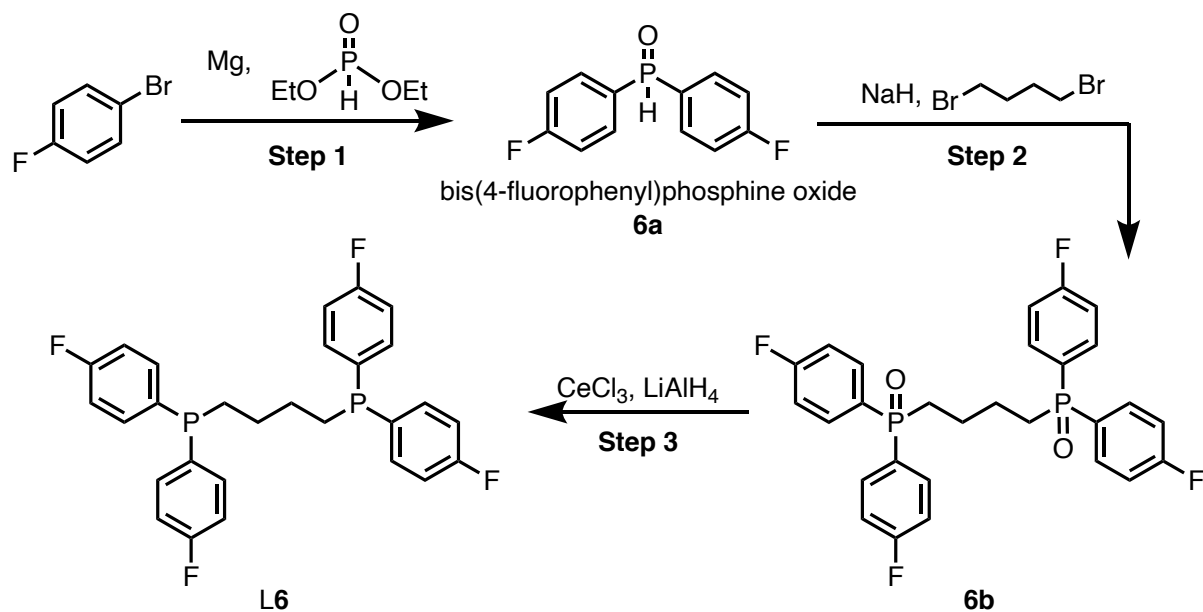
To a 300 mL two-necked flask were added **5a** (5.0 mmol, 1.68 g), THF (30 mL), and a magnetic stirrer bar. NaH (4.5 mmol, 0.23 g) was added to the solution under Ar flow at r.t. and stirred for 1 h. Then, 1,4-dibromobutane (2.4 mmol, 0.52 g) was added to the mixture dropwise. After stirring for 16 h, THF was removed under reduced pressure, the resulting white solid was dissolved in water and extracted with CH₂Cl₂. The organic layer was collected and dried over

Na₂SO₄, and concentrated under reduced pressure. The crude product **5b** was obtained in ~100% yield, 1.71 g). ¹H NMR (600 MHz, CDCl₃) δ 6.82 (d, 4H, *J* = 2.0 Hz, *CH*), 6.80 (d, 4H, *J* = 2.8 Hz, *CH*), 6.55 (t, 4H, *J* = 2.4 Hz, *CH*), 3.80 (s, 24H, *CH*₃), 2.18 (dd, 4H, *J* = 11.0, 15.8 Hz, *CH*₂), 1.20 (t, 4H, *J* = 3.4 Hz, *CH*₂); ³¹P{¹H} NMR (243 MHz, CDCl₃) δ 33.5; ¹³C{¹H} NMR (151 MHz, CDCl₃): δ 161.0 (d, *J* = 17.4 Hz), 135.0, 134.4, 108.3 (d, *J* = 10.1 Hz), 103.9, 55.6, 29.7, 29.2, 23.0 (d, *J* = 2.9 Hz), 22.9.

(Step 3) 1,4-Bis[bis(3,5-dimethoxyphenyl)phosphino]butane (L5)

Grinded CeCl₃·7H₂O (16.5 mmol, 6.1 g) and a magnetic stirrer bar were added to a 300 mL two-necked flask and dried *in vacuo* at 140 °C for 2 h. After cooling to ambient temperature, THF (30 mL) and **5b** (2.2 mmol, 1.53 g) were added to the flask at once and the resulting mixture was stirred for 30 min. Then, the mixture was cooled to 0 °C, before LiAlH₄ (66 mmol, 2.5 g) was added portionwise. The resulting mixture was stirred at r.t. for 16 h. At 0 °C, H₂O (2.5 mL), 2 M NaOH aq (5.0 mL), and H₂O (7.5 mL) were added in this order to the mixture to quench the reaction. The resulting mixture was filtered through Celite[®] using CHCl₃ as eluent. The filtrate was concentrated under reduced pressure. The resulting product was extracted with CH₂Cl₂ and the organic layer as dried over Na₂SO₄, and concentrated under reduced pressure. The crude product was purified with Florisil chromatography (AcOEt/hexane = 1/3.5) as eluent to give **L5** as white solid (55% yield, 0.81 g). ¹H NMR (600 MHz, CDCl₃) δ 6.56 (d, 4H, *J* = 2.1 Hz), 6.55 (d, 4H, *J* = 2.1 Hz), 6.39 (t, 4H, *J* = 2.0 Hz), 3.75 (s, 24H, *CH*₃), 1.98 (t, 4H, *J* = 7.2 Hz, *CH*₂), 1.56 (m, 4H, *CH*₂); ³¹P{¹H} NMR (243 MHz, CDCl₃) δ -11.0; ¹³C{¹H} NMR (151 MHz, CDCl₃): δ 150.6 (d, ³*J*_{PC} = 10.1 Hz), 140.7 (d, ¹*J*_{PC} = 13.0 Hz), 110.4 (d, ²*J*_{PC} = 20.2 Hz), 100.7, 55.3, 30.9, 27.7, 27.6 (dd, ^{2,3}*J*_{PC} = 15.2 Hz); HRMS (ESI, (M+H)⁺) Calcd for C₃₆H₄₅O₈P₂⁺: 667.2584, Found *m/z* = 667.2573.

Synthesis of 1,4-bis[bis(4-fluorophenyl)phosphino]butane (L6).



(Step 1) Bis(4-fluorophenyl)phosphine oxide (6a)

Mg turnings (2.4 g, 100 mmol) and a magnetic stirrer bar were placed in a 500 mL three-necked flask under Ar flow. THF (7 mL) and a small amount of I₂ (51 mg, 0.2 mmol) were added in and the mixture was stirred for 30 min at ambient temperature. A THF solution (40 mL) of 1-bromo-4-fluorobenzene (15.8 g, 90 mmol) was added dropwise into the flask at 0 °C (ice bath) for 1.5 h. Then, the solution was stirred at 40 °C (oil bath) for 40 min. After that, THF solution (20 mL) of diethyl phosphite (4.1 g, 30 mmol) was added dropwise over ca. 30 min. at 0 °C (ice bath) and stirred at r.t. for 15 h. The reaction was quenched with 5.9 M K₂CO₃ aq. (20 mL) at 0 °C, and stirred at r.t. for 30 min. Then, the mixture was filtrated through Celite[®] using ethanol as eluent. The solvent was removed under reduced pressure, then CHCl₃ and activated molecular sieves 4A were added to the residue, stirred for 2 h at r.t., filtered through Celite[®] using CHCl₃ as eluent, and concentrated under reduced pressure. The crude product was purified with silica gel chromatography (eluent; AcOEt/hexane = 3/1) to give L6 as a colorless oil (70% yield, 5.0 g). ¹H NMR (600 MHz, CDCl₃) δ 8.04 (d, 1H, *J* = 485 Hz), 7.69–7.63 (m, 4H), 7.17 (td, 4H, *J* = 8.9, 2.1 Hz); ³¹P{¹H} NMR (243 MHz, CDCl₃) δ 19.3.

(Step 2) Butane-1,4-diylbis[bis(4-fluorophenyl)phosphine oxide] (6b)

To a 100 mL two-necked flask were added 6a (5.0 mmol, 1.4 g), DMF (15 mL), and a magnetic stirrer bar. NaH (5.0 mmol, 0.24 g) was added to the solution under Ar flow at r.t. and stirred for 1 h. Then, 1,4-dibromobutane (4.5 mmol, 0.97 g, 530 μL) was added to the mixture

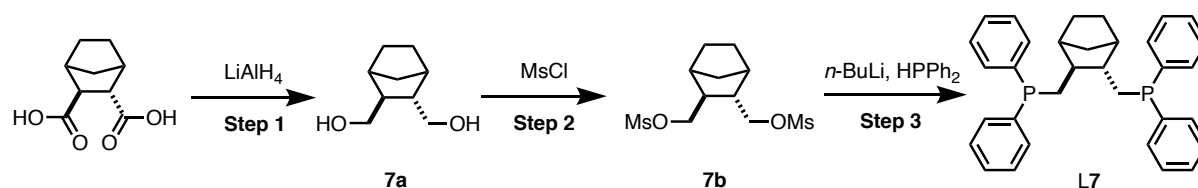
dropwise. After stirring for 2 h, THF was removed under reduced pressure, the resulting white solid was dissolved in water and extracted with CHCl_3 . The organic layer was collected and dried over Na_2SO_4 , and concentrated under reduced pressure (~ 5 mmHg, 70 °C for removing DMF). The obtained crude product was purified with silica gel chromatography (eluent; AcOEt 100%) to give **6b** as a white solid (69% yield, 0.91 g). ^1H NMR (600 MHz, CDCl_3) δ 7.69–7.65 (m, 8H), 7.16 (td, 8H, $J = 8.6, 1.6$ Hz), 2.24–2.20 (m, 4H), 1.73–1.67 (m, 4H); $^{31}\text{P}\{^1\text{H}\}$ NMR (243 MHz, CDCl_3) δ 31.2.

(Step 3) 1,4-Bis[bis(4-fluorophenyl)phosphino]butane (L6)

Grinded $\text{CeCl}_3 \cdot 7\text{H}_2\text{O}$ (12 mmol, 4.5 g) and a magnetic stirrer bar were added to a 500 mL two-necked flask and dried *in vacuo* at 140 °C for 2 h. After cooling to ambient temperature, THF (300 mL) and **6b** (1.5 mmol, 0.8 g) were added to the flask and the resulting mixture was stirred for 30 min. Then, the mixture was cooled to 0 °C, before LiAlH_4 (40 mmol, 1.5 g) was added portionwise. The resulting mixture was stirred at r.t. for 16 h. At 0 °C, H_2O (1.5 mL), 2 M NaOH aq (1.5 mL), and H_2O (7.5 mL) were added in this order to the mixture to quench the reaction. The resulting mixture was filtered through Celite[®] using CHCl_3 as eluent. The filtrate was concentrated under reduced pressure. The resulting product was extracted with CHCl_3 and the organic layer as dried over Na_2SO_4 , and concentrated under reduced pressure. The crude product was purified with Florisil chromatography (eluent; CHCl_3) to give L6 as a white solid (87% yield, 0.65 g). ^1H NMR (600 MHz, CDCl_3) δ 7.31–7.35 (m, 4H, C_6H_2), 7.02 (t, 8H, $J = 4.1$ Hz, C_6H_2), 1.96 (t, 4H, $J = 7.2$ Hz, CH_2), 1.48–1.52 (m, 4H, CH_2); $^{31}\text{P}\{^1\text{H}\}$ NMR (243 MHz, CDCl_3) δ –18.0. $^{13}\text{C}\{^1\text{H}\}$ NMR (151 MHz, CDCl_3): δ 163.2 (d, $^1J_{\text{FC}} = 248.7$ Hz), 134.4 (dd, $^2J_{\text{PC}} = 20.3$ Hz, $^3J_{\text{FC}} = 8.6$ Hz), 133.95 (dd, $^1J_{\text{PC}} = 13.0$ Hz, $^4J_{\text{FC}} = 2.9$ Hz), 115.66 (dd, $^3J_{\text{PC}} = 20.2$ Hz, $^2J_{\text{FC}} = 7.2$ Hz), 28.2 (d, $^1J_{\text{PC}} = 11.6$ Hz), 27.2 (dd, $^{2,3}J_{\text{PC}} = 14.5$ Hz); ^{19}F NMR (564 MHz, CDCl_3): δ –112.4; HRMS (ESI, $(\text{M}+2\text{O}+\text{Na})^+$) Calcd for $\text{C}_{28}\text{H}_{24}\text{O}_2\text{P}_2\text{F}_4\text{Na}^+$: 553.1080, Found $m/z = 552.1068$.

1.4.6. Ligand preparation (L7–L12)

Synthesis of 2,3-bis[(diphenylphosphino)methyl]bicyclo[2.2.1]hexane (L7).



(Step 1) Bicyclo[2.2.1]heptane-2,3-dimethanol (7a)

Under N₂, LiAlH₄ (37.5 mmol, 1.42 g) and 33 mL THF was added to a 100 mL three-necked flask. The mixture was cooled to 0 °C, followed by the addition of 2,3-norbornanedicarboxylic acid (15.0 mmol, 2.58 g) in portions. The mixture was warmed to r.t. and stirred overnight. The mixture was then moved to 60 °C and stirred for another 4 h. The mixture was cooled to 0 °C and 15% NaOH solution (10 mL) was added to the mixture. Ethyl acetate (30 mL, 3 times) was then used to extract. The organic phase was collected and dried over Na₂SO₄. Removal of the solvent under reduced pressure gave **7a** as a white solid (73 % yield, 1.71 g). The spectral data were consistent with the literature.^[39]

(Step 2) Bicyclo[2.2.1]heptane-2,3-dimethanol dimethanesulfonate (7b)

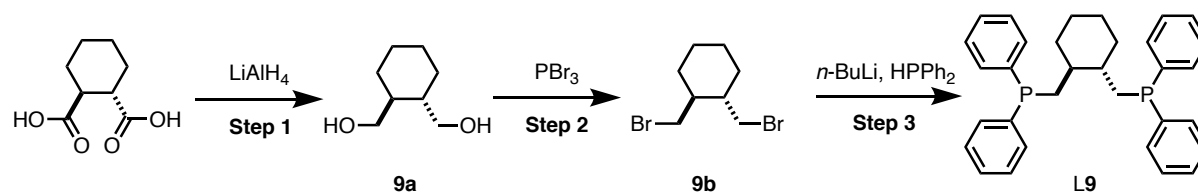
7a (4.86 mmol, 760.0 mg), 20 mg of DMAP, 8 mL pyridine and 5 mL CH₂Cl₂ was added to a 100 mL two-necked flask under N₂. After stirring for 30 min at 0 °C, MsCl (19.50 mmol, 1.5 mL) was added to the mixture dropwise in 10 min. The resulting mixture was moved to r.t. and stirred for 4 h. 50 mL 2N HCl solution was added to the mixture and CH₂Cl₂ (20 mL, 3 times) was used to extract. The organic phase was washed with H₂O (20 mL) and saturated NaHCO₃ (20 mL) and dried over Na₂SO₄. Removal of the solvent and purification by chromatography (hexane/ethyl acetate = 1/1) gave the product **7b** as a white sticky solid (52% yield, 803.3 mg).

(Step 3) 2,3-Bis[(diphenylphosphino)methyl]bicyclo[2.2.1]hexane (L7)

Under N₂, HPPPh₂ (5.88 mmol, 1.05 mL) and 20 mL THF was added to a 100 mL three-necked flask. At 0 °C, *n*-BuLi (7.00 mmol, 4.6 mL, 1.6 M in hexane) was added to the mixture dropwise. The resulting mixture was stirred for 1 h at r.t. **7b** (2.35 mmol, 731.3mg) in 10 mL THF was added to the mixture dropwise in 20 min. The resulting mixture was stirred overnight. Ether (30 mL) and saturated NH₄Cl (15 mL) was added to the mixture. The resulting mixture was extracted by ether (30ml, 3 times). The organic phase was collected and dried over Na₂SO₄. Removal of the solvent under reduced pressure and chromatography (hexane/ethyl acetate =

1/2) on a short column gave the product **L7** as a white solid (22% yield, 299.91 mg). ^1H NMR (600 MHz, CDCl_3) δ 7.47 (dt, 4H, $J = 2.0, 7.6$ Hz), 7.40 (dt, 4H, $J = 6.8, 7.6$ Hz), 7.35–7.29 (m, 12H), 2.36–2.34 (m, 4H), 2.00–1.95 (m, 2H), 1.89 (m, 2H), 1.54 (dd, 2H, $J = 2.1, 7.6$ Hz), 1.30 (d, 3H, $J = 8.9$ Hz), 1.23 (d, 1H, $J = 9.7$ Hz); $^{31}\text{P}\{^1\text{H}\}$ NMR (243 MHz, CDCl_3) δ -16.9; $^{13}\text{C}\{^1\text{H}\}$ NMR (151 MHz, CDCl_3): δ 163.2 (d, $^1J_{\text{FC}} = 248.7$ Hz), 134.4 (dd, $^2J_{\text{PC}} = 20.3$ Hz, $^3J_{\text{FC}} = 8.6$ Hz), 133.95 (dd, $^1J_{\text{PC}} = 13.0$ Hz, $^4J_{\text{FC}} = 2.9$ Hz), 115.66 (dd, $^3J_{\text{PC}} = 20.2$ Hz, $^2J_{\text{FC}} = 7.2$ Hz), 28.2 (d, $^1J_{\text{PC}} = 11.6$ Hz), 27.2 (dd, $^{2,3}J_{\text{PC}} = 14.5$ Hz).

Synthesis of *trans*-1,2-bis[(diphenylphosphino)methyl]cyclohexane (**L9**).



(Step 1) *trans*-1,2-bis(hydroxymethyl)cyclohexane (**9a**)

Trans-1,2-bis(hydroxymethyl)cyclohexane (**9a**) was synthesized using typical procedure.^[54] Under N_2 , LiAlH_4 (37.5 mmol, 1.42 g) and 30 mL THF was added to a 100 mL three-necked flask. The mixture was cooled to 0 °C, followed by the addition of *trans*-cyclohexanedicarboxylic acid (15.0 mmol, 2.58 g) in portions. The mixture was warmed to r.t. and stirred overnight. The mixture was then moved to 60 °C and stirred for another 4 h. The mixture was cooled to 0 °C and 15% NaOH solution (10 mL) was added to the mixture. Ethyl acetate (30 mL, 3 times) was then used to extract. The organic phase was collected and dried over Na_2SO_4 . Removal of the solvent under reduced pressure gave **9a** as a white solid (88 % yield, 1.90 g). ^1H NMR (600 MHz, CDCl_3) δ 3.64 (d, 2H, $J = 10.3$ Hz), 3.55 (dd, 2H, $J = 6.3, 10.9$ Hz), 2.88 (d, 2H, $J = 8.0$ Hz), 1.75 (m, 2H, CyH), 1.65 (m, 2H, CyH), 1.34 (m, 2H, CyH), 1.24 (m, 2H, CyH), 1.06 (m, 2H, CyH).

(Step 2) (1*S*,2*S*)-1,2-bis(bromomethyl)cyclohexane (**9b**)

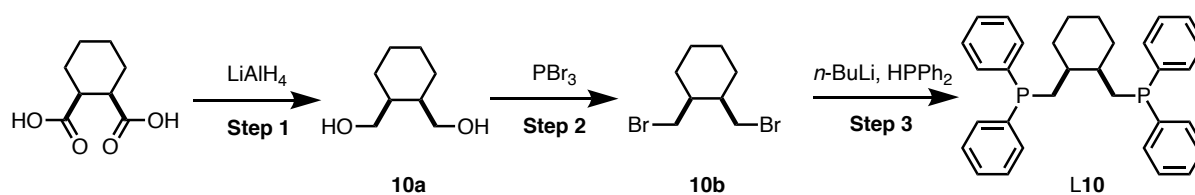
Trans-1,2-bis(bromomethyl)cyclohexane (**9b**) was synthesized using typical procedure.^[55] Under N_2 , PBr_3 (11.0 mmol, 1.05 mL) and 3 mL Et_2O was added directly to a 50 mL two-necked flask. The mixture was stirred at -10 °C. **37a** (10.0 mmol, 1.48 g) in 20 mL Et_2O was added to the mixture dropwise. After adding, Et_2O was removed by reduced pressure and the resulting mixture was moved to 90 °C and stirred overnight under N_2 . 20 mL H_2O was added to the mixture to quench and CH_2Cl_2 (30 mL, 3 times) was used to extract. The organic phase was collected and dried over Na_2SO_4 . Removal of the solvent under reduced pressure gave **9b**

as a light yellow oil (78% yield, 2.21 g). ^1H NMR (600 MHz, CDCl_3) δ 3.59 (d, 2H, $J = 4.1$, 11.0 Hz), 3.45 (dd, 2H, $J = 2.0$, 11.0 Hz), 1.77 (m, 2H, CyH), 1.71 (m, 2H, CyH), 1.64 (m, 2H, CyH), 1.44 (m, 2H, CyH), 1.31 (m, 2H, CyH).

(Step 3) *Trans*-1,2-bis[(diphenylphosphino)methyl]cyclohexane (L9)

Trans-1,2-bis[(diphenylphosphino)methyl]cyclohexane was synthesized using typical procedure.^[55] Under N_2 , HPPH_2 (4.0 mmol, 715 μL) and 20 mL THF was added to a 100 mL three-necked flask. At -78 °C, *n*-BuLi (4.5 mmol, 2.9 mL, 1.6 M in hexane) was added to the mixture dropwise. The resulting mixture was stirred for 1 h at r.t. **9b** (2.0 mmol, 534 mg) in 10 mL THF was added to the mixture dropwise in 20 min. The resulting mixture was stirred overnight. The THF was removed after the reaction. The resulting mixture was extracted by ether (30 mL, 3 times) and washed with H_2O (30 mL). The organic phase was collected and dried over Na_2SO_4 . Removal of the solvent under reduced pressure and chromatography (hexane/ethyl acetate = 1/2) on a short column gave the product **L9** as a colorless oil (29 % yield, 100.0 mg). ^1H NMR (600 MHz, CDCl_3) δ 7.40–7.42 (m, 4H), 7.27–7.35 (m, 16H), 2.37 (t, 1H, $J = 3.4$ Hz), 2.34 (t, 1H, $J = 3.1$ Hz), 2.04 (d, 2H, $J = 13.7$ Hz), 1.59–1.63 (m, 4H), 1.26–1.30 (m, 2H), 1.11–1.18 (m, 2H), 0.99–1.06 (m, 2H); $^{31}\text{P}\{^1\text{H}\}$ NMR (243 MHz, CDCl_3) δ –19.3; $^{13}\text{C}\{^1\text{H}\}$ NMR (151 MHz, CDCl_3): δ 139.8 (d, $^1J_{\text{PC}} = 13.0$ Hz), 139.0 (d, $^1J_{\text{PC}} = 14.5$ Hz), 133.3 (d, $^2J_{\text{PC}} = 20.0$ Hz), 132.4 (d, $^2J_{\text{PC}} = 18.8$ Hz), 128.7, 128.4 (d, $^3J_{\text{PC}} = 7.2$ Hz), 128.3 (d, $^3J_{\text{PC}} = 6.3$ Hz), 128.2, 40.9 (dd, $^2J_{\text{PC}} = 13.0$ Hz, $^3J_{\text{PC}} = 7.2$ Hz), 33.3, 33.2, 25.7.

Synthesis of *cis*-1,2-bis[(diphenylphosphino)methyl]cyclohexane (**L10**).



(Step 1) *cis*-1,2-bis(hydroxymethyl)cyclohexane (**10a**)

Under N_2 , LiAlH_4 (37.5 mmol, 1.42 g) and 30 mL THF was added to a 100 mL three-necked flask. The mixture was cooled to $0\text{ }^\circ\text{C}$, followed by the addition of *cis*-cyclohexanedicarboxylic acid (15.0 mmol, 2.58 g) in portions. The mixture was warmed to r.t. and stirred overnight. The mixture was then moved to $60\text{ }^\circ\text{C}$ and stirred for another 4 h. The mixture was cooled to $0\text{ }^\circ\text{C}$ and 15% NaOH solution (10 mL) was added to the mixture. Ethyl acetate (30 mL, 3 times) was then used to extract. The organic phase was collected and dried over Na_2SO_4 . Removal of the solvent under reduced pressure gave **10a** as a colorless oil (84% yield, 1.81 g). $^1\text{H NMR}$ (600 MHz, CDCl_3) δ 3.75 (dd, 2H, $J = 11.0, 8.2$ Hz), 3.57 (dd, 2H, $J = 11.0, 4.1$ Hz), 3.31 (bs, 2H), 1.95–1.92 (m, 2H), 1.57–1.52 (m, 2H), 1.48–1.42 (m, 4H), 1.40–1.35 (m, 2H).

(Step 2) *cis*-1,2-bis(bromomethyl)cyclohexane (**10b**)

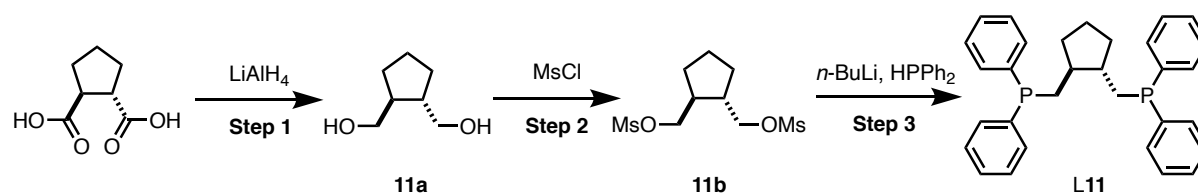
Under N_2 , PBr_3 (11.0 mmol, 1.05 mL) and 3 mL Et_2O was added directly to a 50 mL two-necked flask. The mixture was stirred at $-10\text{ }^\circ\text{C}$. **10a** (10.0 mmol, 1.48 g) in 20 mL Et_2O was added to the mixture dropwise. After adding, Et_2O was removed by reduced pressure and the resulting mixture was moved to $90\text{ }^\circ\text{C}$ and stirred overnight under N_2 . 20 mL H_2O was added to the mixture to quench and CH_2Cl_2 (30 mL, 3 times) was used to extract. The organic phase was collected and dried over Na_2SO_4 . Removal of the solvent under reduced pressure gave **10b** as a yellow solid (71% yield, 2.01 g). $^1\text{H NMR}$ (600 MHz, CDCl_3) δ 3.34–3.40 (m, 4H, CH_2Br), 2.18–2.23 (m, 2H, CyH), 1.62–1.65 (m, 2H, CyH), 1.52–1.58 (m, 4H, CyH), 1.37–1.41 (m, 2H, CyH).

(Step 3) *cis*-1,2-bis[(diphenylphosphino)methyl]cyclohexane (**L10**)

Under N_2 , HPPPh_2 (7.0 mmol, 1.25 mL) and 20 mL THF was added to a 100 mL three-necked flask. At $-78\text{ }^\circ\text{C}$, $n\text{-BuLi}$ (8.0 mmol, 5.1 mL, 1.6 M in hexane) was added to the mixture dropwise. The resulting mixture was stirred for 1 h at r.t. **10b** (3.3 mmol, 881 mg) in 10 mL THF was added to the mixture dropwise in 20 min. The resulting mixture was stirred overnight. The THF was removed after the reaction. The resulting mixture was extracted by ether (30 mL, 3 times) and washed with H_2O (30 mL). The organic phase was collected and dried over

Na₂SO₄. Removal of the solvent under reduced pressure and chromatography (hexane/ethyl acetate = 1/2) on a short column gave the product **L10** as a colorless oil (23 % yield, 80.0 mg). ¹H NMR (500 MHz, CDCl₃) δ 7.26–7.41 (m, 20H), 2.02 (d, 2H, *J* = 16.5 Hz), 1.93 (t, 2H, *J* = 3.6 Hz), 1.65 (m, 4H), 1.48–1.53 (m, 4H), 1.27 (m, 2H); ³¹P {¹H} NMR (202 MHz, CDCl₃) δ –19.2; ¹³C {¹H} NMR (126 MHz, CDCl₃): δ 139.8 (d, ¹*J*_{PC} = 14.4 Hz), 138.6 (d, ¹*J*_{PC} = 13.2 Hz), 133.2 (d, ²*J*_{PC} = 19.2 Hz), 132.6 (d, ²*J*_{PC} = 19.2 Hz), 128.7, 128.4 (d, ³*J*_{PC} = 7.2 Hz), 128.3 (d, ³*J*_{PC} = 9.7 Hz), 128.3, 37.3 (dd, ²*J*_{PC} = 13.2 Hz, ³*J*_{PC} = 8.4 Hz), 29.4, 29.4, 23.3.

Synthesis of *trans*-1,2-bis[(diphenylphosphino)methyl]cyclopentane (**L11**).



(Step 1) *trans*-1,2-bis(hydroxymethyl)cyclopentane (**11a**)

Under N₂, LiAlH₄ (15.6 mmol, 593.9 mg) and 20 mL THF was added to a 100 mL three-necked flask. The mixture was cooled to 0 °C, followed by the addition of *trans*-cyclopentanedicarboxylic acid (6.26 mmol, 990 mg) in portions. The mixture was warmed to r.t. and stirred overnight. The mixture was then moved to 60 °C and stirred for another 4 h. The mixture was cooled to 0 °C and 15% NaOH solution (8 mL) was added to the mixture. Ethyl acetate (30 mL, 3 times) was then used to extract. The organic phase was collected and dried over Na₂SO₄. Removal of the solvent under reduced pressure gave **11a** as a colorless oil (81 % yield, 659.6 mg). ¹H NMR (600 MHz, CDCl₃) δ 3.92 (bs, 2H), 3.74 (dd, 2H, *J* = 10.0, 3.8 Hz), 3.35 (t, 2H, *J* = 12.0 Hz), 1.86–1.77 (m, 4H), 1.60–1.55 (m, 2H), 1.29–1.21 (m, 2H).

(Step 2) *trans*-1,2-cyclopentanedimethanol dimethanesulfonate (**11b**)

11a (5.0 mmol, 650.0 mg), 20 mg of DMAP, 10 mL pyridine and 5 mL CH₂Cl₂ was added to a 100 mL two-necked flask under N₂. After stirring for 30 min at 0 °C, MsCl (20.0 mmol, 1.5 mL) was added to the mixture dropwise in 10 min. The resulting mixture was moved to r.t. and stirred for 4 h. 50 mL 2N HCl solution was added to the mixture and CH₂Cl₂ (20 mL, 3 times) was used to extract. The organic phase was washed with H₂O (20 mL) and saturated NaHCO₃ (20 mL) and dried over Na₂SO₄. Removal of the solvent and purification by chromatography using hexane: ethyl acetate (1:1) gave the product **11b** as a yellow sticky solid (82% yield, 1.17 g). ¹H NMR (600 MHz, CDCl₃) δ 4.20–4.15 (m, 4H), 3.04 (s, 6H), 2.16–2.10 (m, 2H), 1.92–

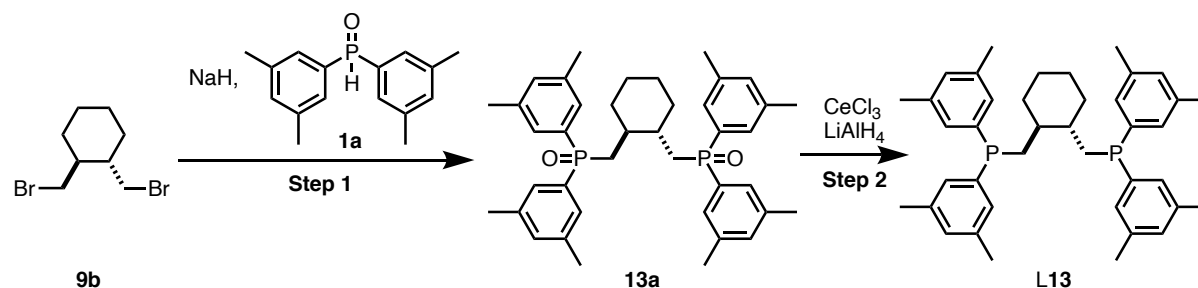
1.86 (m, 2H), 1.66 (quin, $J = 6.9$ Hz), 1.51–1.45 (m, 2H).

(Step 3) *trans*-1,2-bis[(diphenylphosphino)methyl]cyclopentane (L11)

Under N_2 , $HPPPh_2$ (10.00 mmol, 1.8 mL) and 20 mL THF was added to a 100 mL three-necked flask. At 0 °C, *n*-BuLi (13.00 mmol, 8.5 mL, 1.6 M in hexane) was added to the mixture dropwise. The resulting mixture was stirred for 1 h at r.t. **11b** (3.91 mmol, 1.12 g) in 10 mL THF was added to the mixture dropwise in 20 min. The resulting mixture was stirred overnight. Ether (30 mL) and saturated NH_4Cl (15 mL) was added to the mixture. The resulting mixture was extracted by ether (30 mL, 3 times). The organic phase was collected and dried over Na_2SO_4 . Removal of the solvent under reduced pressure and chromatography (hexane/ethyl acetate = 1/2) on a short column gave the product as a colorless oil (56% yield, 1.02 g). 1H NMR (600 MHz, $CDCl_3$) δ 7.29–7.46 (m, 20H), 2.40 (t, 1H, $J = 6.8$ Hz), 2.38 (t, 1H, $J = 6.2$ Hz), 1.91 (m, 2H), 1.78 (t, 2H), 1.55 (m, 4H), 1.27 (m, 2H); $^{31}P\{^1H\}$ NMR (243 MHz, $CDCl_3$) δ -18.4; $^{13}C\{^1H\}$ NMR (151 MHz, $CDCl_3$): δ 139.7 (d, $^1J_{PC} = 13.0$ Hz), 138.6 (d, $^1J_{PC} = 14.5$ Hz), 133.1 (d, $^2J_{PC} = 18.8$ Hz), 132.5 (d, $^2J_{PC} = 18.8$ Hz), 128.6, 128.4 (d, $^3J_{PC} = 7.2$ Hz), 128.3 (d, $^3J_{PC} = 5.8$ Hz), 128.3, 45.0 (dd, $^2J_{PC} = 116.0$ Hz, $^3J_{PC} = 8.7$ Hz), 33.8 (d, $^3J_{PC} = 13.0$ Hz), 33.2 (d, $^3J_{PC} = 7.2$ Hz), 23.5; HRMS (ESI, $(M+H)^+$) Calcd for $C_{31}H_{33}P_2^+$: 467.2052, Found $m/z = 467.2030$.

1.4.7. Ligand preparation (L13–L17)

Synthesis of *trans*-1,2-bis[(dixylylphosphino)methyl]cyclohexane (L13).



(Step 1) ((*trans*-cyclohexane-1,2-diyl)bis(methylene))bis(bis(3,5-dimethylphenyl)phosphine oxide) (13a)

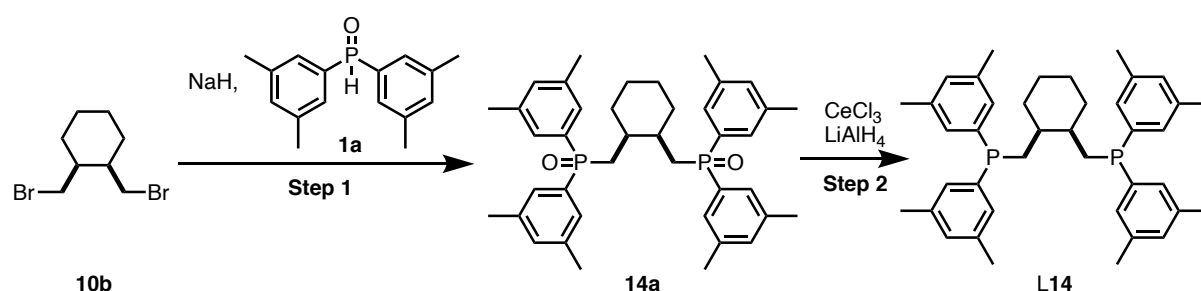
To a 100 mL two-necked flask were added **1a** (2.6 g, 10 mmol), THF (30 mL), and a magnetic stirrer bar. NaH (0.44 g, 10 mmol) was added to the solution under Ar flow at r.t. and stirred for 20 min. Then, **9b** (1.35 g, 5 mmol) was added to the mixture dropwise. After stirring for overnight, the crude product was collected by filtration with CH₂Cl₂, washed with water and brine, and dried over Na₂SO₄. Removal of the solvent and purification by chromatography using ethyl acetate (100%) gave the product **13a** as white solid (2.26g, 72% yield). ¹H NMR (600 MHz, CDCl₃) δ 7.32 (t, 8H, *J* = 10.7 Hz), 7.08 (d, 4H, *J* = 13.7 Hz), 2.43 (t, 2H, *J* = 13.7 Hz), 2.29 (d, 24H, *J* = 40.8 Hz), 1.98 (ddd, 2H, *J* = 16.5, 8.9, 6.9 Hz), 1.84 (d, 2H, *J* = 13.1 Hz), 1.74–1.66 (m, 2H), 1.48 (d, 2H, *J* = 7.6 Hz), 1.14–1.06 (m, 2H), 1.01 (t, 2H, *J* = 11.0 Hz); ³¹P{¹H} NMR (243 MHz, CDCl₃) δ 31.9.

(Step 2) *trans*-1,2-bis[(dixylylphosphino)methyl]cyclohexane (L13)

Grinded CeCl₃·7H₂O (15 mmol, 5.6 g) and a magnetic stirrer bar were added to a 100 mL two-necked flask and dried *in vacuo* at 140 °C for 2 h. After cooling to ambient temperature, THF (40 mL) and **13a** (2 mmol, 1.25 g) were added to the flask at once and the resulting mixture was stirred for 30 min. Then, the mixture was cooled to 0 °C, before LiAlH₄ (54 mmol, 2.05 g) was added portionwise. The resulting mixture was stirred at r.t. for 1 h, then at 40 °C for 24 h. At 0 °C, H₂O (2.1 mL), 2 M NaOH aq (4.2 mL), and H₂O (6.3 mL) were added in this order to the mixture to quench the reaction. The resulting mixture was filtered through Celite[®] using CHCl₃ as eluent. The filtrate was concentrated under reduced pressure. The resulting product was extracted with CH₂Cl₂ and the organic layer as dried over Na₂SO₄, and concentrated under reduced pressure. The crude product was purified with Florisil chromatography (AcOEt/hexane = 1/10) to give **L13** as a white solid (66% yield, 0.787 g). ¹H NMR (600 MHz,

CDCl_3): δ 7.07 (d, 4H, $J = 8.3$ Hz), 6.94 (s, 2H), 6.93 (s, 4H), 6.89 (s, 2H), 2.45–2.46 (m, 1H), 2.43–2.44 (m, 1H), 2.25 (d, 24H, $J = 2.3$ Hz), 2.12 (d, 2H, $J = 13.1$ Hz), 1.60–1.61 (m, 2H), 1.51–1.55 (m, 2H), 1.21–1.25 (m, 2H), 1.15 (t, 2H, $J = 9.6$ Hz), 0.95–1.01 (m, 2H); $^{31}\text{P}\{^1\text{H}\}$ NMR (243 MHz, CDCl_3): δ -19.8; $^{13}\text{C}\{^1\text{H}\}$ NMR (151 MHz, CDCl_3): δ 140.0 (d, $^3J_{\text{PC}} = 13.0$ Hz), 138.4 (d, $^3J_{\text{PC}} = 13.0$ Hz), 137.6 (d, $^1J_{\text{PC}} = 7.2$ Hz), 137.5 (d, $^1J_{\text{PC}} = 7.2$ Hz), 130.8 (d, $^2J_{\text{PC}} = 20.2$ Hz), 130.4, 130.1 (d, $^2J_{\text{PC}} = 17.4$ Hz), 130.0, 45.1 (dd, $^{2,3}J_{\text{PC}} = 10.1$ Hz), 33.7 (d, $^1J_{\text{PC}} = 11.6$ Hz), 33.3 (d, $^1J_{\text{PC}} = 13.0$ Hz), 25.9, 21.3, 21.3; HRMS (ESI, $(\text{M}+\text{H})^+$) Calcd for $\text{C}_{40}\text{H}_{51}\text{P}_2^+$: 593.3461, Found $m/z = 593.3465$.

Synthesis of *cis*-1,2-bis[(dixylylphosphino)methyl]cyclohexane (L14).



(Step 1) ((*cis*-cyclohexane-1,2-diyl)bis(methylene))bis(bis(3,5-dimethylphenyl) phosphine oxide) (14a)

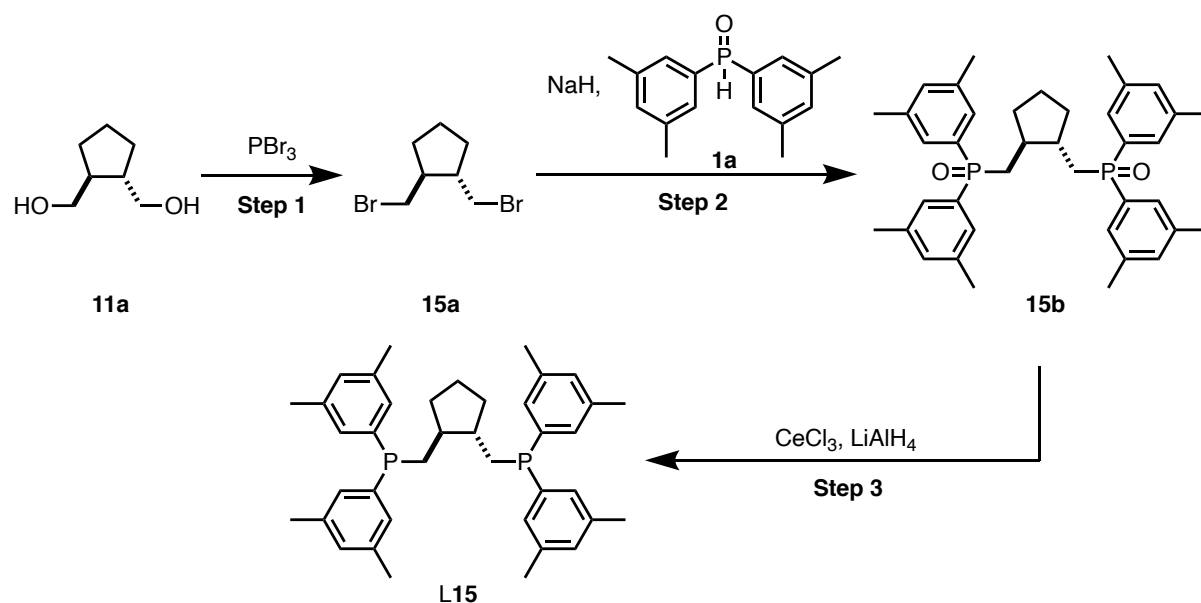
To a 300 mL two-necked flask were added **1a** (3.9 g, 15 mmol), THF (100 mL), and a magnetic stirrer bar. NaH (0.698 g, 16 mmol) was added to the solution under Ar flow at r.t. and stirred for 20 min. Then, **10b** (1.89 g, 7 mmol) was added to the mixture dropwise. After stirring for overnight, the crude product was collected by filtration with CH_2Cl_2 , washed with water and brine, and dried over Na_2SO_4 . Removal of the solvent and purification by chromatography using ethyl acetate (100%) gave the product **14a** as white solid (2.9 g, 67% yield). ^1H NMR (600 MHz, CDCl_3): δ 7.34 (t, 8H, $J = 12.4$ Hz), 7.10 (s, 4H), 2.32 (d, 24H, $J = 10.3$ Hz), 2.16–2.09 (m, 6H), 1.63–1.57 (m, 2H), 1.48–1.43 (m, 2H), 1.42–1.36 (m, 2H), 1.27–1.21 (m, 2H); $^{31}\text{P}\{^1\text{H}\}$ NMR (243 MHz, CDCl_3): δ 33.2.

(Step 2) *cis*-1,2-bis[(dixylylphosphino)methyl]cyclohexane (L14)

Grinded $\text{CeCl}_3 \cdot 7\text{H}_2\text{O}$ (24 mmol, 8.9 g) and a magnetic stirrer bar were added to a 1000 mL two-necked flask and dried *in vacuo* at 140 °C for 2 h. After cooling to ambient temperature, THF (500 mL) and **14a** (3 mmol, 1.87 g) were added to the flask at once and the resulting mixture was stirred for 30 min. Then, the mixture was cooled to 0 °C, before LiAlH_4 (80 mmol, 3.04 g) was added portionwise. The resulting mixture was stirred at r.t. for 1 h, then at 40 °C

for 24 h. At 0 °C, H₂O (3 mL), 2 M NaOH aq (3 mL), and H₂O (9 mL) were added in this order to the mixture to quench the reaction. The resulting mixture was filtered through Celite[®] using CHCl₃ as eluent. The filtrate was concentrated under reduced pressure. The resulting product was extracted with CH₂Cl₂ and the organic layer as dried over Na₂SO₄, and concentrated under reduced pressure. The crude product was purified with Florisil chromatography (AcOEt/hexane = 1/10) to give **L14** as a white solid (88% yield). ¹H NMR (600 MHz, CDCl₃) δ 7.07 (d, 4H, *J* = 7.6 Hz), 6.98 (d, 4H, *J* = 7.6 Hz), 6.92 (d, 4H, *J* = 19.9 Hz), 2.26 (d, 24H, CH₃, *J* = 2.8 Hz), 2.07 (d, 2H, *J* = 13.2 Hz), 1.87–1.91 (m, 2H), 1.54–1.56 (m, 2H), 1.47–1.50 (m, 2H), 1.28–1.31 (m, 2H); ³¹P{¹H} NMR (243 MHz, CDCl₃) δ -20.1; ¹³C{¹H} NMR (151 MHz, CDCl₃): δ 139.7 (d, ³*J*_{PC} = 13.0 Hz), 137.9 (d, ³*J*_{PC} = 13.0 Hz), 137.7 (d, ¹*J*_{PC} = 7.2 Hz), 137.6 (d, ¹*J*_{PC} = 7.2 Hz), 130.8 (d, ²*J*_{PC} = 20.3 Hz), 130.4, 130.2, 130.1 (d, ²*J*_{PC} = 11.6 Hz), 37.3 (dd, ²*J*_{PC} = 11.5 Hz, ³*J*_{PC} = 7.2 Hz), 29.3 (d, ¹*J*_{PC} = 8.7 Hz), 23.3, 21.3, 21.3; HRMS (ESI, (M+H)⁺) Calcd for C₄₀H₅₁P₂⁺: 593.3461, Found *m/z* = 593.3471.

Synthesis of *trans*-1,2-bis[(dixylylphosphino)methyl]cyclopentane (**L15**).



(Step 1) *trans*-1,2-bis(bromomethyl)cyclopentane (**15a**)

Under Ar, PBr₃ (7.3 mmol, 0.69 mL) and Et₂O (10 mL) were added to a vessel equipped with a Young's stopcock (75 mL). The mixture was stirred at -10 °C, and **11a** (5.1 mmol, 0.66 g) in 12 mL Et₂O was added to the mixture dropwise at the same temperature. Et₂O was removed by reduced pressure under Ar, and the resulting mixture was heated at 90 °C for 10 h. H₂O (20 mL) was added to the mixture to quench and CH₂Cl₂ (30 mL, 4 times) was used to extract. The organic phase was collected and dried over Na₂SO₄. Removal of the solvent under reduced

pressure gave **15a** as a colorless oil (57% yield, 0.75 g). ^1H NMR (600 MHz, CDCl_3) δ 3.53 (dd, 2H, $J = 9.6, 4.8$ Hz), 3.42 (dd, 2H, $J = 10.3, 6.2$ Hz), 2.16–2.09 (m, 2H), 1.97–1.91 (m, 2H), 1.65 (quint, 2H, $J = 7.1$ Hz), 1.57–1.53 (m, 2H).

(Step 2) ((trans-cyclopentane-1,2-diyl)bis(methylene))bis(bis(3,5-dimethylphenyl)phosphine oxide) (15b)

To a 100 mL two-necked flask were added **1a** (1.5 g, 5.8 mmol), THF (30 mL), and a magnetic stirrer bar. NaH (0.3 g, 6.8 mmol) was added to the solution under Ar flow at r.t. and stirred for 1 h. Then, **15a** (0.75 g, 2.9 mmol) and THF (20 mL) were added to the mixture dropwise. After stirring for 2 h at r.t., additional amount of NaH (0.26 g, 6 mmol) was added. After stirring for 1 h at r.t., H_2O was added to the reaction mixture to quench, then solvents were removed under a reduced pressure. The obtained crude products were extracted with CH_2Cl_2 and H_2O . The organic phase was collected and dried over Na_2SO_4 . Removal of the solvent under reduced pressure and purification by silica gel chromatography using ethyl acetate (100%) gave the product **15b** as a white solid (1.0 g, 57% yield).

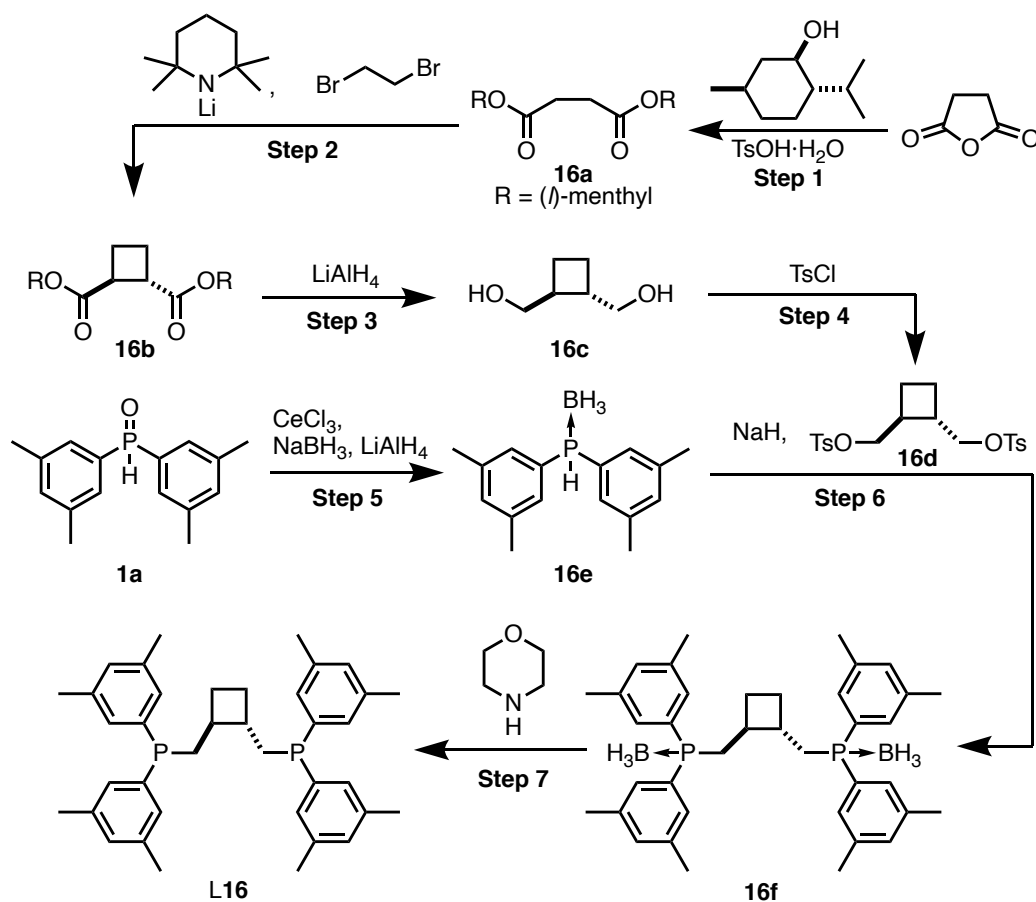
^1H NMR (600 MHz, CDCl_3): δ 7.36 (d, 4H, $J = 5.5$ Hz), 7.34 (d, 4H, $J = 6.2$ Hz), 7.10 (s, 4H), 2.54 (t, 2H, $J = 13.4$ Hz), 2.32 (d, 24H, $J = 4.1$ Hz), 2.13–2.05 (m, 2H), 1.95–1.88 (m, 2H), 1.69–1.63 (m, 2H), 1.45–1.40 (m, 2H), 1.02–0.95 (m, 2H). $^{31}\text{P}\{^1\text{H}\}$ NMR (243 MHz, CDCl_3): δ 31.5. $^{13}\text{C}\{^1\text{H}\}$ NMR (151 MHz, CDCl_3): δ 138.3 (d, $J = 13.0$ Hz), 138.2 (d, $J = 13.0$ Hz), 134.1, 133.8, 133.5, 133.3, 133.1, 128.3 (d, $J = 10.1$ Hz), 128.1 (d, $J = 8.7$ Hz), 41.6 (d, $J = 2.9$ Hz), 41.5 (d, $J = 4.3$ Hz), 34.1, 33.6, 32.5, 23.7, 21.3.

(Step 3) trans-1,2-bis[(dixylylphosphino)methyl]cyclopentane (L15)

Grinded $\text{CeCl}_3 \cdot 7\text{H}_2\text{O}$ (16 mmol, 6.0 g) and a magnetic stirrer bar were added to a 200 mL two-necked flask and dried *in vacuo* at 140 °C for 2 h. After cooling to ambient temperature, THF (70 mL) and **15b** (2 mmol, 1.2 g) were added to the flask and the resulting mixture was stirred for 30 min. Then, the mixture was cooled to 0 °C, before LiAlH_4 (57 mmol, 2.2 g) was added portionwise. The resulting mixture was stirred at r.t. for 12 h, then additional amount of LiAlH_4 (40 mmol, 1.5 g) was added at 0 °C and stirred at r.t. for 8 h. At 0 °C, H_2O (3.7 mL), 2 M NaOH aq (3.7 mL), and H_2O (18.5 mL) were added in this order to the mixture to quench the reaction. The resulting mixture was filtered through Celite[®] using CHCl_3 as eluent. The filtrate was concentrated under reduced pressure. The resulting product was extracted with CHCl_3 and water. The organic layer was dried over Na_2SO_4 , and concentrated under reduced pressure. The

crude product was purified with Florisil chromatography (AcOEt/hexane = 1/10) to give **L15** as a colorless oil (62% yield, 0.71 g). ^1H NMR (600 MHz, CDCl_3): δ 7.10 (d, 4H, $J = 7.6$ Hz), 6.98 (d, 4H, $J = 6.8$ Hz), 6.95 (s, 2H), 6.90 (s, 2H), 2.44 (t, 1H, $J = 2.8$ Hz), 2.42 (t, 1H, $J = 3.4$ Hz), 2.28 (d, 24H, $J = 14.0$ Hz), 1.89–1.95 (m, 2H), 1.68–1.73 (m, 2H), 1.50–1.54 (m, 4H), 1.22–1.28 (m, 2H); $^{31}\text{P}\{^1\text{H}\}$ NMR (243 MHz, CDCl_3): δ -19.1; $^{13}\text{C}\{^1\text{H}\}$ NMR (151 MHz, CDCl_3): δ 139.8 (d, $^3J_{\text{PC}} = 13.0$ Hz), 138.1 (d, $^3J_{\text{PC}} = 14.5$ Hz), 137.7 (d, $^1J_{\text{PC}} = 7.2$ Hz), 137.6 (d, $^1J_{\text{PC}} = 7.2$ Hz), 130.8 (d, $^2J_{\text{PC}} = 20.2$ Hz), 130.4, 130.0 (d, $^2J_{\text{PC}} = 18.9$ Hz), 130.0, 45.0 (dd, $^2J_{\text{PC}} = 11.6$ Hz, $^3J_{\text{PC}} = 8.6$ Hz), 33.7 (d, $^1J_{\text{PC}} = 11.6$ Hz), 33.3 (d, $^1J_{\text{PC}} = 7.2$ Hz), 23.7, 21.3, 21.3; HRMS (ESI, $(\text{M}+\text{H})^+$) Calcd for $\text{C}_{39}\text{H}_{49}\text{P}_2^+$: 579.3304, Found $m/z = 579.3296$.

Synthesis of *trans*-1,2-bis[(dixylylphosphino)methyl]cyclobutane (L16).



(Step 1) dimethyl succinate (16a)

The titled compound **16a** was synthesized by the literature procedure.^[52,53] To a 300 mL one-necked round-bottomed flask equipped with a magnetic stirrer, and a reflux condenser with a Dean-Stark trap, were added succinic anhydride (150 mmol, 15.0 g), (*l*)-menthol (300 mmol, 46.9 g), *p*-toluenesulfonic acid monohydrate (1 mmol, 0.19 g), and toluene (115 mL) under air. The mixture is heated under reflux in an oil bath (bath temperature: 145 °C) for 24 h under air (open system). During this period the water was trapped. The mixture was allowed to cool to ambient temperature, diluted with hexane (150 mL), and poured into a mixture of aqueous saturated NaHCO₃ (200 mL), methanol (75 mL), and water (150 mL). The organic phase was separated, and the aqueous phase was extracted twice with 100 mL of hexane. The organic phases are combined, washed once with 150 mL of saturated brine, and dried over Na₂SO₄. The solvent was removed under a reduced pressure, and the resulting crude product in a 100 mL one-necked round-bottomed flask was dissolved in 75 mL of methanol. After the solution stands in a refrigerator (4 °C) overnight, colorless crystals appeared in the mixture and were collected by filtration with suction washing with a cold methanol. The pure product was obtained in 75% yield (44.3 g) as a colorless crystal. The spectral data were consistent with the

literature.^[52]

(Step 2) dimethyl *trans*-cyclobutane-1,2-dicarboxylate (**16b**)

The titled compound **16b** was synthesized by the literature procedure.^[52,53] A dry 500 mL three-necked round-bottomed flask containing a magnetic stirring bar was equipped with a 100 mL pressure-equalizing dropping funnel, a rubber septum, and a three-way stopcock with an Ar balloon. The air in the system was replaced with Ar. The flask was charged with dehydrated THF (100 mL) and cooled with an ice bath; a 1.55 M hexane solution of butyllithium (105 mmol, 67.7 mL) was added. This solution was stirred while 2,2,6,6-tetramethylpiperidine (105 mmol, 17.9 mL) was added dropwise with a syringe through the septum over a 10 min period. The resulting solution of lithium 2,2,6,6-tetramethylpiperidide (LTMP) was cooled to $-78\text{ }^{\circ}\text{C}$ and stirred. A solution of **16a** (50 mmol, 19.7 g) in THF (100 mL) was then added dropwise through the addition funnel over a 1 h period at $-78\text{ }^{\circ}\text{C}$. The resulting yellow solution of succinate dianion was stirred for 1 h at $-78\text{ }^{\circ}\text{C}$. To the solution was added dropwise 1,2-dibromoethane (50 mmol, 4.3 mL) with a syringe through the septum over a 10 min period at $-78\text{ }^{\circ}\text{C}$. The reaction mixture was stirred for 2 h at $-78\text{ }^{\circ}\text{C}$, and for 12 h at $-20\text{ }^{\circ}\text{C}$. To the resulting mixture, isobutyraldehyde (20 mmol, 1.8 mL) was added dropwise to quench any unreacted anions. After being stirred for an additional 30 min, the reaction mixture was poured into ice-cooled 1 M HCl aq (200 mL) with stirring and the product was extracted 3 times with diethylether (100 mL). The combined organic phases were washed with 200 mL of brine, dried over sodium sulfate, filtered, and concentrated with a rotary evaporator. The residue was purified with silica gel chromatography (eluent; diethylether:hexane = 1:18 as eluant). The appropriate fractions were collected and concentrated, and recrystallization with methanol (100 mL) standing in a freezer ($-30\text{ }^{\circ}\text{C}$) overnight gave the product **16b** as a colorless crystal (18.9 g, 90% yield). The spectral data were consistent with the literature.^[52]

(Step 3) (*trans*-cyclobutane-1,2-diyl)dimethanol (**16c**)

To a 500 mL three-necked round-bottom flask were added **16b** (20 mmol, 8.4 g) and dehydrated THF (200 mL) under Ar. The mixture was cooled to $0\text{ }^{\circ}\text{C}$, followed by the addition of LiAlH_4 (40 mmol, 1.5 g) in portions. The mixture was warmed to r.t. and stirred overnight. The mixture was cooled to $0\text{ }^{\circ}\text{C}$, and H_2O (1.5 mL), 2 M NaOH aq (1.5 mL), and H_2O (4.5 mL) were added in this order to the mixture to quench the reaction. The resulting mixture was filtered through Celite[®] using CHCl_3 as eluent. The filtrate was concentrated under reduced pressure. The resulting product was extracted with CHCl_3 and water. The organic layer as dried over Na_2SO_4 , and concentrated under reduced pressure. The crude product was purified with

silica gel chromatography (eluent; AcOEt:hexane, 3:1 to 1:0) to give **16c** as a colorless oil (58% yield, 1.4 g). The spectral data were consistent with the literature.^[54]

(Step 4) (*trans*-cyclobutane-1,2-diyl)bis(methylene) bis(4-methylbenzenesulfonate) (16d)

The titled compound **16d** was synthesized by referring the synthesis procedure of propane-1,3-dilybis(4-methylbenzenesulfonate).^[55] In a 100 mL three-necked round-bottom flask containing a stirring bar, a solution of **16c** (5.0 mmol) in CH₂Cl₂ (10 mL) was stirred at 0 °C (ice bath) for 10 min. The flask was covered with aluminum foil, and triethylamine (20 mmol, 2.8 mL) were added dropwise. Afterward, a solution of 4-methylbenzenesulfonyl chloride (10 mmol, 1.9 g) in CH₂Cl₂ (10 mL) was added over a period of 15–30 min followed by the addition of DMAP (10 mol %, 0.5 mmol) at 0 °C under Ar. The reaction mixture was stirred for 1 h at 0 °C and overnight at ambient temperature. The white precipitate (triethylamine hydrochloride) was filtered through Celite[®] using CH₂Cl₂. The filtrate was washed once with each 1 M HCl, aq. saturated solution of NaHCO₃, water, and brine. The aqueous phase was extracted once with CH₂Cl₂. The organic phase was dried over Na₂SO₄ and filtered. Evaporation of the solvent and subsequent purification by short silica gel column chromatography (eluent: CHCl₃) afforded **16d** as a white solid (85% yield, 1.8 g). ¹H NMR (600 MHz, CDCl₃): δ 7.76 (d, 4H, *J* = 8.2 Hz), 7.35 (d, 4H, *J* = 8.2 Hz), 3.95–3.90 (m, 4H), 2.46 (s, 6H), 2.39–2.33 (m, 2H), 1.92–1.85 (m, 2H), 1.69–1.62 (m, 2H).

(Step 5) bis(*m*-xylyl)phosphine–borane complex (16e)

The titled compound **16e** was synthesized by modifications of the literature procedure.^[56] Grinded CeCl₃·7H₂O (36 mmol, 13.4 g) and a magnetic stirrer bar were added to a 300 mL two-necked flask and dried *in vacuo* at 140 °C for 2 h. After cooling to ambient temperature, THF (150 mL) was added to the flask and the resulting mixture was stirred for 30 min. Then, NaBH₄ (36 mmol, 1.36 g) was added and stirring was continued for 1 h. The flask was immersed in an ice bath (0 °C) and **1a** (12 mmol, 3.1 g) was added and stirring was continued for 1 h. Finally, LiAlH₄ (19.8 mmol, 0.75 g) was added by portions. The ice bath was removed, and the mixture was stirred at room temperature overnight. At 0 °C, 5.3 M HCl aq (36 mL) was added to the mixture to quench the reaction. The resulting mixture was filtered through Celite[®] using CHCl₃ as eluent. The filtrate was concentrated under reduced pressure. The resulting product was purified with silica gel column chromatography (AcOEt/hexane = 1/7) to give **16e** as a white solid (57% yield, 1.8 g). The spectral data were consistent with the literature.^[56]

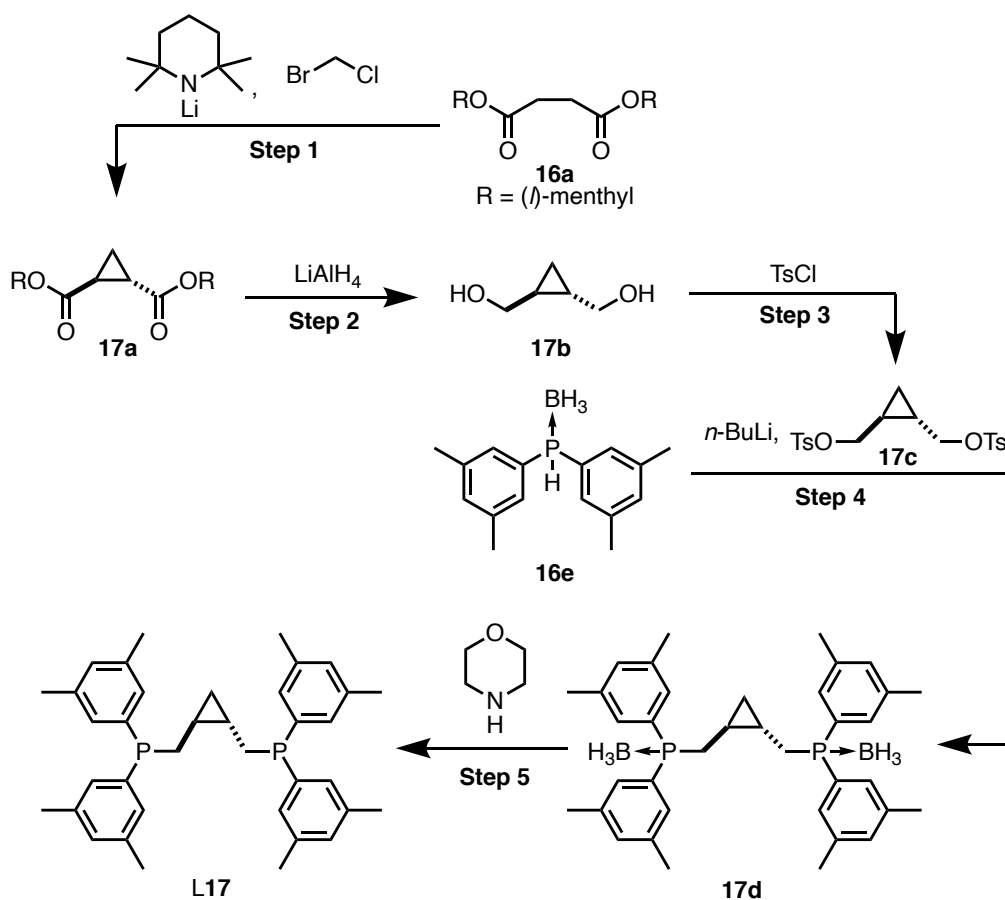
(Step 6) *trans*-1,2-bis[(dixylylphosphino)methyl]cyclobutane–diborane complex (16f)

To a 100 mL two-neck flask, **16e** (512 mg, 2 mmol), anhydrous THF (30 mL), and a magnetic stirring bar were placed under Ar. To the solution was added NaH (2.1 mmol, 91.6 mg) at 0 °C. After stirring for a 1 hour at room temperature, to the solution was added **16d** (382 mg, 0.9 mmol) in anhydrous THF (5 mL) at 0 °C. The reaction mixture was allowed to warm to r.t. After stirring for 4 h, the reaction mixture was quenched with water (20 mL) at 0 °C, and the organic phase was removed under reduced pressure. The residue was extracted with CH₂Cl₂ (30 mL×2) washed with brine. The organic layer was dried over Na₂SO₄ and filtrated. The evaporation of the filtrate gave a crude solid, which was purified by column chromatography on silica gel (hexane/AcOEt = 5/1) to afford **16f** as a white solid (56% yield, 297 mg). ¹H NMR (600 MHz, CDCl₃) δ 7.25 (s, 2H), 7.23 (s, 4H), 7.21 (s, 2H), 7.06 (s, 4H), 2.32 (d, 24H, *J* = 7.5 Hz), 2.15–2.21 (m, 2H), 1.90–1.96 (m, 2H), 0.91 (bs, 6H, BH₃), 0.65–0.68 (m, 2H), 0.35 (t, 2H, CH₂, *J* = 6.9 Hz); ³¹P{¹H} NMR (243 MHz, CDCl₃) δ 14.7–15.4 (m).

(Step 7) *trans*-1,2-bis[(dixylylphosphino)methyl]cyclobutane (L16)

To a 75 mL Schlenk tube equipped with Young's stopcock, **16f** (118 mg, 0.2 mmol), degassed morpholine (2.5 mL) and a magnetic stirring bar were placed under Ar. The mixture was heated at 120 °C for 2 h. The solution was cooled to r.t. and morpholine was removed *in vacuo* (*ca.* 0.01 mmHg, r.t.). The crude product was purified by alumina column chromatography (hexane/AcOEt = 10/1) to afford **L16** as a colorless sticky oil (101 mg, 85% yield). ¹H NMR (600 MHz, CDCl₃) δ 7.04 (d, 4H, *J* = 7.6 Hz), 7.02 (d, 4H, *J* = 7.6 Hz), 6.92 (d, 4H, *J* = 6.2 Hz), 6.92 (d, 4H, *J* = 19.9 Hz), 2.27 (d, 2H, CH₃, *J* = 8.9 Hz), 2.01–2.04 (m, 2H), 1.98–2.00 (m, 2H), 1.87–1.91 (m, 2H), 1.38–1.44 (m, 2H); ³¹P{¹H} NMR (243 MHz, CDCl₃) δ –21.6; ¹³C{¹H} NMR (151 MHz, CDCl₃): δ 139.0 (d, ³*J*_{PC} = 13.0 Hz), 138.5 (d, ³*J*_{PC} = 13.0 Hz), 137.6 (d, ¹*J*_{PC} = 7.2 Hz), 137.6 (d, ¹*J*_{PC} = 7.2 Hz), 130.6, 130.5 (d, ²*J*_{PC} = 8.7 Hz), 130.3, 130.2 (d, ²*J*_{PC} = 4.3 Hz), 41.4 (dd, ^{2,3}*J*_{PC} = 11.6 Hz), 35.2 (d, ¹*J*_{PC} = 13.0 Hz), 26.5 (d, ³*J*_{PC} = 10.1 Hz), 21.3, 21.3; HRMS (ESI, (M+H)⁺) Calcd for C₃₈H₄₇P₂⁺: 565.3148, Found *m/z* = 565.3136.

Synthesis of *trans*-1,2-bis[(dixylylphosphino)methyl]cyclopropane (L17).



(Step 1) dimethyl *trans*-cyclopropane-1,2-dicarboxylate (**17a**)

The titled compound **17a** was synthesized by the literature procedure.^[52,53] A dry 500 mL three-necked round-bottomed flask containing a magnetic stirring bar was equipped with a 100 mL pressure-equalizing dropping funnel, a rubber septum, and a three-way stopcock with an Ar balloon. The air in the system was replaced with Ar. The flask was charged with dehydrated THF (100 mL) and cooled with an ice bath; a 1.55 M hexane solution of butyllithium (105 mmol, 67.7 mL) was added. This solution was stirred while 2,2,6,6-tetramethylpiperidine (105 mmol, 17.9 mL) was added dropwise with a syringe through the septum over a 10 min period. The resulting solution of lithium 2,2,6,6-tetramethylpiperidide (LTMP) was cooled to $-78\text{ }^\circ\text{C}$ and stirred. A solution of **16a** (50 mmol, 19.7 g) in THF (100 mL) was then added dropwise through the addition funnel over a 1 h period at $-78\text{ }^\circ\text{C}$. The resulting yellow solution of succinate dianion was stirred for 1 h at $-78\text{ }^\circ\text{C}$. To the solution was added dropwise 1,2-dibromoethane (50 mmol, 4.3 mL) with a syringe through the septum over a 10 min period at $-78\text{ }^\circ\text{C}$. The reaction mixture was stirred for 2 h at $-78\text{ }^\circ\text{C}$. To the resulting mixture, isobutyraldehyde (20 mmol, 1.8 mL) was added dropwise to quench any unreacted anions. After being stirred for an additional 30 min, the reaction mixture was poured into ice-cooled 1

M HCl aq (200 mL) with stirring and the product was extracted 3 times with diethylether (100 mL). The combined organic phases were washed with 200 mL of brine, dried over sodium sulfate, filtered, and concentrated with a rotary evaporator. The residue was purified with silica gel chromatography (diethylether/hexane = 1/18) to give the product **17a** as a colorless crystal (10.4 g, 51% yield). The spectral data were consistent with the literature.^[52,53]

(Step 2) (*trans*-cyclopropane-1,2-diyl)dimethanol (17b)

To a 500 mL three-necked round-bottom flask were added **17a** (22 mmol, 8.8 g) and dehydrated THF (220 mL) under Ar. The mixture was cooled to 0 °C, followed by the addition of LiAlH₄ (45 mmol, 1.7 g) in portions. The mixture was warmed to r.t. and stirred for 14 h. The mixture was cooled to 0 °C, and H₂O (1.7 mL), 2 M NaOH aq (1.7 mL), and H₂O (8.5 mL) were added in this order to the mixture to quench the reaction. The resulting mixture was filtered through Celite® using CHCl₃ as eluent. The filtrate was concentrated under reduced pressure. The resulting product was extracted with CHCl₃ and water. The organic layer was dried over Na₂SO₄, and concentrated under reduced pressure. The crude product was purified with silica gel chromatography (eluent; AcOEt/hexane = 3/1 to 1/0) to give **17b** as a colorless oil (81% yield, 1.8 g). ¹H NMR (600 MHz, CDCl₃) δ 3.84 (dd, 2H, *J* = 11.0, 4.8 Hz), 3.83 (bs, 2H), 3.07 (dd, 2H, *J* = 11.0, 8.9 Hz), 1.06–1.00 (m, 2H), 0.44 (t, 2H, *J* = 6.9 Hz).

(Step 3) (*trans*-cyclopropane-1,2-diyl)bis(methylene) bis(4-methylbenzenesulfonate) (17c)

The titled compound **17c** was synthesized by referring the synthesis procedure of propane-1,3-dilybis(4-methylbenzenesulfonate).^[55] A solution of **17b** (5.0 mmol, 0.51 g) in CH₂Cl₂ (10 mL) was stirred at 0 °C (ice bath) for 10 min. The round bottom flask was covered using aluminum foil and triethylamine (20 mmol, 2.0 g) were added dropwise. Afterward, a solution of 4-methylbenzenesulfonyl chloride (10 mmol, 1.9 g) in CH₂Cl₂ (10 mL) was added over a period of 15 min, followed by the addition of DMAP (0.5 mmol, 61 mg). The reaction mixture was stirred each for 1 h at 0 °C and at ambient temperature. The white precipitate (triethylamine hydrochloride) was filtered off. The light yellow filtrate was washed once with each 1 M HCl, aq. saturated solution of NaHCO₃, water, and brine. The aqueous phase was extracted once with CH₂Cl₂. The organic phase was dried over Na₂SO₄ and filtered. Evaporation of the solvent and subsequent purification by column chromatography (CHCl₃) afforded a white solid (55% yield, 1.1 g). ¹H NMR (600 MHz, CDCl₃) δ 7.77 (d, 4H, *J* = 8.2 Hz), 7.35 (d, 4H, *J* = 8.2 Hz), 3.87–3.82 (m, 4H), 2.45 (s, 6H), 1.09–1.03 (m, 2H), 0.59 (t, 2H, *J* = 7.2 Hz).

(Step 4) *trans*-1,2-bis[(dixylylphosphino)methyl]cyclopropane–diborane complex (17d)

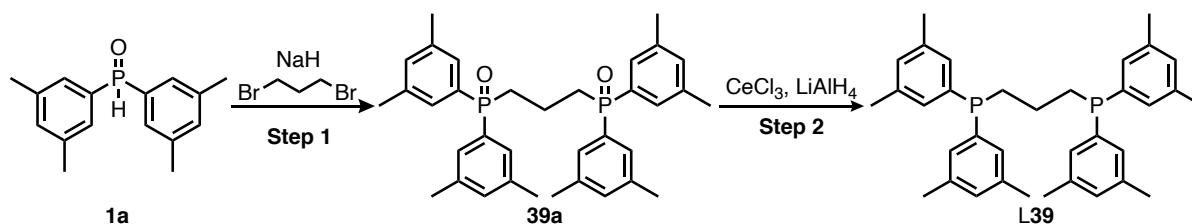
To a 200 mL two-neck flask, **16e** (1.45 g, 5.6 mmol), anhydrous THF (70 mL), and a magnetic stirring bar were placed under Ar. The flask was immersed in an ice bath (0 °C). To the solution was added *n*-BuLi (1.6 M in hexane, 3.6 mL, 5.6 mmol) at 0 °C. After stirring for a 1 hour at 0 °C, to the solution was added **17c** (1.60 g, 2.76 mmol) in anhydrous THF (10 mL) at 0 °C. The reaction mixture was allowed to warm to r.t. After stirring overnight at r.t., the reaction mixture was quenched with water (50 mL) at 0 °C, and the organic phase was removed *in vacuo*. The residue was extracted with CH₂Cl₂ (70 mL×2) washed with brine (70 mL). The organic layer was dried over Na₂SO₄ and filtrated. The evaporation of the filtrate gave a crude solid, which was purified by column chromatography on silica gel (hexane/AcOEt = 10/1) to afford **17d** as white solid (0.37 g, 23%). ¹H NMR (600 MHz, CDCl₃) δ 7.25 (s, 2H), 7.23 (s, 4H), 7.21 (s, 2H), 7.06 (s, 4H), 2.32 (d, 24H, *J* = 7.5 Hz), 2.15–2.21 (m, 2H), 1.90–1.96 (m, 2H), 0.91 (bs, 6H, BH₃), 0.65–0.68 (m, 2H), 0.35 (t, 2H, CH₂, *J* = 6.9 Hz); ³¹P{¹H} NMR (243 MHz, CDCl₃) δ 14.7–15.4 (m).

(Step 5) *trans*-1,2-bis[(dixylylphosphino)methyl]cyclopropane (L17)

To a 75 mL Schlenk tube equipped with Young's stopcock, **17d** (0.17 g, 0.3 mmol), degassed morpholine (7.5 mL) and a magnetic stirring bar were placed under Ar gas atmosphere. The mixture was heated at 120 °C for 2 h under Ar. The solution was cooled to r.t. and morpholine was removed *in vacuo* (*ca.* 0.01 mmHg, r.t.). The crude product was purified by alumina column chromatography (hexane/AcOEt = 10/1) to afford **L17** as a colorless sticky oil (0.13 g, 79%). ¹H NMR (600 MHz, CDCl₃) δ 7.01 (t, 8H, *J* = 7.2 Hz), 6.92 (s, 4H), 2.27 (d, 24H, *J* = 4.0 Hz), 2.06 (dd, 2H, *J* = 5.2, 13.7 Hz), 1.73 (dd, 2H, *J* = 7.4, 13.7 Hz), 0.54 (bs, 2H), 0.35 (t, 2H, *J* = 6.6 Hz); ¹³C{¹H} NMR (151 MHz, CDCl₃): δ 138.2 (d, *J* = 10.1 Hz), 137.6–137.5 (m), 133.3 (d, *J* = 8.8 Hz), 130.6 (d, *J* = 18.9 Hz), 130.4 (d, *J* = 18.7 Hz), 130.2 (d, *J* = 20.2 Hz), 128.4 (d, *J* = 10.1 Hz), 34.0 (d, *J* = 71.0 Hz), 33.2 (d, *J* = 11.6 Hz), 21.3, 21.3, 12.3; ³¹P{¹H} NMR (243 MHz, CDCl₃) δ -17.5; HRMS (ESI, (M+H)⁺) Calcd for C₃₇H₄₅P₂⁺: 551.2991, Found *m/z* = 551.3000.

1.4.8. Ligand preparation (L39–L45)

Synthesis of 1,3-bis[bis(3,5-dimethylphenyl)phosphino]propane (L38).



(Step 1) propane-1,3-diylbis[bis(3,5-dimethylphenyl)phosphine oxide (38a)]

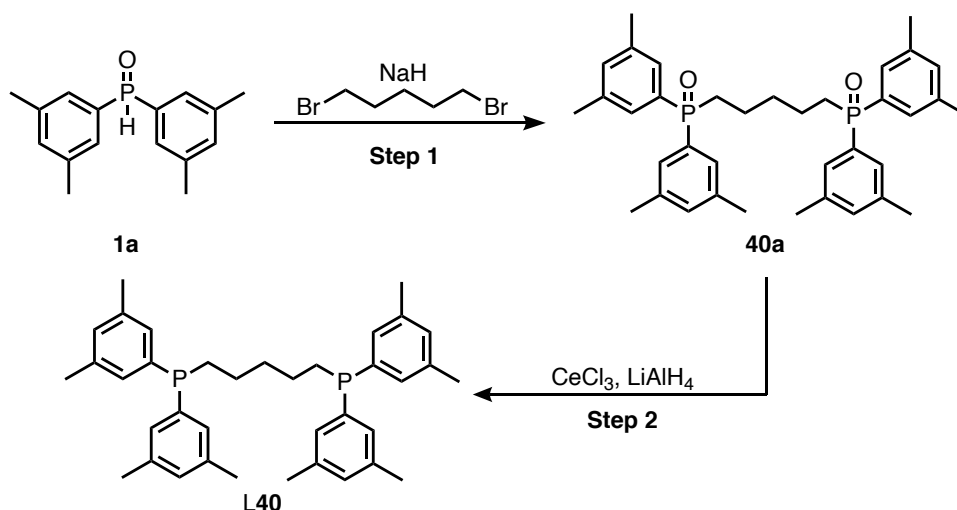
To a 100 mL two-necked flask were added **1a** (9.0 mmol, 2.34 g), THF (40 mL), and a magnetic stirrer bar. NaH (10 mmol, 0.45 g) was added to the solution under Ar flow at r.t. and stirred for 40 min. Then, 1,4-dibromobutane (908 mg, 4.5 mmol) was added to the mixture dropwise. After stirring for 16 h, THF was removed under reduced pressure, the resulting white solid was dissolved in water and extracted with CH₂Cl₂. The organic layer was collected and dried over Na₂SO₄, and concentrated under reduced pressure. The crude product was purified by chromatography (AcOEt/CH₃OH = 20/1) to give **38a** as a white solid (76% yield, 1.90 g). ¹H NMR (500 MHz, CDCl₃) δ 7.31 (s, 4H, C₆H₃), 7.28 (s, 4H, C₆H₃), 7.09 (s, 4H, C₆H₃), 2.40–2.46 (m, 4H), 2.30 (s, 24H, CH₃), 2.00 (m, 2H, CH₂); ³¹P{¹H} NMR (202 MHz, CDCl₃) δ 33.1; ¹³C{¹H} NMR (126 MHz, CDCl₃): δ 138.3 (d, *J* = 13.2 Hz), 133.4, 133.2, 132.4, 128.2 (d, *J* = 9.6 Hz), 30.6 (d, *J* = 5.4 Hz), 30.0 (d, *J* = 5.4 Hz), 21.3, 14.9 (d, *J* = 3.6 Hz).

(Step 2) 1,3-bis[bis(3,5-dimethylphenyl)phosphino]propane (L38)

Grinded CeCl₃·7H₂O (22.5 mmol, 8.36 g) and a magnetic stirrer bar were added to a 300 mL two-necked flask and dried *in vacuo* at 140 °C for 2 h. After cooling to ambient temperature, THF (45 mL) and **38a** (3.0 mmol, 1.67 g) were added to the flask at once and the resulting mixture was stirred for 30 min. Then, the mixture was cooled to 0 °C, before LiAlH₄ (81 mmol, 3.1 g) was added portionwise. The resulting mixture was stirred at r.t. for 16 h. At 0 °C, H₂O (3.1 mL), 2 M NaOH aq (6.2 mL), and H₂O (9.3 mL) were added in this order to the mixture to quench the reaction. The resulting mixture was filtered through Celite[®] using CHCl₃ as eluent. The filtrate was concentrated under reduced pressure. The resulting product was extracted with CH₂Cl₂ and the organic layer as dried over Na₂SO₄, and concentrated under reduced pressure. The crude product was purified with Florisil chromatography using hexane as eluent to give **L38** as white solid (82% yield, 1.29 g). ¹H NMR (600 MHz, CDCl₃) δ 6.99 (s, 4H, C₆H₃), 6.98 (s, 4H, C₆H₃), 6.91 (s, 4H, C₆H₃), 2.26 (s, 24H, CH₃), 2.14 (t, 4H, *J* = 7.6

Hz, PCH₂), 1.58 (m, 2H, CH₂); ³¹P{¹H} NMR (243 MHz, CDCl₃) δ -17.1; ¹³C{¹H} NMR (151 MHz, CDCl₃): δ 138.4 (d, ³J_{PC} = 11.6 Hz), 137.7 (d, ¹J_{PC} = 7.2 Hz), 130.4, 130.3 (d, ²J_{PC} = 5.8 Hz), 29.6 (dd, ^{2,3}J_{PC} = 12.3 Hz), 22.7 (t, ²J_{PC} = 18.1 Hz), 21.3; HRMS (ESI, (M+H)⁺) Calcd for C₃₅H₄₃P₂⁺: 525.2835, Found *m/z* = 528.2807.

Synthesis of 1,5-bis[bis(3,5-dimethylphenyl)phosphino]pentane (L39).



(Step 1) pentane-1,5-diylbis[bis(3,5-dimethylphenyl)phosphine oxide (39a)

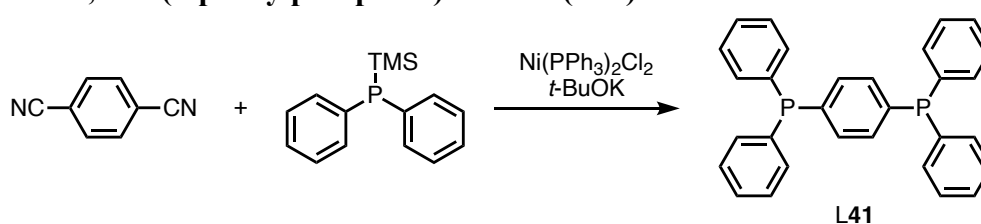
To a 100 mL two-necked flask were added phosphine **1a** (9.0 mmol, 2.35 g), THF (40 mL), and a magnetic stirrer bar. NaH (10 mmol, 0.44 g) was added to the solution under Ar flow at r.t. and stirred for 1 h. Then, 1,4-dibromobutane (1.04 g, 4.5 mmol) was added to the mixture dropwise. After stirring for 16 h, THF was removed under reduced pressure, the resulting white solid was dissolved in water and extracted with CH₂Cl₂. The organic layer was collected and dried over Na₂SO₄, and concentrated under reduced pressure. The crude product was purified by chromatography (AcOEt/CH₃OH = 20/1) to give **39a** as a white solid (70% yield, 1.73 g). ¹H NMR (500 MHz, CDCl₃) δ 7.31 (s, 4H, C₆H₃), 7.29 (s, 4H, C₆H₃), 7.11 (s, 4H, C₆H₃), 2.32 (s, 24H, CH₃), 2.16 (m, 4H), 1.59 (m, 4H), 1.54 (m, 2H); ³¹P{¹H} NMR (202 MHz, CDCl₃) δ 33.4; ¹³C{¹H} NMR (126 MHz, CDCl₃): δ 138.3 (d, *J* = 12.0 Hz), 133.4 (d, *J* = 2.4 Hz), 133.3, 132.5, 128.2 (d, *J* = 9.6 Hz), 32.1 (t, *J* = 14.4 Hz), 29.6, 29.1, 21.3, 20.9 (d, *J* = 3.6 Hz).

(Step 2) 1,5-bis[bis(3,5-dimethylphenyl)phosphino]pentane (L39)

Grinded CeCl₃·7H₂O (23 mmol, 8.55 g) and a magnetic stirrer bar were added to a 300 mL two-necked flask and dried *in vacuo* at 140 °C for 2 h. After cooling to ambient temperature, THF (45 mL) and **39a** (3.0 mmol, 1.67 g) were added to the flask at once and the resulting mixture was stirred for 30 min. Then, the mixture was cooled to 0 °C, before LiAlH₄ (81 mmol,

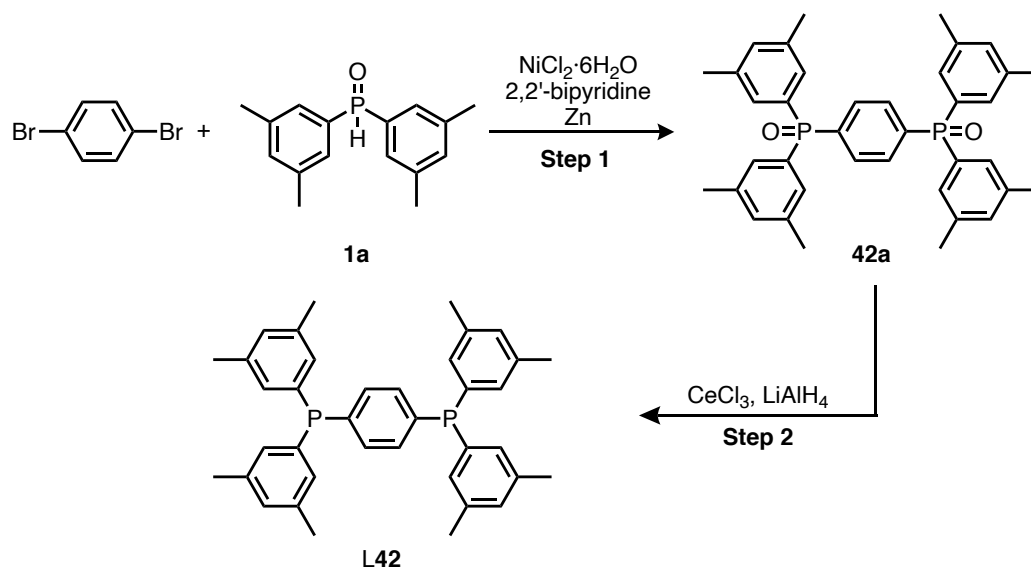
3.1 g) was added portionwise. The resulting mixture was stirred at r.t. for 16 h. At 0 °C, H₂O (3.1 mL), 2 M NaOH aq (6.2 mL), and H₂O (9.3 mL) were added in this order to the mixture to quench the reaction. The resulting mixture was filtered through Celite[®] using CHCl₃ as eluent. The filtrate was concentrated under reduced pressure. The resulting product was extracted with water (50 mL) and CH₂Cl₂ (15 × 5 mL) and the organic layer as dried over Na₂SO₄, and concentrated under reduced pressure. The crude product was purified with Florisil chromatography (AcOEt/hexane = 1/40) to give **L39** as white solid (85% yield, 1.41 g). ¹H NMR (600 MHz, CDCl₃) δ 7.01 (s, 4H, C₆H₃), 7.00 (s, 4H, C₆H₃), 6.92 (s, 4H, C₆H₃), 2.27 (s, 24H, CH₃), 1.95 (t, 4H, *J* = 7.9 Hz, PCH₂), 1.55 (m, 2H, CH₂), 1.41 (m, 4H, CH₂); ³¹P{¹H} NMR (243 MHz, CDCl₃) δ -15.9; ¹³C{¹H} NMR (151 MHz, CDCl₃): δ 138.6 (d, ³*J*_{PC} = 11.6 Hz), 137.7 (d, ¹*J*_{PC} = 7.2 Hz), 130.4, 130.3 (d, ²*J*_{PC} = 10.1 Hz), 32.7 (t, ³*J*_{PC} = 13.0 Hz), 27.7 (d, ¹*J*_{PC} = 10.1 Hz), 25.6 (d, ²*J*_{PC} = 15.9 Hz), 21.3; HRMS (ESI, (M+H)⁺) Calcd for C₃₇H₄₇P₂⁺:553.3148, Found *m/z* = 553.3104.

Synthesis of 1,4-bis(diphenylphosphino)benzene (**L40**).



1,4-Bis(diphenylphosphino)benzene was synthesized using typical procedure.^[40] In a 100 mL two-necked flask was added terephthalonitrile (0.90 mmol, 116.9 mg), Ni(PPh₃)₂Cl₂ (0.054 mmol, 35.3 mg), *t*-BuOK (2.70 mmol, 303.0 mg) and dehydrate 1,4-dioxane (8.0 mL) under Ar. The resulting mixture was stirred at r.t. for 10 min followed by the addition of TMS-PPh₂ (2.10 mmol, 538.0 μL) at once. The mixture was moved to 90 °C and stirred overnight. The mixture was cooled down at r.t. and the solvent was removed. The resulting sticky mixture was charged with H₂O (20 mL) and extracted by CH₂Cl₂ (20 mL, 3 times). The organic phase was collected and dried over Na₂SO₄. Removal of the solvent under reduced pressure and chromatography using hexane: ethyl acetate (50:1) gave the product **L40** as a white solid (34% yield, 138.41 mg). ¹H NMR (600 MHz, CDCl₃) δ 7.29–7.34 (m, 24H); ³¹P{¹H} NMR (243 MHz, CDCl₃) δ -4.82; ¹³C{¹H} NMR (151 MHz, CDCl₃): δ 137.2 (d, ¹*J*_{PC} = 11.6 Hz), 133.8 (d, ²*J*_{PC} = 20.2 Hz), 128.7, 128.5 (d, ³*J*_{PC} = 7.2 Hz).

Synthesis of 1,4-bis[bis(3,5-dimethylphenyl)phosphino]benzene (L41).



(Step 1) 1,4-Phenylenebis[bis(3,5-dimethylphenyl)phosphine oxide] (41a)

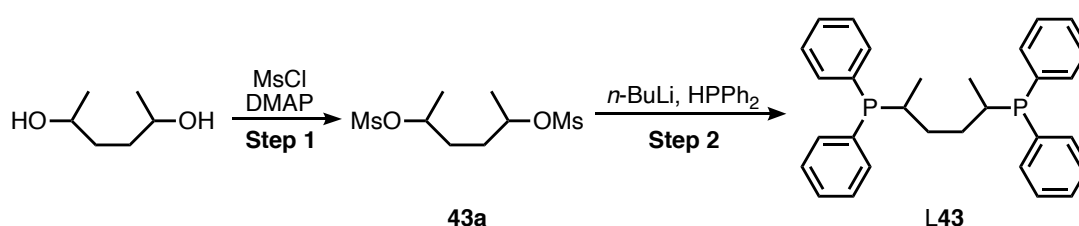
1,4-Phenylenebis[bis(3,5-dimethylphenyl)phosphine oxide] was synthesized using typical procedure.^[41] Under air, added 1,4-dibromobenzene (2.4 mmol, 568.3 mg), $\text{NiCl}_2 \cdot 6\text{H}_2\text{O}$ (1.8 mmol, 430.0 mg), bipyridine (3.6 mmol, 565.0 mg), Zn powder (9.6 mmol, 526.0 mg) and de-ionized H_2O (20 mL) into a 100 mL two-necked flask. The mixture was stirred for 10 min followed by the addition of bis(3,5-dimethylphenyl)phosphine oxide (6.0 mmol, 1214.6 mg) at once. The resulting mixture was stirred under air at 70 °C for 24 h. The reaction was stopped and cooled down at r.t. and extracted by CH_2Cl_2 (20 mL, 3 times). The organic phase was collected and dried over Na_2SO_4 . Removal of the solvent under reduced pressure and chromatography ($\text{CH}_2\text{Cl}_2/\text{MeOH} = 20/1$), followed by recrystallization using hexane and CH_2Cl_2 gave the product **41a** as a white solid (69% yield, 994.1 mg). ^1H NMR (600 MHz, CDCl_3) δ 7.34 (d, 8H, $J = 13.1$ Hz), 7.30 (d, 2H, $J = 14.4$ Hz), 7.16 (d, 2H, $J = 19.2$ Hz), 7.06 (s, 4H), 2.26 (s, 24H); $^{31}\text{P}\{^1\text{H}\}$ NMR (243 MHz, CDCl_3) δ 35.3.

(Step 2) 1,4-Bis[bis(3,5-dimethylphenyl)phosphino]benzene (L41)

Grinded $\text{CeCl}_3 \cdot 7\text{H}_2\text{O}$ (1.5 mmol, 562.6 mg) was added to 100 mL three-necked flask and stirred under vacuum at 140 °C for 2 h. Under Ar, the reaction was cooled to r.t. THF (5 mL) and **41a** (0.2 mmol, 118.5 mg) was added to the flask at once and the resulting mixture was stirred for 30 min. After the stirring, the mixture was cooled to 0 °C, LiAlH_4 (3.6 mmol, 144.3 mg) was added to the mixture in portions. The resulting mixture was stirred for 16 h at r.t. At 0 °C, 5 mL H_2O was added to the mixture to quench the reaction. The resulting mixture was filtered by Celite[®] and washed with acetone. The filtrate was collected and the solvent was removed by reduced pressure. Recrystallization using hexane and CH_2Cl_2 gave the product **L41**

as a white solid (75% yield, 84.13 mg). ^1H NMR (600 MHz, CDCl_3) δ 7.22 (s, 1H), 7.21 (d, 2H, $J = 1.4$ Hz), 7.20 (s, 1H), 6.92 (d, 8H, $J = 8.22$ Hz), 2.25 (s, 24H, CH_3); $^{31}\text{P}\{^1\text{H}\}$ NMR (243 MHz, CDCl_3) δ -5.09; $^{13}\text{C}\{^1\text{H}\}$ NMR (151 MHz, CDCl_3): δ 137.9 (d, $^3J_{\text{PC}} = 8.7$ Hz), 136.5 (d, $^1J_{\text{PC}} = 10.1$ Hz), 133.3 (dd, $^2J_{\text{PC}} = 18.9$ Hz, $^3J_{\text{PC}} = 5.7$ Hz), 131.6 (d, $^2J_{\text{PC}} = 18.8$ Hz), 130.6, 21.3.

Synthesis of 2,5-bis(diphenylphosphino)hexane (L42).



(Step 1) 1,4-Bis(methylsulfonyloxy)-1,4-dimethylbutane (42a)

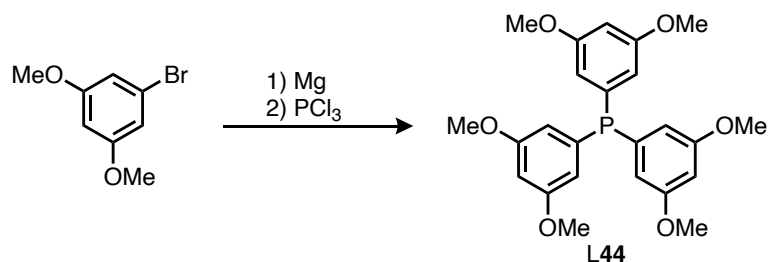
1,4-Bis(methylsulfonyloxy)-1,4-dimethylbutane was synthesized using typical procedure.^[42] 2,5-hexanediol (10.0 mmol, 1.24 mL), 20 mg of DMAP, 10 mL pyridine and 5 mL CH_2Cl_2 was added to a 100 mL two-necked flask under N_2 . After stirring for 30 min at 0 °C, MsCl (40.0 mmol, 3.1 mL) was added to the mixture dropwise in 10 min. The resulting mixture was moved to r.t. and stirred for 4 h. 50 mL 2N HCl solution was added to the mixture and CH_2Cl_2 (30 mL, 3 times) was used to extract. The organic phase was washed with H_2O (30 mL) and saturated NaHCO_3 (30 mL) and dried over Na_2SO_4 . Removal of the solvent and purification by chromatography using hexane: ethyl acetate (1:1) gave the product **42a** as a white sticky solid (52% yield, 1.42 g). ^1H NMR (600 MHz, CDCl_3) δ 2.92 (s, 6H, SCH_3), 1.74–1.86 (m, 6H), 1.44 (dd, 6H, $J = 2.1, 6.1$ Hz, CH_3).

(Step 2) 2,5-Bis(diphenylphosphino)hexane (L42)

2,5-Bis(diphenylphosphino)hexane was synthesized using typical procedure.^[42] Under N_2 , HPPH₂ (1.68 mmol, 300.0 μL) and 10 mL THF was added to a three-necked flask. At 0 °C, *n*-BuLi (2.02 mmol, 1.3 mL, 1.6 M in hexane) was added to the mixture dropwise. The resulting mixture was stirred for 1 h at r.t. **42a** (0.67 mmol, 183.3 mg) in 5 mL THF was added to the mixture dropwise in 20 min. The resulting mixture was stirred overnight. Ether (20 mL) and saturated NH_4Cl (10 mL) was added to the mixture. The resulting mixture was extracted by ether (20 mL, 3 times). The organic phase was collected and dried over Na_2SO_4 . Removal of

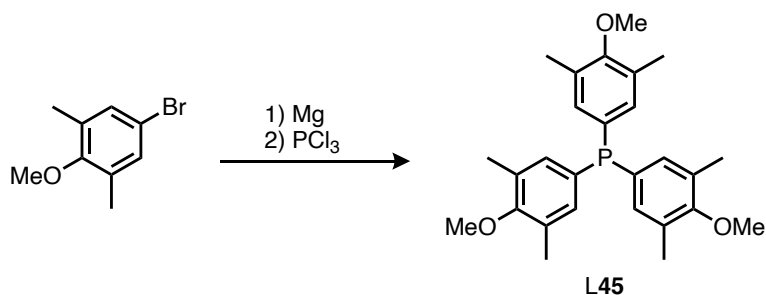
the solvent under reduced pressure and chromatography (hexane/ethyl acetate = 1/2) on a short column gave the product **L42** as a white solid (67% yield, 205.4 mg). ^1H NMR (600 MHz, CDCl_3) δ 7.45–7.41 (m, 8H), 7.33–7.29 (m, 12H), 2.24–2.17 (m, 2H), 1.82–1.74 (m, 2H), 1.25–1.19 (m, 2H), 0.94 (d, 3H, $J = 6.9$ Hz), 0.92 (d, 3H, $J = 6.9$ Hz); $^{31}\text{P}\{^1\text{H}\}$ NMR (243 MHz, CDCl_3) δ -1.33.

Synthesis of tris(3,5-dimethoxyphenyl)phosphine (**L43**).



Tris(3,5-dimethoxyphenyl)phosphine was synthesized using typical procedure.^[54] Under Ar, Mg turnings (18 mmol, 433.60 mg) was added to a 100 mL two-necked flask and stirred for 1 h at r.t.. THF (7 mL) was added to the flask at r.t., followed by the addition of one bead of I_2 . The mixture was stirred for 15 min. 1-bromo-3,5-dimethoxybenzene (6 mmol, 1.31 mL) in 6 mL THF was added to the mixture dropwise in 30 min. The mixture was stirred for further 1 h at r.t. PCl_3 (2 mmol, 175 μL) in 6 mL THF was added to the mixture dropwise in 20 min and stirred for 1 h at r.t. After the reaction finished, 20 mL H_2O was added to the mixture, the resulting mixture was extracted with CH_2Cl_2 (20 mL, 3 times) and the organic layer was dried over Na_2SO_4 . Removal of the solvent under reduced pressure and chromatography (hexane/ethyl acetate = 30/1) gave pure product **L43** as white solid (761 mg, 86.0% yield). ^1H NMR (500 MHz, CDCl_3) δ 6.49 (d, $J = 2.3$ Hz), 6.43 (d, $J = 2.3$ Hz), 6.43 (t, $J = 2.3$ Hz), 3.72 (s, 18H, OCH_3); $^{31}\text{P}\{^1\text{H}\}$ NMR (202 MHz, CDCl_3) δ 1.48; $^{13}\text{C}\{^1\text{H}\}$ NMR (126 MHz, CDCl_3): δ 160.7 (d, $^3J_{\text{PC}} = 13.2$ Hz), 138.9 (d, $^1J_{\text{PC}} = 12.0$ Hz), 111.5 (d, $^2J_{\text{PC}} = 21.6$ Hz), 101.1, 55.3.

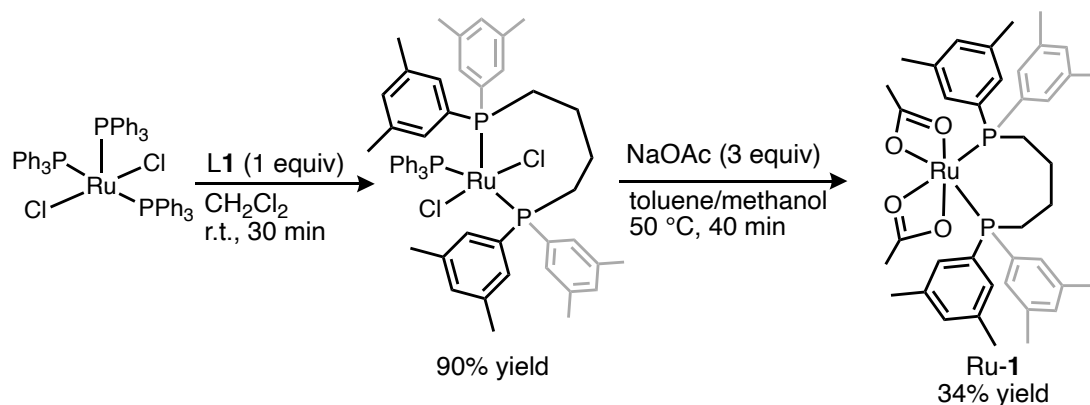
Synthesis of tris(3,5-dimethyl-4-methoxyphenyl)phosphine (L44).



Tris(3,5-dimethyl-4-methoxyphenyl)phosphine was synthesized using typical procedure.^[43] Under Ar, Mg turnings (9 mmol, 217.06 mg) was added to a 50 mL two-necked flask and stirred for 1 h at r.t. THF (4 mL) was added to the flask at r.t., followed by the addition of one bead of I₂. The mixture was stirred for 15 min. 5-bromo-2-methoxy-1,3-dimethylbenzene (3 mmol, 480 μL) in 3 mL THF was added to the mixture dropwise in 30 min. The mixture was stirred for further 1 h at r.t. PCl₃ (1 mmol, 88 μL) in 3 mL THF was added to the mixture dropwise in 20 min and stirred for 1 h at r.t. After the reaction finished, 10 mL H₂O was added to the mixture, the resulting mixture was extracted with CH₂Cl₂ (20 mL, 3 times) and the organic layer was dried over Na₂SO₄. Removal of the solvent under reduced pressure and chromatography (hexane/ethyl acetate = 30/1) gave pure product L44 as white solid (226.9 mg, 52% yield). ¹H NMR (600 MHz, CDCl₃) δ 6.94 (s, 3H), 6.93 (s, 3H), 3.73 (s, 9H, OCH₃), 2.23 (s, 18H, CH₃); ³¹P{¹H} NMR (243 MHz, CDCl₃) δ -7.15; ¹³C{¹H} NMR (151 MHz, CDCl₃): δ 157.5, 134.2 (d, ²J_{PC} = 20.4 Hz), 132.3 (d, ¹J_{PC} = 10.1 Hz), 130.9 (d, ³J_{PC} = 7.2 Hz), 59.6, 16.2.

1.4.9. Precatalyst preparation (Ru-1–Ru-3)

Synthesis of (L1)Ru(OAc)₂ complex (Ru-1).



(Step 1) (L1)RuCl₂(PPh₃)

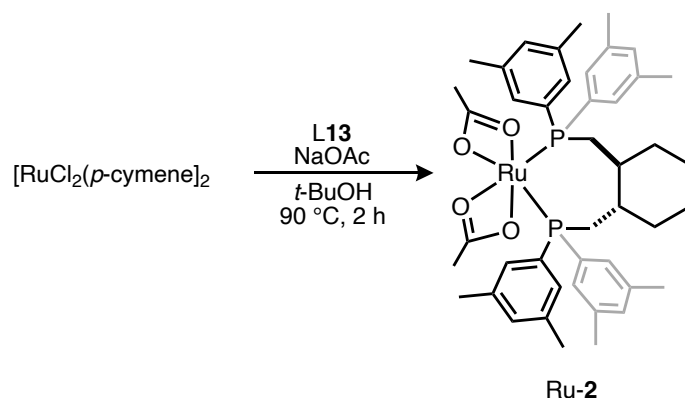
The synthesis of (L1)RuCl₂(PPh₃) was carried out with modification of the literature procedure for the synthesis of (dppb)RuCl₂(PPh₃) complex.^[29] RuCl₂(PPh₃)₃ (958.8 mg, 1.0 mmol), L1 (538.7 mg, 1.0 mmol), dehydrated CH₂Cl₂ (50 mL), and a magnetic stirring bar were placed in a vessel equipped with a Young's stopcock (100 mL) under Ar gas atmosphere. The mixture was stirred at room temperature for 30 min. The resulting dark green color solution was concentrated under reduced pressure (keep under Ar gas atmosphere) to ca. 5 mL. To the slurry was added excess degassed EtOH (ca. 80 mL) to afford the precipitate. Then, the green precipitate was collected under air by filtration washing with degassed EtOH and *n*-hexane, and vacuum dried; yield 90%. HRMS (ESI) (*m/z*): [(L1)RuCl(CH₃CN)]⁺ calcd. for C₃₈H₄₇ClNP₂Ru⁺, 716.1910; found, 716.1893.

(Step 2) (L1)Ru(OAc)₂ complex (Ru-1)

(L1)RuCl₂(PPh₃) (0.2 mmol), NaOAc (0.6 mmol), degassed dehydrated toluene (2 mL), methanol (1 mL), and a magnetic stirring bar were placed in a vessel equipped with a Young's stopcock (75 mL) under Ar gas atmosphere. The mixture was stirred at 50 °C for 1 h and cooled to room temperature. The resulting pale orange solution was extracted with degassed H₂O (1 mL, 2 times) flowing Ar gas continuously, and water layer was removed by syringe. On the resulting organic layer was layered excess degassed dehydrated *n*-hexane (ca. 50 mL) under Ar. After very slow shaking to vanish the clear interface between dark orange layer and *n*-hexane layer, the mixture was kept on a lab bench at room temperature for several days to give yellow crystal. The crystal was collected by filtration under Ar, washed with *n*-hexane, and dried *in vacuo* to obtain the product (34% yield). ¹H NMR (600 MHz, CDCl₃): δ 7.02 (bs, 8H), 6.98 (s, 4H), 2.48 (s, 4H), 2.26 (s, 24H), 1.97 (bs, 4H), 1.65 (s, 6H); ³¹P{¹H} NMR (243 MHz,

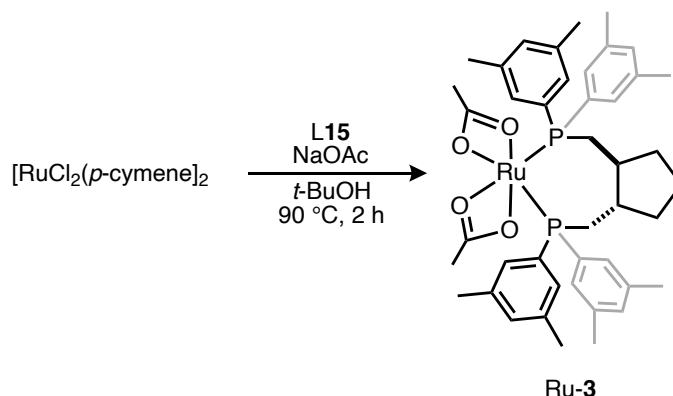
CDCl_3): δ 62.2; $^{13}\text{C}\{^1\text{H}\}$ NMR (151 MHz, CDCl_3): δ 187.1, 137.2 (t, $J = 4.3$ Hz), 130.9, 130.3, 23.9, 23.7, 21.4; HRMS (ESI) (m/z): $[(\text{L1})\text{Ru}(\text{OAc})(\text{CH}_3\text{CN})]^+$ calcd. for $\text{C}_{40}\text{H}_{50}\text{NO}_2\text{P}_2\text{Ru}^+$, 740.2355; found, 740.2289.

Synthesis of $(\text{L13})\text{Ru}(\text{OAc})_2$ complex (Ru-2).



$[\text{RuCl}_2(p\text{-cymene})]_2$ (0.1 mmol), highly pure **L13** (0.2 mmol), NaOAc (0.6 mmol), degassed *t*-BuOH (13 mL), and a magnetic stirring bar were placed in a vessel equipped with a Young's stopcock (75 mL) under Ar gas atmosphere. The mixture was stirred at 90 °C for 2 h and cooled to room temperature. To the resulting dark red solution was added directly excess *n*-hexane (ca. 50 mL) to precipitate inorganic salt. This salt was removed by filtration under Ar atmosphere, and the resulting filtrate was concentrated under Ar to afford the desired solid. The solid was heated at 80 °C, 9 h *in vacuo* to remove *p*-cymene, and the resulting product was collected to obtain the desired Ru complex (44% yield). ^1H NMR (600 MHz, CDCl_3): δ 7.22 (s, 4H), 7.06 (s, 2H), 6.91 (s, 2H), 6.76 (s, 4H), 2.48–2.55 (m, 2H), 2.27 (d, 24H, $J = 37.9$ Hz), 2.17–2.20 (m, 2H), 1.54 (bs, 2H), 1.52 (s, 6H), 1.33 (bs, 2H), 1.04–1.07 (m, 2H), 0.96–1.01 (m, 2H); $^{31}\text{P}\{^1\text{H}\}$ NMR (243 MHz, CDCl_3): δ 61.3; $^{13}\text{C}\{^1\text{H}\}$ NMR (151 MHz, CDCl_3): δ 187.5, 137.3 (t, $J = 5.1$ Hz), 136.8 (t, $J = 4.3$ Hz), 131.7, 130.1, 128.8, 39.1, 38.3 (t, $J = 14.5$ Hz), 37.6, 31.2, 26.0, 23.8, 21.5 (d, $J = 17.4$ Hz); HRMS (ESI) (m/z): $[(\text{L13})\text{Ru}(\text{OAc})(\text{CH}_3\text{CN})]^+$ calcd. for $\text{C}_{44}\text{H}_{56}\text{NO}_2\text{P}_2\text{Ru}^+$, 794.2824; found, 794.2804.

Synthesis of (L15)Ru(OAc)₂ complex (Ru-3).



[RuCl₂(*p*-cymene)]₂ (0.1 mmol), *highly pure* L15 (0.2 mmol), NaOAc (0.6 mmol), degassed *t*-BuOH (13 mL), and a magnetic stirring bar were placed in a vessel equipped with a Young's stopcock (75 mL) under Ar. The mixture was stirred at 90 °C for 2 h and cooled to r.t. To the resulting dark red solution was added directly excess *n*-hexane (ca. 50 mL) to precipitate inorganic salt under Ar. This salt was removed by filtration under Ar atmosphere, and the resulting filtrate was concentrated under Ar to afford the desired solid. The solid was heated at 80 °C, 9 h *in vacuo* to remove *p*-cymene, and the resulting product was collected to obtain desired Ru complex (106 mg, 80% yield). ¹H NMR (600 MHz, CDCl₃): δ 7.22 (s, 4H), 7.04 (s, 2H), 6.93 (s, 2H), 6.84 (s, 4H), 2.82–2.77 (m, 2H), 2.34–2.32 (m, 2H), 2.26 (d, 24H, *J* = 16.5 Hz), 1.86–1.80 (m, 2H), 1.61 (bs, 2H), 1.40–1.33 (m, 2H), 1.27 (s, 2H). ¹³C{¹H} NMR (151 MHz, CDCl₃): δ 186.7, 136.3 (t, *J* = 5.8 Hz), 135.8 (t, *J* = 4.3 Hz), 130.6 (d, *J* = 4.3 Hz), 129.2, 127.8 (d, *J* = 2.9 Hz), 41.1, 36.0, 30.2, 22.6, 22.1, 20.5, 20.4; ³¹P{¹H} NMR (243 MHz, CDCl₃): δ 58.9; HRMS (ESI) (*m/z*): [(L15)Ru(OAc)(CH₃CN)]⁺ calcd. for C₄₃H₅₄NO₂P₂Ru⁺, 780.2668; found, 780.2700.

1.4.10. Cartesian Coordinates

Ru-1: (L1)Ru(OAc)₂

Element	X	Y	Z
Ru	-0.659406	3.472423	0.000484
P	-2.948381	3.589417	0.134276
P	-0.542958	1.191936	0.097205
C	-3.946558	2.055976	0.501602
H	-5.001055	2.347646	0.462499
H	-3.782588	1.347621	-0.316676
C	-3.632883	1.380608	1.857360
H	-4.586097	1.046505	2.283464
H	-3.231025	2.107903	2.573119
C	-2.713679	0.149730	1.790429
H	-3.058370	-0.514898	0.988610
H	-2.848314	-0.413110	2.723466
C	-1.200528	0.389383	1.653919
H	-0.857073	1.047276	2.459928
H	-0.684436	-0.569382	1.776077
O	-0.559560	5.631597	-0.647414
O	0.049696	3.507237	2.059473
O	-0.666662	3.969054	-2.080012
O	1.511328	3.741355	0.433886
C	2.310108	4.095280	2.686977
H	2.074071	3.647313	3.654329
H	2.347732	5.183281	2.811104
H	3.287374	3.758904	2.335794
C	-0.224733	6.160141	-2.986605
H	0.852402	6.160125	-3.186988
H	-0.525551	7.175608	-2.722622
H	-0.739892	5.828983	-3.890689
C	1.249564	3.755307	1.670023
C	-0.509234	5.218138	-1.844585
C	-3.553622	4.726478	1.468507
C	-2.663716	5.225710	2.422372

Chapter 1. Development of Effective Bidentate Diphosphine Ligands of Ruthenium Catalysts toward Practical Hydrogenation of Carboxylic Acids

C	-4.915575	5.069141	1.552435
C	-3.116064	6.062002	3.457574
H	-1.613470	4.957495	2.370590
C	-5.389779	5.893116	2.572947
H	-5.613992	4.703113	0.804210
C	-4.472701	6.380072	3.518671
H	-4.831118	7.025079	4.319377
C	-3.823218	4.270706	-1.352439
C	-4.528630	3.454543	-2.248681
C	-3.754673	5.648249	-1.604403
C	-5.171413	3.994723	-3.369703
H	-4.596712	2.384525	-2.080885
C	-4.380431	6.213355	-2.722058
H	-3.207273	6.290968	-0.921310
C	-5.089003	5.374474	-3.588921
H	-5.593435	5.806047	-4.451842
C	-1.273674	0.213861	-1.290220
C	-1.664886	0.876169	-2.458887
C	-1.401395	-1.183499	-1.214539
C	-2.181537	0.158782	-3.550645
H	-1.548460	1.953788	-2.528261
C	-1.930055	-1.916957	-2.279152
H	-1.077819	-1.712827	-0.322088
C	-2.315811	-1.226984	-3.438580
H	-2.723589	-1.789871	-4.276636
C	1.212899	0.602049	0.083280
C	1.884454	0.501478	-1.139165
C	1.914929	0.333401	1.268636
C	3.233662	0.128911	-1.196621
H	1.355820	0.715019	-2.064262
C	3.260313	-0.045974	1.240007
H	1.421492	0.422133	2.231701
C	3.902866	-0.145219	-0.001184
H	4.950359	-0.439265	-0.034763

Chapter 1. Development of Effective Bidentate Diphosphine Ligands of Ruthenium Catalysts toward Practical Hydrogenation of Carboxylic Acids

C	-5.944930	3.112022	-4.323298
H	-6.951998	3.504607	-4.502679
H	-5.448366	3.045642	-5.298845
H	-6.045475	2.094747	-3.934760
C	-4.278621	7.697087	-2.992851
H	-3.405066	7.926257	-3.616103
H	-5.161192	8.069454	-3.522190
H	-4.172473	8.266042	-2.064637
C	-6.852731	6.262045	2.665805
H	-7.289255	5.929762	3.615085
H	-6.995085	7.347627	2.611002
H	-7.431088	5.809151	1.855736
C	-2.135765	6.612263	4.467627
H	-1.482020	5.824230	4.855815
H	-1.487260	7.371177	4.013533
H	-2.649375	7.077285	5.314173
C	4.009786	-0.353315	2.516544
H	4.306302	-1.408205	2.561752
H	4.927466	0.240574	2.593365
H	3.400051	-0.142507	3.399643
C	3.943620	0.041093	-2.527939
H	4.947677	-0.378836	-2.419523
H	3.389950	-0.585901	-3.235561
H	4.044143	1.031811	-2.986499
C	-2.095912	-3.416573	-2.187772
H	-3.152027	-3.695715	-2.087124
H	-1.716468	-3.915841	-3.085773
H	-1.562875	-3.825726	-1.324963
C	-2.550467	0.878164	-4.827343
H	-1.667469	1.029907	-5.460544
H	-3.279448	0.309761	-5.413084
H	-2.968459	1.866967	-4.617646

Ru-2: (L13)Ru(OAc)₂

Element	X	Y	Z
Ru	-0.530792	1.451657	-0.237081
P	-2.808941	1.544671	-0.083441
P	-0.463312	-0.830626	-0.213649
O	-0.417630	3.634213	-0.812751
O	0.185132	1.403253	1.817092
O	-0.552637	2.020247	-2.298034
O	1.648326	1.690976	0.200412
C	2.449561	1.950299	2.465342
H	2.218009	1.453389	3.409755
H	2.482769	3.030697	2.644979
H	3.427102	1.636312	2.094893
C	-0.106708	4.235941	-3.138316
H	0.955411	4.182885	-3.401525
H	-0.334595	5.253545	-2.816823
H	-0.689291	3.974547	-4.024379
C	1.386955	1.657747	1.435541
C	-0.383462	3.260164	-2.022955
C	-3.435185	2.607781	1.300326
C	-2.551415	3.088697	2.269238
C	-4.804838	2.912737	1.405357
C	-3.017663	3.868796	3.341432
H	-1.495185	2.848647	2.199714
C	-5.292637	3.680792	2.462942
H	-5.498191	2.562712	0.644821
C	-4.381642	4.149353	3.423624
H	-4.750867	4.750075	4.253304
C	-3.694981	2.280052	-1.537633
C	-4.392105	1.498521	-2.468865
C	-3.634256	3.668427	-1.730231
C	-5.033101	2.082534	-3.570313
H	-4.448818	0.420996	-2.350085
C	-4.265110	4.277149	-2.820360

Chapter 1. Development of Effective Bidentate Diphosphine Ligands of Ruthenium Catalysts toward Practical Hydrogenation of Carboxylic Acids

H	-3.086502	4.283719	-1.022552
C	-4.960737	3.470000	-3.728822
H	-5.460028	3.933980	-4.577721
C	-1.189773	-1.756924	-1.637172
C	-1.535466	-1.055418	-2.796972
C	-1.357543	-3.151633	-1.597765
C	-2.045582	-1.731710	-3.917776
H	-1.393001	0.020891	-2.832904
C	-1.879253	-3.844068	-2.692656
H	-1.070601	-3.710245	-0.710660
C	-2.218766	-3.115516	-3.843305
H	-2.622232	-3.646426	-4.704070
C	1.282172	-1.454781	-0.220538
C	1.961830	-1.553854	-1.442363
C	1.974637	-1.733665	0.964569
C	3.304798	-1.938001	-1.494660
H	1.442083	-1.324307	-2.368290
C	3.320114	-2.124436	0.941037
H	1.479946	-1.637133	1.926348
C	3.968093	-2.219946	-0.293888
H	5.016021	-2.513021	-0.321929
C	-3.770879	-0.026082	0.199731
H	-3.522259	-0.717561	-0.611178
H	-4.825973	0.235319	0.067140
C	-1.140142	-1.651318	1.324127
H	-0.792617	-0.995105	2.130826
H	-0.598494	-2.597577	1.433286
C	-2.643218	-1.952209	1.535687
H	-2.992010	-2.602893	0.720261
C	-2.723015	-2.769138	2.852426
H	-2.112735	-3.674429	2.743401
H	-2.256013	-2.180691	3.655862
C	-3.585786	-0.718339	1.579560
H	-3.166003	-0.002641	2.300604

Chapter 1. Development of Effective Bidentate Diphosphine Ligands of Ruthenium Catalysts toward Practical Hydrogenation of Carboxylic Acids

C	-4.145420	-3.140731	3.279569
H	-4.117561	-3.691596	4.227523
H	-4.592443	-3.816840	2.536795
C	-5.005405	-1.881338	3.403900
H	-4.610240	-1.246064	4.209135
H	-6.034899	-2.136832	3.682555
C	-4.997729	-1.106483	2.085123
H	-5.590570	-0.188884	2.179194
H	-5.489819	-1.716082	1.312218
C	-2.368064	-0.970793	-5.182838
H	-1.467869	-0.824373	-5.792624
H	-3.097447	-1.505432	-5.799066
H	-2.766119	0.022361	-4.955489
C	-2.080354	-5.341384	-2.647691
H	-3.144226	-5.602875	-2.697221
H	-1.589279	-5.835308	-3.493562
H	-1.675225	-5.771778	-1.727695
C	4.046754	-2.455981	2.224696
H	3.667481	-1.865095	3.064189
H	3.923657	-3.513664	2.490700
H	5.120884	-2.267097	2.136171
C	4.019728	-2.066494	-2.819893
H	5.074978	-1.789560	-2.732454
H	3.984403	-3.098186	-3.192628
H	3.563895	-1.427775	-3.581773
C	-4.229285	5.778539	-2.992023
H	-4.194637	6.060963	-4.049073
H	-5.122634	6.247529	-2.560577
H	-3.359734	6.216181	-2.493521
C	-5.775522	1.230690	-4.575246
H	-6.680799	1.732106	-4.932353
H	-5.155174	1.018947	-5.455030
H	-6.069200	0.268469	-4.145459
C	-6.762860	4.013115	2.576984

Chapter 1. Development of Effective Bidentate Diphosphine Ligands of Ruthenium Catalysts toward Practical Hydrogenation of Carboxylic Acids

H	-7.178554	3.666112	3.530152
H	-6.932016	5.095302	2.529382
H	-7.340702	3.550753	1.771905
C	-2.045294	4.400352	4.369019
H	-1.366216	3.614597	4.716076
H	-1.422394	5.197772	3.946119
H	-2.565128	4.811213	5.239444

Ru-3: (L15)Ru(OAc)₂

Element	X	Y	Z
Ru	-0.540971	1.412820	-0.196614
P	-2.829669	1.486574	0.000915
P	-0.382122	-0.865425	-0.136567
O	-0.491864	3.583473	-0.812943
O	0.227229	1.428292	1.840101
O	-0.621647	1.941483	-2.267363
O	1.635228	1.715204	0.176569
C	2.495357	2.044857	2.410759
H	2.290390	1.585457	3.379805
H	2.526455	3.131990	2.543931
H	3.465684	1.721209	2.029539
C	-0.238256	4.152400	-3.152712
H	0.831955	4.170287	-3.386632
H	-0.544485	5.159261	-2.863484
H	-0.777361	3.828338	-4.045286
C	1.410629	1.703903	1.420064
C	-0.473852	3.189067	-2.017423
C	-3.421877	2.572988	1.382892
C	-2.515222	3.075655	2.318998
C	-4.789581	2.873643	1.519624
C	-2.956505	3.872706	3.389323
H	-1.460077	2.839751	2.225841
C	-5.252795	3.658584	2.575539
H	-5.501986	2.506636	0.785195

Chapter 1. Development of Effective Bidentate Diphosphine Ligands of Ruthenium Catalysts toward Practical Hydrogenation of Carboxylic Acids

C	-4.319029	4.148720	3.503054
H	-4.669057	4.762731	4.331338
C	-3.751726	2.199359	-1.442160
C	-4.472230	1.403637	-2.341839
C	-3.705212	3.586437	-1.653748
C	-5.151514	1.971057	-3.429889
H	-4.526102	0.328298	-2.204420
C	-4.368129	4.177537	-2.733445
H	-3.145829	4.214025	-0.966602
C	-5.091956	3.355971	-3.607463
H	-5.626321	3.807462	-4.441736
C	-1.121457	-1.839558	-1.521810
C	-1.570273	-1.167550	-2.664086
C	-1.199074	-3.241383	-1.471820
C	-2.094427	-1.880125	-3.755041
H	-1.492805	-0.085311	-2.713235
C	-1.734162	-3.971233	-2.535966
H	-0.830745	-3.776441	-0.600276
C	-2.177815	-3.271885	-3.668536
H	-2.590871	-3.831747	-4.506082
C	1.385007	-1.417981	-0.196885
C	2.034069	-1.475224	-1.434928
C	2.117146	-1.692804	0.967768
C	3.390926	-1.808499	-1.526864
H	1.481514	-1.254056	-2.344162
C	3.471564	-2.037064	0.904281
H	1.641416	-1.635349	1.942098
C	4.091411	-2.090183	-0.350400
H	5.145985	-2.352696	-0.410691
C	-3.797852	-0.070869	0.344248
H	-3.639684	-0.759091	-0.492714
H	-4.856859	0.209738	0.328515
C	-3.465501	-0.773635	1.677472
H	-3.063678	-0.045277	2.395993

Chapter 1. Development of Effective Bidentate Diphosphine Ligands of Ruthenium Catalysts toward Practical Hydrogenation of Carboxylic Acids

C	-2.491861	-1.974091	1.592392
H	-2.826888	-2.597402	0.751798
C	-4.718253	-1.419039	2.306959
H	-5.416306	-0.670739	2.696513
H	-5.251744	-1.986935	1.532487
C	-2.750495	-2.762247	2.909510
H	-2.004751	-2.483486	3.662863
H	-2.640940	-3.839775	2.747871
C	-4.176642	-2.372262	3.388997
H	-4.123473	-1.858717	4.354760
H	-4.824204	-3.242890	3.531139
C	-0.991069	-1.694185	1.424032
H	-0.647452	-1.034472	2.229124
H	-0.449133	-2.641456	1.529421
C	4.246919	-2.368177	2.159158
H	4.367961	-3.452234	2.278865
H	5.251699	-1.933709	2.134660
H	3.739833	-1.994801	3.053652
C	4.078926	-1.840864	-2.872125
H	5.079644	-2.276467	-2.800220
H	3.506690	-2.426401	-3.599882
H	4.184722	-0.830233	-3.284023
C	-2.523935	-1.150224	-5.006646
H	-1.678838	-1.021002	-5.694328
H	-3.302022	-1.699628	-5.545883
H	-2.902823	-0.151550	-4.771821
C	-1.845467	-5.477289	-2.471699
H	-2.888614	-5.795416	-2.353336
H	-1.469563	-5.945116	-3.387963
H	-1.278670	-5.884237	-1.629632
C	-1.959323	4.426361	4.380835
H	-1.271074	3.648369	4.727396
H	-1.347850	5.214777	3.925636
H	-2.457640	4.855322	5.255109

Chapter 1. Development of Effective Bidentate Diphosphine Ligands of Ruthenium Catalysts toward Practical Hydrogenation of Carboxylic Acids

C	-6.721397	3.984639	2.723488
H	-7.113015	3.638075	3.687064
H	-6.896765	5.065848	2.677293
H	-7.315930	3.517409	1.933524
C	-4.302433	5.670786	-2.959123
H	-3.627542	5.917061	-3.788205
H	-5.285721	6.081310	-3.212564
H	-3.936069	6.192389	-2.070749
C	-5.925033	1.102269	-4.396061
H	-6.817847	1.615246	-4.767291
H	-5.316629	0.838015	-5.270074
H	-6.243029	0.166058	-3.927562

References

- [1] J. Klankermayer, S. Wesselbaum, K. Beydoun, W. Leitner, *Angew. Chem. Int. Ed.* **2016**, *55*, 7296–7343.
- [2] For reviews, see: a) W. H. Wang, Y. Himeda, J. T. Muckerman, G. F. Manbeck, E. Fujita, *Chem. Rev.* **2015**, *115*, 12936–12973; b) A. Otto, T. Grube, S. Schiebahn, D. Stolten, *Energy Environ. Sci.* **2015**, *8*, 3283–3297; c) Q. Liu, L. Wu, R. Jackstell, M. Beller, *Nat. Commun.* **2015**, *6*, 5933; d) T. G. Ostapowicz, M. Schmitz, M. Krystof, J. Klankermayer, W. Leitner, *Angew. Chem. Int. Ed.* **2013**, *52*, 12119–12123.
- [3] For selected examples of the UV-light-driven carboxylation reactions with CO₂, see: a) S. Tazuke, S. Kazama, N. Kitamura, *J. Org. Chem.* **1986**, *51*, 4548–4553; b) Y. Ito, Y. Uozu, T. Matsuura, *J. Chem. Soc., Chem. Commun.* **1988**, 562–564; c) H. Tagaya, M. Onuki, Y. Tomioka, Y. Wada, M. Karasu, K. Chiba, *Bull. Chem. Soc. Jpn.* **1990**, *63*, 3233–3237; d) M. Aresta, A. Dibenedetto, T. Baran, S. Wojtyła, W. Macyk, *Faraday Discuss.* **2015**, *183*, 413–427; e) Y. Masuda, N. Ishida, M. Murakami, *J. Am. Chem. Soc.* **2015**, *137*, 14063–14066; f) N. Ishida, Y. Masuda, S. Uemoto, M. Murakami, *Chem. Eur. J.* **2016**, *22*, 6524–6527; g) H. Seo, M. H. Katcher, T. F. Jamison, *Nat. Chem.* **2017**, *9*, 453–456; f) K. Shimomaki, K. Murata, R. Martin, N. Iwasawa, *J. Am. Chem. Soc.* **2017**, *139*, 9467–9470; g) Q.-Y. Meng, S. Wang, B. König, *Angew. Chem. Int. Ed.* **2017**, *56*, 13426–13430; h) Q.-Y. Meng, S. Wang, G. S. Huff, B. König, *J. Am. Chem. Soc.* **2018**, *140*, 3198–3201; i) Q.-Y. Meng, T. E. Schirmer, A. L. Berger, K. Donabauer, B. König, *J. Am. Chem. Soc.* **2019**, *141*, 11393–11397; h) K. Kamada, J. Jung, T. Wakabayashi, K. Sekizawa, S. Sato, T. Morikawa, S. Fukuzumi, S. Saito, *J. Am. Chem. Soc.* **2020**, *142*, 10261–10266.
- [4] T. Werpy, G. Petersen, A. Aden, J. Bozell, J. Holladay, J. White, A. Manheim, “Top value-added chemicals from biomass” U.S. Department of Energy (DOE) report number DOE/GO-102004-1992, Golden, CO, **2004**; www.nrel.gov/docs/fy04osti/35523.pdf.
- [5] R. F. Nystrom, W. G. Brown, *J. Am. Chem. Soc.* **1947**, *69*, 2548–2549.
- [6] N. M. Yoon, C. S. Pak, H. C. Brown, S. Krishnamurthy, T. P. Stocky, *J. Org. Chem.* **1973**, *38*, 2786–2792.
- [7] J. A. Olah, *Angew. Chem. Int. Ed.* **2005**, *44*, 2636–2639.
- [8] a) S. Sato, T. Arai, T. Morikawa, K. Uemura, T. M. Suzuki, H. Tanaka, T. Kajino, *J. Am. Chem. Soc.* **2011**, *133*, 15240–15243; b) T. Arai, S. Sato, T. Kajino, T. Morikawa, *Energy Environ. Sci.* **2013**, *6*, 1274–1282; c) T. Arai, S. Sato, T. Morikawa, *Energy Environ. Sci.* **2015**, *8*, 1998–2002.
- [9] S. Yoshioka, S. Saito, *Chem. Commun.* **2018**, *54*, 13319–13330.

- [10] For selected reviews for the heterogeneous catalysts, see: a) J. Pritchard, G. A. Filonenko, R. van Putten, J. M. Hensen, E. A. Pidko, *Chem. Soc. Rev.* **2015**, *44*, 3808–3833; b) M. Besson, P. Gallezot, C. Pinel, *Chem. Rev.* **2014**, *114*, 1827–1870; c) M. Besson, C. Pinel, *Sci. Synth.* **2018**, *6*, 255–285; d) P. Mäki-Arvela, J. Hájek, T. Salmi, D. Y. Murzin, *Appl. Catal. A* **2005**, *292*, 1–49; e) T. Toyao, S. M. A. H. Siddiki, K. Kon, K.-i. Shimizu, *Chem. Rec.* **2018**, *18*, 1374–1393; f) M. Tamura, Y. Nakagawa, L. Tomishige, *Asian J. Org. Chem.* **2020**, *9*, 126–143; g) T. Toyao, S. M. A. H. Siddiki, K. Kon, K.-i. Shimizu, *Chem. Rec.* **2018**, *18*, 1374–1393.
- [11] K. Kandel, U. Chaudhary, N. C. Nelson, I. I. Slowing, *ACS Catal.* **2015**, *5*, 6719–6723.
- [12] H. G. Manyar, C. Paun, R. Pilus, D. W. Rooney, J. M. Thompson, C. Hardacre, *Chem. Commun.* **2010**, *46*, 6279–6281.
- [13] K. Tahara, E. Nagahara, Y. Itoi, S. Nishiyama, S. Tsuruya, M. Masai, *Appl. Catal. A Gen.* **1997**, *154*, 75–86.
- [14] T. Toyao, S. M. A. H. Siddiki, A. S. Touchy, W. Onodera, K. Kon, Y. Morita, T. Kamachi, K. Yoshizawa, K. Shimizu, *Chem. Eur. J.* **2017**, *23*, 1001–1006.
- [15] J. Ullrich, B. Breit, *ACS Catal.* **2018**, *8*, 785–789.
- [16] H. T. Teunissen, C. J. Elsevier, *Chem. Commun.* **1997**, 667–668.
- [17] H. T. Teunissen, C. J. Elsevier, *Chem. Commun.* **1998**, 1367–1368.
- [18] a) A. A. Núñez Magro, G. R. Eastham, D. J. Cole-Hamilton, *Chem. Commun.* **2007**, 3154–3156; b) J. Coetzee, D. L. Dodds, J. Klankermayer, S. Brosinski, W. Leitner, A. M. Z. Slawin, D. J. Cole-Hamilton, *Chem. Eur. J.* **2013**, *19*, 11039–11050; c) J. R. Cabrero-Antonino, E. Alberico, K. Junge, H. Junge, M. Beller, *Chem. Sci.* **2016**, *7*, 3432–3442.
- [19] T. vom Stein, M. Meuresch, D. Limper, M. Schmitz, M. Hölscher, J. Coetzee, D. J. Cole-Hamilton, J. Klankermayer, W. Leitner, *J. Am. Chem. Soc.* **2014**, *136*, 13217–13225.
- [20] X. Cui, Y. Li, C. Topf, K. Junge, M. Beller, *Angew. Chem. Int. Ed.* **2015**, *54*, 10596–10599.
- [21] T. J. Korstanje, J. I. van der Vlugt, C. J. Elsevier, B. de Bruin, *Science* **2015**, *350*, 298–302.
- [22] L. Deng, B. Kang, U. Englert, J. Klankermayer, R. Palkovits, *ChemSusChem* **2016**, *9*, 177–180.
- [23] F. M. A. Geilen, B. Engendahl, M. Hölscher, J. Klankermayer and W. Leitner, *J. Am. Chem. Soc.*, **2011**, *133*, 14349–14358.
- [24] M. Naruto, S. Saito, *Nat. Commun.* **2015**, *6*, 8140.
- [25] a) S. Yoshioka, S. Nimura, M. Naruto, S. Saito, *Sci. Adv.* **2020**, *6*, eabc0274; b) S. Yoshioka, J. Jung, S. Saito, *J. Synth. Chem. Soc. Jpn.* **2020**, *78*, 856–866; c) M. Naruto, S. Agrawal, K. Toda, S. Saito, *Sci. Rep.* **2017**, *7*, 3425.
- [26] T. Saito, A. Yoshida, K. Matsuda, T. Miura, H. Kumobayashi, JP Patent 3830180, **1997**.

- [27] X. Zhang, K. Huang, G. Hou, B. Cao, X. Zhang, *Angew. Chem. Int. Ed.* **2010**, *49*, 6421–6424.
- [28] S. Doherty, J. G. Knight, A. L. Bell, R. W. Harrington, W. Clegg, *Organometallics* **2007**, *26*, 2465–2468.
- [29] a) C. W. Jung, P. E. Garrou, P. R. Hoffman, K. G. Caulton, *Inorg. Chem.* **1984**, *23*, 726–729; b) S. L. Queiroz, M. P. de Araujo, A. A. Batista, K. S. MacFarlane, B. R. James, *J. Chem. Educ.* **2001**, *78*, 87.
- [30] A. Saito, S. Yoshioka, M. Naruto, S. Saito, *Adv. Synth. Catal.* **2020**, *362*, 424–429.
- [31] Q. Lu, J. Song, M. Zhang, J. Wei, C. Li, *Dalton Trans.*, **2018**, *47*, 2460–2469.
- [32] a) T. Oshiki, K. Takai, M. Utsunomiya, K. Takahashi, K. Kawakami, JP Patent 2003128686A, **2003**; b) M. Utsunomiya, K. Kawakami, K. Takahashi, JP Patent 2004010568A, **2004**.
- [33] N. Hideki, S. Noboru, F. Takahiro, JP Patent 201070510A, **2010**.
- [34] Gaussian 09, revision B.01; M. J. Frisch, G. W. Trucks, H. B. Schlegel, G. E. Scuseria, M. A. Robb, J. R. Cheeseman, G. Scalmani, V. Barone, B. Mennucci, G. A. Petersson, H. Nakatsuji, M. Caricato, X. Li, H. P. Hratchian, A. F. Izmaylov, J. Bloino, G. Zheng, J. L. Sonnenberg, M. Hada, M. Ehara, K. Toyota, R. Fukuda, J. Hasegawa, M. Ishida, T. Nakajima, Y. Honda, O. Kitao, H. Nakai, T. Vreven, J. A. Montgomery, Jr., J. E. Peralta, F. Ogliaro, M. Bearpark, J. J. Heyd, E. Brothers, K. N. Kudin, V. N. Staroverov, T. Keith, R. Kobayashi, J. Normand, K. Raghavachari, A. Rendell, J. C. Burant, S. S. Iyengar, J. Tomasi, M. Cossi, N. Rega, J. M. Millam, M. Klene, J. E. Knox, J. B. Cross, V. Bakken, C. Adamo, J. Jaramillo, R. Gomperts, R. E. Stratmann, O. Yazyev, A. J. Austin, R. Cammi, C. Pomelli, J. W. Ochterski, R. L. Martin, K. Morokuma, V. G. Zakrzewski, G. A. Voth, P. Salvador, J. J. Dannenberg, S. Dapprich, A. D. Daniels, O. Farkas, J. B. Foresman, J. V. Ortiz, J. Cioslowski, D. J. Fox, Gaussian, Inc., Wallingford CT, **2010**.
- [35] R. S. Loewe, K. Tomizaki, J. S. Lindsey, US Patent 2003075216, **2003**.
- [36] T. Wiedemann, G. Voit, A. Tchernook, P. Roesle, I. Göttker-Schnetmann, S. Mecking, *J. Am. Chem. Soc.* **2014**, *136*, 2078–2085.
- [37] O. Mitsutaka, N. Mitsuhisa, EP 1452537 A1, **2004**.
- [38] C. Tejo, J. H. Pang, D. Y. Ong, M. Oi, M. Uchiyama, R. Takita, S. Chiba, *Chem. Commun.* **2018**, *54*, 1782–1785.
- [39] T. Nishikubo, H. Kubo, JP Patent 2005272787, **2005**.
- [40] M. Sun, H. Zhang, Q. Han, K. Yang, S. Yang, *Chem. Eur. J.* **2011**, *17*, 9566–9570.
- [41] X. Zhang, H. Liu, X. Hu, G. Tang, J. Zhu, Y. Zhao, *Org. Lett.* **2011**, *13*, 3478–3481.
- [42] Y. Yan, T. V. RajanBabu, *Org. Lett.* **2000**, *2*, 4137–4140.

- [43] D. Sinou, D. Maillard, A. Aghmiz, A. M. M. i-Bultó, *Adv. Synth. Catal.* **2003**, *345*, 603–611.
- [44] N. N. B. Kumar, O. A. Mukhina, A. G. Kutateladze, *J. Am. Chem. Soc.* **2013**, *135*, 9608–9611.
- [45] J. A. Murphy, F. Schoenebeck, N. J. Findlay, D. W. Thomson, S.-Z. Zhou, J. Garnier, *J. Am. Chem. Soc.* **2009**, *131*, 6475–6479.
- [46] T. Taniguchi, D. Hirose, H. Ishibashi, *ACS Catal.* **2011**, *1*, 1469–1474.
- [47] S. David, A. Thieffry, *J. Org. Chem.* **1983**, *48*, 441–447.
- [48] N. Mori, H. Togo, *Tetrahedron* **2005**, *61*, 5915–5925.
- [49] J. A. Schiffner, T. H. Wöste, M. Oestreich, *Eur. J. Org. Chem.* **2010**, 174–182.
- [50] A. P. Dieskau, J.-M. Begouin, B. Plietker, *Eur. J. Org. Chem.* **2011**, 5291–5296.
- [51] B. S. Bodnar, P. F. Vogt, *J. Org. Chem.* **2009**, *74*, 2598–2600.
- [52] K. Furuta, K. Iwanaga, H. Yamamoto, *Org. Synth.* **1989**, *67*, 76.
- [53] A. Misumi, K. Iwanaga, K. Furuta, H. Yamamoto, *J. Am. Chem. Soc.* **1985**, *107*, 3343–3345.
- [54] C. Pichon, C. Alexandre, F. Huet, *Tetrahedron Asymmetry* **2004**, *15*, 1103–1111.
- [55] S. Schröder, B. Wenzel, W. Deuther-Conrad, R. Teodoro, U. Egerland, M. Kranz, M. Scheunemann, N. Höfgen, J. Steinbach, P. Brust, *Molecules* **2015**, *20*, 9591–9615.
- [56] T. Imamoto, T. Kusumoto, N. Suzuki, K. Sato, *J. Am. Chem. Soc.* **1985**, *107*, 5301–5303.

Chapter 2.

Catalytic Hydrogenation of N-protected α -Amino Acids Using Ruthenium Complexes with Monodentate Phosphine Ligands

Abstract: A ruthenium complex with a monodentate phosphine ligand was used to catalytically hydrogenate N-protected α -amino acids under essential retention of the configuration of their α -chiral centers. Among the ligands tested for this hydrogenation, which proceeds at a relatively low temperature, tris(*para*-fluorophenyl)phosphine exhibited the best performance. In comparison, electron-rich monodentate, bidentate, and tridentate phosphines were far less effective. The precatalyst $\text{Ru}(\text{OAc})_2[(p\text{-FC}_6\text{H}_4)_3\text{P}]_2$ was synthesized and isolated, and its structure was determined by a single-crystal X-ray diffraction analysis. N-protected α -amino acids with neutral alkyl side chains, including polar functional groups such as sulfides, indoles, ethers, phenols, pyrroles, and arenes, are compatible with the applied hydrogenation conditions, affording the corresponding optically active 2-substituted-2-(1*H*-pyrrol-1-yl)ethan-1-ol (2-amino ethanol) derivatives in moderate to high yield.

2.1. Introduction

Optically pure 2-aminoalkan-1-ol derivatives (β -amino alcohols) have a long history as supporting chiral ligands for molecular metal catalysts,^[1] chiral auxiliaries,^[2] synthetic intermediates for pharmaceuticals/bioactive compounds,^[3] organocatalysts,^[4] and as organic frameworks for the dehydrative trapping of CO₂^[5] (Figure 1).

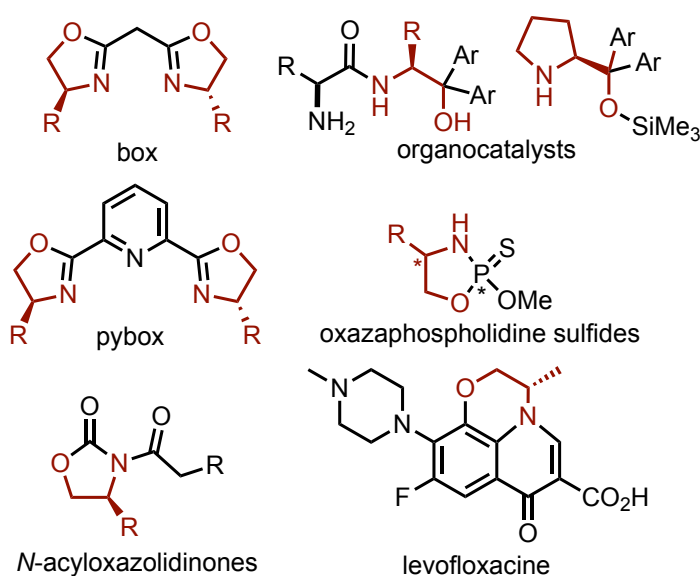


Figure 1 | Chiral β -amino alcohol motifs found in high-value-added chemicals. R = side chains of natural α -amino acids.

Metal hydrides, including LiAlH₄ and BH₃,^[6] are privileged hydroxophilic reductants, converting natural α -amino acids into optically active/pure β -amino alcohols. Although these reagents serve without reservation as useful and promising hydrides, these methods usually produce more than stoichiometric amounts of (metal) salt waste. This drawback hampers future applications of these methods in large-scale syntheses or in the industrial production of optically active/pure 2-aminoalkan-1-ols. In contrast, Noyori-type (metal–ligand bifunctional) (PP)(NH,NH)Ru^[7a] and (P,NH,N)Mn^[7b] complexes such as RuH(η^1 -BH₄)(dppp)(dpen) can catalyze the hydrogenation of *N*-Boc- and C-protected α -amino acids, i.e. the respective esters, with alkyl side chains to *N*-protected-2-aminoalkan-1-ols under with retention of their optical purity (dppp = Ph₂P(CH₂)₃PPh₂; dpen = H₂N[CH(Ph)CH(Ph)]NH₂).^[7] We report herein that ruthenium complexes of the type (PP)Ru, which contain two molecules of a monodentate phosphine, especially tris(*para*-fluorophenyl)phosphine (e.g., Ru-1 in Figure 2), effectively catalyze the hydrogenation of *N*-protected- α -amino acids at relatively low temperature (100–120 °C). Although several examples of molecular catalyst systems based e.g. on [(Ph₂P)CH₂]₃CMe (Triphos)–Ru^[8a–c] and Co^[9] complexes ((PPP)M complexes^[8]), as well as

our (PP)Ru^[10] and (PP)Re^[11] complexes, have been reported to promote the hydrogenation of carboxylic acids selectively to alcohols,^[12] these require relatively high hydrogenation temperatures (140–200 °C), which often results in racemization (epimerization) at the α -chiral centers of natural α -amino acids. Another notable issue associated with these methods is the involvement of notorious α -amino aldehydes^[13] and/or their hydrate forms as short-lived reaction intermediates, which undergo racemization at their α -stereogenic center more readily than the parent α -amino acids. To the best of our knowledge, our results represent the first example of a molecular catalyst that promotes the hydrogenation of α -amino acids under preservation of their chirality over weakly acidic (near neutral) conditions. Even though the heterogeneously catalyzed hydrogenation of *N*-unprotected α -amino acids at low hydrogenation temperature *T* (60–125 °C) with high hydrogen (H₂) pressure *P*_{H₂} (7–20 MPa) has already been achieved,^[14–16] those precedents exhibit limited substrate scope with respect to α -amino acids, i.e. only substrates with alkyl side chains are compatible, as aromatic groups in the side chains could potentially undergo dearomatic hydrogenation under the strongly acidic conditions (e.g., excess H₂SO₄ or H₃PO₄) used in these methods, with very few exceptions.^[16c] In contrast, the characteristic features of molecular catalysis, i.e. higher functional-group tolerance and substrate compatibility, would pave a new and practical avenue for a ‘greener’ synthesis of various optically active/pure β -amino alcohols from naturally rich carbon resources.

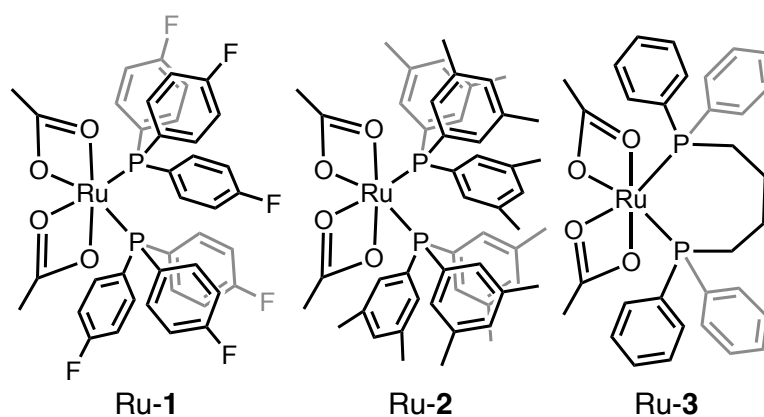


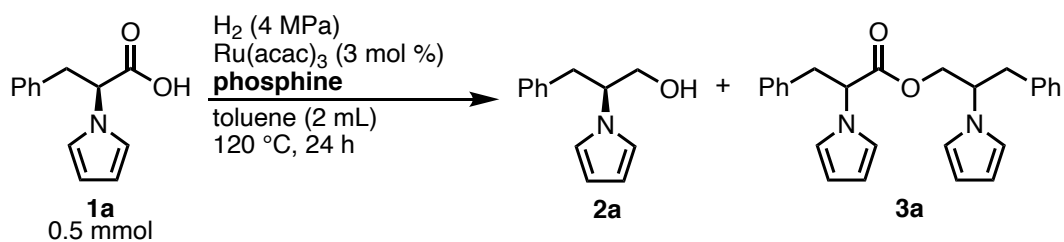
Figure 2 | Ru complexes for the catalytic hydrogenation of carboxylic acids. Ru-1: this work; Ru-2 and Ru-3: previous work.^[10,11]

2.2. Results and discussion

We have previously reported^[10] that the Ru complexes **Ru-2** and **Ru-3** are among the most effective precatalysts for the hydrogenation of carboxylic acids in toluene. Using a catalytic amount of these complexes (3 mol %), the *N*-unprotected α -amino acid (*S*)-phenylalanine did barely undergo hydrogenation under standard conditions ($P_{\text{H}_2} = 4$ MPa; $T = 160$ °C; toluene). Among the α -amino acids with *N*-protected primary amine moieties tested, those with pyrrolyl-protected amine moieties exhibited the best performance, i.e. the **Ru-2**-catalyzed hydrogenation ($[\text{Ru-2}]_0 = 7.5$ mM; $P_{\text{H}_2} = 4$ MPa; $T = 160$ °C; 24 h) of 2-pyrrolyl-(*S*)-phenylalanine **1a** furnished 3-phenyl-2-(1*H*-pyrrol-1-yl)propan-1-ol (**2a**) in 94% together with merely a negligible amount of ester **3a**; regretfully, the β -carbon of **2a**, which is derived from the α -carbon atom of the α -amino acid **1a**, effectively racemized at 160 °C. Sterically more rigid (conformationally more confined) **Ru-3** provided even worse results (**2a**: 63% together with unknown side products). In an attempt to prevent the racemization, the hydrogenation was carried out with no less than 5 mol % of **Ru-2** ($[\text{Ru-2}]_0 = 13$ mM) at $T = 110$ °C, which resulted in a sluggish hydrogenation that required 53 h and afforded **2a** in 99% yield with a considerable loss of enantiomeric purity (**1a**: 99:1 er; **2a**: 91:9 er).

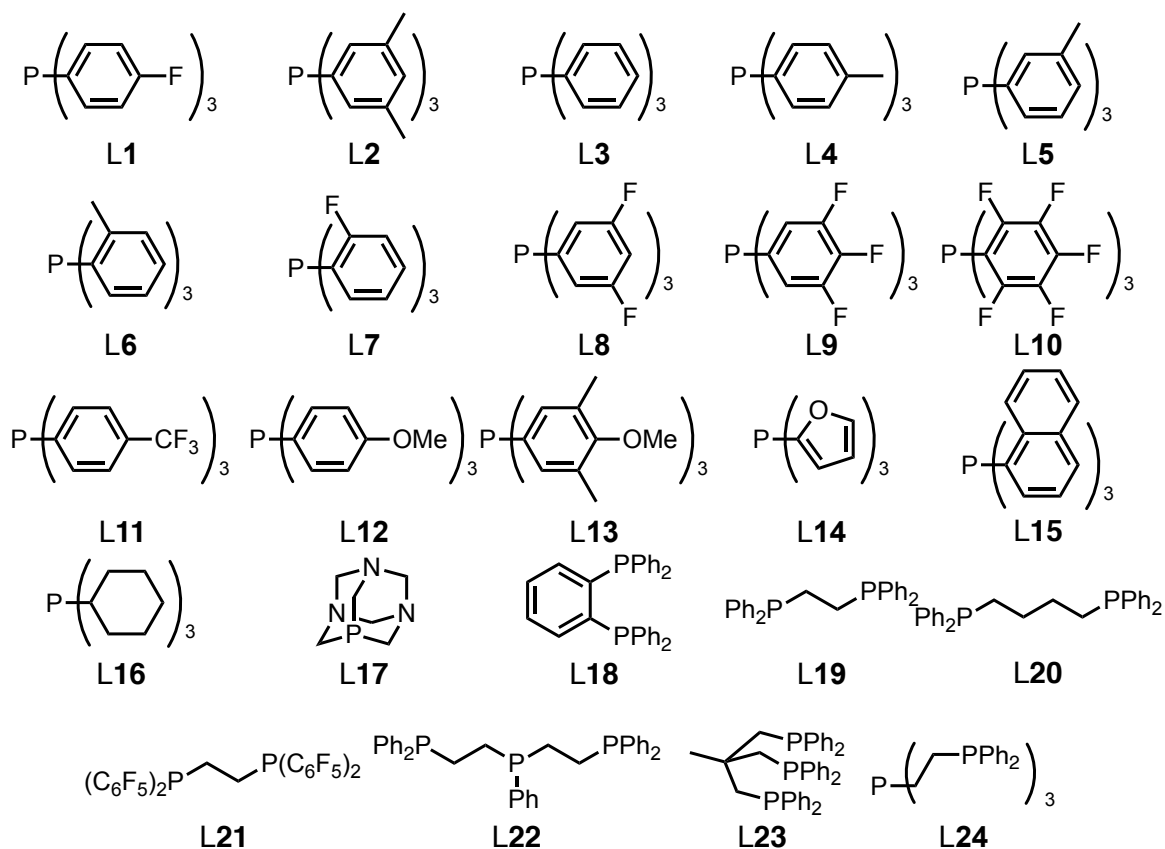
We thus rescreened a range of monodentate phosphine ligands (6 mol %), combined with $\text{Ru}(\text{acac})_3$ (3 mol %) under $P_{\text{H}_2} = 4$ MPa and $T = 120$ °C for the hydrogenation of **1a**, and eventually found that (*p*- FC_6H_4)₃P (**L1**) outperformed the other phosphine ligands examined thus far (**2a**: 63%), with simple PPh_3 (**2a**: 49%) as the second-most effective (Table 1). The ligand of **Ru-2**, **L2**, was not as effective as **L1** or PPh_3 in this low-temperature hydrogenation. We discovered that the yield of **2a** decreases with increasing electron-donating properties of the group from the *p*-fluorine group that is attached to the arene ring of the phosphines. However, the increment of electron-deficient natures of the arene rings also substantially decelerated the reaction, so that a precise adjustment of the substituent of the arene rings seems necessary either for the formation of the (PP)Ru structure, or after which, for inducing catalytically active species. Neither bidentate nor tridentate phosphines such as *dppe* ($\text{Ph}_2\text{P}(\text{CH}_2)_2\text{PPh}_2$), *dppb* ($\text{Ph}_2\text{P}(\text{CH}_2)_4\text{PPh}_2$), or *Triphos* can be used for this low-temperature hydrogenation. It should also be noted here that **L1** is unsuitable for the hydrogenation of 2-phenylpropanoic acid at $T = 160$ °C ($P_{\text{H}_2} = 4$ MPa).^[10]

Table 1 | Phosphine ligands screening with a combination of Ru(acac)₃ in the hydrogenation of 1a.



entry	phosphine	conv (%)	yield (%)	
			2a	3a
1	L1 (6)	72	63	5
2	L2 (6)	60	38	6
3	L3 (6)	60	49	4
4	L4 (6)	52	30	5
5	L5 (6)	64	13	7
6	L6 (6)	60	8	10
7	L7 (6)	18	7	3
8	L8 (6)	30	0	1
9	L9 (6)	7	3	1
10	L10 (6)	47	8	7
11	L11 (6)	58	35	5
12	L12 (6)	26	<1	1
13	L13 (6)	26	6	1
14	L14 (6)	22	4	1
15	L15 (6)	16	1	7
16	L16 (6)	48	5	1
17	L17 (6)	23	<1	<1
18	L18 (3)	42	9	5
19	L19 (3)	54	13	5
20	L20 (3)	16	0	1
21	L21 (3)	14	1	<1
22	L22 (3)	9	13	5
23	L23 (3)	10	0	0
24	L24 (3)	39	9	4

Table 1 (continued) | Phosphine ligands screening with a combination of Ru(acac)₃ in the hydrogenation of 1a.



Unless otherwise specified, the reactions were carried out with **1a**:Ru(acac)₃:monodentate phosphine (L1–L17) (mol %) = 100:3:6 or **1a**:Ru(acac)₃:multidentate phosphine (L18–L24) (mol %) = 100:3:3, $T = 120\text{ }^{\circ}\text{C}$, $P_{\text{H}_2} = 4\text{ MPa}$ and $t = 24\text{ h}$ ($[\mathbf{1a}]_0 = 250\text{ mM}$, $[\text{Ru}]_0 = 7.5\text{ mM}$, $[\text{L1–L17}]_0 = 15\text{ mM}$ or $[\text{L18–L24}]_0 = 7.5\text{ mM}$ in toluene). The conversion and yields were determined by $^1\text{H NMR}$ (600 MHz, CDCl_3) based on the integral ratio of the signals of products and internal standard (mesitylene).

When starting the hydrogenation of **1a** at $T = 120\text{ }^{\circ}\text{C}$ using **L1** (6 mol %) and $\text{Ru}(\text{acac})_3$ (3 mol %), an induction period (ca. 13 h) of the catalyst was observed. When using $\text{Ru}(\text{cod})(\eta^3\text{-methallyl})_2$ instead of $\text{Ru}(\text{acac})_3$, the induction period decreased significantly ($\leq 2\text{ h}$) (Figure 3).

entry	Ru source	t (h)	conv (%)	yield (%)		TON
				2a	3a	
1	$\text{Ru}(\text{acac})_3$	8	0	0	0	0
2		15	5	6	<1	2
3		24	72	63	5	23
4		36	84	68	16	28
5		48	95	92	5	32
6	$\text{Ru}(\text{cod})(\eta^3\text{-methallyl})_2$	2	–	3	0	1
7		4	7	11	<1	4
8		8	38	33	2	12
9		16	88	64	11	25
10		24	92	78	7	28
11		36	99	86	6	31
12		48	94	81	7	29

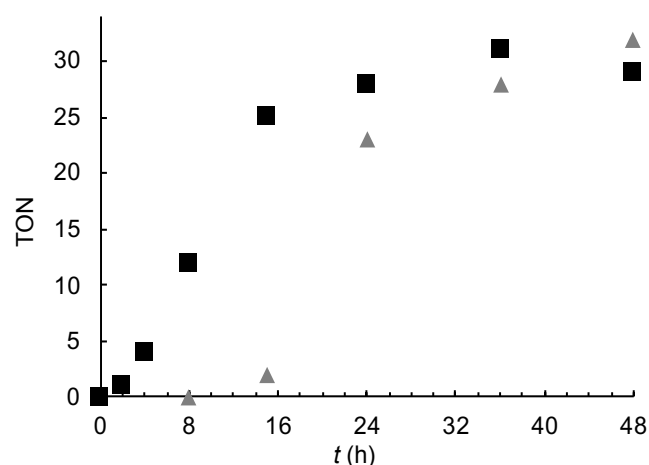


Figure 3 | Change in turnover number (TON) of the catalyst as a function of the reaction time (t) during the hydrogenation of **1a using $\text{Ru}(\text{acac})_3$ (grey triangles) or $\text{Ru}(\text{cod})(\eta^3\text{-methallyl})_2$ (black squares). Reaction conditions: **L1** (6 mol %); Ru source (3 mol %) ($[\text{Ru}]_0 = 7.5\text{ mM}$); toluene; $P_{\text{H}_2} = 4\text{ MPa}$; $T = 120\text{ }^{\circ}\text{C}$. The TONs were calculated by $(\mathbf{2a} + \mathbf{3a})/\text{Ru}$, assuming that **3a** was obtained from the condensation of **1a** with **2a**.**

When the hydrogenation was carried out at $T = 110\text{ }^{\circ}\text{C}$ under otherwise identical conditions, almost no reaction was observed for $\text{Ru}(\text{acac})_3$ ($\text{TON} \approx 0$), while $\text{Ru}(\text{cod})(\eta^3\text{-methallyl})_2$ afforded a substantially higher TON (~ 12). These results suggest that the initial Ru(III) species are reduced by H_2 to Ru(II) during the preactivation that does not occur below $T \sim 120\text{ }^{\circ}\text{C}$ ($P_{\text{H}_2} = 4\text{ MPa}$). Subsequently, we re-examined different *N*-protection groups using $\text{Ru}(\text{cod})(\eta^3\text{-methallyl})_2$ (3 mol %) and **L1** (6 mol %) at $T = 120\text{ }^{\circ}\text{C}$ and again obtained the best results for the pyrrolyl protection group (Table 2).

Table 2 | Screening of *N*-protecting groups.

entry	PG = Protecting Group	yield (%)	
		AL	ES
1	Boc	0	0
2	Cbz	0	0
3	Bz	0	0
4	Phth	0	0
5	Fmoc	0	0
6	pyrrole (1a)	78 (2a)	7 (3a)
7	dimethylpyrrole	0	0

Unless otherwise specified, the reactions were carried out with **AM**: $\text{Ru}(\text{cod})(\eta^3\text{-methallyl})_2\text{:L1}$ (mol %) = 100:3:6, $T = 120\text{ }^{\circ}\text{C}$, $P_{\text{H}_2} = 4\text{ MPa}$ and $t = 24\text{ h}$ ($[\text{AM}]_0 = 250\text{ mM}$, $[\text{Ru}]_0 = 7.5\text{ mM}$ and $[\text{L1}]_0 = 15\text{ mM}$ in toluene). The yields were determined by $^1\text{H NMR}$ based on the integral ratio of the signals of products and internal standard (mesitylene).

In order to circumvent the need for such a lengthy preactivation step and the complexation of Ru(II) with two monodentate phosphine ligands, we synthesized a Ru(II) complex bearing L1, i.e. Ru-1 (Figure 2), which is a bright orange powder that is shelf-stable in air. For that purpose, we used a procedure similar to that used for the preparation of Wilkinson-type RuCl₂(PPP) complexes,^[17] followed by a Cl–OAc exchange reaction that we have already developed.^[10] The structure of Ru-1 was ascertained by a single-crystal X-ray diffraction analysis (Figures 4). The stabilization of Ru-1 in the solid state may be, at least partially, ascribed to intramolecular, offset π – π stacked interactions^[18] (Figure 4) between two *p*-FC₆H₄ groups of L1 (shortest C···C distance between two *p*-FC₆H₄ groups: 3.157 Å). Also noteworthy is the intramolecular “weak” hydrogen bonding^[19] formed at two distinct internal sites, i.e. between the *ortho*-C–H of the *p*-FC₆H₄ groups and the oxygen atoms of the OAc groups (C–H···O: 3.094 Å), which suggests that the C–H bond could potentially undergo bond cleavage through a concerted deprotonation–metalation (CMD) process^[20] under harsher conditions such as higher temperatures to induce a partial decomposition of catalyst. This result is consistent with our previous observations and interpretations, i.e. intramolecular Ru–C bond formation was introduced as a possible means to induce catalyst deactivation (Figure 5).^[10] Indeed, L1 was not a suitable ligand for the hydrogenation of carboxylic acids at *T* = 160 °C (*vide supra*), presumably due to the dominance of this deactivation step.

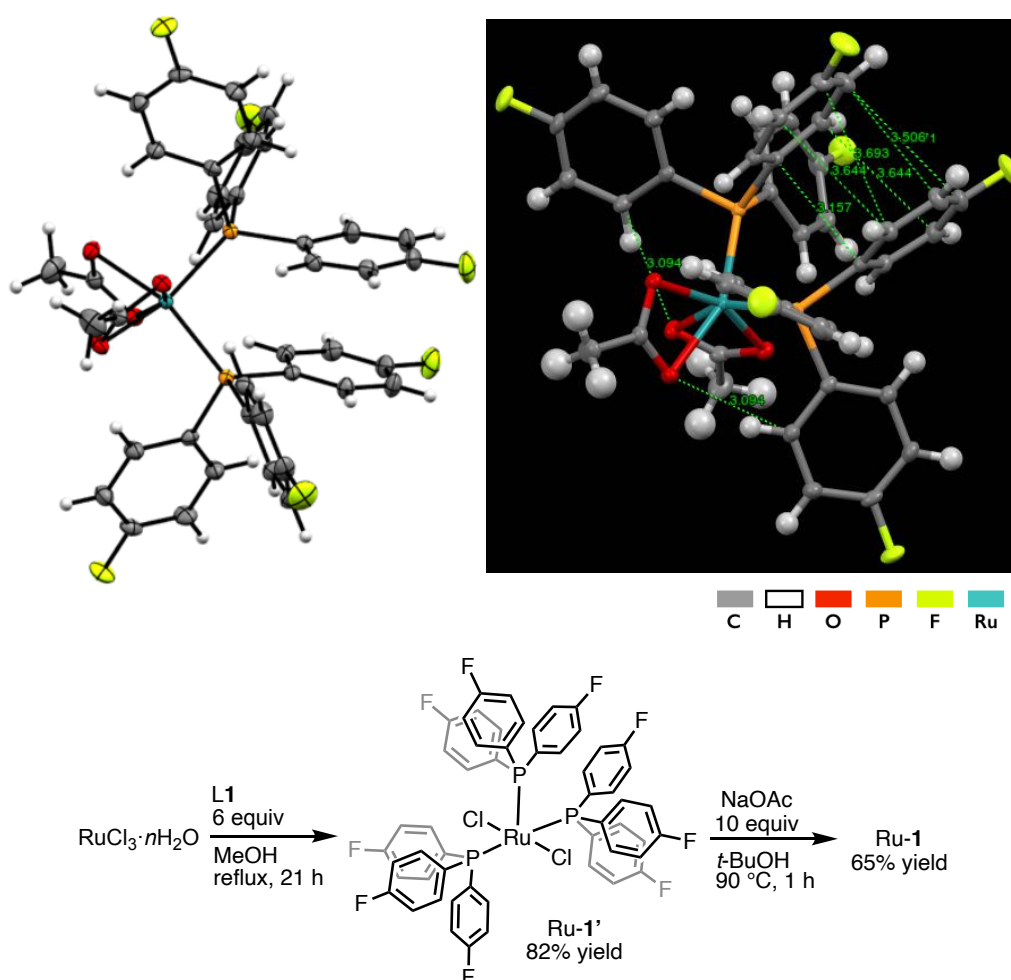


Figure 4 | Single-crystal X-ray diffraction structure of Ru-1 (up) and synthetic route of Ru-1' and Ru-1 (down). Upper left: ORTEP drawing of Ru-1 (50% probability ellipsoids). Upper right: ball and stick drawing of Ru-1 (white: H; gray: C; red: O; green: F; orange: P; blue: Ru). Bottom: synthetic route to Ru-1' and Ru-1.

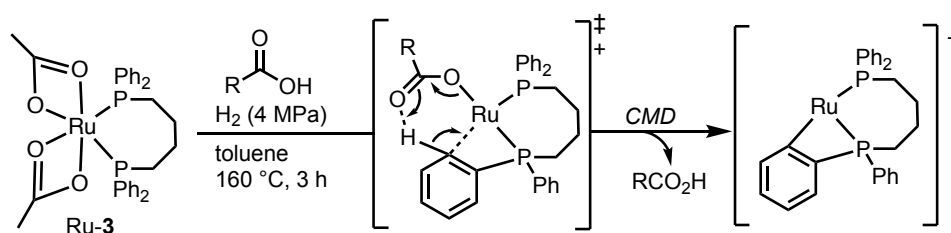


Figure 5 | Our previously proposed plausible catalyst-deactivation process.^[10,12a]

We subsequently discovered that the hydrogenation temperature (T) is the most critical parameter for the preservation of the chirality of the α -carbon of **1a** (β -carbon of **2a**) before and after the hydrogenation (Table 3). At $T = 120$ °C and $T = 100$ °C ($t = 24$ h), **2a** (**3a**) was obtained in 58% (7%) and 9% (6%), respectively, with 89:11 er and >99:1 er (entries 1 and 4). As $T = 100$ °C is too low to effectively accelerate the Ru-**1**-catalyzed hydrogenation, we chose $T = 110$ °C, which furnished **2a** (**3a**) in 36% (6%) yield with 98:2 er (entry 2). The performance of the combination of **L1** and Ru(cod)(η^3 -methallyl)₂ was comparable to that of Ru-**1**, albeit that the reproducibility of the former was lower than that of the latter (entry 3). For comparison, RuCl₂(PPP) complex, Ru-**1'** (3 mol %; Figure 4), was also tested with NaBPh₄ (15 mol %) for the hydrogenation of **1a** ($P_{\text{H}_2} = 4$ MPa; $t = 24$ h). However, at $T = 110$ °C and $T = 120$ °C, **2a** was obtained only in 15% and 35% yield, respectively, under complete racemization at the latter temperature. This may be due to a potential detachment of the third phosphine ligand from Ru-**1'**; the thus liberated phosphine could engage in a deprotonation–protonation at the chiral C–H group of **1a** to promote racemization.

Table 3 | Temperature-depending hydrogenation of 1a with Ru-1.^a

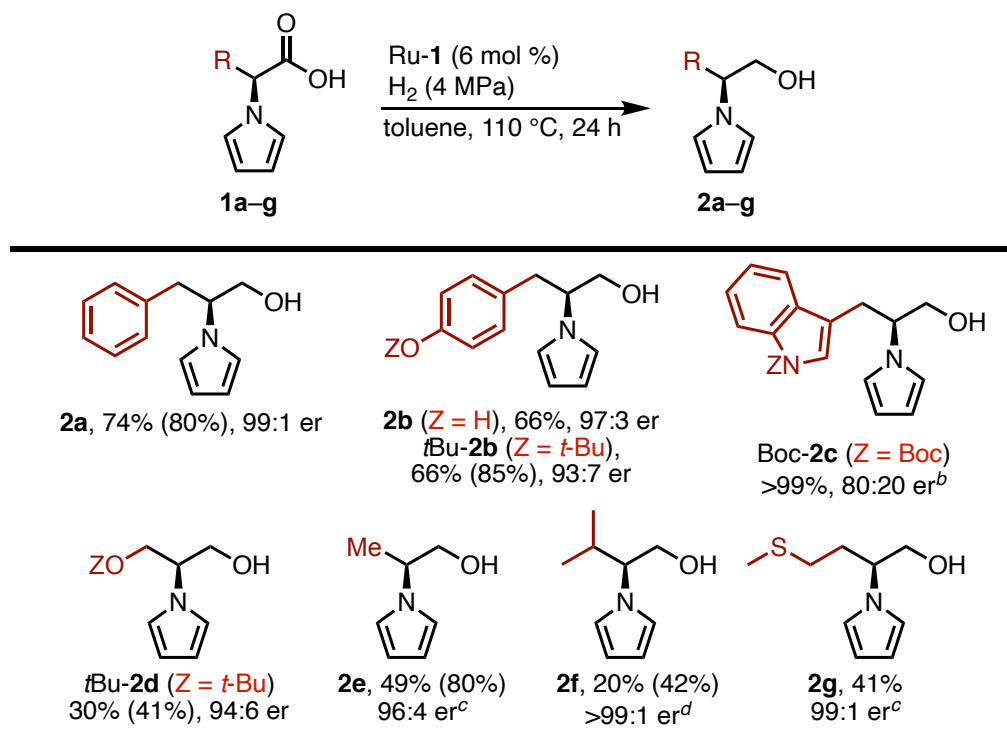
entry	T (°C)	conv (%) ^b	yield (%) ^b		TON ^c	er of 2a
			2a	3a		
1	120	84	58	7	22	89:11
2	110	48	36	6	14	98:2
3 ^{d,e}	110	55	30	7	12	97:3
4	100	45	9	6	5	>99:1

^aUnless otherwise specified, reactions were conducted using: [Ru-**1**]₀ = 7.5 mM; $P_{\text{H}_2} = 4$ MPa; $T = 25$ °C. ^bThe conversion of **1a** and the yields of **2a** and **3a** were determined by ¹H NMR analysis, using mesitylene as the internal standard. ^cCalculated by (**2a**+**3a**)/Ru-**1**, assuming that **3a** was obtained from the condensation of **1a** with **2a**. ^dRu(cod)(η^3 -methallyl)₂ (3 mol %) and **L1** (6 mol %) were used instead of Ru-**1**. ^eAverage of two runs.

The catalytic performance of Ru-1 in the hydrogenation of **1a** was further investigated by varying P_{H_2} , solvents, and [Ru-1]₀ (and thus [1a]₀). Within $P_{H_2} = 4\text{--}8$ MPa, the hydrogenation rate at $T = 110$ °C was not affected significantly. A coordinating solvent such as cyclopentyl methyl ether (CPME) and THF afforded was better for results than toluene in terms of **2a/3a** selectivity (~15:1), albeit that they were also detrimental to the catalytic activity. Increasing [1a]₀ to e.g. 500 mM and $T = 120$ °C resulted in the formation of a considerable amount of ester **3a** through dehydrative esterification of **1a** with *in-situ*-generated **2a**. These tests allowed us to identify the optimal amount of Ru-1 (6 mol %) and [Ru-1]₀ (5.0–23 mM) in order to promote the selective hydrogenation of **1a** to **2a** at $T = 110$ °C under concomitant suppression of the esterification into **3a**.

To examine the scope and limitations with respect to a range of pyrrolyl-protected natural amino acids with non-polar/neutral or polar/neutral side chains, α -pyrrolyl-protected **1a–1g** were subjected to the aforementioned optimized hydrogenation conditions (Ru-1: 6 mol %; [Ru-1]₀ = 15 mM; $P_{H_2} = 4$ MPa; $T = 110$ °C) (Table 4). For example, in the presence of 6 mol % of Ru-1, almost full conversion of **1a** was achieved within 24 h to afford **2a** (**3a**) in 80% (6%) yield with 99:1 er (**2a**). One advantage of the present method relative to heterogeneous catalysis is that different arene rings, including the indole of Trp-derived **1c**, the unprotected phenol of Tyr-derived **1b**, the ethers of *t*Bu-**1b** and *t*Bu-**1d**, as well as the Boc group of the side chains, are all tolerated under the applied reaction conditions. Unlike heterogeneous catalysts, which are frequently poisoned by sulfur-containing groups, the hydrogenation of Met-derived **1g** proceeded acceptably. Although a small amount of the corresponding ester is always the major side product, the amount of ester formed decreases with increasing steric demand of the side chain. In the case of Trp-derived **1c**, essentially no ester was produced. The ether of Ser-derived **1d** as well as the sterically demanding *i*-Pr group of Val-derived **1f**, were rather detrimental to the catalytic activity of Ru-1, and thus a longer reaction time and/or a larger amount of Ru-1 was required to induce a reasonable hydrogenation rate at $T = 110$ °C. However, the chirality of the stereogenic center in **1a–1g** was consistently well preserved in all cases. Authentic (racemic and scalemic) samples of **2a–g** were obtained by (PP)Re-catalyzed hydrogenation^[11] of **1a–g** (Section 2.4.10, Schemes S1 and S2).

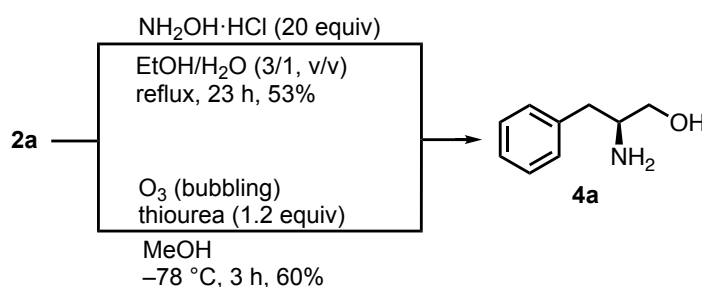
Table 4 | Catalytic hydrogenation of various optically active α -pyrrolyl- α -amino acids using Ru-1.^a



^aUnless otherwise specified, reactions were conducted using: [Ru-1]₀ = 15 mM; toluene; *P*_{H₂} = 4 MPa; *T* = 110 °C; *t* = 24 h. Isolated yields are shown. ¹H NMR yields are shown in parentheses. The enantiomeric ratio (er) was determined by chiral HPLC or GC-MS analysis.
^bBoc-1c, 91:9 er. ^cRu-1 (12 mol %) was used. ^d*t* = 48 h.

To complete the synthetic route to chiral *N*-unprotected-2-aminoalkan-1-ols from hydrogenation products, we examined the deprotection of the pyrrolyl amine group in **2a** (Scheme 1). The use of NH₂OH in refluxing EtOH/H₂O (3/1, v/v)^[21] and the ozonolysis in MeOH at -78 °C^[22] were both effective, affording 2-amino-3-phenylpropan-1-ol (**4a**) in isolated yields of 53% and 60%, respectively. Racemization was not observed in the **4a** produced by either of the two different deprotection methods.

Scheme 1 | Deprotection of the pyrrolyl group of 2a.



2.3. Conclusion

We have demonstrated that the catalytic hydrogenation of N-protected α -amino acids is possible at relatively low temperatures when using a newly devised Ru complex. The chirality of the α -amino-acids is well preserved before and after the hydrogenation, giving optically active β -aminoalkan-1-ols under almost complete retention of the absolute configuration. Stoichiometric metal salt-wastes are essentially not mandated from the synthesis of **1** (removal of MeOH) through the deprotection of the pyrrolyl group of **2** (ozonolysis). Although the catalytic activity performance attained in this proof-of-concept study leaves room for substantial improvement for scalable and practical applications, in terms of H₂ pressure and catalyst loading, in addition to the meticulous control of reaction temperature, the results shed for the first time light on the importance of further molecular design of metal complexes as a powerful and practical alternative that complements the future (large-scale) supply of optically active/pure divergently functionalized 2-aminoalkan-1-ols.

2.4. Experimental section

2.4.1. Material.

Bis(2-methylallyl)(1,5-cyclooctadiene)ruthenium(II), potassium tetraphenylborate, 1,2-dichloroethane, (*S*)-phenylalanine, tris(4-trifluoromethylphenyl)phosphine, tris(4-methoxyphenyl)phosphine, tricyclohexylphosphine, tri(1-naphthyl)phosphine, 1,3,5-triaza-7-phosphaadamantane, 1,1,1-tris(diphenylphosphinomethyl)ethane and 1-bromo-3,4,5-trifluorobenzene were purchased from Aldrich. Cyclopentyl methyl ether (CPME), sodium borohydride, 2,5-dimethoxytetrahydrofuran, tris(2-methylphenyl)phosphine, tris(pentafluorophenyl)phosphine, tri(2-furyl)phosphine, 1,4-bis(diphenylphosphino)butane, *N*-(*tert*-butoxycarbonyl)-(*S*)-phenylalanine, *N*-phthaloyl-(*S*)-phenylalanine, hydroxylamine hydrochloride, (*S*)-phenylalaninol, *O*-*tert*-butyl-(*S*)-tyrosine, (*S*)-tryptophan ethyl ester hydrochloride, *O*-*tert*-butyl-(*S*)-serine, di-*tert*-butyl dicarbonate, ethanolamine and 4-dimethylaminopyridine were purchased from TCI, Ltd. Hydrochloric acid, THF (anhydrous), toluene (anhydrous), EtOAc (anhydrous), dichloromethane, ethanol, chloroform, mesitylene, Na₂SO₄, NaOH, and diethyl ether, Celite 545[®], sodium hydride (dispersion in paraffin liquid, 55% purity), lithium aluminium hydride, *n*-butyllithium (1.6 M *n*-hexane solution), sodium acetate, potassium acetate, triphenylphosphine, tris(4-methylphenyl)phosphine, 2,5-hexanedione, 1-bromo-3,5-difluorobenzene, (*R*)-phenylalaninol, *n*-hexane for HPLC, ethanol for HPLC and methanol-*d*₄ were purchased from Kanto Chemicals, Ltd. Ruthenium(III) acetylacetonate, tri(3,5-xylyl)phosphine, sodium hydroxide, *t*-butyl alcohol, ethyl acetate and hexane, thiourea, tris(4-fluorophenyl)phosphine, (*S*)-alanine, (*S*)-methionine, phosphorotrichloride, tris(3-methylphenyl)phosphine, tris(4-methoxy-3,5-dimethylphenyl)phosphine, 1,2-bis(diphenylphosphino)ethane, 1,2-bis[bis(pentafluorophenyl)phosphino]ethane, 1,2-bis(diphenylphosphino)benzene, bis(2-diphenylphosphinoethyl)phenylphosphine, tris[2-(diphenylphosphino)ethyl]phosphine, *N*-Cbz-(*S*)-phenylalanine, formic acid, *o*-bromofluorobenzene, 2-propanol for HPLC and Wakogel[®] 50NH₂ were purchased from FUJIFILM Wako Pure Chemical Corporation, Ltd. Magnesium (turnings) and chlorotrimethylsilane were purchased from Across Organics, Ltd. Chloroform-*d* was purchased from Cambridge Isotope Laboratories, Inc. RuCl₃·*n*H₂O and dichlorotris(triphenylphosphine)ruthenium(II) were purchased from Furuya Metal Co., Ltd. Hydrogen gas (99.99% purity) was purchased from Alphasystem. These chemicals were used without further purification. Oxotrichloro[(*S,S*)-chiraphos]rhenium (Re-chiraphos) was prepared according to our report.^[11]

2.4.2. General methods.

All experiments were performed under an argon atmosphere unless otherwise noted. ^1H NMR spectra were measured on JEOL ECA-600 (600 MHz) or JEOL ECA-500 (500 MHz) at ambient temperature unless otherwise noted. Data were recorded as follows: chemical shift in ppm from internal tetramethylsilane (δ 0 ppm) or residual peak of methanol- d_4 (δ 3.30 ppm), multiplicity (bs = broad singlet, s = singlet, d = doublet, t = triplet, quin = quintet, dd = double doublet, dt = double triplet and m = multiplet), coupling constant (Hz), integration, and assignment. $^{13}\text{C}\{^1\text{H}\}$ NMR spectra were measured on JEOL ECA-600 (150 MHz) or JEOL ECA-500 (126 MHz) at ambient temperature unless otherwise noted. Chemical shifts were recorded in ppm from the solvent resonance employed as the internal standard (tetramethylsilane at 0 ppm). $^{31}\text{P}\{^1\text{H}\}$ NMR spectra were measured on JEOL ECA-600 (243 MHz) at ambient temperature unless otherwise noted. Chemical shifts were recorded in ppm from the solvent resonance employed as the external standard (phosphoric acid (85 wt% in H_2O) at 0.0 ppm). High-resolution mass spectra (HRMS) were obtained from PE Biosystems QSTAR (ESI). For thin-layer chromatography (TLC) analysis through this work, Merck precoated TLC plates (silica gel 60 GF254 0.25 mm) were used. The products were purified by preparative column chromatography on silica gel 60 N (spherical, neutral, 40–100 μm ; Kanto) or Wakogel[®] 50NH₂ (Wako).

Chiral GC-MS analysis was performed on Agilent 7820 series network GC system and Agilent 5977 series Mass Selective Detector (EI). The following conditions were used unless otherwise noted: [column: Cyclosil-B (l = 30 m, d = 0.25 mm, film thickness = 0.25 μm); chromatographic elution: isothermal at 50 $^\circ\text{C}$ for 1 min, 50–140 $^\circ\text{C}$ at a rate of 25 $^\circ\text{C}/\text{min}$, isothermal at 140 $^\circ\text{C}$ for 180 min, 140–160 $^\circ\text{C}$ at a rate of 1 $^\circ\text{C}/\text{min}$, isothermal at 160 $^\circ\text{C}$ for 15 min, 160–230 $^\circ\text{C}$ at a rate of 25 $^\circ\text{C}/\text{min}$, isothermal at 230 $^\circ\text{C}$ for 1 min; carrier gas: He (1.5 mL/min, at 27 psi)]. High performance liquid chromatography (HPLC) spectra were recorded on Prominence 2000 (SHIMADZU). Optical rotation values were recorded on Polarimeter P-1010-GT (JASCO).

2.4.3. X-ray single crystal structural analysis of Ru-1

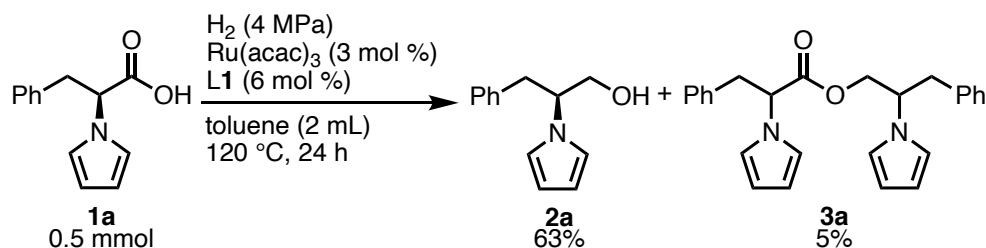
Ru-1 (328 mg, 0.39 mmol), acetic acid (20 mL) were placed in a vessel equipped with a Young's stopcock under argon atmosphere, and the mixture was stirred at 90 °C for 10 min. The solution became dark red. After cooling to room temperature, hexane (ca. 80 mL) was layered on the mixture under argon atmosphere. The mixture was kept on a lab bench at room temperature for 2 months to give reddish orange crystal. The crystal was collected by filtration and dried *in vacuo* to obtain Ru-1 (191 mg, 0.22 mmol, 58 %) as a single crystal.

Intensity data were collected at 123 K on a Rigaku Single Crystal CCD X-ray Diffractometer (Saturn 70 with MicroMax-007) with Mo K α radiation ($\lambda = 0.71075 \text{ \AA}$) and graphite monochromator. A total of 29170 reflections were measured at a maximum 2θ angle of 52.0°, of which 3294 were independent reflections ($R_{\text{int}} = 0.0176$). The structure was solved by direct methods (SHELXS-97) and refined by the full-matrix least-squares on F^2 (SHELXL-97). All non-hydrogen atoms were refined anisotropically. All hydrogen atoms were placed using AFIX instructions. The following crystal structure has been deposited at the Cambridge Crystallographic Data Centre and allocated the deposition number CCDC 1838638.

The crystal data are as follows: $\text{C}_{40}\text{H}_{30}\text{F}_6\text{O}_4\text{P}_2\text{Ru}_1$; FW = 851.65, crystal size $0.20 \times 0.30 \times 0.50 \text{ mm}^3$, monoclinic, $C2/c$, $a = 14.278(3) \text{ \AA}$, $b = 13.391(2) \text{ \AA}$, $c = 19.330(4) \text{ \AA}$, $\alpha = 90^\circ$, $\beta = 104.782(3)^\circ$, $\gamma = 90^\circ$, $V = 3573.5(12) \text{ \AA}^3$, $Z = 4$, $D_c = 1.583 \text{ g cm}^{-3}$. The refinement converged to $R_1 = 0.0222$ $wR_2 = 0.0901$ ($I > 2\sigma(I)$), GOF = 1.053.

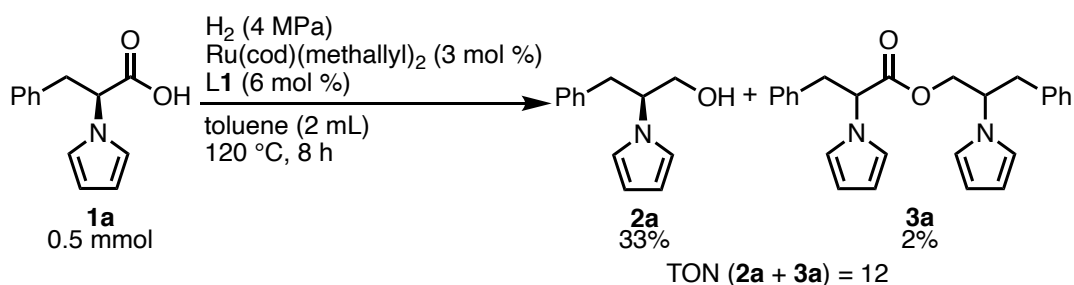
2.4.4. General procedures of hydrogenation experiments

Representative procedure for hydrogenation of **1a** with Ru(acac)₃ and L1 (Table 1, entry 1; Figure 3, entry 3)



N-protected (*S*)-phenylalanine (**1a**, 107.6 mg, 0.5 mmol), Ru(acac)₃ (6.0 mg, 0.015 mmol), tris(4-fluorophenyl)phosphine (L1, 9.5 mg, 0.030 mmol), and a magnetic stirring bar were placed in a glass tube (21 mL), which was inserted into an autoclave that was closed tightly and refilled with argon. Under a continuous flow of argon, anhydrous toluene (2 mL) was added to the mixture. The autoclave was purged 10 times with H₂ (ca. 1 MPa) and then pressurized at 25 °C with H₂ (4 MPa) and subsequently heated to 120 °C for 24 h under stirring (500 rpm). Thereafter, the autoclave was cooled to ~25 °C in an ice–water bath (0 °C). The reaction mixture was transferred into a round-bottom flask (100 mL) with CHCl₃ and concentrated under a reduced pressure (ca. 30 mmHg, 40 °C). The thus obtained residue was dissolved in CDCl₃ and analyzed by ¹H NMR. The yields of **2a** (63%) and **3a** (5%) were calculated based on the integral ratio between the signals of these compounds with respect to an internal standard (mesitylene).

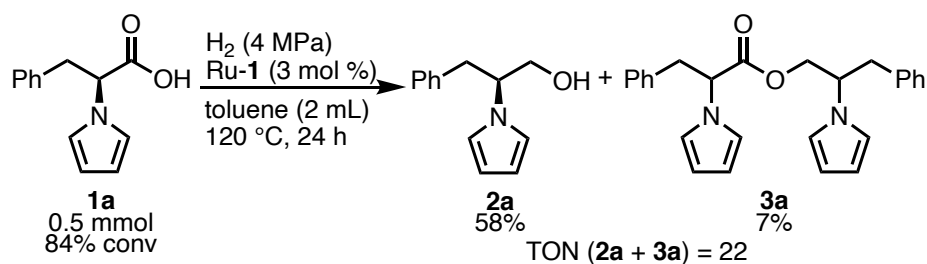
Representative procedure for hydrogenation of **1a** with Ru(cod)(methallyl)₂ and L1 (Figure 3, entry 8)



N-protected (*S*)-phenylalanine (**1a**, 107.6 mg, 0.5 mmol), Ru(cod)(methallyl)₂ (4.8 mg, 0.015 mmol), tris(4-fluorophenyl)phosphine (L1, 9.5 mg, 0.030 mmol), and a magnetic stirring bar were placed in a glass tube (21 mL), which was inserted into an autoclave that was closed tightly and refilled with argon. Under a continuous flow of argon, anhydrous toluene (2 mL) was added to the mixture. The autoclave was purged 10 times with H₂ (ca. 1 MPa) and then pressurized at 25 °C with H₂ (4 MPa) and subsequently heated to 120 °C for 8 h under stirring

(500 rpm). Thereafter, the autoclave was cooled to ~ 25 °C in an ice–water bath (0 °C). The reaction mixture was transferred into a round-bottom flask (100 mL) with CHCl_3 and concentrated under a reduced pressure (ca. 30 mmHg, 40 °C). The thus obtained residue was dissolved in CDCl_3 and analyzed by ^1H NMR. The yields of **2a** (33%) and **3a** (2%) were calculated based on the integral ratio between the signals of these compounds with respect to an internal standard (mesitylene). The TON (12) was calculated by $(\mathbf{2a}+\mathbf{3a})/\text{Ru}$, assuming that **3a** was obtained from the condensation of **1a** with **2a**.

Representative procedure for hydrogenation of **1a** with Ru-1 (Table 3, entry 1)



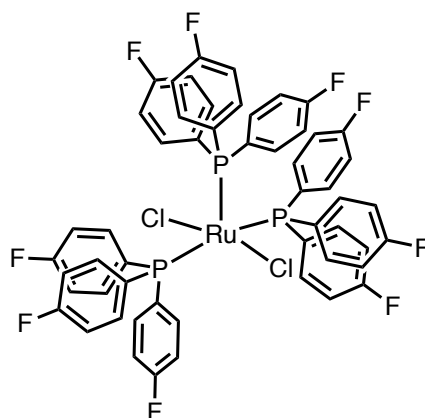
N-protected (*S*)-phenylalanine (**1a**, 107.6 mg, 0.5 mmol), Ru-1 (12.8 mg, 0.015 mmol), and a magnetic stirring bar were placed in a glass tube (21 mL), which was inserted into an autoclave that was closed tightly and refilled with argon. Under a continuous flow of argon, anhydrous toluene (2 mL) was added to the mixture. The autoclave was purged 10 times with H_2 (ca. 1 MPa) and then pressurized at 25 °C with H_2 (4 MPa) and subsequently heated to 120 °C for 24 h under stirring (500 rpm). Thereafter, the autoclave was cooled to ~ 25 °C in an ice–water bath (0 °C). The reaction mixture was transferred into a round-bottom flask (100 mL) with CHCl_3 and concentrated under a reduced pressure (ca. 30 mmHg, 40 °C). The thus obtained residue was dissolved in CDCl_3 and analyzed by ^1H NMR. The conversion of **1a** (84%) and yields of **2a** (58%) and **3a** (7%) were calculated based on the integral ratio between the signals of these compounds with respect to an internal standard (mesitylene). The TON (22) was calculated by $(\mathbf{2a}+\mathbf{3a})/\text{Ru-1}$, assuming that **3a** was obtained from the condensation of **1a** with **2a**.

2.4.5. Ligand preparation

Tris(2-fluorophenyl)phosphine (L7),^[22] tris(3,5-difluorophenyl)phosphine (L8)^[23] and tris(3,4,5-trifluorophenyl)phosphine (L9)^[24] are all known compounds and synthesized according to the corresponding literature. All other ligands are commercially available and were used without further purification.

2.4.6. Precatalyst preparation

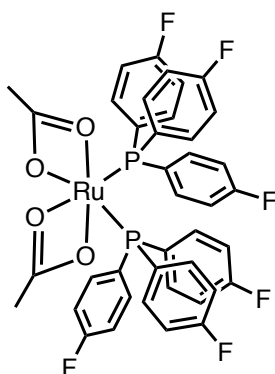
RuCl₂[P(4-fluorophenyl)₃]₃ (Ru-1', Figure 4, step 1)



The complex Ru-1' was prepared by minor modifications of the literature procedure^[25] as shown below.

RuCl₃·*n*H₂O (containing Ru in 42.18 wt %) (225.4 mg, 1.0 mmol), degassed and argon gas-purged methanol (45 mL), and a magnetic stirring bar were placed in a vessel equipped with a Young's stopcock under argon atmosphere. The mixture was stirred at 90 °C for 10 min and cooled to room temperature. To this reaction mixture was added tris(4-fluorophenyl)phosphine (L1, 1.90 g, 6.0 mmol), and stirred at 80 °C for 21 h and cooled to room temperature. The solution was concentrated under a reduced pressure until green precipitation was generated under argon atmosphere. The precipitation was collected by filtration under argon atmosphere, washed with degassed hexane (3×10 mL) and degassed hexane–diethyl ether (1:1 v/v 3×10 mL), and dried *in vacuo* to obtain the target Ru complex Ru-1' (915.2 mg, 0.82 mmol, 82% yield) as a moss green powder. ¹H NMR (600 MHz, CDCl₃): δ 7.66–7.62 (m, 18H, C₆H₄F), 7.18 (dt, *J* = 8.3, 2.0 Hz, 18H, C₆H₄F); ³¹P{¹H} NMR (243 MHz, CDCl₃): δ 27.3; HRMS (ESI) (*m/z*): [Ru[P(C₆H₄F)₃]₂Cl(CH₃CN)]⁺ calcd. for C₃₈H₂₇ClF₆NP₂Ru⁺, 810.0249; found, 810.0257.

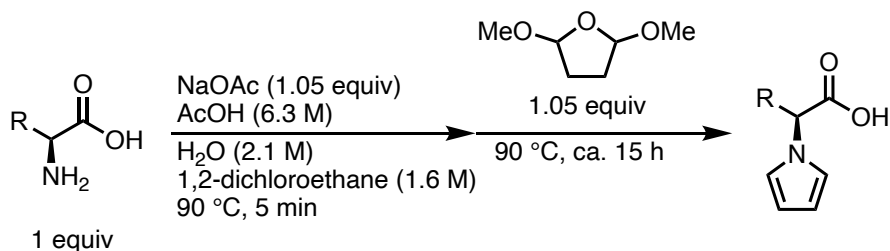
Ru(OAc)₂[P(4-fluorophenyl)₃]₂ (Ru-1, Figure 4, step 2)



Ru complex Ru-1 (669 mg, 0.70 mmol), NaOAc (490 mg, 6.0 mmol), degassed and argon gas-purged *t*-BuOH (28 mL), and a magnetic stirring bar were placed in a vessel equipped with a Young's stopcock under argon atmosphere. The mixture was stirred at 90 °C for 1 h and cooled to room temperature to afford orange solid. The solid was collected by filtration and washed with H₂O, methanol and Et₂O under argon atmosphere. The orange powder was dried *in vacuo* to obtain the target Ru complex Ru-1 (328 mg, 0.39 mmol, 65 % yield). ¹H NMR (600 MHz, CDCl₃): δ 7.14–7.10 (m, 12H, C₆H₄F), 6.89 (t, *J* = 8.3 Hz, 12H, C₆H₄F), 1.54 (s, 6H, CH₃COO); ¹³C{¹H} NMR (151 MHz, CDCl₃): δ 189.0, 164.4, 162.8, 136.0, 115.1, 23.5; ³¹P{¹H} NMR (243 MHz, CDCl₃): δ 62.6; HRMS (ESI) (*m/z*): [Ru[P(C₆H₄F)₃]₂(OAc)(CH₃CN)]⁺ calcd. for C₄₀H₃₀F₆NO₂P₂Ru⁺, 834.0694; found, 834.0661; Elemental analysis: calcd. C 56.41, H 3.55; found C 56.47, H 3.56.

2.4.7. Substrate preparation for hydrogenation

General procedure (modified by the literature procedure^[26])

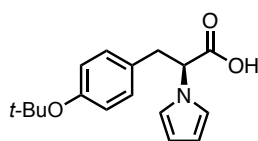


To a two-necked round bottom flask containing a stirring bar with a reflux condenser completely jacketed with an aluminum foil to exclude light inside, were added α -amino acid (1 equiv), sodium acetate (1.05 equiv), acetic acid (6.3 M), H₂O (2.1 M) and 1,2-dichloroethane (1.6 M) at room temperature under argon. After closing the flask with a rubber septum, the resulting mixture was immersed to pre-heated oil bath (set temperature: 90 °C) with vigorous stirring for 5 min. To the mixture was added 2,5-dimethoxytetrahydrofuran (1.05 equiv) dropwise using a syringe through the septum at 90 °C. The resulting mixture was stirred vigorously at the same temperature for ca. 15 h. The reaction mixture was allowed to cool to room temperature, diluted with water and ethyl acetate. The organic layer was washed with water several times, and then removing organic solvents gave a crude product. The target product was purified by silica gel chromatography.

(*S*)-3-Phenyl-2-(1*H*-pyrrol-1-yl)propanoic acid (**1a**),^[26a] (*S*)-3-(4-hydroxyphenyl)-2-(1*H*-pyrrol-1-yl)propanoic acid (**1b**),^[26b] (*S*)-2-(1*H*-pyrrol-1-yl)propanoic acid (**1e**),^[26a] (*S*)-3-methyl-2-(1*H*-pyrrol-1-yl)butanoic acid (**1f**)^[26a] and (*S*)-4-(methylthio)-2-(1*H*-pyrrol-1-yl)butanoic acid (**1g**)^[26a] are all known compounds and synthesized according to the aforementioned general procedure.

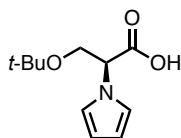
As for the *N*-protected substrates in Table 2, Boc (entry 1), Cbz (entry 2), Bz (entry 3), Phth (entry 4) and Fmoc (entry 5)-phenylalanine are commercially available. (*S*)-2,5-dimethyl- α -(phenylmethyl)-1*H*-pyrrole-1-acetic acid (entry 7) was synthesized according to the literature procedure.^[27]

(*S*)-3-(4-(*tert*-butoxy)phenyl)-2-(1*H*-pyrrol-1-yl)propanoic acid (*t*Bu-1b)



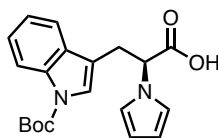
(*S*)-3-(4-(*tert*-butoxy)phenyl)-2-(1*H*-pyrrol-1-yl)propanoic acid was synthesized according to the aforementioned general procedure from *O*-*t*-Bu-(*S*)-tyrosine (1 g, 4.2 mmol). Purification by silica gel column chromatography (eluent: ethyl acetate/chloroform= 1/4) gave pure product *t*Bu-1b as a white solid (0.68 g, 2.4 mmol, 56% yield). ^1H NMR (600 MHz, CDCl_3): δ 6.89 (d, $J = 8.4$ Hz, 2H, C_6H_4), 6.85 (d, $J = 9.0$ Hz, 2H, C_6H_4), 6.68 (t, $J = 2.1$ Hz, 2H, C_4NH_4), 6.15 (t, $J = 2.1$ Hz, 2H, C_4NH_4), 4.75 (dd, $J = 9.6, 6.0$ Hz, 1H, CH), 3.41 (dd, $J = 15.0, 6.6$ Hz, 1H, CH_2), 3.24 (dd, $J = 14.4, 9.6$ Hz, 1H, CH_2), 1.31 (s, 9H, $\text{C}(\text{CH}_3)_3$); $^{13}\text{C}\{^1\text{H}\}$ NMR (CDCl_3 , 150 MHz) δ : 175.2, 154.3, 130.9, 129.2, 124.2, 120.2, 108.9, 78.5, 63.5, 38.5, 28.8; HRMS (ESI) (m/z): $[\text{M}-\text{H}]^-$ calcd. for $\text{C}_{17}\text{H}_{20}\text{NO}_3^-$, 286.1449; found, 286.1446; $[\alpha]_{\text{D}}^{24} = -49.2$ (c 1.0, CHCl_3).

(*S*)-3-(*tert*-butoxy)-2-(1*H*-pyrrol-1-yl)propanoic acid (*t*Bu-1d)



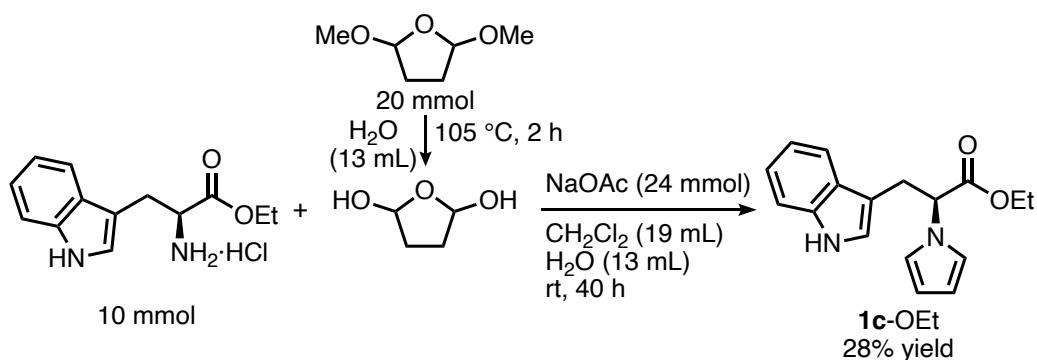
(*S*)-3-(*tert*-butoxy)-2-(1*H*-pyrrol-1-yl)propanoic acid was synthesized according to the aforementioned general procedure from *O*-*t*-Bu-(*S*)-serine (1 g, 6.2 mmol). Purification by silica gel column chromatography (eluent: ethyl acetate/chloroform= 1/3) gave pure product *t*Bu-1d as a white solid (0.57 g, 2.7 mmol, 44% yield). ^1H NMR (600 MHz, CDCl_3): δ 6.82 (t, 2H, $J = 2.4$ Hz, C_4NH_4), 6.19 (t, 2H, $J = 2.4$ Hz, C_4NH_4), 4.79 (t, $J = 5.1$ Hz, 1H, CH), 3.93 (d, $J = 5.4$ Hz, 2H, CH_2), 1.19 (s, 9H, $\text{C}(\text{CH}_3)_3$); $^{13}\text{C}\{^1\text{H}\}$ NMR (CDCl_3 , 150 MHz) δ : 174.3, 121.0, 108.7, 74.5, 62.8, 61.9, 27.3; HRMS (ESI) (m/z): $[\text{M}-\text{H}]^-$ calcd. for $\text{C}_{11}\text{H}_{16}\text{NO}_3^-$, 210.1136; found, 210.1140; $[\alpha]_{\text{D}}^{20} = +48.1$ (c 1.0, CHCl_3).

(*S*)-3-(1-(*tert*-butoxycarbonyl)-1*H*-indol-3-yl)-2-(1*H*-pyrrol-1-yl)propanoic acid (Boc-1c)



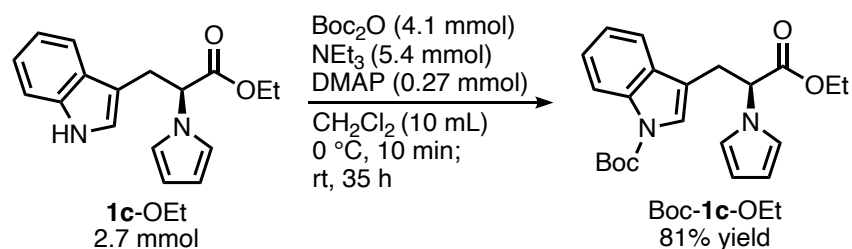
(*S*)-3-(1-(*tert*-butoxycarbonyl)-1*H*-indol-3-yl)-2-(1*H*-pyrrol-1-yl)propanoic acid (**Boc-1c**) was synthesized according to the literature procedure for the synthesis of *racemic* Boc-1c in three steps^[28] with minor modifications as shown below.

Step 1: ethyl (*S*)-3-(1*H*-indol-3-yl)-2-(1*H*-pyrrol-1-yl)propanoate (**1c-OEt**)



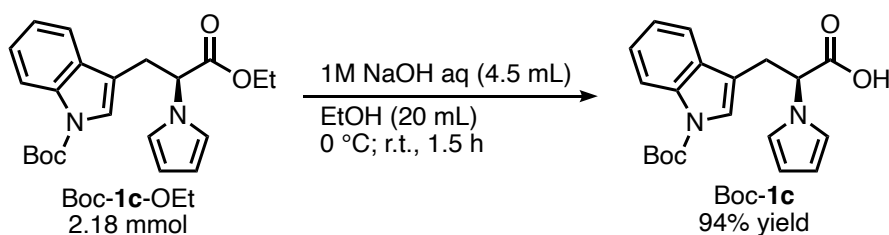
A mixture of 2,5-dimethoxytetrahydrofuran (20.0 mmol) and water (13 mL) was refluxed at 105 °C for 2 h. After cooling to 0 °C, dichloromethane (9.6 mL), sodium acetate (984 mg, 12.0 mmol) and DL-tryptophan ethyl ester hydrochloride (1.34 g, 5.00 mmol) were added to the reaction mixture. After the reaction mixture had been stirred for 40 h at room temperature with the vessel jacketed with an aluminum foil to exclude light inside, water was added. The mixture was extracted with chloroform, and the organic layer was dried over sodium sulfate. After the mixture was filtrated and the filtrate was evaporated, the crude product was purified by column chromatography on Wakogel[®] 50NH₂ (ethyl acetate/hexane = 1/9) to afford **1c-OEt** (0.78 g, 2.8 mmol, 28% yield) as a colorless oil. NMR spectrum was matched with reported spectrum data.^[28]

Step 2: *tert*-butyl (*S*)-3-(3-ethoxy-3-oxo-2-(1*H*-pyrrol-1-yl)propyl)-1*H*-indole-1-carboxylate (Boc-1c-OEt)



To a solution of **1c-OEt** (0.76 g, 2.7 mmol) and triethylamine (0.75 mL, 5.4 mmol) in dichloromethane (10 mL) at $0\text{ }^\circ\text{C}$ was added di-*tert*-butyl dicarbonate (Boc_2O , 0.89 g, 4.1 mmol) and *N,N*-dimethyl-4-aminopyridine (DMAP, 33 mg, 0.27 mmol). The reaction mixture was stirred at $0\text{ }^\circ\text{C}$ for 10 min and at room temperature for 35 h. The reaction mixture was purified by column chromatography on a neutral silica (ethyl acetate/hexane = 1/19) to afford **Boc-1c-OEt** (0.84 g, 2.2 mmol, 81% yield) as a colorless oil. ^1H NMR (500 MHz, CDCl_3): δ 8.11 (d, $J = 7.5$ Hz, 1H, indole), 7.46 (d, $J = 7.5$ Hz, 1H, indole), 7.31 (t, $J = 7.2$ Hz, 1H, indole), 7.24 (t, $J = 6.9$ Hz, 1H, indole), 7.05 (bs, 1H, indole), 6.78 (t, $J = 2.0$ Hz, 2H, pyrrole), 6.18 (t, $J = 2.0$ Hz, 2H, pyrrole), 4.84 (dd, $J = 10.3, 8.2$ Hz, 1H, 2-H), 4.21–4.15 (m, 2H, OCH_2CH_3), 3.56 (dd, $J = 14.9, 6.9$ Hz, 1H, 3- CH_2), 3.32 (dd, $J = 14.9, 7.4$ Hz, 1H, 3- CH_2), 1.63 (s, 9H, $\text{C}(\text{CH}_3)_3$), 1.21 (t, $J = 7.2$ Hz, OCH_2CH_3).

Step 3: Boc-1c



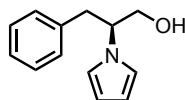
To a solution of **Boc-1c-OEt** (0.84 g, 2.2 mmol) in ethanol (20 mL) at $0\text{ }^\circ\text{C}$ was added aqueous sodium hydroxide (1 M, 4.5 mL, 4.5 mmol), and then the mixture was stirred at room temperature for 1.5 h. After removal of organic solvents by evaporation, the residue was diluted with a 1 M aq hydrochloric acid (17 mL) at $0\text{ }^\circ\text{C}$. After the mixture was extracted with ethyl acetate, the organic layer was washed with water, and dried over sodium sulfate. After filtration of the mixture, evaporation of the filtrate solvents afforded **Boc-1c** (0.73 g, 2.0 mmol, 94% yield) as a white solid. ^1H NMR (600 MHz, CDCl_3): δ 8.10 (bs, 1H, indole), 7.46 (d, $J = 7.8$ Hz, 1H, indole), 7.32 (t, $J = 7.2$ Hz, 1H, indole), 7.24 (t, $J = 7.5$ Hz, 1H, indole), 7.01 (bs, 1H, indole), 6.77 (t, $J = 2.1$ Hz, 2H, pyrrole), 6.20 (t, $J = 2.1$ Hz, 2H, pyrrole), 4.90 (dd, $J = 9.6,$

6.0 Hz, 1H, 2-*H*), 3.61 (dd, $J = 15.0, 5.4$ Hz, 1H, 3- CH_2), 3.36 (dd, $J = 15.0, 8.4$ Hz, 1H, 3- CH_2), 1.63 (s, 9H, $\text{C}(\text{CH}_3)_3$); $^{13}\text{C}\{^1\text{H}\}$ NMR (CDCl_3 , 150 MHz) δ : 174.5, 149.5, 135.2, 129.9, 124.6, 124.2, 122.6, 120.2, 118.3, 115.3, 114.6, 109.2, 83.7, 61.5, 28.4, 28.2; HRMS (ESI) (m/z): $[\text{M}-\text{H}]^-$ calcd. for $\text{C}_{20}\text{H}_{21}\text{N}_2\text{O}_4^-$, 353.1507; found, 353.1514; $[\alpha]_{\text{D}}^{24} = -14.2$ (c 1.0, CHCl_3). The enantiomeric ratio (er) of Boc-**1c** was determined by chiral HPLC analysis after derivatization to the corresponding ethyl ester Boc-**1c**-OEt' (91:9 er). For further detail, see Section 2.4.10, Scheme S4.

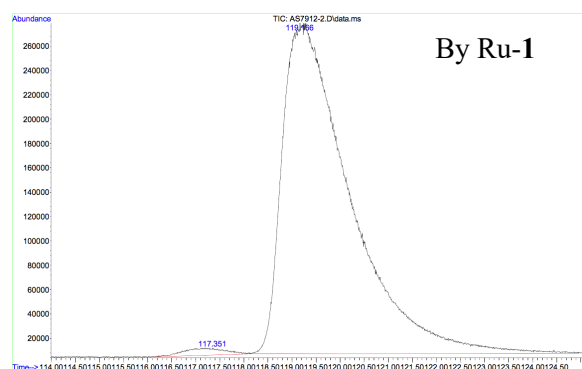
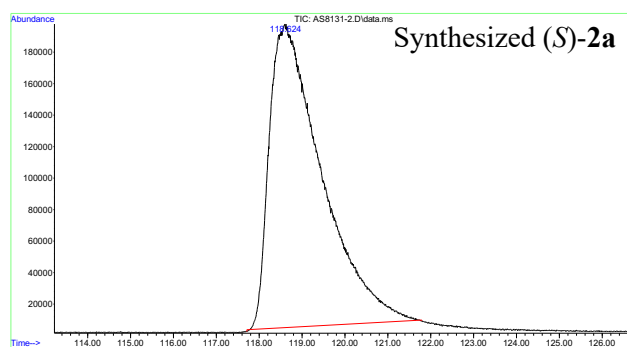
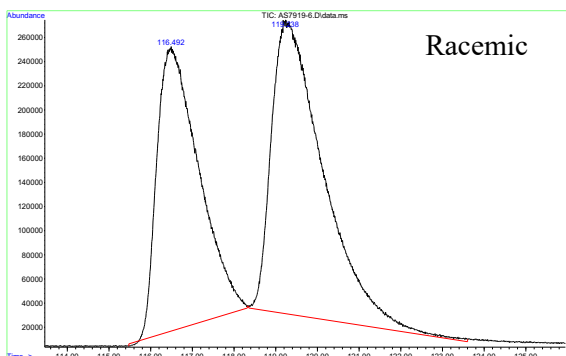
2.4.8. Alcohol products obtained in hydrogenation experiments

(*S*)-3-Phenyl-2-(1*H*-pyrrol-1-yl)propan-1-ol (**2a**),^[28] (*S*)-2-(1*H*-pyrrol-1-yl)propan-1-ol (**2e**)^[29] and (*S*)-3-methyl-2-(1*H*-pyrrol-1-yl)butan-1-ol (**2f**)^[30] are all known compounds.

(*S*)-3-Phenyl-2-(1*H*-pyrrol-1-yl)propan-1-ol (**2a**)

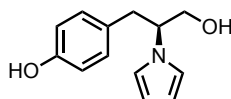


The reaction mixture obtained after hydrogenation was purified by column chromatography on silica gel (eluent: hexane/ethyl acetate = 4/1), giving **2a** (75 mg, 0.37 mmol, 74% yield) as a brown oil. ¹H NMR (600 MHz, CDCl₃): δ 7.23–7.11 (m, 3H, C₆H₅), 6.98–6.97 (m, 2H, C₆H₅), 6.63 (t, 2H, *J* = 2.1 Hz, C₄NH₄), 6.13 (t, 2H, *J* = 2.1 Hz, C₄NH₄), 4.12–4.07 (m, 1H, CH), 3.71 (d, 2H, *J* = 6.2 Hz, CH₂), 3.01–2.96 (m, 2H, CH₂). $[\alpha]_D^{20} = -84.3$ (*c* 1.0, CHCl₃). NMR spectrum was matched with reported spectrum data.^[28] The enantiomeric ratio (er) of **2a** was determined by chiral GC-MS analysis (99:1 er). A racemic sample was prepared from a 1:1 mixture of (*S*) and (*R*)-phenylalaninol (Section 2.4.10).

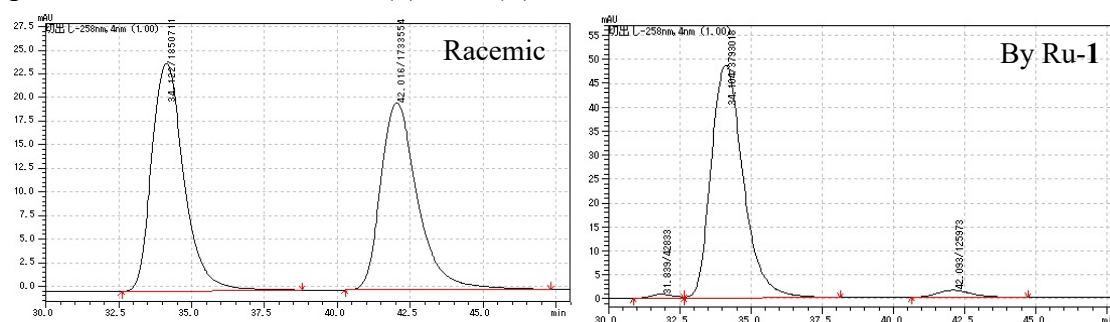


Peak No.	Retention time (min)	Area	Area ratio (%)
1	117.4	3536295	1.3
2	119.2	264859014	98.7
Total		268395309	100

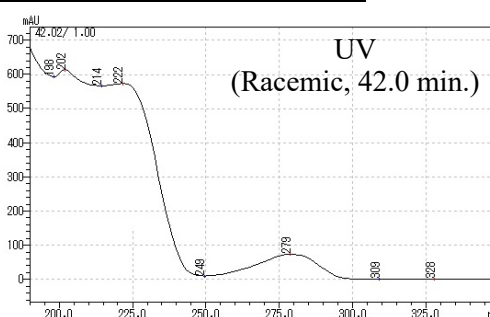
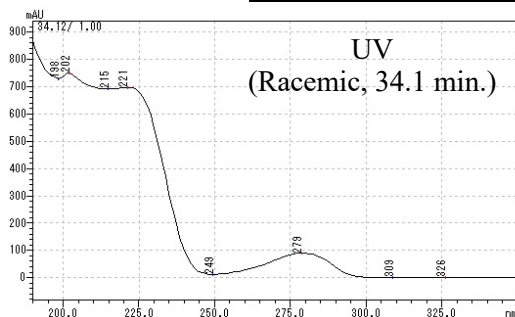
(*S*)-3-(4-hydroxyphenyl)-2-(1*H*-pyrrol-1-yl)propan-1-ol (2b)



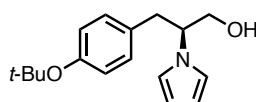
The reaction mixture obtained after hydrogenation was purified by column chromatography on silica gel (eluent: $\text{CHCl}_3/\text{MeOH} = 20/1$), giving **2b** (72 mg, 0.33 mmol, 66% yield) as a brown oil. ^1H NMR (600 MHz, CD_3OD): δ 6.85 (d, 2H, $J = 8.2$ Hz, C_6H_4), 6.68–6.65 (m, 4H, C_6H_4 , C_4NH_4), 6.16 (m, 2H, C_4NH_4), 4.11 (m, 1H, CH), 3.78 (d, 2H, $J = 5.5$ Hz, CH_2), 2.96 (d, 2H, $J = 6.9$ Hz, CH_2); ^{13}C $\{^1\text{H}\}$ NMR (151 MHz, CD_3OD): δ 157.7, 131.8, 131.3, 121.2, 116.8, 109.3, 66.6, 39.9; HRMS (ESI) (m/z): $[\text{M}+\text{Na}]^+$ calcd. for $\text{C}_{13}\text{H}_{15}\text{NNaO}_2$, 240.0995; found, 240.1007; $[\alpha]_{\text{D}}^{22} = -64.0$ (c 1.0, MeOH). The enantiomeric ratio (er) of **2b** was determined by chiral HPLC analysis (97:3 er). Conditions for HPLC analysis: CHIRALPAK AD-H (ϕ 0.46 cm \times 25 cm), *n*-hexane/2-propanol = 9/1, flow rate 0.50 mL/min, detection at 258 nm, $t_{\text{R}} = 34.1$ min. (major) and 42.1 min. (minor). A racemic sample was prepared by hydrogenation of **1b** using our Re catalyst (Section 2.4.10). We confirmed both peaks were derived from the (*S*)- and (*R*)-enantiomers which have the same UV absorbance.



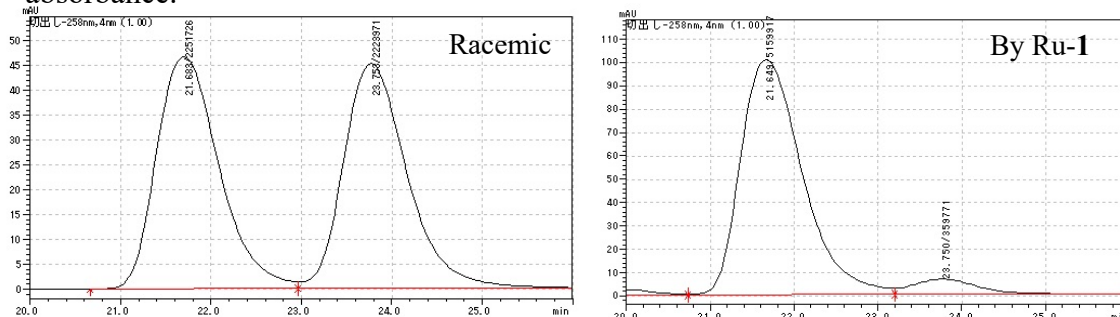
Peak No.	Retention time (min)	Area	Height	Area ratio (%)
1	34.1	3793018	48557	96.8
2	42.1	125973	1476	3.2
Total		3918991	50033	100



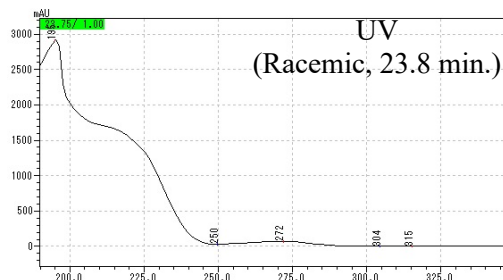
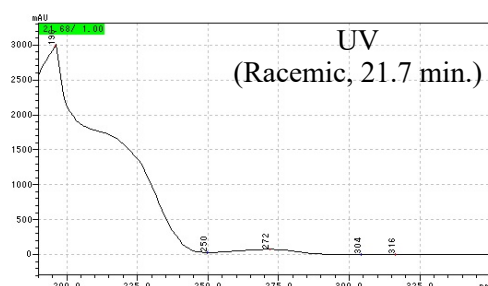
(*S*)-4-(3-hydroxy-2-(1*H*-pyrrol-1-yl)propyl)phenol (*t*Bu-2b)



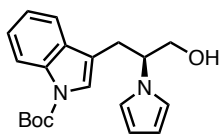
The reaction mixture obtained after hydrogenation was purified by column chromatography on silica gel (eluent: CHCl_3), giving *t*Bu-2b (90 mg, 0.33 mmol, 66% yield) as a brown oil. ^1H NMR (600 MHz, CDCl_3): δ 6.92 (d, $J = 8.4$ Hz, 2H, C_6H_4), 6.87 (d, $J = 7.8$ Hz, 2H, C_6H_4), 6.69 (t, $J = 2.1$ Hz, 2H, C_4NH_4), 6.16 (t, $J = 2.1$ Hz, 2H, C_4NH_4), 4.16 (quin, $J = 6.6$ Hz, 1H, CH), 3.82 (d, $J = 6.0$ Hz, 2H, CH_2OH), 3.02 (dd, $J = 7.8, 4.8$ Hz, 2H, CH), 6.16 (m, 2H, C_4NH_4), 4.11 (m, 1H, CH), 3.78 (d, 2H, $J = 5.5$ Hz, CH_2), 2.96 (d, 2H, $J = 6.9$ Hz, CH_2), 1.31 (s, 9H, $\text{C}(\text{CH}_3)_3$); $^{13}\text{C}\{^1\text{H}\}$ NMR (150 MHz, CDCl_3): δ 154.1, 132.4, 129.3, 124.3, 119.2, 108.5, 78.4, 65.2, 63.6, 38.0, 28.8; HRMS (ESI) (m/z): $[\text{M}+\text{Na}]^+$ calcd. for $\text{C}_{17}\text{H}_{23}\text{NNaO}_2^+$, 296.1621; found, 296.1600; $[\alpha]_{\text{D}}^{20} = -68.1$ (c 1.0, CHCl_3). The enantiomeric ratio (er) of *t*Bu-2b was determined by chiral HPLC analysis (93:7 er). Conditions for HPLC analysis: CHIRALPAK AD-H (ϕ 0.46 cm \times 25 cm), *n*-hexane/2-propanol = 24/1, flow rate 0.50 mL/min, detection at 258 nm, $t_{\text{R}} = 21.7$ min. (major) and 23.7 min. (minor). A racemic sample was prepared by hydrogenation of **1b** using our Re catalyst (Section 2.4.10). We confirmed both peaks were derived from the (*S*)- and (*R*)-enantiomers which have the same UV



Peak No.	Retention time (min)	Area	Height	Area ratio (%)
1	21.7	3655038	69828	93.1
2	23.7	272600	4887	6.9
Total		3927638	74715	100

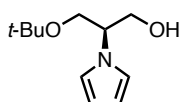


***tert*-butyl (S)-3-(3-hydroxy-2-(1*H*-pyrrol-1-yl)propyl)-1*H*-indole-1-carboxylate (Boc-2c)**

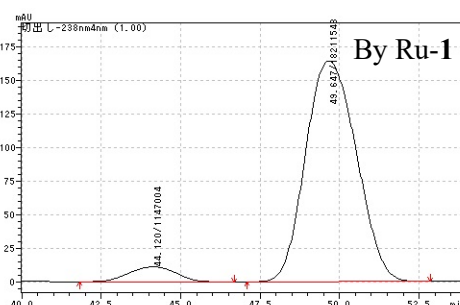
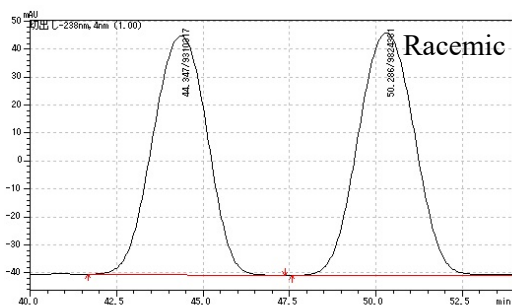


The reaction mixture obtained after hydrogenation was purified by column chromatography on silica gel (eluent: CHCl_3), giving Boc-2c (171 mg, 0.5 mmol, >99% yield) as a brown solid. ^1H NMR (600 MHz, CDCl_3): δ 8.12 (bs, 1H, indole), 7.45 (d, $J = 7.2$ Hz, 1H, indole), 7.31 (t, $J = 7.8$ Hz, 1H, indole), 7.23 (t, $J = 7.5$ Hz, 1H, indole), 7.11 (bs, 1H, indole), 6.78 (t, $J = 2.1$ Hz, 2H, pyrrole), 6.20 (t, $J = 2.1$ Hz, 2H, pyrrole), 4.33 (quin, $J = 6.8$ Hz, 1H, NCH), 3.88 (t, $J = 5.4$ Hz, OCH_2), 3.23 (dd, $J = 15.0, 6.8$ Hz, 1H, CH_2), 3.14 (dd, $J = 15.0, 8.2$ Hz, 1H, CH_2), 1.67 (s, 9H, $\text{C}(\text{CH}_3)_3$); $^{13}\text{C}\{^1\text{H}\}$ NMR (150 MHz, CDCl_3): δ 167.8, 149.6, 135.3, 132.5, 130.9, 130.2, 128.8, 127.2, 124.5, 123.8, 122.5, 122.1, 119.6, 119.3, 119.2, 118.5, 118.4, 116.1, 115.3, 111.6, 111.2, 108.7, 108.4, 83.6, 68.2, 65.8, 65.6, 62.4, 61.7, 38.7, 30.4, 29.7, 28.9, 28.2, 28.0, 27.7, 23.7, 23.0, 14.1, 11.0; HRMS (ESI) (m/z): $[\text{M}+\text{Cl}]^-$ calcd. for $\text{C}_{20}\text{H}_{24}\text{ClN}_2\text{O}_3^-$, 375.1481; found, 375.1364; $[\alpha]_{\text{D}}^{20} = -18.5$ (c 1.0, CHCl_3). The enantiomeric ratio (er) of Boc-2c was determined by chiral HPLC analysis after deprotection of the Boc group (80:20 er). For further detail, see Section 2.4.10, Scheme S3.

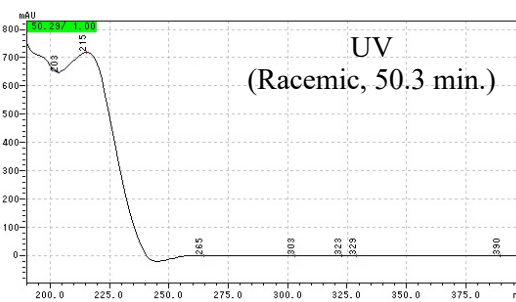
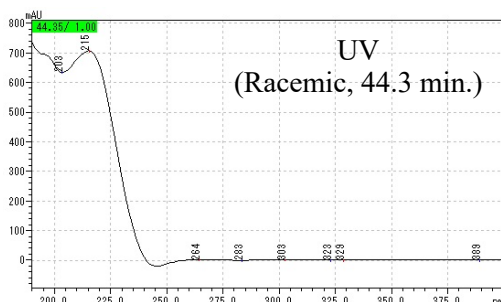
(*R*)-3-(*tert*-butoxy)-2-(1*H*-pyrrol-1-yl)propan-1-ol (*t*Bu-2d)



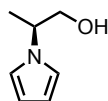
The reaction mixture obtained after hydrogenation was purified by column chromatography on silica gel (eluent: CHCl_3), giving *t*Bu-2d (30 mg, 0.15 mmol, 30% yield) as a brown oil. ^1H NMR (600 MHz, CDCl_3): δ 6.77 (t, $J = 2.1$ Hz, 2H, C_4NH_4), 6.17 (t, $J = 2.1$ Hz, 2H, C_4NH_4), 4.17 (quin, $J = 6.0$ Hz, 1H, CH), 3.99 (dd, $J = 10.8, 5.4$ Hz, 1H, CH_2), 3.94 (dd, $J = 11.4, 6.0$ Hz, 1H, CH_2), 3.72 (d, $J = 6.6$ Hz, 2H, CH_2OH), 1.19 (s, 9H, $\text{C}(\text{CH}_3)_3$); $^{13}\text{C}\{^1\text{H}\}$ NMR (150 MHz, CDCl_3): δ 119.8, 108.2, 73.9, 64.9, 63.6, 60.7, 27.3; HRMS (ESI) (m/z): $[\text{M}+\text{Na}]^+$ calcd. for $\text{C}_{11}\text{H}_{19}\text{NNaO}_2^+$, 220.1308; found, 220.1271; $[\alpha]_{\text{D}}^{20} = +12.8$ (c 0.51, CHCl_3). The enantiomeric ratio (er) of *t*Bu-2d was determined by chiral HPLC analysis (94:6 er). Conditions for HPLC analysis: CHIRALPAK OD-H (ϕ 0.46 cm \times 25 cm), *n*-hexane/2-propanol = 49/1, flow rate 0.25 mL/min, detection at 238 nm, $t_{\text{R}} = 49.6$ min (major) and 44.1 min. (minor). A racemic sample was prepared by hydrogenation of *t*Bu-1d using our Re catalyst (Section 2.4.10). We confirmed both peaks were derived from the (*S*)- and (*R*)-enantiomers which have the same UV absorbance.



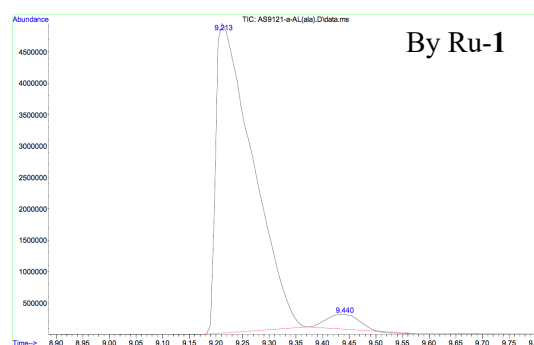
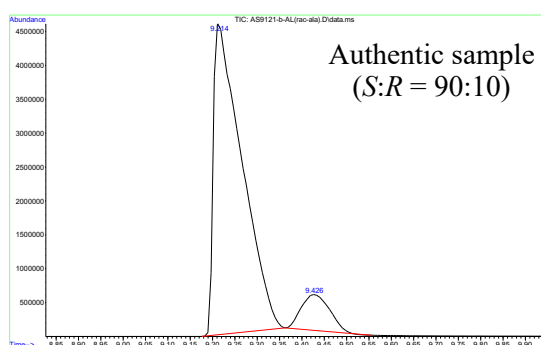
Peak No.	Retention time (min)	Area	Height	Area ratio (%)
1	44.1	1147004	11184	5.9
2	49.6	18211548	164118	94.1
Total		19358552	175302	100



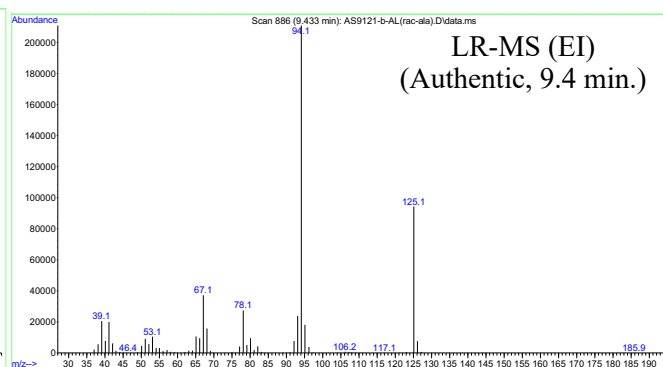
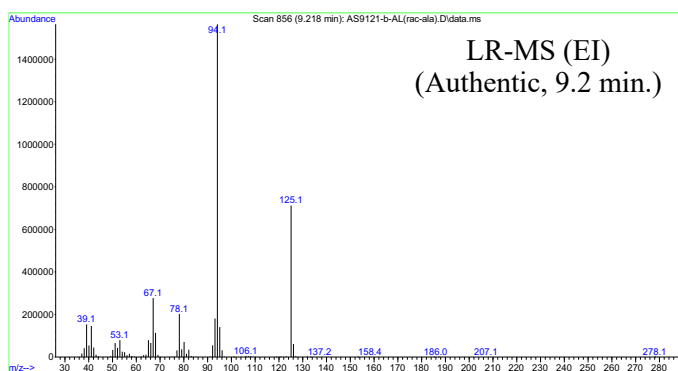
(*S*)-2-(1*H*-pyrrol-1-yl)propan-1-ol (2e**)**



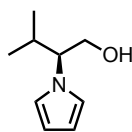
The reaction mixture obtained after hydrogenation was purified by column chromatography on silica gel (eluent: CHCl_3), giving **2e** (31 mg, 0.24 mmol, 49% yield) as a brown oil. $^1\text{H NMR}$ (600 MHz, CDCl_3): δ 6.73 (t, $J = 2.1$ Hz, 2H, C_4NH_4), 6.17 (t, $J = 2.1$ Hz, 2H, C_4NH_4), 4.18–4.13 (m, 1H, *CH*), 3.70–3.63 (m, 2H, CH_2), 1.43 (d, $J = 6.9$ Hz, 2H, CH_3). NMR spectrum was matched with reported spectrum data.^[29] Measurement of the optical rotation was failed because **2e** (c 1.1, CHCl_3) gave fluctuating readings. The reported value is $[\alpha]_{\text{D}}^{20} = +8.25$ (c 2.2, CHCl_3).^[29] The enantiomeric ratio (er) of **2e** was determined by chiral GC-MS analysis (96:4 er). An authentic sample (a mixture of (*S*)- and (*R*)-**2e**) was prepared by hydrogenation of **1e** using our Re catalyst (Section 2.4.10). The LR-MS (EI) spectra of these two peaks are consistent with each other.



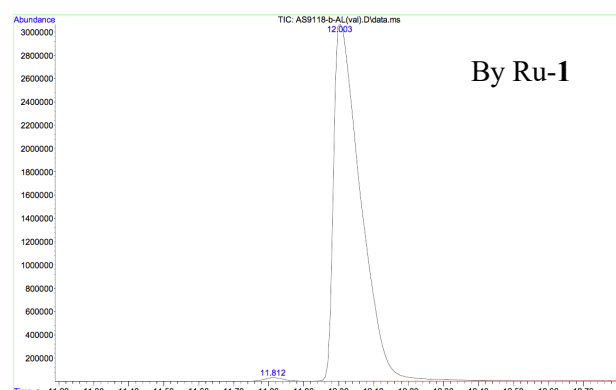
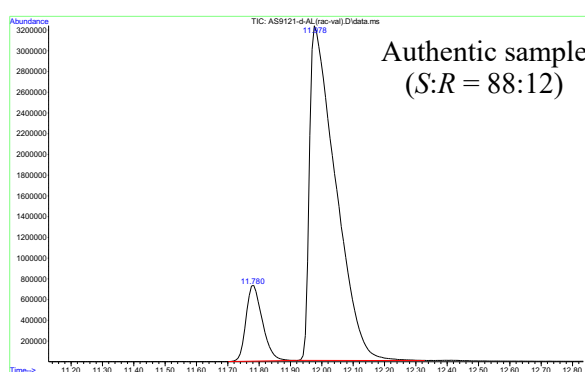
Peak No.	Retention time (min)	Area	Area ratio (%)
1	9.2	236394635	95.8
2	9.4	10476062	4.2
Total		246870697	100



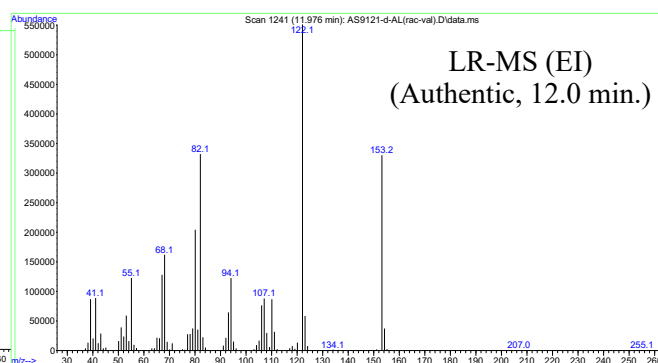
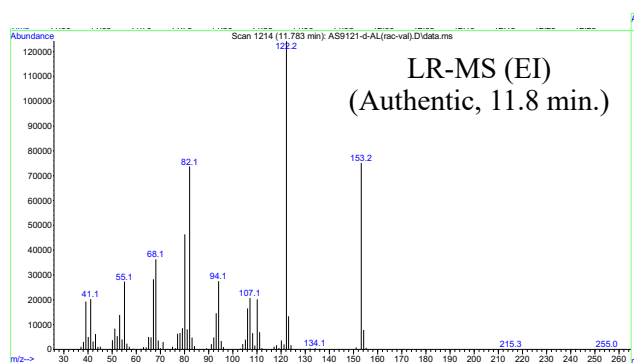
(*S*)-3-methyl-2-(1*H*-pyrrol-1-yl)butan-1-ol (2f**)**



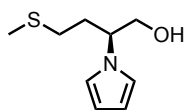
The reaction mixture obtained after hydrogenation was purified by column chromatography on silica gel (eluent: hexane/ethyl acetate = 5/1), giving **2f** (15 mg, 0.10 mmol, 20% yield) as a brown oil. ^1H NMR (600 MHz, CDCl_3): δ 6.68 (t, $J = 2.0$ Hz, 2H, C_4NH_4), 6.17 (t, $J = 2.0$ Hz, 2H, C_4NH_4), 3.91 (dd, $J = 11.7, 4.1$ Hz, 1H, OCH_2), 3.82 (dd, $J = 11.7, 10.3$ Hz, 1H, OCH_2), 3.59 (dt, $J = 8.9, 4.1$ Hz, 1H, NCH), 2.04–1.98 (m, 1H, CH), 1.00 (d, $J = 6.9$ Hz, 3H, CH_3), 0.73 (d, $J = 6.9$ Hz, 3H, CH_3). NMR spectrum was matched with the reported spectrum data.^[30] Measurement of the optical rotation was failed because **2f** (c 0.1, CHCl_3) gave fluctuating readings. The enantiomeric ratio (er) of **2f** was determined by chiral GC-MS analysis (>99:1 er). An authentic sample (a mixture of (*S*)- and (*R*)-**2f**) was prepared by hydrogenation of **1f** using our Re catalyst (Section 2.4.10). The LR-MS (EI) spectra of these two peaks are consistent with each other.



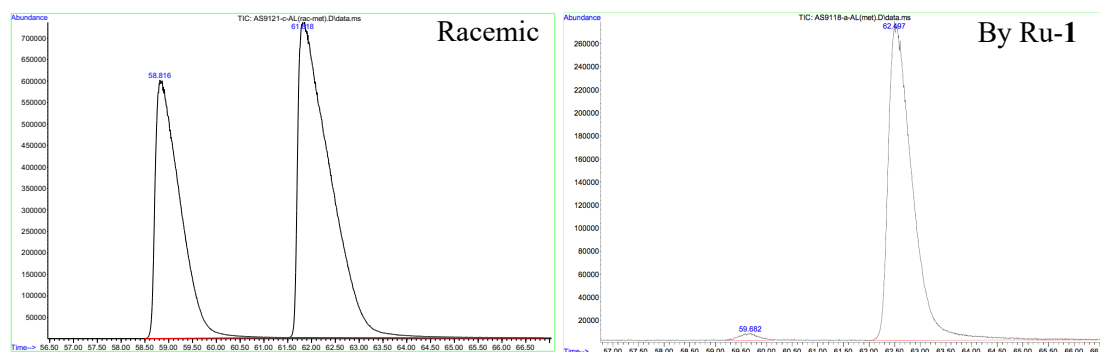
Peak No.	Retention time (min)	Area	Area ratio (%)
1	11.8	1152388	0.7
2	12.0	163145736	99.3
Total		165268341	100



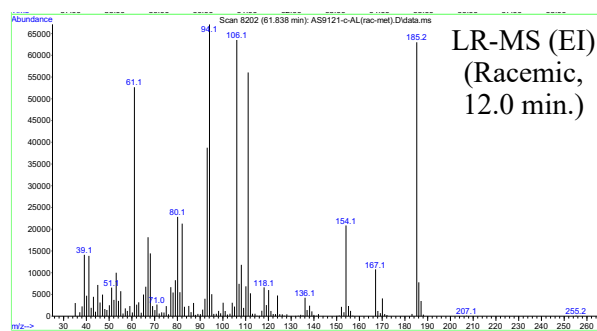
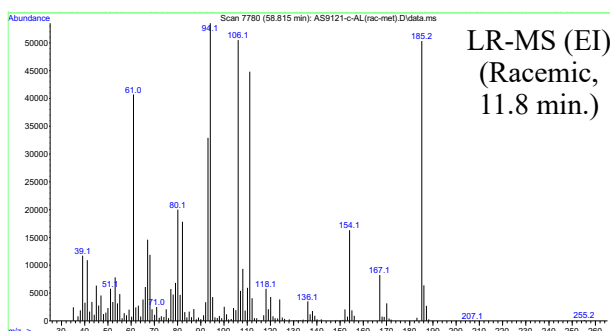
(*S*)-4-(methylthio)-2-(1*H*-pyrrol-1-yl)butan-1-ol (2g)



The reaction mixture obtained after hydrogenation was purified by column chromatography on silica gel (eluent: hexane/ethyl acetate = 3/1), giving **2g** (38 mg, 0.20 mmol, 41% yield) as a brown oil. ^1H NMR (600 MHz, CDCl_3): δ 6.72 (t, $J = 2.4$ Hz, 2H, C_4NH_4), 6.19 (t, $J = 1.8$ Hz, 2H, C_4NH_4), 4.21–4.16 (m, 1H, CH), 3.78 (d, $J = 6.6$ Hz, 2H, CH_2), 2.41–2.37 (m, 1H, CH_2), 2.29–2.24 (m, 1H, CH_2), 2.06–1.71 (m, 5H, CH_2 , CH_3); $^{13}\text{C}\{^1\text{H}\}$ NMR (151 MHz, CDCl_3): δ 119.2, 108.6, 66.1, 60.5, 31.0, 30.4, 15.5; HRMS (ESI) (m/z): $[\text{M}]^+$ calcd. for $\text{C}_9\text{H}_{15}\text{NOS}$, 185.0869; found, 184.0811; $[\alpha]_{\text{D}}^{20} = -44.9$ (c 1.0, CHCl_3). The enantiomeric ratio (er) of **2g** was determined by chiral GC-MS analysis (99:1 er). A racemic sample was prepared by hydrogenation of **1g** using our Re catalyst (Section 2.4.10). We confirmed both peaks were derived from the (*S*)- and (*R*)-enantiomers which have the same LR-MS (EI) spectra.

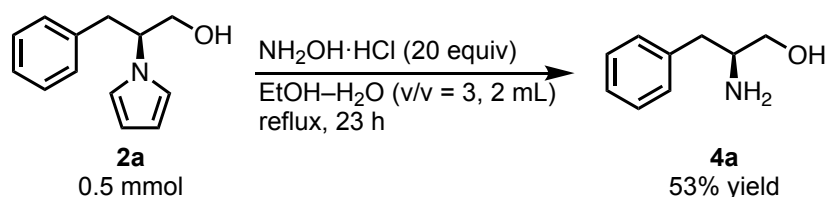


Peak No.	Retention time (min)	Area	Area ratio (%)
1	59.7	1048420	1.2
2	62.5	88735372	98.8
Total		89783792	100



2.4.9. Deprotection of the pyrrolyl group from **2a** (Scheme 1)

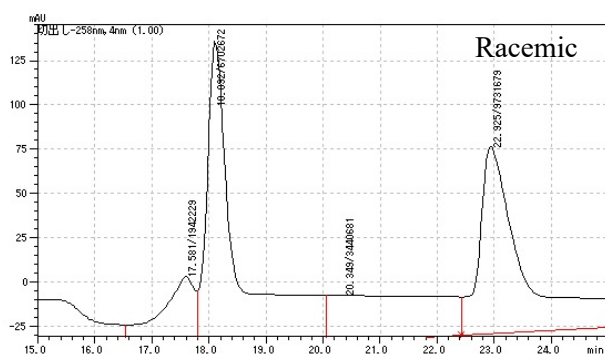
Deprotection using $\text{NH}_2\text{OH}\cdot\text{HCl}$



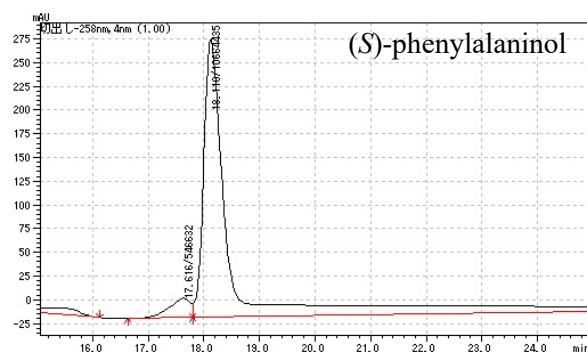
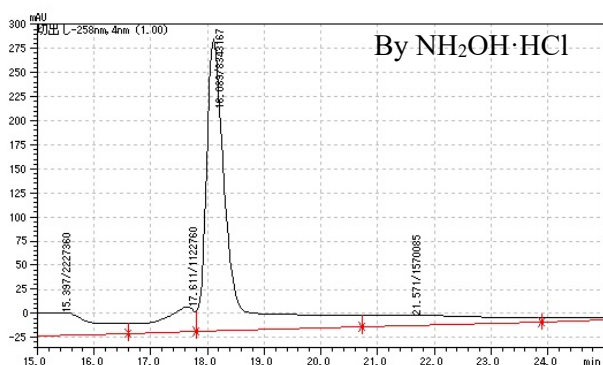
Deprotection of the pyrrolyl group from **2a** using $\text{NH}_2\text{OH}\cdot\text{HCl}$ was carried out with modification of the literature procedure.^[21]

To a vessel equipped with a Young's stopcock were added $\text{NH}_2\text{OH}\cdot\text{HCl}$ (695 mg, 10 mmol), EtOH (1.5 mL), H_2O (0.5 mL) and a stirring bar under argon. The solution was put in a pre-heated block (set temperature: 95 °C) for 15 min. After the mixture was cooled to room temperature, **2a** (101 mg, 0.5 mmol) was added to the mixture under argon. The resulting mixture was stirred at 95 °C with reflux for 23 h, poured into a 2 M aq HCl, washed with chloroform, and basified with a 2 M aq NaOH, extracted with EtOAc. Evaporation of the collected organic solvents afforded a crude product as yellow oil. The crude product was purified by column chromatography on Wakogel[®] 50NH₂ (chloroform/methanol = 30/1) to afford **4a** (26 mg, 0.17 mmol, 53% yield) as a white solid. ¹H NMR (600 MHz, CD₃OD) δ : 7.71 (dd, $J = 6.0, 3.6$ Hz, 1H), 7.62 (dd, $J = 5.4, 2.4$ Hz, 1H), 7.29 (t, $J = 7.8$ Hz, 1H), 7.21 (t, $J = 6.0$ Hz, 2H), 4.24–4.18 (m, 2H), 3.52 (dd, $J = 10.8, 4.2$ Hz, 1H), 3.36 (dd, $J = 11.4, 7.2$ Hz, 1H), 3.04 (quin, $J = 5.3$ Hz, 1H), 2.77 (dd, $J = 13.8, 6.6$ Hz, 1H), 2.57 (dd, $J = 13.8, 8.4$ Hz, 1H).

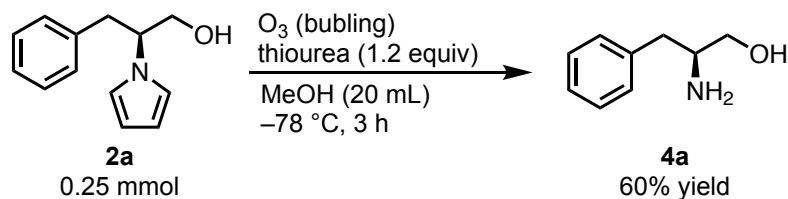
The enantiomeric ratio (er) of **2a** was determined by chiral HPLC analysis (100:0 er). Conditions for HPLC analysis (modified by the literature procedure^[31]): CHIRALPAK AY-H (ϕ 0.46 cm \times 25 cm), column temperature at 35 °C, *n*-hexane/ethanol/ethanolamine = 90/10/0.1, flow rate 0.5 mL/min, detection at 258 nm, *t*R = 18.1 min. (major, *S*) and 22.9 min. (minor, *R*). A racemic sample was prepared from commercially available (*S*)- and (*R*)-phenylalaninol.



Peak No.	Retention time (min)	Area	Height	Area ratio (%)
1	18.1	8348167	303055	100
2	—	—	—	—
Total		8348167	303055	100

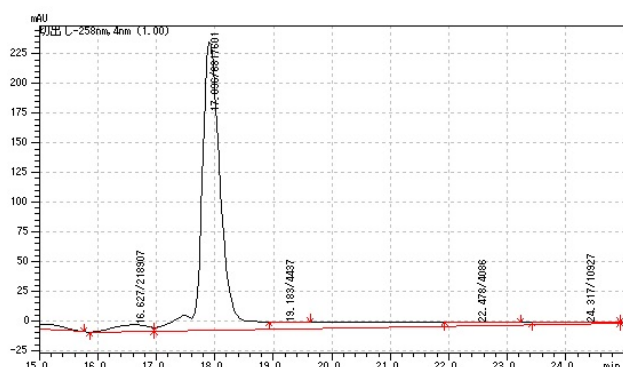


Deprotection using O₃ and thiourea



Deprotection of the pyrrolyl group from **2a** using O₃ and thiourea was carried out with modification of the literature procedure for the deprotection of methyl (*S*)-3-phenyl-2-(1*H*-pyrrol-1-yl)propanoate.^[28]

2a (50 mg, 0.25 mmol) was dissolved in methanol (20 mL) and the solution was cooled to -78 °C. Ozone was bubbled (flow rate: ~2 mL/min) through the solution for 2.5 h with vigorously stirring, after which argon was bubbled for 15 min. A solution of thiourea (40.2 mg, 0.529 mmol) in methanol (4 mL) was added. The reaction mixture was stirred for 30 min at -78 °C and for 1 h at 0 °C and then filtered through Celite to remove the generated white precipitate. The filtrate was concentrated to be dryness under a reduced pressure. To the mixture was added hydrochloride in 1,4-dioxane (4.0 M, 5 mL, 2 mmol) at 0 °C and then the resulting mixture was stirred for 19 h at room temperature. The reaction mixture was concentrated to be dryness under a reduced pressure with a KOH trap, basified with a 2 M aq NaOH, extracted with EtOAc. Evaporation of the collected organic solvents afforded a crude product as yellow oil. The crude product was purified by column chromatography on Wakogel[®] 50NH₂ (chloroform/methanol = 30/1) to afford **4a** (23 mg, 0.15 mmol, 60% yield) as a white solid. The enantiomeric ratio (er) of **4a** was determined by chiral HPLC analysis (99.9:0.1 er). For conditions of HPLC analysis, see section 2.4.9.

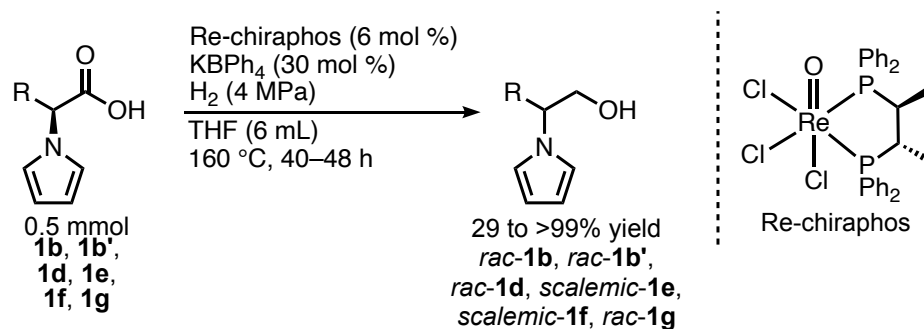


Peak No.	Retention time (min)	Area	Height	Area ratio (%)
1	17.9	6817601	243319	99.9
2	22.5	4086	111	0.1
Total		6821687	243430	100

2.4.10. Experimental procedure for preparation of authentic samples to determine enantiomeric ratio (er) by chiral GC-MS or HPLC analysis

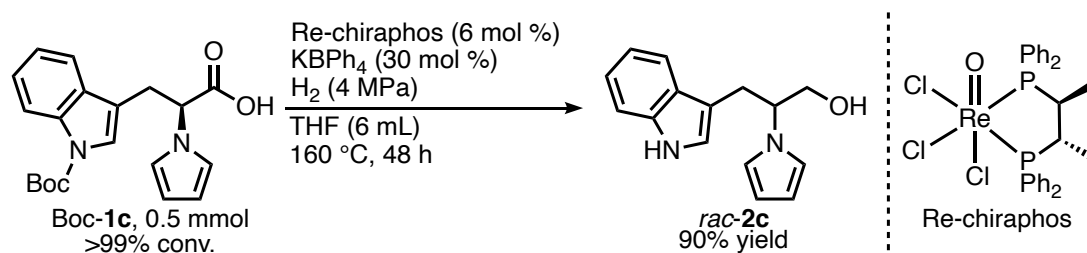
Racemic 3-Phenyl-2-(1*H*-pyrrol-1-yl)propan-1-ol (*rac*-**2a**) was synthesized from 1:1 mixture of (*S*) and (*R*)-phenylalaninol (total 454 mg, 3 mmol) according to the general procedure (section 2.4.7) instead of α -amino acids (527 mg, 2.6 mmol, 87% isolated yield) as a white solid.

Racemic 3-(4-hydroxyphenyl)-2-(1*H*-pyrrol-1-yl)propan-1-ol (*rac*-**2b**), racemic 4-(3-hydroxy-2-(1*H*-pyrrol-1-yl)propyl)phenol (*rac*-**2b'**), racemic 3-(*tert*-butoxy)-2-(1*H*-pyrrol-1-yl)propan-1-ol (*rac*-**2d**), scalemic 2-(1*H*-pyrrol-1-yl)propan-1-ol (*scalemic*-**2e**), scalemic 3-methyl-2-(1*H*-pyrrol-1-yl)butan-1-ol (*scalemic*-**2f**) and (*S*)-4-(methylthio)-2-(1*H*-pyrrol-1-yl)butan-1-ol (*rac*-**2g**) were prepared by hydrogenation of the corresponding *N*-protected amino acids using our Re catalyst (Re-chiraphos), under which the racemization occurs (Scheme S1).^[11] Procedure for the hydrogenation was following the general procedure in section 2.4.4.

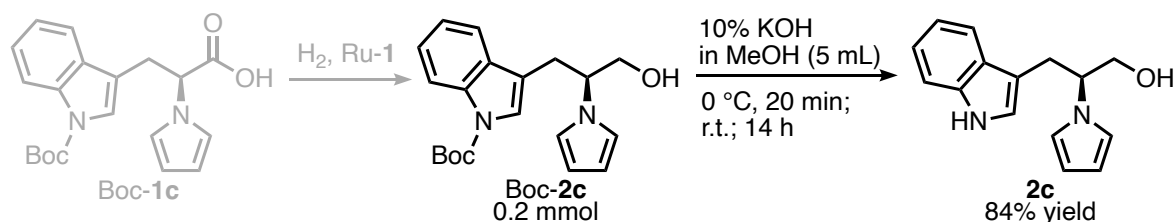


Scheme S1 | Preparation of authentic samples via hydrogenation using Re-chiraphos.

As for the preparation of racemic *tert*-butyl-3-(3-hydroxy-2-(1*H*-pyrrol-1-yl)propyl)-1*H*-indole-1-carboxylate (*rac*-Boc-**2c**), hydrogenation of Boc-**1c** using Re-chiraphos complex as the above provided racemic 3-(1*H*-indol-3-yl)-2-(1*H*-pyrrol-1-yl)propan-1-ol (*rac*-**2c**) free from the Boc group (Scheme S2). Therefore, in order to determine er of Boc-**2c** which was obtained by the hydrogenation with Ru-**1**, deprotection of the Boc group from Boc-**2c** was carried out under basic conditions (Scheme S3).

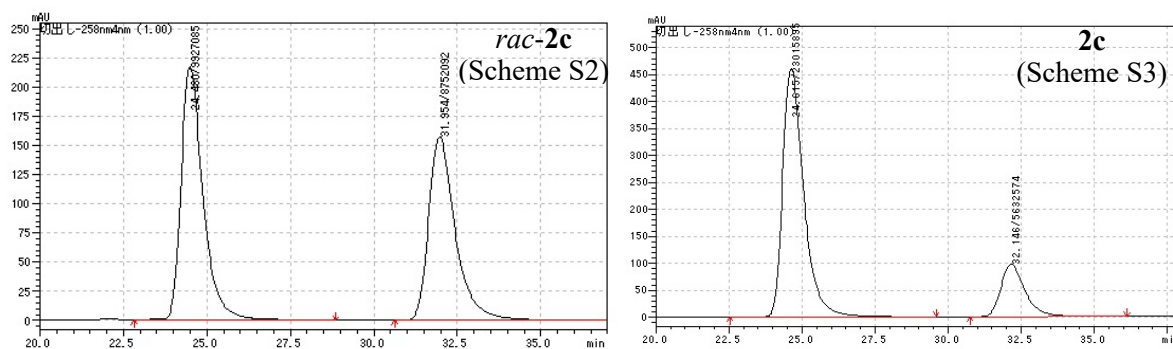


Scheme S2 | Hydrogenation of Boc-1c using the Re-chiraphos to *rac*-2c. The yield was determined by ¹H NMR analysis using mesitylene as internal standard. The reaction mixture obtained after hydrogenation was purified by column chromatography on Wakogel[®] 50NH₂ (eluent: chloroform), giving *rac*-2c. ¹H NMR (600 MHz, CDCl₃): δ 7.95 (bs, 1H, indole), 7.56 (d, J = 8.2 Hz, 1H, indole), 7.35 (d, J = 8.2 Hz, 1H, indole), 7.20 (t, J = 7.5 Hz, 1H, indole), 7.13 (t, J = 7.5 Hz, 1H, indole), 6.76 (t, J = 2.0 Hz, 2H, pyrrole), 6.70 (d, J = 1.4 Hz, 1H, indole), 6.19 (t, J = 2.0 Hz, 2H, pyrrole), 4.33 (quin, J = 6.8 Hz, 1H, NCH), 3.89 (t, J = 6.1 Hz, OCH₂), 3.30 (dd, J = 14.3, 6.8 Hz, 1H, CH₂), 3.20 (dd, J = 14.6, 7.8 Hz, 1H, CH₂), 1.48 (t, J = 6.5 Hz, OH). NMR spectrum was matched with reported spectrum data.^[28] HRMS (ESI) (m/z): [M+Cl]⁻ calcd. for C₁₅H₁₆N₂OCl⁻, 275.0957; found, 275.0985.

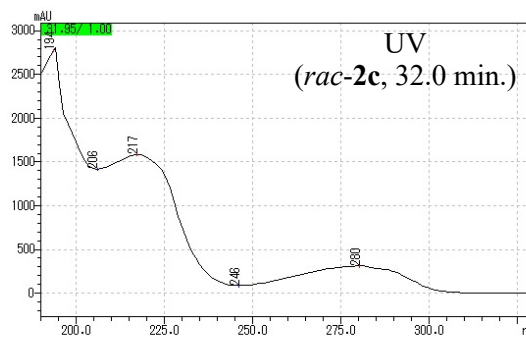
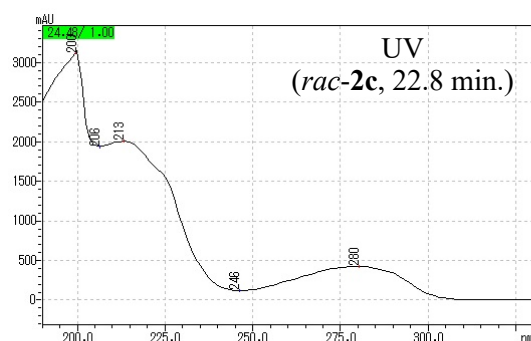


Scheme S3 | Deprotection of the Boc group from Boc-2c under basic conditions. This reaction was carried out according to the literature procedure for deprotection of the Boc group from 2-amino-3-(1-(*tert*-butoxycarbonyl)-1*H*-indol-3-yl)-2-methylpropanoic acid (*N*₁-Boc- α -Metryptophan).^[32] Experimental procedure is as follows. To a flask containing a stirring bar and Boc-2c (68 mg, 0.2 mmol), which was isolated after the hydrogenation using Ru-1, was added a 10% KOH in methanol (5 mL) at 0 °C under argon, and then the mixture was stirred at 0 °C for 20 min, and at room temperature for 14 h. After removal of solvents by evaporation, the residue was dissolved in chloroform and purification with column chromatography on Wakogel[®] 50NH₂ (eluent: chloroform) afforded 2c (41 mg, 0.17 mmol, 84% yield) as a colorless oil. ¹H NMR (600 MHz, CDCl₃): δ 7.95 (bs, 1H, indole), 7.56 (d, J = 7.5 Hz, 1H, indole), 7.35 (d, J = 8.2 Hz, 1H, indole), 7.20 (t, J = 7.8 Hz, 1H, indole), 7.14 (t, J = 7.1 Hz, 1H, indole), 6.76 (t, J = 2.1 Hz, 2H, pyrrole), 6.69 (d, J = 2.0 Hz, 1H, indole), 6.19 (t, J = 2.4 Hz, 2H, pyrrole), 4.33 (quin, J = 6.8 Hz, 1H, NCH), 3.88 (t, J = 5.7 Hz, OCH₂), 3.29 (dd, J = 15.0, 6.8 Hz, 1H, CH₂), 3.20 (dd, J = 14.6, 8.5 Hz, 1H, CH₂), 1.48 (t, J = 6.5 Hz, OH); ¹³C {¹H}

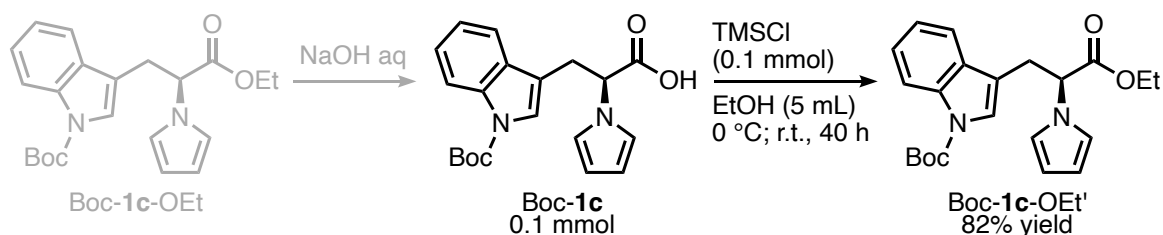
NMR (149 MHz, CDCl_3): δ 136.0, 127.2, 122.5, 122.1, 119.6, 119.3, 118.4, 111.6, 111.2, 108.4, 65.8, 62.4, 27.9. The enantiomeric ratio (er) of **2c** was determined by chiral HPLC analysis (80:20 er). Conditions for HPLC analysis^[28]: CHIRALPAK AD-H (ϕ 0.46 cm \times 25 cm), column temperature at 40 °C, *n*-hexane/2-propanol = 9/1, flow rate 0.75 mL/min, detection at 258 nm, *t*R = 24.6 min. (major) and 32.1 min. (minor). We confirmed both peaks were derived from the (*S*)- and (*R*)-enantiomers which have the same UV absorbance.



Peak No.	Retention time (min)	Area	Height	Area ratio (%)
1	24.6	23015895	460449	80.3
2	32.1	5662354	97071	19.7
Total		28678249	557520	100

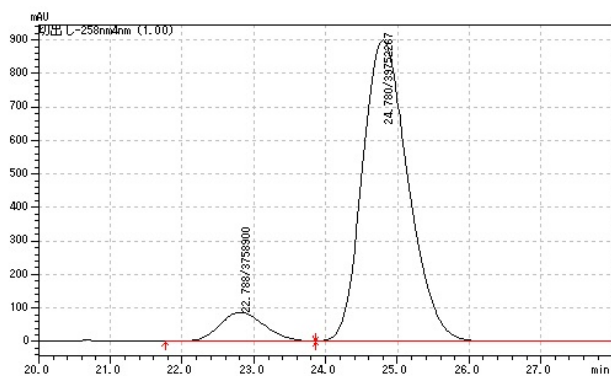


In order to determine *er* of Boc-**1c** which had been used as substrate for the hydrogenation, esterification of Boc-**1c** was carried out (Scheme S4).

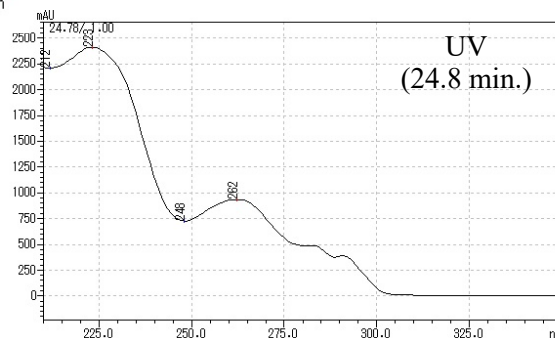
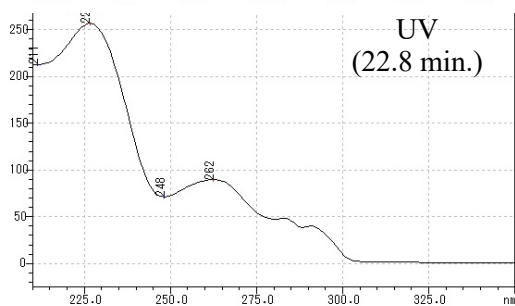


Scheme S4 | Esterification of Boc-**1c**. This reaction was carried out according to the literature procedure for ethyl esterification of tryptophan^[33] with a modification. Experimental procedure is as follows. To a flask containing a stirring bar and Boc-**1c** (35 mg, 0.1 mmol), which was obtained in section 2.4.7., were added ethanol (5 mL) and trimethylsilyl chloride (13 μ L, 0.1 mmol) at 0 °C under argon, and then stirred at room temperature for 40 h. After removal of solvents by evaporation, the residue was dissolved in chloroform and purification with column chromatography on neutral silica (ethyl acetate/hexane = 1/19) to afford Boc-**1c**-OEt' (31 mg, 0.08 mmol, 82% yield) as a colorless oil. ¹H NMR (600 MHz, CDCl₃): δ 8.11 (bs, 1H, indole), 7.47 (d, *J* = 8.4 Hz, 1H, indole), 7.32 (t, *J* = 7.2 Hz, 1H, indole), 7.24 (t, *J* = 7.8 Hz, 1H, indole), 7.05 (bs, 1H, indole), 6.79 (t, *J* = 2.4 Hz, 2H, pyrrole), 6.18 (t, *J* = 1.8 Hz, 2H, pyrrole), 4.84 (t, *J* = 7.8 Hz, 1H, 2-H), 4.20–4.15 (m, 2H, OCH₂CH₃), 3.56 (dd, *J* = 15.6, 7.8 Hz, 1H, 3-CH₂), 3.32 (dd, *J* = 15.6, 7.8 Hz, 1H, 3-CH₂), 1.63 (s, 9H, C(CH₃)₃), 1.21 (t, *J* = 7.2 Hz, OCH₂CH₃); ¹³C{¹H} NMR (149 MHz, CDCl₃): δ 170.2, 149.6, 135.3, 130.1, 124.6, 124.2, 122.6, 120.1, 118.5, 115.4, 115.0, 108.9, 83.7, 62.0, 61.8, 28.9, 28.2, 14.1; HRMS (ESI) (*m/z*): [M+Na]⁺ calcd. for C₂₂H₂₆N₂O₄Na⁺, 405.1785; found, 405.1785; [α]_D²⁰ = -25.2 (*c* 0.1, CHCl₃).

The enantiomeric ratio (er) of Boc-**1c**-OEt' was determined by chiral HPLC analysis (91:9 er). Conditions for HPLC analysis: CHIRALPAK OD-H (ϕ 0.46 cm \times 25 cm), column temperature at 40 °C, *n*-hexane/2-propanol = 49/1, flow rate 0.30 mL/min, detection at 258 nm, *t*R = 22.8 min. (major) and 24.8 min. (minor). We confirmed both peaks were derived from the (*S*)- and (*R*)-enantiomers which have the same UV absorbance.



Peak No.	Retention time (min)	Area	Height	Area ratio (%)
1	22.8	3761274	86556	8.6
2	24.8	39754657	899509	91.4
Total		43515931	986065	100



References

- [1] a) *Comprehensive Asymmetric Catalysis* (Eds.: E. N. Jacobsen, A. Pfaltz, H. Yamamoto), Springer-Verlag, Berlin Heidelberg, **1999**; b) A. K. Ghosh, P. Mathivanan, J. Cappiello, *Tetrahedron: Asymmetry* **1998**, *9*, 1–45; c) J. S. Johnson, D. A. Evans, *Acc. Chem. Res.* **2000**, *33*, 325–335; d) G. Desimoni, G. Faita, P. Quadrelli, *Chem. Rev.* **2003**, *103*, 3119–3154; e) T. P. Yoon, E. N. Jacobsen, *Science* **2003**, *299*, 1691–1693; f) R. Noyori, M. Kitamura, *Angew. Chem.* **1991**, *103*, 34–55; *Angew. Chem. Int. Ed. Engl.* **1991**, *30*, 49–69; g) M. Kitamura, S. Suga, H. Oka, R. Noyori, *J. Am. Chem. Soc.* **1998**, *120*, 9800–9809; h) A. Pfaltz, *Acc. Chem. Res.* **1993**, *26*, 339–345; i) F. Fache, E. Schulz, M. L. Tommasino, M. Lemaire, *Chem. Rev.* **2000**, *100*, 2159–2231; j) D. Rechavi, M. Lemaire, *Chem. Rev.* **2002**, *102*, 3467–3494; k) O. B. Sutcliffe, M. R. Bryce, *Tetrahedron: Asymmetry* **2003**, *14*, 2297–2325; l) H. A. McManus, P. J. Guiry, *Chem. Rev.* **2004**, *104*, 4151–4202.
- [2] a) M. M. Heravi, V. Zadsirjan, B. Farajpour, *RSC Adv.* **2016**, *6*, 30498–30551; b) D. J. Ager, I. Prakash, D. R. Schaad, *Chem. Rev.* **1996**, *96*, 835–875; c) G. Proctor in *Asymmetric Synthesis*, Oxford University Press, Oxford, **1996**, Chapter 5; d) D. A. Evans in *Asymmetric Synthesis*, Vol. 3 (Ed.: J. D. Morison), Academic Press, San Diego CA, **1984**, Chapter I.
- [3] a) C.-X. Ye, Y. Y. Melcamu, H.-H. Li, J.-T. Cheng, T.-T. Zhang, Y.-P. Ruan, X. Zheng, X. Lu, P.-Q. Huang, *Nat. Commun.* **2018**, *9*, 410; b) S. B. Kang, Park, Y. H. Kim, Y. Kim, *Heterocycles* **1997**, *45*, 137–145; c) S.-Y. Wu, A. Hirashima, E. Kuwano, M. Eto, *Agric. Biol. Chem.* **1987**, *51*, 537–547.
- [4] a) H. Nakano, I. A. Owolabi, M. Chennapuram, Y. Okuyama, E. Kwon, C. Seki, M. Tokiwa, M. Takeshita, *Heterocycles* **2018**, *97*, 647–667; b) C. R. Shugrue, S. J. Miller, *Chem. Rev.* **2017**, *117*, 11894–11951; c) Y. Hayashi, *Chem. Sci.* **2016**, *7*, 866–880; d) X.-Y. Xu, Y.-Z. Wang, L.-Z. Gong, *Org. Lett.* **2007**, *9*, 4247–4249; e) E. R. Jarvo, S. J. Miller, *Tetrahedron* **2002**, *58*, 2481–2495.
- [5] a) Y. Takada, S. W. Foo, Y. Yamazaki, S. Saito, *RSC Adv.* **2014**, *4*, 50851–50857; b) S. W. Foo, Y. Takada, Y. Yamazaki, S. Saito, *Tetrahedron Lett.* **2013**, *54*, 4714–4720.
- [6] H. C. Brown, *Science* **1980**, *210*, 485–492.
- [7] a) W. Kuriyama, Y. Ino, O. Ogata, N. Sayo, T. Saito, *Adv. Synth. Catal.* **2010**, *352*, 92–96; b) M. B. Widegren, M. L. Clarke, *Org. Lett.* **2019**, *20*, 2654–2658.
- [8] a) F. M. A. Geilen, B. Engendahl, M. Hölscher, J. Klankermayer, W. Leitner, *J. Am. Chem. Soc.* **2011**, *133*, 14349–14358; b) T. vom Stein, M. Meuresch, D. Limper, M. Schmitz, M. Hölscher, J. Coetzee, D. J. Cole-Hamilton, J. Klankermayer, W. Leitner, *J. Am. Chem. Soc.* **2014**, *136*, 13217–13225; c) X. Cui, Y. Li, C. Topf, K. Junge, M. Beller, *Angew. Chem.*

- 2015**, *127*, 10742–10745; *Angew. Chem. Int. Ed.* **2015**, *54*, 10596–10599; d) F. M. A. Geilen, B. Engendahl, A. Harwardt, W. Marquardt, J. Klankermayer and W. Leitner, *Angew. Chem.* **2010**, *122*, 5642–5646; *Angew. Chem., Int. Ed.* **2010**, *49*, 5510–5514; e) A. Salvini, P. Frediani, C. Giannelli and L. Rosi, *J. Organomet. Chem.* **2005**, *690*, 371–382; f) A. Phanopoulos, A. J. P. White, N. J. Long, W. Miller, *ACS Catal.* **2015**, *5*, 2500–2512; g) L. Deng, B. Kang, U. Englert, J. Klankermayer and R. Palkovits, *ChemSusChem* **2016**, *9*, 177–180.
- [9] T. J. Korstanje, J. I. van der Vlugt, C. J. Elsevier, B. de Bruin, *Science* **2015**, *350*, 298–302.
- [10] a) M. Naruto, S. Saito, *Nat. Commun.* **2015**, *6*, 8140; b) Q. Lu, J. Song, M. Zhang, J. Wei, C. Li, *Dalton Trans.* **2018**, *47*, 2460–2469.
- [11] M. Naruto, S. Agrawal, K. Toda, S. Saito, *Sci. Rep.* **2017**, *7*, 3425.
- [12] a) S. Yoshioka, S. Saito, *Chem. Commun.* **2018**, *54*, 13319–13330; b) J. Pritchard, G. A. Filonenko, R. van Putten, E. J. M. Hensen, E. A. Pidko, *Chem. Soc. Rev.* **2015**, *44*, 3808–3833; c) P. A. Dub, T. Ikariya, *ACS Catal.* **2012**, *2*, 1718–1741.
- [13] a) K. Iida, T. Miura, J. Ando, S. Saito, *Org. Lett.* **2013**, *15*, 1436–1439; b) Y. Takada, M. Iida, K. Iida, T. Miura, S. Saito, *J. Org. Syn. Chem. Jpn.* **2016**, *74*, 1078–1089.
- [14] a) F. T. Jere, D. J. Miller, J. E. Jackson, *Org. Lett.* **2003**, *4*, 527–530; b) F. T. Jere, J. E. Jackson, D. J. Miller, *Ind. Eng. Chem. Res.* **2004**, *43*, 3297–3303; c) K. P. Pimparkar, D. J. Miller, J. E. Jackson, *Ind. Eng. Chem. Res.* **2008**, *47*, 7648–7653.
- [15] a) W. Mägerlein, C. Dreisbach, H. Hugl, M. K. Tse, M. Klawonn, S. Bhor, M. Beller, *Catal. Today* **2007**, *121*, 140–150.
- [16] a) M. Tamura, R. Tamura, Y. Takeda, Y. Nakagawa, K. Tomishige, *Chem. Commun.* **2014**, *50*, 6656–6659; b) M. Tamura, R. Tamura, Y. Takeda, Y. Nakagawa, K. Tomishige, *Chem. Eur. J.* **2015**, *21*, 3097–3107; c) T. Toyao, S. M. A. Hakim Siddiki, A. S. Touchy, W. Onodera, K. Kon, Y. Morita, T. Kamachi, K. Yoshizawa, K. Shimizu, *Chem. Eur. J.* **2017**, *23*, 1001–1006.
- [17] T. A. Stephenson, G. Wilkinson *J. Inorg. Nucl. Chem.* **1966**, *28*, 945–956.
- [18] a) C. A. Hunter, J. K. M. Sanders, *J. Am. Chem. Soc.* **1990**, *112*, 5525–5534; b) M. J. Tashkin, M. L. Waters, *J. Am. Chem. Soc.* **2002**, *124*, 1860–1861; c) E. A. Meyer, R. K. Castellano, F. Diederich, *Angew. Chem.* **2003**, *115*, 1244–1287; *Angew. Chem. Int. Ed.* **2003**, *42*, 1210–1250.
- [19] G. R. Desiraju, T. Steiner in *The Weak Hydrogen bond: In Structural Chemistry and Biology*, Oxford University Press, New York, **1999**.
- [20] a) L. Ackermann, *Chem. Rev.* **2011**, *111*, 1315–1345; b) P. B. Arockiam, C. Bruneau, P. H. Dixneuf, *Chem. Rev.* **2012**, *112*, 5879–5918.

- [21] S. P. Bruekelman, S. E. Leach, G. D. Meakins, M. D. Tirel, *J. Chem. Soc., Perkin Trans. I* **1984**, 2801–2807.
- [22] A. Goto, K. Otake, O. Kubo, Y. Sawama, T. Maegawa, H. Fujioka, *Chem. Eur. J.* **2012**, *18*, 11423–11432.
- [23] H.-C. Wu, S. A. Hamid, J.-Q. Yu, J. B. Spencer, *J. Am. Chem. Soc.* **2009**, *131*, 9604–9605.
- [24] M. L. Clarke, D. Ellis, K. L. Mason, A. G. Orpen, R. L. W. Pringle, D. A. Zaher, R. T. Baker, *Dalton Trans.* **2005**, 1294–1300.
- [25] L.-C. Yang, T. Ishida, T. Yamakawa, S. Shinoda, *J. mol. Catal. A: Chemical.* **1996**, *108*, 87–93.
- [26] a) N. N. B. Kumar, O. A. Mukhina, A. G. Kutateladze, *J. Am. Chem. Soc.* **2013**, *135*, 9608–9611; b) C. D’Silva, D. A. Walker, *J. Org. Chem.* **1998**, *63*, 6715–6718.
- [27] X. M. Ji, M. Q. Zhao, Y. Zhang, X. Y. Zhang, Y. Lu, *J. Food Agric. Environ.* **2013**, *11*, 902–905.
- [28] E. Tokumaru, A. Tengeiji, T. Nakahara, I. Shiina, *Chem. Lett.* **2015**, *44*, 1768–1770.
- [29] F. Aydogan, M. Basarir, C. Yolacan, A. S. Demir, *Tetrahedron* **2007**, *63*, 9746–9750.
- [30] M. T. Valahovic, W. H. Myers, W. D. Harman, *Organometallics* **2002**, *21*, 4581–4589.
- [31] S. Zhang, J. Yu, H. Li, D. Mao, G. Lu, *Sci. Rep.* **2016**, *6*, 33196.
- [32] M. Googman, J. Zhang, P. Gantzel, E. Benedetti, *Tetrahedron Lett.* **1998**, *39*, 9589–9592.
- [33] D. Quiroga, L. D. Becerra, J. Sadat-Bernal, N. Vargas, E. Coy-Barrera, *Molecules* **2016**, *21*, 1349–1356.

Chapter 3.

Reaction of H₂ with Mitochondria-Relevant Metabolites Using a Multifunctional Molecular Catalyst

Abstract: The Krebs cycle is the fuel/energy source for cellular activity, and therefore of paramount importance for oxygen-based life. The cycle occurs in the mitochondrial matrix, where it produces and transfers electrons to generate energy-rich NADH and FADH₂, as well as C₄-, C₅-, and C₆-polycarboxylic acids as energy-poor metabolites. These metabolites are bio-renewable resources that represent potential sustainable carbon feedstocks, provided that carbon–hydrogen bonds are restored to these molecules. In the present study, these polycarboxylic acids and other mitochondria-relevant metabolites underwent dehydration (alcohol-to-olefin and/or dehydrative cyclization) and reduction (hydrogenation and hydrogenolysis) to diols or triols upon reaction with H₂, catalyzed by sterically confined iridium-bipyridyl complexes. The investigation of these single-metal-site catalysts provides valuable molecular insights into the development of molecular technologies for the reduction and dehydration of highly functionalized carbon resources.

3.1. Introduction

The recent depletion of fossil fuel resources has impelled industrial and academic researchers to search for alternative carbon-based energy sources. Considerable effort has been invested in biotechnology and sustainable/green technologies to develop a chemical industry in which renewable energy resources complement dwindling fossil fuel sources for the new millennium. A round-table discussion of the US Department of Energy (DOE) identified the top 30 value-added chemicals derived from biomass, which included various (poly)carboxylic acids and polyols.^[1] These chemicals exist in high oxidation and/or highly oxygenated states, and thus, current state-of-the-art oxidation catalysts must be substantially modified in order to achieve the reduction and dehydration of such bio-renewable resources.^[2,3]

The top 30 value-added chemicals re-evaluated were further narrowed to a top 12 list, in which the highest value-added carboxylic acid (CA) is succinic acid (SucA).^[4,5] Succinic acid has been produced in conventional petrochemical or coal industry, mainly from acetylene, butane, or 1,4-butadiene, and hydrogenated to 1,4-butanediol (1,4-BDO) using heterogeneous catalysts.^[5] In particular, the eight-hydrogen-atom (or 8e)-reduced, doubly dehydrated form of succinic acid, 1,4-BDO, is a highly versatile synthetic intermediate. 1,4-BDO is an important commodity chemical used to manufacture over 2.5 million tons of valuable polymers per year, including poly(butylene) terephthalate and poly(urethane)s.^[6] Yet, reports dealing with the selective reduction of succinic acid to 1,4-BDO using molecular catalysis are still limited,^[5,7-9] particularly those reporting systematic trial-and-error investigations. Various patents and scientific articles on the topic of heterogeneous catalysts for the hydrogenation of succinic acid have reported that numerous reaction parameters influence the product distribution;^[5,10] thus, the development of more sophisticated catalysts is required to control the product yields.

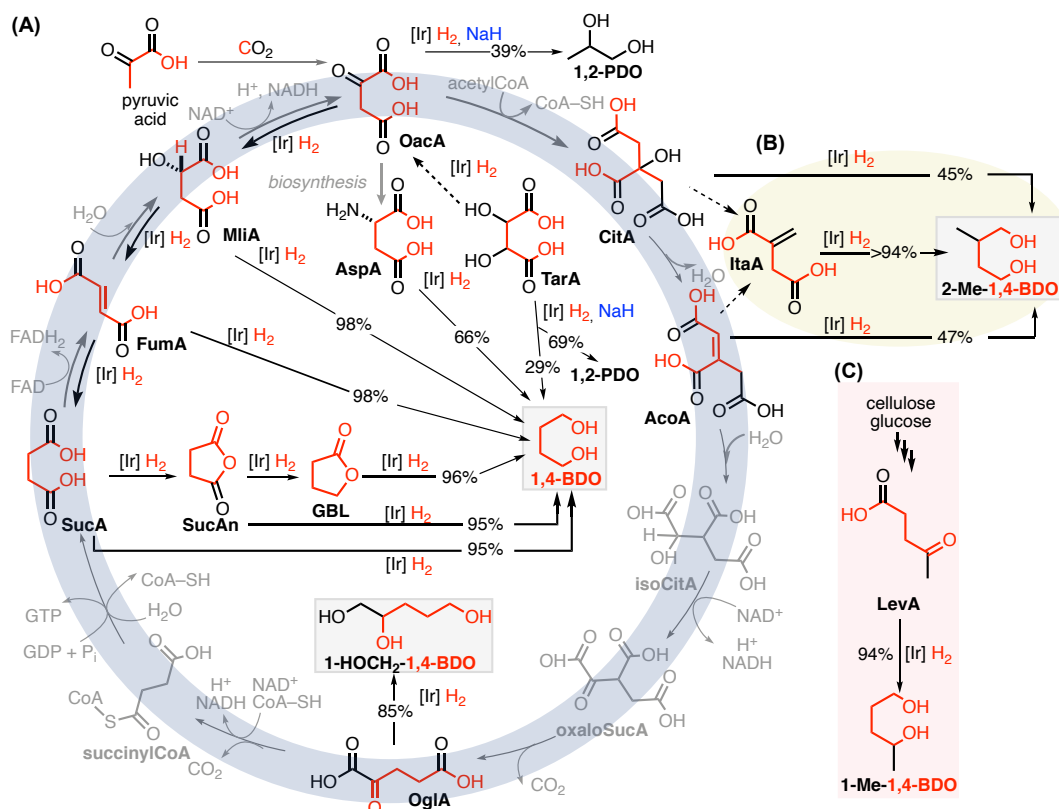


Figure 1 | Redrawing the map for the chemical transformation of Krebs-cycle-relevant metabolites. (A) Single-[Ir]-site-catalyzed hydrogenation and dehydration reactions in this work (black arrows and red text), and the original Krebs cycle (blue ring and gray text/arrows). Dotted arrows are proposed partial pathways in the hydrogenation of each substrate with Ir-a. (B) Hydrogenation of cytoplasm metabolites (pale green ellipse). (C) Hydrogenation of the sugar-derived artificial feedstock LevA. IsoCitA, oxaloSucA, and succinylCoA are rarely available.

In addition to succinic acid, significant attention should be paid to the reduction and dehydration of more highly functionalized C_4 -, C_5 -, and C_6 -polycarboxylic acids (PCAs, including dicarboxylic acids (DCAs) and tricarboxylic acids (TCAs)), such as fumaric acid (FumA),^[11] malic acid (MliA),^[12] oxaloacetic acid (OacA),^[13] 2-oxoglutaric acid (OglA),^[14] aconitic acid (AcoA),^[15] and citric acid (CitA),^[16] which are potential carbon feedstocks produced as metabolites in the Krebs cycle^[17] (also known as the tricarboxylic acid (TCA) cycle or citric acid cycle) (Figures 1A and 2A), which operates in the mitochondrial matrix in the cells of most plants, animals, fungi, and many bacteria. Further biotechnological modification of this energy-yielding metabolic pathway could enable the scalable production of C_4 -, C_5 -, and C_6 -PCAs, which can be expected to be upgraded subsequently using catalysts that

effectively reduce and dehydrate these compounds (the goal of this research). The Krebs cycle is mainly controlled by oxidation and hydration (with decarboxylation) reactions of various enzymes. The hydrogen (electron)-trapping cofactors NAD⁺ and FAD⁺ are involved in controlling the product distribution across different C₄-, C₅-, and C₆-PCAs. If an artificial catalyst was able to reverse the natural Krebs cycle (written formally in a clockwise fashion in Figure 1A) by promoting the usually unfavorable reduction (hydrogenation) and dehydration [hydrogenolysis/hydrodeoxygenation (HDO)]:^[18,19] reactions in an anti-clockwise fashion, diverse functionalized C₄-, C₅-, and C₆-metabolites could be transformed into a family of energy-rich polyols without recruiting natural enzymes. In this context, the development of novel, robust, and unidirectional catalysts, i.e., catalysts that promote hydrogenations and dehydrations while they suppress the reverse processes, represents a great challenge, since the highly oxygenated or nitrogenated substrates abundant in nature can easily poison catalytically active sites via substrate/product inhibition, and the reverse dehydrogenation reaction sometimes occurs, particularly at high temperature. Unfortunately, however, systematic studies to establish a molecular rationale and molecularly predictable approaches to obtain high productivity and selectivity in divergent reduction/dehydration reactions of PCAs all the way to different polyol products remain elusive.

As part of our ongoing interest in developing new molecular technologies for the catalytic reduction and/or dehydration of organic compounds in high oxidation states,^[20] peptides and plastics,^[21,22] monocarboxylic acids (MCA) including fatty acids and α -amino acids,^[23–26] bioalcohols,^[27] and CO₂,^[28] we introduce here the coordinatively saturated (PNNP)iridium (Ir) complex **Ir-a** (Figure 2). **Ir-a** is a novel, versatile, and robust precatalyst, whose multifunctional, sterically confined Ir-bipyridyl (bpy) framework can promote various dehydration and hydrogenation processes in a one-pot fashion; the apparent cleavage of C–O and C–N σ bonds under concomitant decarboxylation to induce HDO and even hydrodeamination (HDA) reactions is followed by the hydrogenation of various C=C and C=O bonds of ketones, acid anhydrides, and esters, which affords C₃, C₄, and C₅ polyols (Figure 2A). The catalytic framework generated upon addition of n H₂ ($n = 1–6$) to **Ir-a** maintains its structural robustness, with no detachment of the ligand from the Ir center or C–P bond cleavage.^[21] Thus, the complex retains good catalytic activity even under strenuous conditions (hydrogen pressure (P_{H_2}): 4–8 MPa; reaction temperature (T): 140–200 °C; reaction time (t): 18–120 h). The single catalytic active site of this bespoke Ir–bpy framework is sterically protected by four cyclohexyl (Cy) groups; the small size of the active pocket favors the selective uptake, coordination, and activation of H₂ (Figure 2B, left). The confined environment of the single-metal-site also protects the catalyst from deactivation via bidentate coordination by the relatively large

functional groups of the highly oxygenated and nitrogenated compounds, and even from monodentate coordination to the virtually coordinatively saturated Ir center.

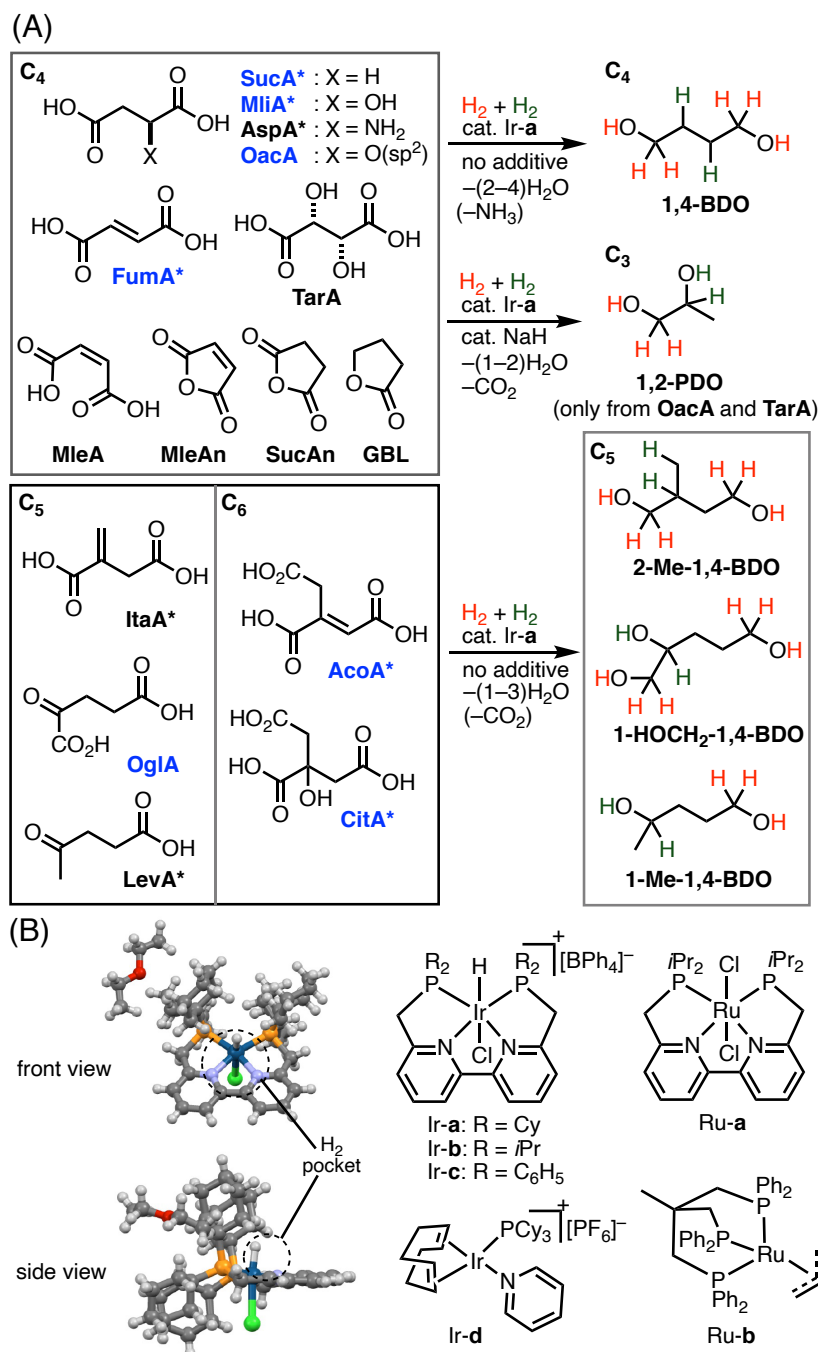


Figure 2 | Summary of this work. (A) Renewable carbon feedstocks that afford various 1,4-butanediol (1,4-BDO) derivatives and 1,2-propanediol (1,2-PDO). Compound names in blue are Krebs cycle metabolites, while those marked with asterisks are possible feedstocks listed as top 30 value-added chemicals in the initial DOE/NREL report in 2004.^[1] Succinic acid (SucA), malic acid (MliA), aspartic acid (AspA), oxaloacetic acid (OacA), tartaric acid (TarA), fumaric acid (FumA), maleic acid (MleA), maleic anhydride (MleAn), succinic anhydride (SucAn), γ -butyrolactone (GBL), itaconic acid (ItaA), 2-oxoglutaric acid (OglA), levulinic acid

(LevA), aconitic acid (AcoA), and citric acid (CitA). (B) Single-crystal x-ray diffraction structure of Ir-**a** (left; Et₂O included). Color key: Ir (blue), N (purple), P (orange), Cl (green), O (red), H (white). [BPh₄]⁻ is omitted for clarity. Ir- and Ru complexes for hydrogenation tested in this work (right).

3.2. Results and Discussion

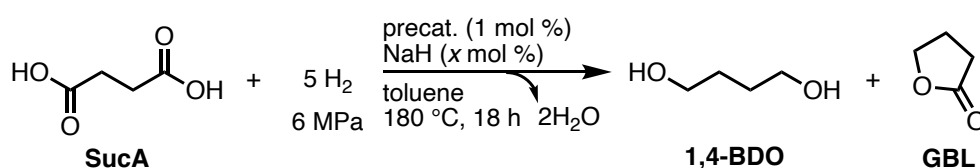
3.2.1. Reaction of H₂ with C₄-DCAs and their anhydrides.

We have recently reported that the (PNNP)ruthenium (Ru) complex Ru-**a** (Figure 2B, right) serves as a molecular precatalyst for the hydrogenation of unactivated amides, including polymer nylons.^[21] However, Ru-**a** (1 mol %) was ineffective for the hydrogenation of succinic acid to 1,4-BDO (Table 1, entry 1) under the reaction conditions used for amide hydrogenation (NaH (10 mol %); P_{H_2} = 6 MPa; T = 180 °C), and only γ -butyrolactone (GBL) was produced in 21% yield. We then screened different metal centers with different tetradentate PNNP ligands in the presence of a catalytic amount of NaH (6 mol %) for the hydrogenation of succinic acid, and found that iridium (Ir) complex Ir-**a** (1 mol %) was the most effective to furnish 1,4-BDO in 95% yield. The state-of-the-art Ir-complex Ir-**d** (Crabtree complex^[29]) was also tested (Table 1, entry 5), albeit that it showed, similar to the water-soluble Vaska complex, merely scant activity, producing only GBL.^[5]

The intended role of NaH was to remove a methylene (CH₂PCy₂) hydrogen atom from Ir-**a** to promote the dearomatization of a bipyridyl (bpy) fragment.^[21,22,30–33] This step may be followed by the full hydrogenation of the bpy framework under strenuous conditions; Ru-**a** undergoes such deprotonation and hydrogenation in the presence of NaH.^[21,22] However, after numerous control experiments for the hydrogenation of succinic acid with Ir-**a** (1.5 mol %), we found that a comparable hydrogenation of succinic acid occurs even *without NaH*, which generates 1,4-BDO in 86±8% yield (average of six runs) (Table 2, entry 1). A mercury test revealed that the reduction of succinic acid occurred by homogeneous catalysis, as there was no significant difference in the amount of 1,4-BDO in the presence of Hg (0.22 M). Ir-**a** derivatives Ir-**b** and Ir-**c**, which bear similar PNNP ligands with different steric demands, showed comparable or lower catalytic activity (Table 2, entries 2 and 3). The groups of Leitner and Klankermayer as well as that of Frediani have previously reported that Ru–Triphos ((Ph₂PCH₂)₃CMe) catalyzes the hydrogenation of succinic acid under harsh conditions.^[7,8] Therefore, we retested Ru-Triphos complex Ru-**b** in both the presence and absence of NaH (Table 1, entries 2 and 3), and found that its catalytic activity (1,4-BDO: 75–90%) was comparable to that of Ir-**a**. Both the P_{H_2} and T values are critical for the production of the desired product 1,4-BDO; GBL was formed exclusively in good to moderate yield at lower temperatures (160 °C, 79% yield) or at lower P_{H_2} (4 MPa, 58% yield). GBL was hydrogenated almost quantitatively to 1,4-BDO by Ir-**a** within 4 h at 180 °C (Table 2, entry 13). Capitalizing on the versatility of Ir-**a**, the dehydrogenated forms of succinic acid, i.e., fumaric acid and its *Z*-isomer maleic acid, were also hydrogenated smoothly to give 1,4-BDO in near quantitative

yield (Table 2, entries 4 and 5). The anhydrides of succinic acid (SucAn) and maleic acid (MleAn) were also hydrogenated to exclusively produce 1,4-BDO (Table 2, entries 11 and 12), although the hydrogenation of maleic anhydride was somewhat sluggish ($t = 18$ h: 35%; $t = 42$ h: 88%; $t = 66$ h: 91%). All control experiments suggest that the hydrogenation of fumaric acid to 1,4-BDO follows the pathway fumaric acid → succinic acid → succinic anhydride → GBL → 1,4-BDO.

Table 1 | Hydrogenation of SucA with different Ir- and Ru complexes.



entry	precat.	NaH x (mol %)	1,4-BDO yield (%) ^b	GBL yield (%) ^b
1 ^{b,d}	Ru-a	10	nd ^c	21
2	Ru-b	6	75	3
3	Ru-b	0	90	3
4	Ir-a	6	95	5
5 ^{b,d}	Ir-d	6	nd ^c	19

^aUnless otherwise specified, the reactions were carried out using precat.:SucA:NaH = 1:100:0–10 mol % in toluene for 18 h, starting with $P_{\text{H}_2} = 6$ MPa at 25 °C. ^bOf ¹H NMR (DMSO-*d*₆) based on internal standard. ^cNot detected by ¹H NMR. ^dDetermined by GC.

Table 2 | Hydrogenation of C₄-feedstocks with Ir-a, Ir-b, and Ir-c.

$$\text{C}_4 \text{ feedstock} + \text{H}_2 \xrightarrow[\text{180 } ^\circ\text{C, } t \text{ (h)}]{\text{Ir-a (1.5 mol \%), toluene, 6 MPa}} \text{HO-CH}_2\text{-CH}_2\text{-CH}_2\text{-CH}_2\text{-OH}$$

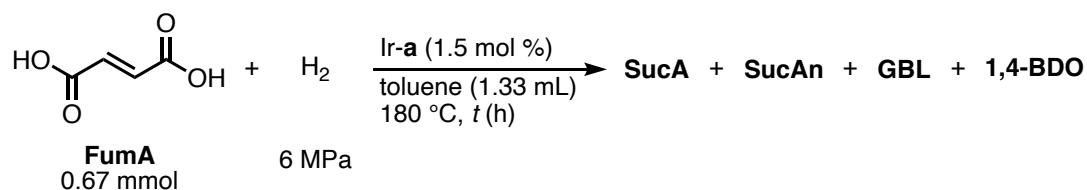
1,4-BDO

entry	C ₄ feedstock	<i>t</i> (h)	1,4-BDO yield (%) ^b	GBL yield (%) ^b
1	SucA	18, 42	86±8 ^h , 91	5±2 ^h , 2
2 ^c	SucA	18	44	41
3 ^d	SucA	18	81	2
4	FumA	18, 42	81, 98	3, 2
5	MleA	18, 42	80, 97	16, 3
6	MliA	42	98	2
7 ^e	AspA	66	66	4
8	TarA	90	29(36) ^g	– ⁱ
9 ^f	TarA	90	14(69) ^g	– ⁱ
10 ^f	OacA	24	~1(38) ^g	– ⁱ
11	MleAn	18, 42, 66	35, 88, 91	28, 2, 3
12	SucAn	4, 8	7, 95	62, 2
13	GBL	4	96	– ⁱ

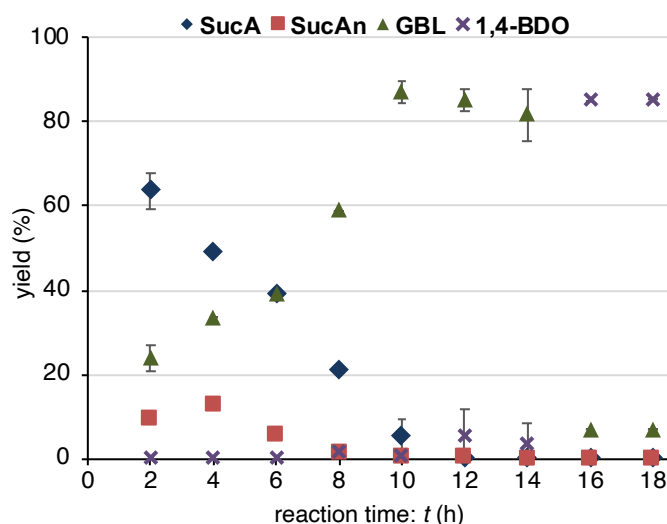
^aUnless otherwise specified, the reactions were carried out using Ir-a:feedstock = 1.5:100 mol % in toluene, starting with P_{H_2} = 6 MPa at 25 °C. ^bOf ¹H NMR (DMSO-*d*₆), based on internal standard. ^cIr-b. ^dIr-c. ^e2-Pyrrolidone (12%) byproduced. ^fNaH (9 mol %) was used. ^gOf yield of 1,2-PDO. ^hAverage of 6 runs. ⁱNot detected.

We then determined the time–conversion profile during the Ir-**a** (1.5 mol %)-promoted hydrogenation of fumaric acid ($P_{H_2} = 6$ MPa; $T = 180$ °C; $t = 0$ –18 h) and plotted the changes in the product distribution as a function of time (Table 3). Fumaric acid was rapidly hydrogenated to succinic acid (2e reduction: $t < 1$ h), which was consistently detected over the first 12 h of reaction. The conversion of succinic acid to GBL was slow (t : 10–12 h), while the concentration of succinic anhydride was negligible until $t = 18$ h, which suggests that succinic anhydride, once formed, was rapidly hydrogenated to GBL (4e reduction), even in the presence of succinic acid, which provided slightly acidic conditions. Interestingly, the subsequent hydrogenation of GBL to 1,4-BDO (4e reduction) did not begin until succinic acid had completely disappeared ($t = \sim 14$ h). Upon complete consumption of succinic acid, the hydrogenation of GBL commenced suddenly, and was completed within 2 h. It can thus be concluded that the catalyst for the hydrogenation of succinic anhydride is alive, but that for GBL is not generated or resting in an inactive form, under acidic conditions provided by the inherent acidity of succinic acid. Unlike significant effects of a base additive observed on ester/lactone hydrogenation by a Ru- or cobalt-pincer complex,^[32,33] base is not necessarily needed for the hydrogenation in the present system. During the overall reaction to produce 1,4-BDO from fumaric acid (fumaric acid \rightarrow succinic acid \rightarrow succinic anhydride \rightarrow GBL \rightarrow 1,4-BDO), the slowest reaction step was the dehydrative cyclization of succinic acid to succinic anhydride, which required ca. 12 h. A similar time profile of the product distribution was observed under the relatively basic conditions provided by the combined use of Ir-**a** and NaH (1.5:9 mol %) (Table 4), except that the complete conversion of succinic acid to succinic anhydride was faster (ca. 10 h vs. 14 h w/o NaH (*vide supra*)) and the hydrogenation of GBL to 1,4-BDO was slower (ca. 6 h vs. 2 h w/o NaH (*vide supra*)).

Table 3 | Time-conversion (yield) plots of the hydrogenation of FumA with Ir-a (1.5 mol %) w/o NaH.

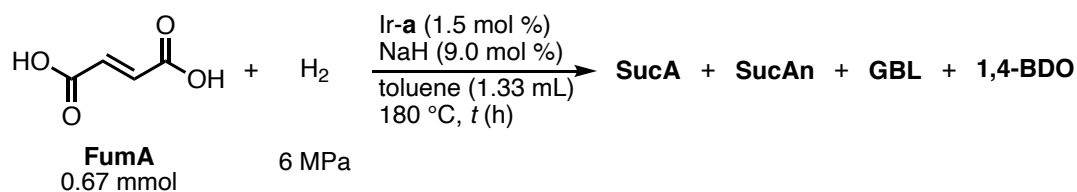


entry	t (h)	yield (%)			
		SucA	SucAn	GBL	1,4-BDO
1	2	64±5 ^a (56) ^b	10±1 ^a (9) ^b	24±3 ^a (30) ^b	nd ^d
2 ^c	4	49	13	34	nd ^d
3 ^c	6	39	6	39	nd ^d
4 ^c	8	21	1	59	<6 ^f
5	10	5±4 ^a (3) ^b	trace ^a (0) ^b	87±3 ^a (83) ^b	trace ^a (0) ^b
6	12	0 ^a (0) ^b	trace ^a (0) ^b	85±3 ^a (82) ^b	5±7 ^a (8) ^b
7	14	0 ^a (<1) ^b	0 ^a (0) ^b	82±6 ^a (80) ^b	3±5 ^a (4) ^b
8 ^c	16	0	0	7	85
9	18	0 ^d (0) ^e	0 ^d (0) ^e	7 ^d (13) ^e	85 ^d (81) ^e

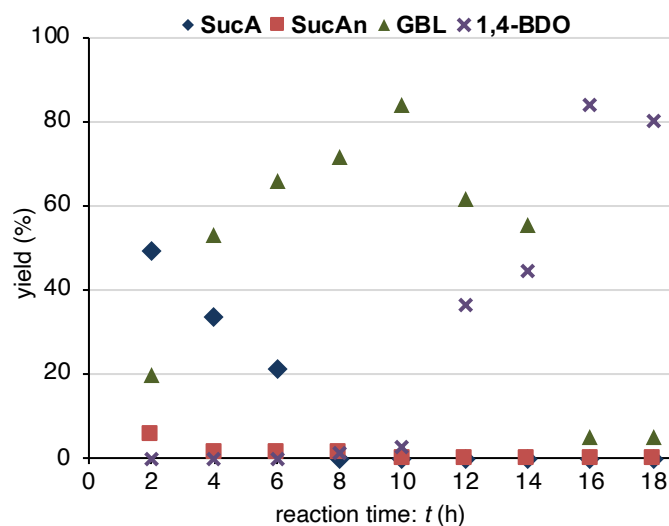


Unless otherwise specified, the reactions were carried out in a Teflon[®] tube with Ir-a:FumA (mol %) = 1.5:100, [Ir-a]₀ = 7.5 mM, [FumA]₀ = 0.50 M, P_{H₂} = 6 MPa, T = 180 °C, and t = 2–18 h. Yields were determined by ¹H NMR (DMSO-*d*₆) and GC-MS analyses based on the integral ratio of the signals of products and internal standard (mesitylene). ^aAverage ¹H NMR yield of 3 runs with standard deviation. ^bAverage GC yield of 2 runs. ^c¹H NMR yield of 1 run. ^dAverage ¹H NMR yield of 2 runs. ^eGC yield of 1 run.

Table 4 | The time profile of the change in product distribution in hydrogenation of FumA in the presence of NaH.



entry	<i>t</i> (h)	yield (%)			
		SucA	SucAn	GBL	1,4-BDO
1	2	49	6	20	0
2	4	34	1	53	0
3	6	21	1	66	0
4	8	21	1	71	1
5	10	0	0	84	3
6	12	0	0	62	36
7	14	0	0	55	45
8	16	0	0	<5	84
9	18	0	0	<5	80



Unless otherwise specified, the reactions were carried out in a Teflon[®] tube with Ir-a:NaH:FumA (mol %) = 1.5:9.0:100, [Ir-a]₀ = 7.5 mM, [FumA]₀ = 0.50 M, P_{H₂} = 6 MPa, T = 180 °C, and t = 2–18 h. Yields were determined by ¹H NMR (DMSO-*d*₆) based on the integral ratio of the signals of products and internal standard (mesitylene).

3.2.2. Reaction of H₂ with more functionalized C₄-DCAs.

Subsequently, we investigated the hydrogenation of malic acid, aspartic acid (AspA), and tartaric acid (TarA), i.e., functionalized C₄-DCAs. Malic acid is a Krebs cycle metabolite;^[12,17] aspartic acid is biosynthesized by the transamination of oxaloacetic acid (OacA: Krebs cycle metabolite) via enzymatic processes involving aspartase.^[34] Tartaric acid can be produced from vitamin C (L-ascorbic acid; or from 5-oxo-D-gluconic acid) by scalable fermentation.^[35] Since Ru-**b** showed catalytic activity similar to that of Ir-**a** for the hydrogenation of succinic acid (*vide supra*), the hydrogenation of these C₄-DCAs using catalytic amounts of Ru-**b** was examined ($P_{\text{H}_2} = 6 \text{ MPa}$; $T = 180 \text{ }^\circ\text{C}$, $t = 18\text{--}90 \text{ h}$) (Table 5). Malic acid was hydrogenated to 1,4-BDO; the yield was found to be the same ($70 \pm 1\%$) at $t = 18 \text{ h}$ and 42 h . This result suggests that the Ru-**b**-derived catalyst is relatively vulnerable and deactivated within 18 h, while the Ir-**a**-derived catalyst continues to show good activity thereafter (1,4-BDO: 63% for $t = 18 \text{ h}$; 98% for $t = 42 \text{ h}$). When aspartic acid and tartaric acid were hydrogenated using Ru-**b**, the yield of 1,4-BDO was marginal in both cases ($\sim 4\%$), probably due to substrate inhibition of the catalyst. In sharp contrast, the Ir-**a**-derived catalyst is more robust and maintains its activity during the hydrogenation of malic acid, aspartic acid, and tartaric acid, to furnish 1,4-BDO in 98%, 66%, and 29% yield, respectively (Table 2, entries 6–8; Tables 5 and 6; see also proposed multistep HDO/HDA and hydrogenation sequences: Figures 3–5). In contrast, 1,2-propanediol (1,2-PDO: 36%) is the main product formed from tartaric acid. When NaH (9 mol %) was used for the preactivation of Ir-**a**, 1,2-propanediol and 1,4-BDO were produced in higher (69%) and lower yield (14%), respectively (Table 2, entry 9; Table 7). Thus, the complex reaction pathway for the formation of 1,2-propanediol with 1,4-BDO as a side product may involve the dehydration of tartaric acid to oxaloacetic acid as a common process, followed by two distinct multistep sequences to generate either 1,2-propanediol or 1,4-BDO (Figure 5). Indeed, when the potential intermediate oxaloacetic acid, which is the starting compound in the Krebs cycle, was hydrogenated, 1,2-propanediol (38%) was detected, while the formation of 1,4-BDO was negligible ($\sim 1\%$) (Table 2, entry 10). The decarboxylation of oxaloacetic acid that leads to pyruvic acid was much faster than the hydrogenation of the ketone. The sequence of dehydration and decarboxylation of tartaric acid giving pyruvic acid was promoted previously by a sub-stoichiometric amount of KHSO₄ at 210–220 °C.^[36] The long-lived catalytic activity of Ir-**a** in the hydrogenation of the three C₄-DCAs is probably due to the almost exhaustive coordinative saturation and steric confinement of the Ir center, which provide structural robustness to the Ir-**a**-derived catalyst. These electronic and steric features prevent substrate/product inhibition of the catalyst, namely, deactivation of the catalyst by the highly

functionalized substrates malic acid, aspartic acid, and tartaric acid, which are probably able to more tightly ligate the coordinatively less saturated Ru center of Ru-**b** through bidentate chelation.

Table 5 | Hydrogenation of MliA, AspA, and TarA using Ir-a**, Ru-**b**, and Re(5 wt %)/TiO₂.**

C4 feedstock + H₂ $\xrightarrow[\text{180 } ^\circ\text{C, } t(\text{h})]{\text{precat. (1.5 mol \%), \text{toluene (1.33-3.0 mL)}}}$ HO-CH₂-CH₂-CH₂-CH₂-OH + GBL + 2-PY + 1,2-PDO

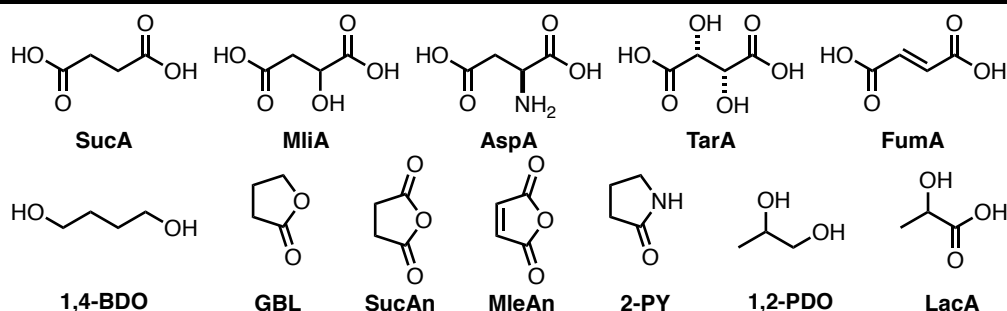
0.67 mmol 6 MPa **1,4-BDO** **GBL** **2-PY** **1,2-PDO**

entry	C4 feedstock	precat.	<i>t</i> (h)	yield (%)				
				1,4-BDO	GBL	2-PY	1,2-PDO	THF
1		Ir-a	18	63	24	–	0	–
2			42	98	2	–	0	–
3		Ru-b	18	71	2	–	5	–
4			42	69	2	–	6	–
5 ^a		Re/TiO ₂ (1.5 mol % Re)	42	20	46	–	1	33
6		Ir-a	66	66	4	12	–	–
7		Ru-b	66	1	trace	trace	–	–
8 ^a		Re/TiO ₂ (1.5 mol % Re)	66	–	–	–	–	<1
9		Ir-a	90	29	–	–	36	–
10		Ru-b	90	5	trace	–	18	–
11 ^a		Re/TiO ₂ (1.5 mol % Re)	90	1	55	–	<1	9

Unless otherwise specified, the reactions were carried out in a Pyrex glass (for MliA and AspA) or Teflon[®] tube (for TarA) with precat.:C4 feedstock (mol %) = 1.5:100, *P*_{H₂} = 6 MPa, *T* = 180 °C, and *t* = 18–90 h ([pre-cat.]₀ = 7.5 mM; [substrate]₀ = 0.50 M; in toluene). Yields were determined by ¹H NMR (DMSO-*d*₆) based on the integral ratio of the signals of products and internal standard (mesitylene). ^aYields were determined by GC-MS analysis.

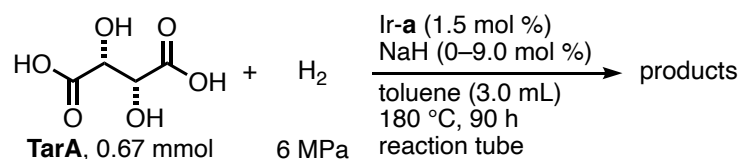
Table 6 | Control experiments for hydrogenation of MliA, AspA, and TarA using Ir-a.

entry	substrate	+	H ₂	or	Ar	Ir-a (0 or 1.5 mol %)	products
	0.67 mmol		6 MPa		1 atm	toluene (3 mL) 180 °C, <i>t</i> (h)	
entry	substrate	atmosphere	reaction tube	Ir-a (mol %)	<i>t</i> (h)	products (yields in %)	
1		H ₂ (6MPa)	Teflon	1.5		1,4-BDO (98), GBL (2)	
2		H ₂ (6MPa)	glass	1.5		1,4-BDO (80), GBL (5)	
3	MliA	H ₂ (6MPa)	Teflon	0	42	FumA (85), SucA (2), SucAn (2)	
4		H ₂ (6MPa)	glass	0		FumA (87), SucA (3), SucAn (2), MleAn (1)	
5		Ar (1 atm)	glass	1.5		FumA (33), SucA (<3), SucAn (0.4), MleAn (42)	
6		Ar (1 atm)	glass	0		FumA (71), MleAn (9)	
7		H ₂ (6MPa)	Teflon	1.5		1,4-BDO (42), GBL (1), 2-PY (14)	
8		H ₂ (6MPa)	glass	1.5		1,4-BDO (66), GBL (4), 2-PY (12)	
9	AspA	H ₂ (6MPa)	Teflon	0	66	1,4-BDO (<1), GBL (1), FumA (<1)	
10		H ₂ (6MPa)	glass	0		FumA (<1)	
11		Ar (1 atm)	glass	1.5		no major product	
12		H ₂ (6MPa)	Teflon	1.5		1,4-BDO (29), GBL (<1), 1,2-PDO (36), LacA (<1)	
13		H ₂ (6MPa)	glass	1.5		1,4-BDO (2), GBL (1), 1,2-PDO (6)	
14	TarA	H ₂ (6MPa)	Teflon	0	90	GBL (2), LacA (5)	
15		H ₂ (6MPa)	glass	0		LacA (6), SucA (<1), SucAn (<1), FumA (<1)	
16		Ar (1 atm)	Teflon	1.5		LacA (8), SucAn (<1), FumA (<1)	
17		Ar (1 atm)	glass	1.5		LacA (7), SucAn (<1)	

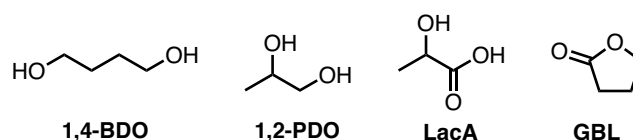


Unless otherwise specified, the reactions were carried out in a Teflon[®] or glass tube with Ir-a:substrate (mol %) = 0–1.5:100, P_{H_2} = 6 MPa or P_{Ar} = 1 atm, T = 180 °C, and t = 42–90 h ([Ir-a]₀ = 0–3.3 mM; [substrate]₀ = 0.22 M; in toluene). Yields were determined by ¹H NMR (DMSO-*d*₆) based on the integral ratio of the signals of products and internal standard (mesitylene).

Table 7 | Hydrogenation of TarA using Ir-a under various conditions.



entry	NaH (mol %)	reaction tube	products (yields in %)
1	0	glass	1,4-BDO (2), GBL (1), 1,2-PDO (6)
2	0	Teflon	1,4-BDO (29), GBL (<1), 1,2-PDO (36), LacA (<1)
3	9.0	Teflon	1,4-BDO (14), 1,2-PDO (69)



Unless otherwise specified, the reactions were carried out in a Pyrex glass or Teflon[®] tube with Ir-a:NaH:TarA (mol %) = 1.5:0–9.0:100, P_{H_2} = 6 MPa, T = 180 °C, and t = 90 h ($[Ir-a]_0$ = 3.3 mM; $[TarA]_0$ = 0.22 M; in toluene). Yields were determined by 1H NMR ($DMSO-d_6$) based on the integral ratio of the signals of products and internal standard (mesitylene).

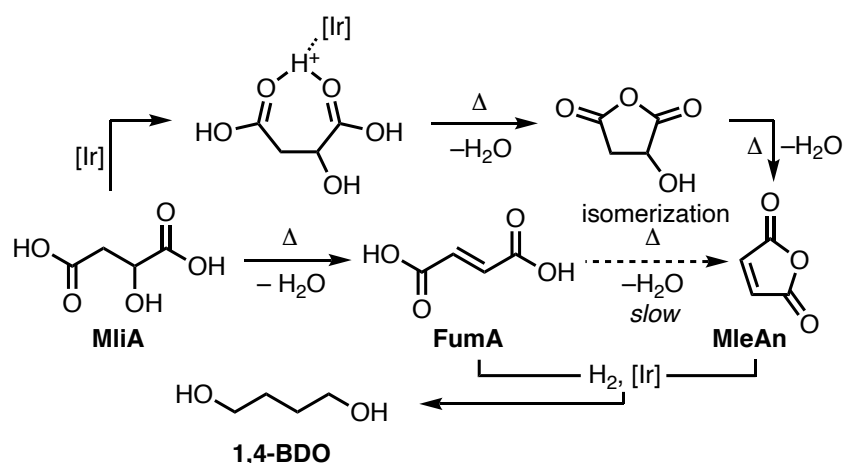


Figure 3 | Possible reaction pathway from MliA to 1,4-BDO. For control experiments for hydrogenation of MliA, see Table 6.

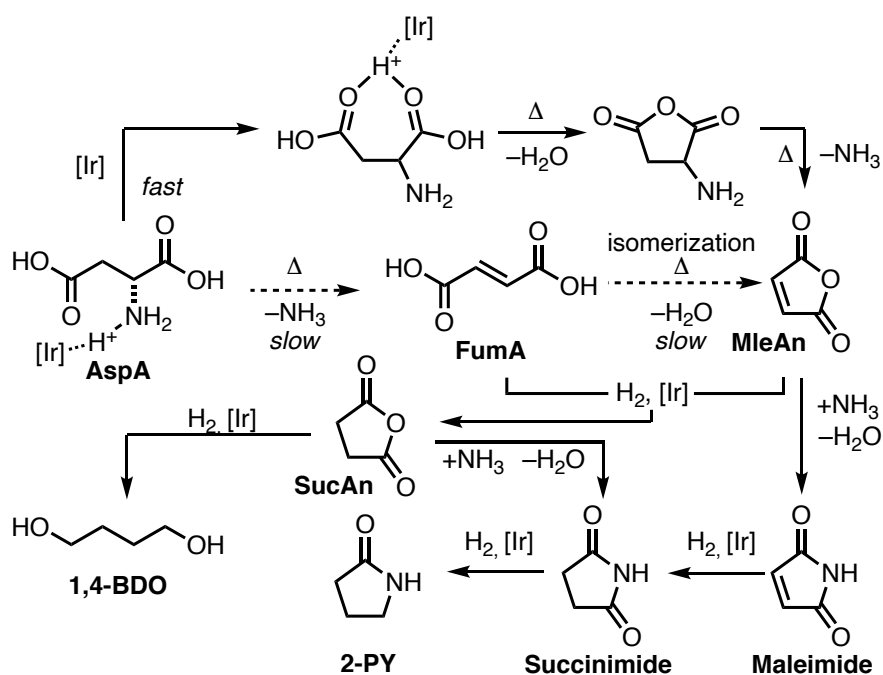


Figure 4 | Possible reaction pathway from AspA to 1,4-BDO. For control experiments for hydrogenation of AspA, see Table 6.

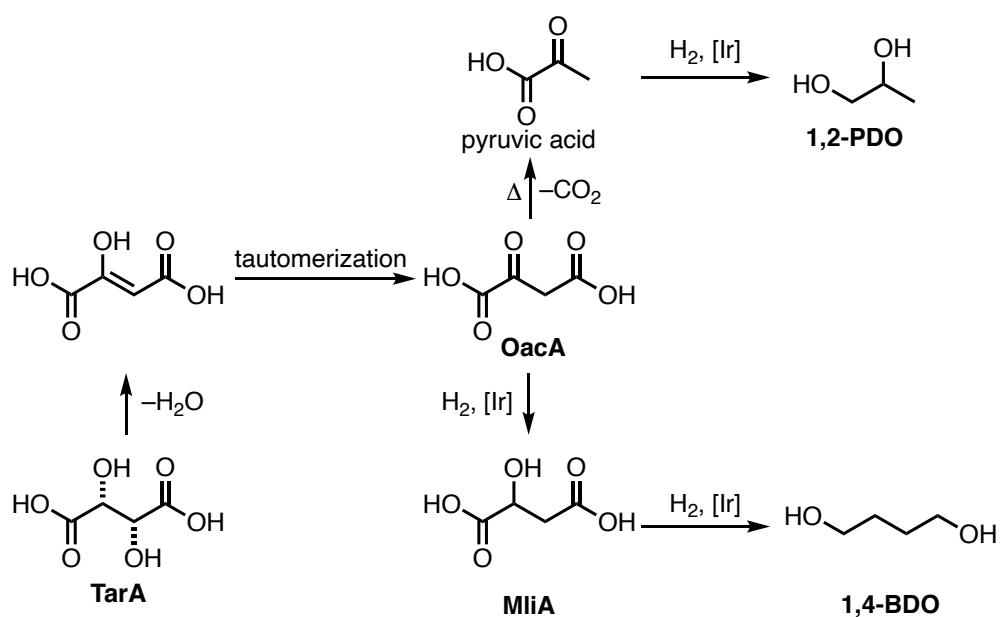


Figure 5 | Possible reaction pathway from TarA to 1,2-PDO and 1,4-BDO. For control experiments for hydrogenation of TarA, see Table 6.

3.2.3. Reaction of H₂ with C₅- and C₆-PCA.

2-Oxoglutaric acid (OglA) and itaconic acid (ItaA) are C₅-DCAs; the former is a Krebs cycle metabolite,^[14,17] while the latter can be fermentatively biosynthesized in the cytoplasm through the *cis*-aconitic acid-decarboxylase-catalyzed decarboxylation of *cis*-aconitic acid (a C₆ acid involved in the Krebs cycle), which is released from the mitochondria.^[37] Both DCAs undergo hydrogenation using H₂ and Ir-**a**, to furnish 1-(HOCH₂)-1,4-BDO in 85% yield (isolated yield: 78%) and 2-Me-1,4-BDO in >94% yield, respectively (Table 8, entries 1 and 4). 1-(HOCH₂)-1,4-BDO (pentane-1,2,5-triol) has been produced from furfural or furfuryl alcohol in different ways.^[38] Itaconic acid has previously been hydrogenated to 2-Me-1,4-BDO using a Ru–Triphos catalyst.^[39] Citric acid and aconitic acid are C₆-TCA metabolites in the Krebs cycle,^[17] and their fermentation has previously been investigated.^[15,16] Although the time required was relatively long (120 h) in both cases, the diol 2-Me-1,4-BDO was obtained uniformly in 45–47% yield (Table 8, entries 2 and 3). The dehydration of citric acid may give *cis*- and/or *trans*-aconitic acid, which is transformed into itaconic acid upon decarboxylation. The subsequent hydrogenation of itaconic acid affords 2-Me-1,4-BDO (Figure 2A).

Table 8 | Hydrogenation of C₅ and C₆ feedstocks with Ir-a**.**

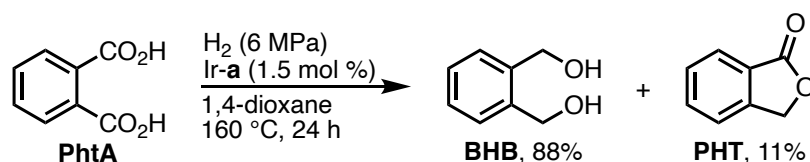
C5 or C6 feedstock		+	H ₂	$\xrightarrow[\text{toluene}]{\text{Ir-a (1.5 mol %)}}\rightarrow$	1,4-BDO derivative	
			6 MPa	180 °C, t (h)		
entry	C5 or C6 feedstock	t (h)	main product		1,4-BDO deriv. yield (%) ^b	GBL deriv. yield (%) ^b
1	OglA	72	1-HOCH₂-1,4-BDO		85(78) ^c	nd ^d
2	AcoA	120	2-Me-1,4-BDO		47(42) ^c	nd ^d
3	CitA	120	2-Me-1,4-BDO		45(32) ^c	nd ^d
4 ^e	ItaA	72	2-Me-1,4-BDO		>94	<6 ^f
5	LevA	18	1-Me-1,4-BDO		94	6

^aUnless otherwise specified, the reactions were carried out using Ir-**a**:feedstock = 1.5:100 mol % in toluene, starting with P_{H_2} = 6 MPa at 25 °C. ^bOf ¹H NMR (DMSO-*d*₆), based on internal standard. ^cOf isolated, purified product. ^dNot determined. ^e1,4-dioxane instead of toluene. ^f2-Me- (<2%) and 3-Me-GBL (<2%).

3.2.4. Reaction of H₂ with miscellaneous DCAs and MCAs.

Phthalic acid (PhtA) is a 1,4-DCA formed via the hydration of phthalic anhydride, which is a commodity chemical. Phthalic acid is an aromatic CA, and its CO₂H group is generally more inert to hydrogenation than that of aliphatic CAs.^[8,39,40] In addition, phthalic acid is difficult to hydrogenate to 1,2-bis(1,2-hydroxymethyl)benzene (BHB). Instead, phthalic acid tends to undergo dearomatic hydrogenation when heterogeneous catalysts are used.^[40] Even using a Ru-Triphos catalyst (1.5 mol %; P_{H₂} = 8.5 MPa),^[41] its ester, dimethyl phthalate, is preferentially hydrogenated to phthalide (PHT); only under specifically arranged strongly acidic conditions is BHB (78%) the major product.^[41] Neither homogeneous nor heterogeneous catalysts have achieved the selective 8e-reduction/dehydration of the two adjacent CO₂H groups on the benzene ring in more than marginal yield. However, the selective hydrogenation of phthalic acid to BHB using Ir-**a** was successful when 1,4-dioxane was used as the solvent, giving BHB in 88% yield (11% PHT) (Eq. 1, Table 9 for control experiments using BHB as a substrate). Reducing the reaction temperature from 160 °C to 140 °C under otherwise identical conditions quantitatively furnished PHT (98%).

Levulinic acid (LevA) is an important C₅-MCA that can be produced artificially from glucose/cellulose with promising scalability.^[42] Levulinic acid also undergoes hydrogenation using H₂ and Ir-**a** to give 1-Me-1,4-BDO (Figure 2A) in 94% yield (Table 8, entry 5). A Ru-Triphos catalyst showed similar reactivity.^[39]



Eq. 1 | Hydrogenation of phthalic acid with Ir-**a**.

Table 9 | Control experiments using BHB as a substrate.

BHB, 0.67 mmol		6 MPa	1 atm			BHB	PHT
entry	solvent (3 mL)	atmosphere	<i>T</i> (°C)	Ir- a (mol %)	recovery (%) BHB	yield (%) PHT	
1		H ₂ (6 MPa)	180	1.5	50	51	
2		H ₂ (6 MPa)	180	0	100	0	
3	toluene	H ₂ (6 MPa)	180	1.5	24	75	
4		H ₂ (6 MPa)	180	1.5	4	94	
5		Ar (1 atm)	180	1.5	0.1	98	
6	1,4-dioxane	H ₂ (6 MPa)	180	1.5	57	44	
7		H ₂ (6 MPa)	160	1.5	90	10	

Unless otherwise specified, the reactions were carried out in a Pyrex glass tube with Ir-**a**:BHB (mol %) = 0–1.5:100, P_{H_2} = 6 MPa or P_{Ar} = 1 atm, T = 160–180 °C, and t = 24 h ($[\text{Ir-}\mathbf{a}]_0$ = 0–3.3 mM; $[\text{BHB}]_0$ = 0.22 M; in solvent). Yields were determined by ¹H NMR (CDCl₃) based on the integral ratio of the signals of products and internal standard (mesitylene).

3.2.5. Molecular insights into the behavior of the single-active-site catalyst.

Unlike with the deprotonation at the CH₂PiPr₂ moiety of Ru-**a**, which is facilitated when NaH is used, Ir-**a** seems to undergo spontaneous tautomerization upon heating in the absence of an alkali base. Indeed, when a CH₃OD/THF-*d*₈ solution of Ir-**a** was heated, the four hydrogen atoms of the two methylene units and the Ir–H were all replaced with deuterium atoms (Figure 6A; Figures S1–S4). The smooth H–D exchange at the methylene units is owing to thermal deprotonation and dearomatization, unlike the previous system where a base additive is needed for deprotonation.^[32,33] In contrast, that occurred on the Ir center under mild conditions was tentatively assigned to the hydricity–proticity interchange that occurs in parallel to Ir(III)–Ir(I) interconversion under near-neutral conditions. Similar H–D exchange has also been observed in a D₂O solution of a Cp*IrH(bpy) complex, but only under relatively acidic conditions (pD = 2.4–6.4).^[43]

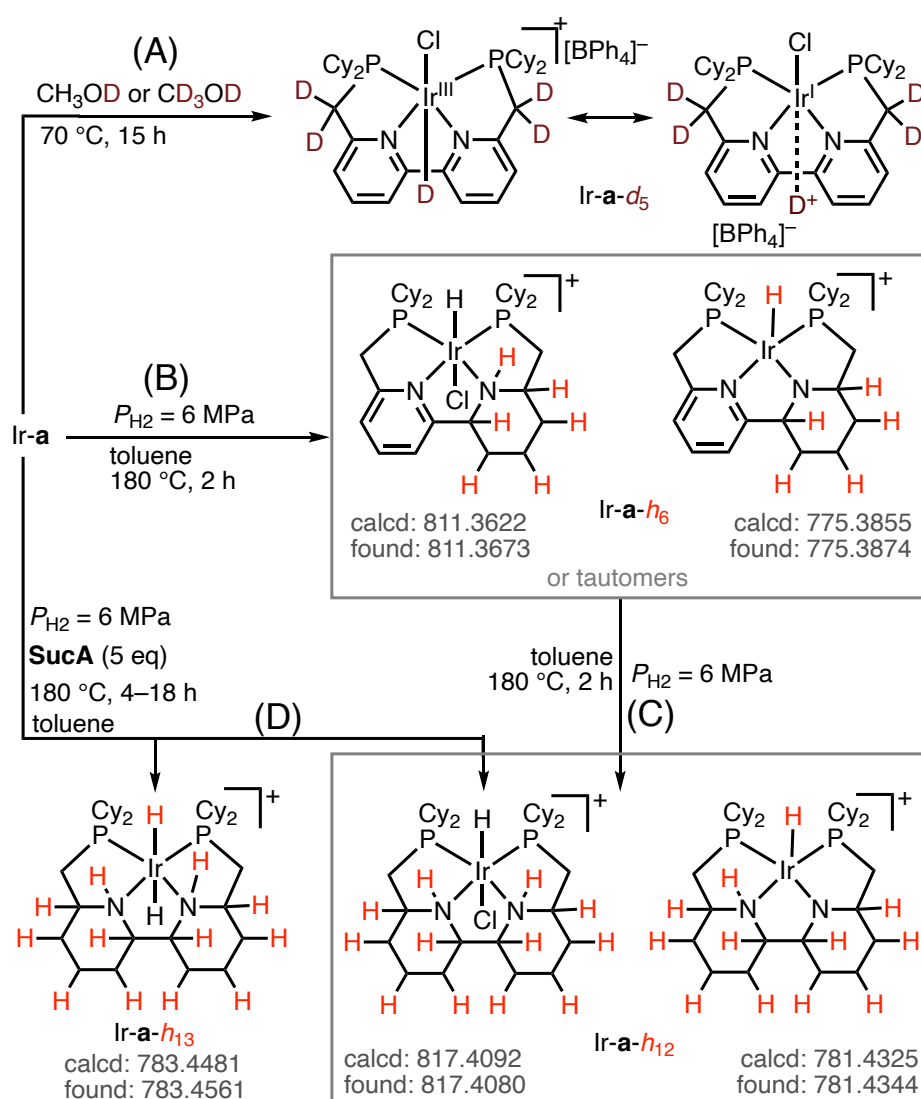
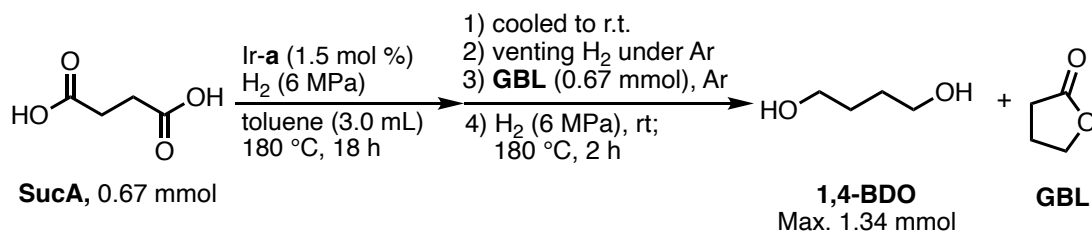


Figure 6 | Representative H/D exchange and structural interconversion of Ir-a under different reaction conditions. (A) Heating in deuterated alcohols without H₂. (B) Shorter heating with H₂. (C) Prolonged heating with H₂. (D) Prolonged heating in the presence of a DCA with H₂. The values below each compound represent theoretical and experimental ESI-MS values.

The facile tautomerization of Ir-**a**, which could lead to the dearomatization of the dipyridyl fragment, suggests that the hydrogenation of bpy might occur in the presence of H₂. To verify this hypothesis, in addition to testing the structural robustness of the resting state of the catalyst derived from Ir-**a**, Ir-**a** was activated under the conditions used for the hydrogenation, and the resulting samples were subjected to electron spray ionization-mass spectrometry (ESI-MS) measurements (Figures S5–S8). When Ir-**a** was preactivated for 2 h in the absence of succinic acid, the mass spectra indicated that Ir-**a**-*h*₆ was the main intermediate (Figure 6B), accompanied by the minor species Ir-**a**-*h*₁₂ (Figure 6C). The partial hydrogenation of bpy was detected. In contrast, heating the sample for an additional 2 h gave Ir-**a**-*h*₁₂ as the major product. Unlike in the case of Ru-**a**,^[21] however, the C–P bonds of Ir-**a** were not cleaved during these processes. When the preactivation of Ir-**a** was carried out in the presence of excess succinic acid, succinic acid was completely consumed, and Ir-**a**-*h*₁₂ (Figure 6D; ¹H NMR (ppm): δ –23.1 (1H, t, *J* = 16.1 Hz, ClIrH) and Ir-**a**-*h*₁₃ (Figure 6D; ¹H NMR (ppm): δ –9.29 (2H, t, *J* = 13.8 Hz, IrH₂) were the two major products observed, with the C–P bonds acting again as spectators. The species that catalyzes the hydrogenation would be produced via the incorporation of multiple hydrogen atoms into Ir-**a**.

It is highly likely that the Ir center of the catalyst is virtually coordinatively saturated between two apical ligands in *trans* configuration. The robustness of the catalyst is further demonstrated by the control experiment: after the hydrogenation of succinic acid for 18 h, the catalyst even promoted effective hydrogenation of a second portion of GBL in one-pot operation (Table 10). It could thus be feasibly concluded that two of the hydrogen atoms on the catalytic species “H(δ⁻)–Ir–N–H(δ⁺)”^[44] are transferred directly onto olefins and the carbonyl groups of esters, anhydrides, and ketones; however, an alternative proton transfer pathway from the C–H bonds^[31,45] of the Ir catalyst cannot be ruled out at this point. To the best of our knowledge, this is the first time that the Noyori-type bifunctional mechanism^[44–48] has been experimentally invoked in the hydrogenation of carboxylic acid anhydrides, assuming that the *trans* configuration of the induced (PNNP)Ir catalyst would be preserved from the precatalyst Ir-**a**. It is worth mentioning that the groups of Khaskin and Gusev have recently reported the catalytic mechanism of the Milstein bipyridyl complex RuH(CO)[PNN] gives a square-pyramidal Ru(II) product RuH(CO)[pPNN] (pPNN = piperidyl PNN) via hydrogenation of the dearomatized PNN ligand, which comprise substantive evidence indicating that the heteroaromatic fragments of the coordinated PN, PNN, and related polydentate ligands may be susceptible to hydrogenation under reducing conditions.^[56]

Table 10 | Sequential hydrogenation of different substrates in one-pot operation using Ir-a**: SucA used in a first timeframe and GBL in the second timeframe.**



entry	yield (%)	
	1,4-BDO	GBL
1	85 (1.14 mmol)	(0.055 mmol)

Unless otherwise specified, the reactions were carried out in a Pyrex glass tube with Ir-**a**:(SucA + GBL) (mol %) = 1.5:(100 + 100), P_{H_2} = 6 MPa, T = 180 °C, and t = 18 + 2 h ($[\text{Ir-}\mathbf{a}]_0$ = 3.3 mM; $[\text{SucA}]_0$ = 0.22 M; in toluene). Yields were determined by ¹H NMR (DMSO-*d*₆) based on the integral ratio of the signals of products and internal standard (mesitylene).

3.3. Conclusion

In summary, this work demonstrates that a bespoke, structurally robust Ir complex with a tetradentate PNNP ligand can achieve the hydrogenative deoxygenation/deamination of a variety of bio-renewable C₄–C₆ feedstocks. The conceptually new sterically confined Ir-bpy framework: (i) prefers the uptake of H₂ relative to that of highly functionalized organic compounds; (ii) promotes reduction (hydricity) and dehydration (proticity); (iii) retains the robust tetracoordinated organic–metal framework under strenuous hydrogenation conditions. This multifunctional, robust, single-active-site molecular catalyst can be used for the hydrogenation of polyacids to polyols as well as for hydrodeoxygenation (HDO) and hydrodeamination (HDA) reactions to give saturated carbon chains under weakly acidic conditions. The structural precatalyst/catalyst platform presented in this work could potentially be extended to develop more versatile catalysis for the hydrogenation and hydrogenolysis of thermodynamically stable and kinetically inert C–O and C–N single bonds as well as other unsaturated bonds; such studies are currently in progress in our laboratory.

3.4. Experimental section

3.4.1. Material.

Maleic anhydride (MleAn), DL-tartaric acid (TarA), 1,2-propanediol (1,2-PDO), diisopropylamine, chlorodiisopropylphosphine, lithium tetraphenylborate tris(1,2-dimethoxyethane), sodium tetraphenylborate, α,α,α -trifluorotoluene, phthalic anhydride (PhtAn), methan(ol-*d*), methanol-*d*₃, and tetrahydrofuran-*d*₈ were purchased from Aldrich Chemical Co. Acetonitrile (anhydrous), sodium sulfate, dichloromethane, THF (anhydrous), chlorodicyclohexylphosphine, dichloromethane (anhydrous), morpholine, methanol (anhydrous), ethanol, diethyl ether (anhydrous), toluene (anhydrous), chloroform, ethyl acetate, sodium hydride (NaH, 55% paraffin dispersion), *n*-BuLi (1.6 M in *n*-hexane solution), mesitylene, DMSO-*d*₆, methanol-*d*₄, Primepure[®] toluene (>99.9% purity), triethylamine, and Celite[®] were purchased from Kanto Chemicals, Ltd. Fumaric acid (FumA), L-aspartic acid (AspA), hexane (anhydrous), hexane, *p*-xylene, 1,4-dioxane (anhydrous), hexafluoro-2-propanol (anhydrous), chloroform-*d*, acetonitrile-*d*₃, γ -butyrolactone (GBL), Crabtree's catalyst (Ir-**d**), tetrafluoroboric acid, and mercury were purchased from FUJIFILM Wako Pure Chemical Corporation. Oxaloacetic acid (OacA), Maleic acid (MleA), DL-malic acid (MliA), chlorodiphenylphosphine, borane–tetrahydrofuran complex (8.5% in THF, ca. 0.9 mol/L), 2-methyltetrahydrofuran (2-Me-THF), cyclopentyl methyl ether (CPME), citric acid (CitA), *trans*-aconitic acid (AcoA), 2-oxoglutaric acid (OglA), phthalic acid (PhtA), 1,4-butanediol (1,4-BDO), 1,2-benzenedimethanol (BHB), acetic anhydride, and *N,N*-dimethyl-4-aminopyridine (DMAP) were purchased from Tokyo Chemical Industry CO., Ltd. Succinic acid (SucA), and succinic anhydride (SucAn) were purchased from Nacalai tesque. Chloro(1,5-cyclooctadiene)iridium(I) dimer was purchased from Furuya Metal Co., Ltd. Hydrogen gas (H₂) (99.99%) was purchased from Alpha system. These chemicals were used without further purification. Dichloro(6,6'-bis((dicyclohexylphosphino)methyl)-2,2'-bipyridine)–ruthenium (II) (Ru-**a**),^[21] [Ru(1,1,1-tris(diphenylphosphinomethyl)ethane)(tri-methylene methane)] (Ru-**b**),^[8] 6,6'-bi-2-picoline,^[52] 6,6'-bis((dicyclohexylphosphino)methyl)-2,2'-bipyridine–diborane complex,^[21] and 6,6'-bis((diisopropylphosphino)methyl)-2,2'-bipyridine–diborane complex^[21] were prepared according to the corresponding reported procedures. An active Re(5 wt %)/TiO₂ was prepared and provided by Dr. T. Toyao and Prof. K. Shimizu at Hokkaido University, Japan according to the reported procedure.^[49]

3.4.2. General methods.

All experiments were performed under an inert gas atmosphere unless otherwise noted. ¹H NMR spectra were measured on JEOL ECA-600 (600 MHz) or JEOL ECA-500 (500 MHz) at ambient temperature unless otherwise noted. Data were recorded as follows: chemical shift in ppm from internal tetramethylsilane (δ 0 ppm) or residual peak of DMSO-*d*₆ (δ 2.50 ppm), multiplicity (br = broad, s = singlet, d = doublet, t = triplet, quint = quintet, m = multiplet, dd = doublet of doublets, td = triplet of doublets, dt = doublet of triplets, dq = doublet of quartets), coupling constant (Hz), integration, and assignment. ¹³C{¹H} NMR spectra were measured on JEOL ECA-600 (150 MHz) or JEOL ECA-500 (126 MHz) at ambient temperature. Chemical shifts were recorded in ppm from the solvent resonance employed as the internal standard (DMSO-*d*₆ at 39.52 ppm). ³¹P{¹H} NMR spectra were measured on JEOL ECA-600 (243 MHz) at ambient temperature. Chemical shifts were recorded in ppm from the solvent resonance as the external standard (phosphoric acid (85 wt % in H₂O) at 0.0 ppm). High-resolution mass spectra (HRMS) were obtained from BRUKER micrOTOF-QII (ESI) and JEOL JMS-T100GCV (EI). For thin-layer chromatography (TLC) analysis through this work, Merck precoated TLC plates (silica gel 60 GF254 0.25 mm) were used. The products were purified by preparative column chromatography on silica gel 60 (230–400 mesh; Merck).

GC-MS analysis was performed on Agilent 6850 series network GC system and Agilent 5975 series Mass Selective Detector (EI). The following conditions were used unless otherwise noted: [column: CYCLODEX-B (*l* = 30 m, *d* = 0.25 mm, film thickness = 0.25 μ m); chromatographic elution: 50–230 °C at a rate of 10 °C/min, isothermal at 230 °C for 2 min; carrier gas: He (1.0 mL/min, at 7.7 psi)]. Retention time of each compound is as following: 1,4-BDO (7.82 min), GBL (7.06 min), THF (2.12 min), succinic acid (10.0 min, detected as succinic anhydride), and succinic anhydride (10.0 min).

For isolation of the products, the reaction mixture was evaporated to dryness. To the resulting mixture methanol or THF was added to dissolve all. Purification was performed using column chromatography (SiO₂, MeOH/CH₂Cl₂ or CHCl₃/EtOAc) for 1,4-BDO (MeOH/CH₂Cl₂ = 1/6, *R_f* = 0.57), 1-HOCH₂-1,4-BDO (MeOH/CH₂Cl₂ = 1/8, *R_f* = 0.09), 1-Me-1,4-BDO (MeOH/CH₂Cl₂ = 1/8, *R_f* = 0.52), 2-Me-1,4-BDO (MeOH/CH₂Cl₂ = 1/8, *R_f* = 0.24), BHB (CHCl₃/EtOAc = 1/1, *R_f* = 0.36), PHT (CHCl₃/EtOAc = 1/1, *R_f* = 0.96) or distillation for GBL and 1,2-PDO. 1,2-PDO and 1,4-BDO were inseparable by distillation, probably due to azeotrope formation.

3.4.3. X-ray single crystal structural analysis of Ir-a

Single crystal of Ir-a suitable for X-ray single crystal analysis was obtained by slow diffusion of diethyl ether into a THF solution of Ir-a. Intensity data were collected at 123 K on a Rigaku Single Crystal CCD X-ray Diffractometer (Saturn 70 with MicroMax-007) with Mo K α radiation ($\lambda = 0.71075$ Å) and graphite monochromator. A total of 29170 reflections were measured at a maximum 2θ angle of 50.0°, of which 7937 were independent reflections ($R_{\text{int}} = 0.0498$). The structure was solved by direct methods (SHELXS-97) and refined by the full-matrix least-squares on F_2 (SHELXL-97). All non-hydrogen atoms were refined anisotropically. All hydrogen atoms were placed using AFIX instructions except for H1. The following crystal structure has been deposited at the Cambridge Crystallographic Data Centre and allocated the deposition number CCDC 1050122.

The crystal data are as follows: C₆₄H₈₅BClIrN₂OP₂; FW = 1198.74, crystal size 0.20 × 0.20 × 0.10 mm³, monoclinic, $P2_1/n$, $a = 15.065$ (3) Å, $b = 19.566$ (4) Å, $c = 20.867$ (4) Å, $\alpha = 90.00^\circ$, $\beta = 108.347$ (3)°, $\gamma = 90.00^\circ$, $V = 5838$ (2) Å³, $Z = 4$, $D_c = 1.364$ g cm⁻³. The refinement converged to $R_1 = 0.0715$, $wR_2 = 0.2148$ ($I > 2\sigma(I)$), GOF = 1.044.

3.4.4. Compound data of products

1,4-Butanediol (1,4-BDO):^[8] ¹H NMR (600 MHz, DMSO-*d*₆): δ 4.36 (t, $J = 5.4$ Hz, 2H), 3.39–3.36 (m, 4H), 1.40–1.44 (m, 4H); ¹³C{¹H} NMR (151 MHz, DMSO-*d*₆): δ 60.7, 29.2; HRMS (ESI, (M+Na)⁺) calcd for C₄H₁₀O₂Na⁺: 113.0573. Found: 113.0538.

γ -Butyrolactone (GBL):^[8] ¹H NMR (600 MHz, methanol-*d*₄): δ 4.34 (t, $J = 8.7$ Hz, 2H), 2.47 (t, $J = 9.6$ Hz, 2H), 2.26–2.20 (m, 2H).

1,2-Propanediol (1,2-PDO):^[8] ¹H NMR (600 MHz, methanol-*d*₄): δ 3.77–3.71 (m, 1H), 3.40 (d, $J = 9.5$ Hz, 2H), 1.12 (d, $J = 6.0$ Hz, 3H); ¹³C{¹H} NMR (151 MHz, methanol-*d*₄): δ 69.2, 68.6, 19.5.

1,2,5-Pentanetriol (1-HOCH₂-1,4-BDO): ¹H NMR (600 MHz, DMSO-*d*₆): δ 4.41 (t, $J = 5.9$ Hz, 1H), 4.37 (d, $J = 4.8$ Hz, 1H), 4.35 (t, $J = 5.2$ Hz, 1H), 3.40–3.36 (m, 3H), 3.27–3.20 (m, 2H), 1.55–1.50 (m, 1H), 1.48–1.38 (m, 2H), 1.23–1.16 (m, 1H); ¹³C{¹H} NMR (151 MHz, DMSO-*d*₆): δ 71.1, 66.0, 61.1, 30.0, 28.8; HRMS (ESI, (M+Na)⁺) calcd for C₅H₁₂O₃Na⁺: 143.0679. Found: 143.0666.

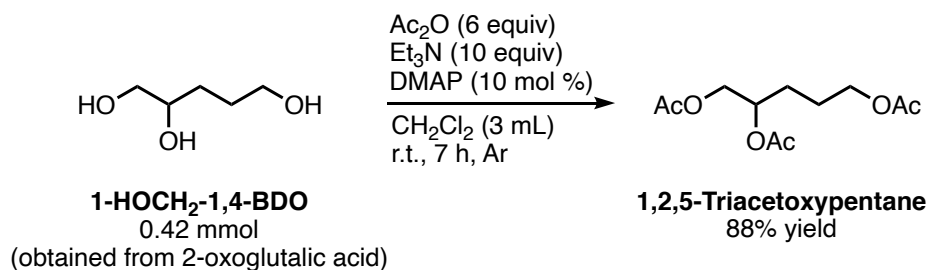
1,4-Pentanediol (1-Me-1,4-BDO):^[8] ¹H NMR (600 MHz, DMSO-*d*₆): δ 4.36 (t, *J* = 5.2 Hz, 1H), 4.34 (d, *J* = 4.8 Hz, 1H), 3.60–3.53 (m, 1H), 3.38–3.35 (m, 1H), 1.51–1.45 (m, 1H), 1.43–1.37 (m, 1H), 1.33–1.29 (m, 1H), 1.03 (d, *J* = 6.6 Hz, 3H); ¹³C{¹H} NMR (151 MHz, DMSO-*d*₆): δ 65.8, 61.0, 35.6, 29.0, 23.7; HRMS (ESI, (M+Na)⁺) calcd for C₅H₁₂O₂Na⁺: 127.0730. Found: 127.0706.

2-Methyl-1,4-butanediol (2-Me-1,4-BDO):^[53] ¹H NMR (500 MHz, DMSO-*d*₆): δ 4.40 (t, *J* = 5.4 Hz, 1H), 4.33 (t, *J* = 5.2 Hz, 1H), 3.47–3.37 (m, 2H), 3.27–3.23 (m, 1H), 3.19–3.15 (m, 1H), 1.64–1.56 (m, 1H), 1.55–1.48 (m, 1H), 1.20–1.13 (m, 1H), 0.82 (d, *J* = 6.9 Hz, 3H); ¹³C{¹H} NMR (126 MHz, DMSO-*d*₆): δ 66.4, 58.9, 36.4, 32.4, 16.9; HRMS (ESI, (M+Na)⁺) calcd for C₅H₁₂O₂Na⁺: 127.0730. Found: 127.0706.

1,2-Benzenedimethanol (BHB):^[54] ¹H NMR (600 MHz, CDCl₃): δ 7.33 (td, *J* = 9.5, 4.5 Hz, 4H), 4.70 (s, 4H), 3.21 (s, 2H); ¹³C{¹H} NMR (151 MHz, CDCl₃): δ 139.4, 129.7, 128.6, 64.2; HRMS (EI, (M+Na)⁺) calcd for C₈H₁₀O₂Na⁺: 161.0573. Found: 161.0646; Elemental analysis: calcd. C 69.55, H 7.30; found C 69.21, H 7.42.

Phthalide (PHT):^[55] ¹H NMR (600 MHz, CDCl₃): δ 7.93 (d, *J* = 7.8 Hz, 1H), 7.70 (td, *J* = 7.5, 1.2 Hz, 1H), 7.55 (td, *J* = 7.8, 0.6 Hz, 1H), 7.51 (dt, *J* = 7.8, 1.2 Hz, 1H), 5.34 (s, 2H); ¹³C{¹H} NMR (151 MHz, CDCl₃): δ 171.1, 146.5, 134.0, 129.1, 125.8, 125.8, 122.1, 69.7; HRMS (EI, M⁺) calcd for C₈H₆O₂⁺: 134.0362. Found: 134.0392; Elemental analysis: calcd. C 71.64, H 4.51; found C 71.42, H 4.46.

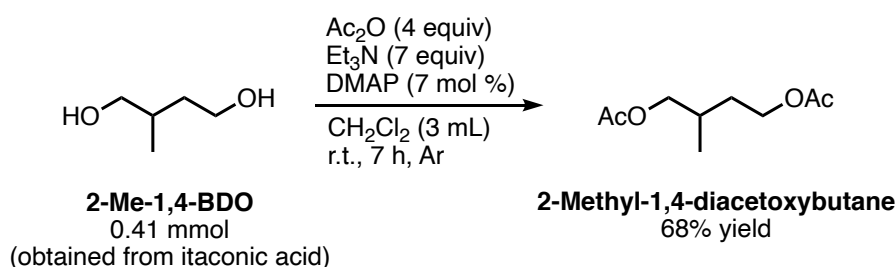
3.4.5. Acetylation of 1-HOCH₂-1,4-BDO obtained from the reaction of 2-oxoglutaric acid with Ir-a



The isolated **1-HOCH₂-1,4-BDO** (50 mg, 0.42 mmol) obtained by the hydrogenation of 2-oxoglutaric acid with Ir-a was treated with acetic anhydride (6 equiv, 2.52 mmol, 240 μL), triethylamine (10 equiv, 4.2 mmol, 580 μL), and DMAP (10 mol %, 0.042 mmol, 5.2 mg) in dichloromethane (3 mL) at room temperature under argon atmosphere. The mixture was stirred for 7 h at the same temperature. To the resulting mixture was added a 1 M aq hydrochloric acid.

After the mixture was extracted with dichloromethane, the organic layer was washed with water, and dried over sodium sulfate. After filtration of the mixture, evaporation of the filtrate solvents afforded **1,2,5-Triacetoxy-pentane** (90.6 mg, 0.37 mmol, 88% yield) as yellow oil. ¹H NMR (500 MHz, DMSO-*d*₆): δ 4.98 (quint, *J* = 7.0 Hz, 1H), 4.17 (dd, *J* = 12.1, 4.2 Hz, 1H), 4.02 (dd, *J* = 12.1, 5.8 Hz, 1H), 4.00–3.96 (m, 2H), 2.01 (s, 3H), 2.01 (s, 3H), 2.00 (s, 3H), 1.64–1.52 (m, 4H); ¹³C{¹H} NMR (126 MHz, DMSO-*d*₆): δ 170.4, 170.2, 170.0, 70.6, 64.4, 63.4, 26.6, 24.0, 20.7, 20.7, 20.5; HRMS (ESI, (M+Na)⁺) calcd for C₁₁H₁₈O₆Na⁺: 269.0996. Found: 269.1007.

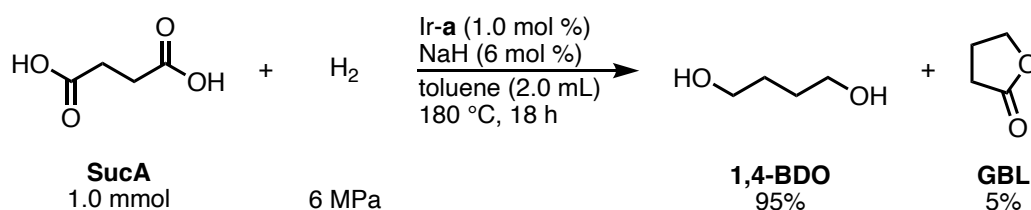
3.4.6. Acetylation of 2-Me-1,4-BDO obtained from the reaction of itaconic acid with Ir-a



The isolated **2-Me-1,4-BDO** (43 mg, 0.41 mmol) obtained by the hydrogenation of itaconic acid with Ir-a was treated with acetic anhydride (4 equiv, 1.6 mmol, 155 μL), triethylamine (7 equiv, 2.9 mmol, 400 μL), and DMAP (7 mol %, 0.029 mmol, 3.5 mg) in dichloromethane (3 mL) at room temperature under argon atmosphere. The mixture was stirred for 7 h at the same temperature. To the resulting mixture was added a 1 M aq hydrochloric acid. After the mixture was extracted with dichloromethane, the organic layer was washed with water, and dried over sodium sulfate. After filtration of the mixture, evaporation of the filtrate solvents afforded **2-Methyl-1,4-diacetoxybutane** (52.4 mg, 0.28 mmol, 68% yield) as yellow oil. ¹H NMR (500 MHz, DMSO-*d*₆): δ 4.09–4.00 (m, 2H), 3.87 (dq, *J* = 9.8, 6.3 Hz, 2H), 2.01 (s, 3H), 1.99 (s, 3H), 1.91–1.80 (m, 1H), 1.70–1.63 (m, 1H), 1.46–1.39 (m, 1H); ¹³C{¹H} NMR (126 MHz, DMSO-*d*₆): δ 170.9, 170.9, 68.7, 62.3, 32.2, 29.8, 21.2, 21.2, 16.9; HRMS (ESI, (M+Na)⁺) calcd for C₉H₁₆O₄Na⁺: 211.0941. Found: 211.0968.

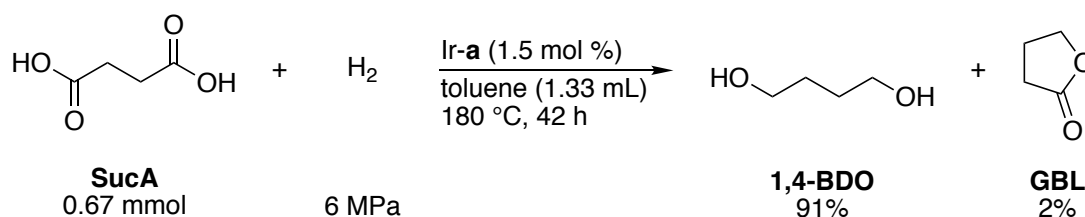
3.4.7. General procedures of hydrogenation experiments

Representative hydrogenation procedure with Ir-a and sodium hydride (NaH) (Table 1, entry 4)



Succinic acid (SucA) (118.1 mg, 1.0 mmol), Ir-a (10.9 mg, 0.01 mmol), sodium hydride (NaH, 55% paraffin dispersion, 2.6 mg, 0.06 mmol), and a magnetic stirring bar were placed in a dried Teflon[®] tube (21 mL capacity). The Teflon[®] tube was inserted into an autoclave, which was closed tightly, evaporated in vacuum, and refilled with Ar gas. To the mixture was added anhydrous toluene (2.0 mL) under a continuous flow of Ar, and inside the autoclave was purged with H₂ gas ($P_{\text{H}_2} = 1$ MPa). The autoclave was pressurized by H₂ gas ($P_{\text{H}_2} = 6$ MPa) at 25 °C, and heated at 180 °C for 18 h with stirring (800 rpm). The autoclave was cooled to 0 °C in an ice–water bath. The reaction mixture was concentrated under a reduced pressure (ca. 35 mmHg, 50 °C). The residue was diluted with DMSO-*d*₆, and analyzed by ¹H NMR. The yields of γ -butyrolactone (GBL) (5%) and 1,4-butanediol (1,4-BDO) (95%) were calculated based on the integral ratio among the signals of these compounds with respect to an internal standard (mesitylene).

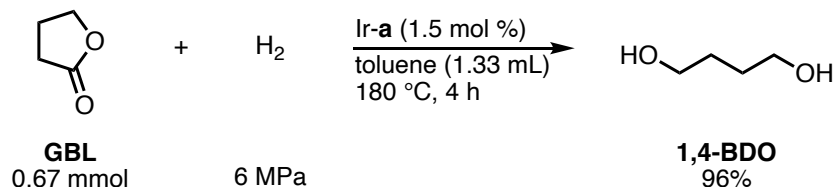
Representative procedure for the hydrogenation of 1,4-dicarboxylic acids: The reaction of SucA (Table 2, entry 1)



SucA (78.7 mg, 0.67 mmol), Ir-a (10.9 mg, 0.01 mmol), and a magnetic stirring bar were placed in a dried Teflon[®] tube (21 mL capacity). The Teflon[®] tube was inserted into an autoclave, which was closed tightly, evaporated in vacuum, and refilled with Ar gas. To the mixture was added anhydrous toluene (1.33 mL) under a continuous flow of Ar, and inside the autoclave was purged with H₂ gas ($P_{\text{H}_2} = 1$ MPa). The autoclave was pressurized by H₂ gas ($P_{\text{H}_2} = 6$ MPa) at 25 °C, and heated at 180 °C for 42 h with stirring (800 rpm). The autoclave was cooled to 0 °C in an ice–water bath. The reaction mixture was concentrated under a reduced pressure (ca. 35 mmHg, 50 °C). The residue was diluted with DMSO-*d*₆, and analyzed by ¹H

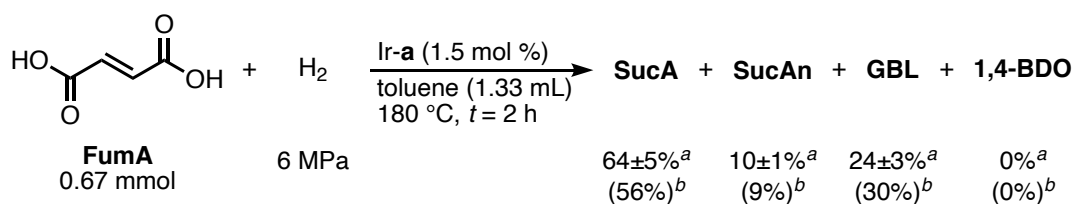
NMR. The yields of GBL (2%) and 1,4-BDO (91%) were calculated based on the integral ratio among the signals of these compounds with respect to an internal standard (mesitylene).

Representative procedure for the hydrogenation of GBL (Table 2, entry 13)



GBL (57.4 mg, 0.67 mmol), Ir-a (10.9 mg, 0.01 mmol), and a magnetic stirring bar were placed in a dried Teflon[®] tube (21 mL capacity). The Teflon[®] tube was inserted into an autoclave, which was closed tightly, evaporated in vacuum, and refilled with Ar gas. To the mixture was added anhydrous toluene (1.33 mL) under a continuous flow of Ar, and inside the autoclave was purged with H₂ gas ($P_{\text{H}_2} = 1$ MPa). The autoclave was pressurized by H₂ gas ($P_{\text{H}_2} = 6$ MPa) at 25 °C, and heated at 180 °C for 4 h with stirring (800 rpm). The autoclave was cooled to 0 °C in an ice–water bath. The reaction mixture was concentrated under a reduced pressure (ca. 35 mmHg, 50 °C). The residue was diluted with DMSO-*d*₆, and analyzed by ¹H NMR. The yield of 1,4-BDO (96%) was calculated based on the integral ratio among the signals of these compounds with respect to an internal standard (mesitylene).

Representative procedure for investigating time dependency on product distribution in hydrogenation of FumA using Ir-a (Table 3, entry 1)



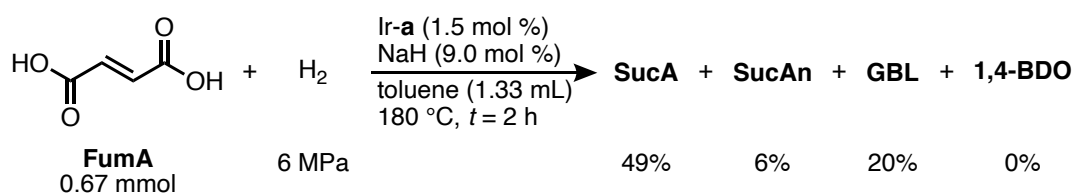
^a Average ¹H NMR yield of 3 runs with standard deviation.

^b Average GC yield of 2 runs.

FumA (77.4 mg, 0.67 mmol), Ir-a (10.9 mg, 0.01 mmol), and a magnetic stirring bar were placed in a dried Teflon[®] tube (21 mL capacity). The Teflon[®] tube was inserted into an autoclave, which was closed tightly, evaporated in vacuum, and refilled with Ar gas. To the mixture was added anhydrous toluene (1.33 mL) under a continuous flow of Ar, and inside the autoclave was purged with H₂ gas ($P_{\text{H}_2} = 1$ MPa). The autoclave was pressurized by H₂ gas ($P_{\text{H}_2} = 6$ MPa) at 25 °C, and heated at 180 °C for 2 h with stirring (800 rpm). The autoclave was cooled to 0 °C in an ice–water bath. After venting H₂ carefully, the reaction mixture was diluted with dehydrated MeOH (5 mL) with washing inside the autoclave, followed by

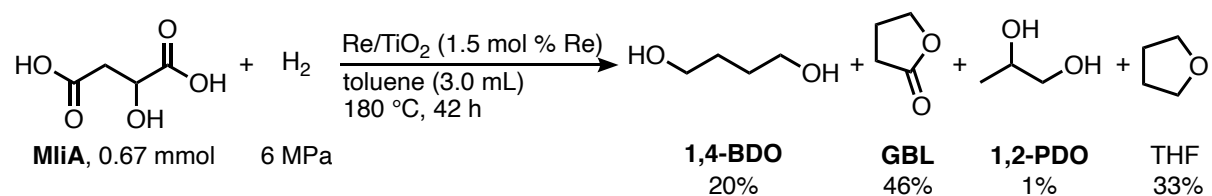
mesitylene (15 μL) was added, and analyzed by GC-MS. A part of the resulted mixture (ca. 0.25 mL) was transferred to an NMR tube containing DMSO-*d*₆ (ca. 0.25 mL), and analyzed by ¹H NMR (600 MHz). The yields of SucA, SucAn, GBL, and 1,4-BDO were calculated based on the integral ratio among the signals of these compounds with respect to an internal standard (mesitylene).

Representative procedure for investigating time dependency on product distribution in hydrogenation of FumA using Ir-a and NaH (Table 4, entry 1)



FumA (77.4 mg, 0.67 mmol), Ir-a (10.9 mg, 0.01 mmol), NaH (55% paraffin dispersion, 2.6 mg, 0.06 mmol), and a magnetic stirring bar were placed in a dried Teflon[®] tube (21 mL capacity). The Teflon[®] tube was inserted into an autoclave, which was closed tightly, evaporated in vacuum, and refilled with Ar gas. To the mixture was added anhydrous toluene (1.33 mL) under a continuous flow of Ar, and inside the autoclave was purged with H₂ gas (*P*_{H₂} = 1 MPa). The autoclave was pressurized by H₂ gas (*P*_{H₂} = 6 MPa) at 25 °C, and heated at 180 °C for 2 h with stirring (800 rpm). The autoclave was cooled to 0 °C in an ice–water bath. The reaction mixture was concentrated under a reduced pressure (ca. 35 mmHg, 50 °C). The residue was diluted with DMSO-*d*₆, and analyzed by ¹H NMR. The yields of SucA (49%), SucAn (6%), GBL (20%), and 1,4-BDO (0%) were calculated based on the integral ratio among the signals of these compounds with respect to an internal standard (mesitylene).

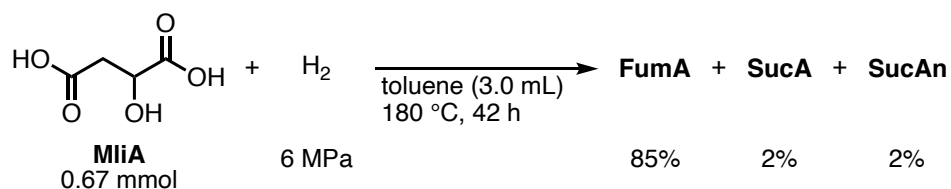
Representative procedure for the hydrogenation of MliA with Re/TiO₂ (Table 5, entry 5)



DL-Malic acid (MliA) (89.4 mg, 0.67 mmol) and a magnetic stirring bar were placed in a dried glass tube (21 mL capacity). The glass tube and an autoclave were introduced into an argon-atmosphere glovebox. To the glass tube was added Re(5 wt %)/TiO₂ (37 mg, 1.5 mol % Re), the the tube was inserted to the autoclave, which was closed tightly. The autoclave was taken out of the glovebox, then to it was added anhydrous toluene (3.0 mL) under a continuous flow of Ar, and inside the autoclave was purged with H₂ gas (*P*_{H₂} = 1 MPa). The autoclave was

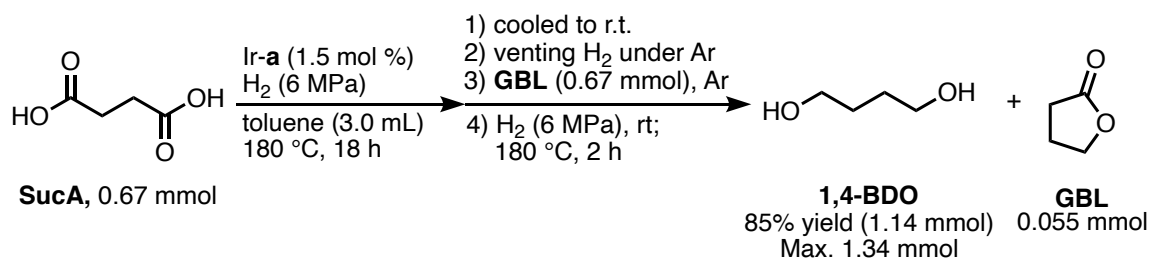
pressurized by H₂ gas ($P_{\text{H}_2} = 6$ MPa) at 25 °C, and heated at 180 °C for 42 h with stirring (500 rpm). The autoclave was cooled to 0 °C in an ice–water bath. After venting H₂ carefully, the reaction mixture was diluted with dehydrated MeOH (5 mL) with washing inside the autoclave, followed by mesitylene (15 μ L) was added. The resulted mixture was directly centrifuged (3500 rpm, 3 min). The supernate was obtained by decantation and analyzed by GC-MS. The yields of 1,4-BDO (20%), GBL (46%), 1,2-PDO (1%), and THF (33%) were calculated based on the integral ratio among the signals of these compounds with respect to an internal standard (mesitylene).

Representative procedure for the hydrogenation of functionalized 1,4-dicarboxylic acids without catalyst: The reaction of MliA (Table 6, entry 3)



DL-Malic acid (MliA) (89.4 mg, 0.67 mmol) and a magnetic stirring bar were placed in a dried Teflon[®] tube (21 mL capacity). The Teflon[®] tube was inserted into an autoclave, which was closed tightly, evaporated in vacuum, and refilled with Ar gas. To the mixture was added anhydrous toluene (3.0 mL) under a continuous flow of Ar, and inside the autoclave was purged with H₂ gas ($P_{\text{H}_2} = 1$ MPa). The autoclave was pressurized by H₂ gas ($P_{\text{H}_2} = 6$ MPa) at 25 °C, and heated at 180 °C for 42 h with stirring (500 rpm). The autoclave was cooled to 0 °C in an ice–water bath. The reaction mixture was concentrated under a reduced pressure (ca. 35 mmHg, 50 °C). The residue was diluted with DMSO-*d*₆, and analyzed by ¹H NMR. The yields of FumA (85%), SucA (2%), and SucAn (2%) were calculated based on the integral ratio among the signals of these compounds with respect to an internal standard (mesitylene).

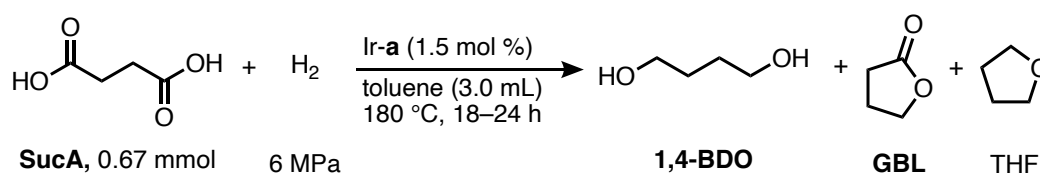
Procedure for the sequential reaction of SucA and GBL using Ir-a (Table 10, entry 1)



SucA (78.7 mg, 0.67 mmol), Ir-a (11.2 mg, 0.01 mmol), and a magnetic stirring bar were placed in a dried glass tube (21 mL capacity). The glass tube was inserted into an autoclave, which was closed tightly, evaporated in vacuum, and refilled with Ar gas. To the mixture was

added dehydrated toluene (3.0 mL) under a continuous flow of Ar, and inside the autoclave was purged with H₂ gas ($P_{\text{H}_2} = 1$ MPa). The autoclave was pressurized by H₂ gas ($P_{\text{H}_2} = 6$ MPa) at 25 °C, and heated at 180 °C for 18 h with stirring (500 rpm). The autoclave was cooled to room temperature in a water bath for ca. 20 min, and hydrogen was blown away under an Ar stream. Under the continuous Ar flow, GBL (51 μL , 0.67 mmol) was added using a gas-tight syringe. The autoclave was closed tightly and purged with H₂ gas ($P_{\text{H}_2} = 1$ MPa). The autoclave was finally pressurized by H₂ gas ($P_{\text{H}_2} = 6$ MPa) at 25 °C, and heated at 180 °C for 2 h with stirring (500 rpm). The autoclave was cooled to 0 °C in an ice–water bath. The reaction mixture was concentrated under a reduced pressure (ca. 15 mmHg, 40 °C). The residue was diluted with DMSO-*d*₆, and analyzed by ¹H NMR. The yield and amount of 1,4-BDO (85%, 1.14 mmol), and GBL (0.055 mmol) were calculated based on the integral ratio among the signals of these compounds with respect to an internal standard (mesitylene).

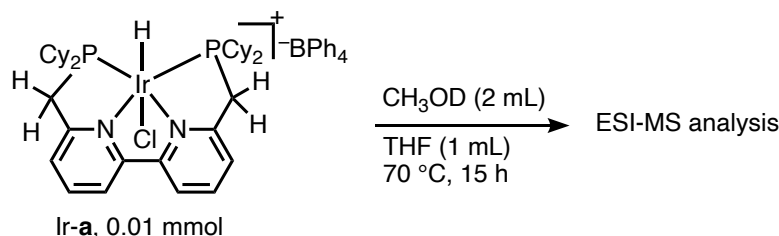
Representative procedure for the hydrogenation of SucA analyzed by ¹H NMR and GC-MS (Table 11, entry 1)



SucA (78.7 mg, 0.67 mmol), Ir-a (11.2 mg, 0.01 mmol), and a magnetic stirring bar were placed in a dried glass tube (21 mL capacity). The glass tube was inserted into an autoclave, which was closed tightly, evaporated in vacuum, and refilled with Ar gas. To the mixture was added Primepure[®] toluene (3.0 mL) under a continuous flow of Ar, and inside the autoclave was purged with H₂ gas ($P_{\text{H}_2} = 1$ MPa). The autoclave was pressurized by H₂ gas ($P_{\text{H}_2} = 6$ MPa) at 25 °C, and heated at 180 °C for 18–24 h with stirring (500 rpm). The autoclave was cooled to 0 °C in an ice–water bath. After venting H₂ carefully, the reaction mixture was diluted with dehydrated MeOH (5 mL) with washing inside the autoclave, followed by mesitylene (15 μL) was added, and analyzed by GC-MS. A part of the resulted mixture (ca. 0.25 mL) was transferred to an NMR tube containing DMSO-*d*₆ (ca. 0.25 mL), and analyzed by ¹H NMR (600 MHz). The yields of 1,4-BDO, GBL, and THF were calculated based on the integral ratio among the signals of these compounds with respect to an internal standard (mesitylene).

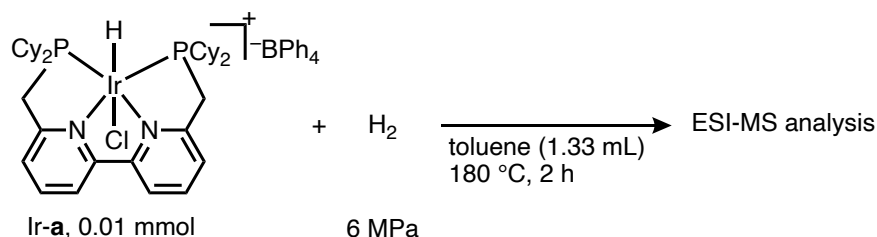
3.4.8. Representative procedure of ESI-MS analyses for investigation of chemical species generated by treatment of Ir-a

Investigation of chemical species generated by treatment of Ir-a with CH₃OD (Figures 6A and S1)



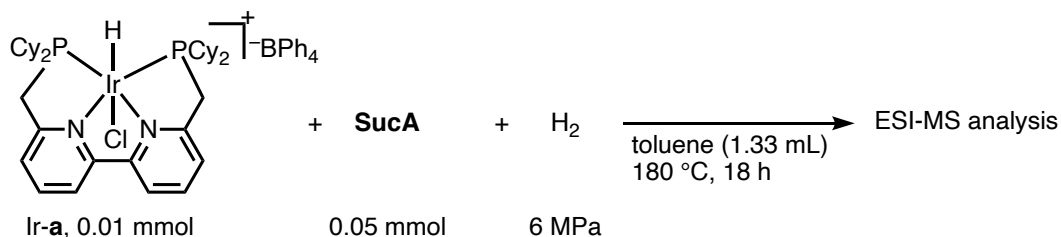
Ir-a (11.2 mg, 0.01 mmol), CH₃OD (2 mL), THF (1 mL), and a magnetic stirring bar were placed in a dried Young Schlenk tube under a continuous flow of Ar. The mixture was heated at 70 °C for 15 h with stirring (800 rpm) and then cooled down to room temperature. The reaction mixture was diluted with acetonitrile and analyzed by ESI-MS.

Representative procedure for investigation of chemical species generated by treatment of Ir-a with H₂ (P_{H₂} = 6 MPa, t = 2 h) (Figures 6B and S5)



Ir-a (11.2 mg, 0.01 mmol) and a magnetic stirring bar were placed in a dried Teflon[®] tube (21 mL capacity). The Teflon[®] tube was inserted into an autoclave, which was closed tightly, evaporated in vacuum, and refilled with Ar gas. To the mixture was added anhydrous toluene (1.33 mL) under a continuous flow of Ar, and inside the autoclave was purged with H₂ gas (P_{H₂} = 1 MPa). The autoclave was pressurized by H₂ gas (P_{H₂} = 6 MPa) at 25 °C, and heated at 180 °C for 2 h with stirring (800 rpm). The autoclave was cooled to 0 °C in an ice–water bath. The reaction mixture was diluted with acetonitrile and analyzed by ESI-MS.

Investigation of chemical species generated from Ir-a in hydrogenation of SucA (Figures 6D and S8)



SucA (5.9 mg, 0.05 mmol), Ir-a (11.2 mg, 0.01 mmol), and a magnetic stirring bar were placed in a dried Teflon[®] tube (21 mL capacity). The Teflon[®] tube was inserted into an autoclave, which was closed tightly, evaporated in vacuum, and refilled with Ar gas. To the mixture was added anhydrous toluene (1.33 mL) under a continuous flow of Ar, and inside the autoclave was purged with H₂ gas ($P_{\text{H}_2} = 1 \text{ MPa}$). The autoclave was pressurized by H₂ gas ($P_{\text{H}_2} = 6 \text{ MPa}$) at 25 °C, and heated at 180 °C for 18 h with stirring (800 rpm). The autoclave was cooled to 0 °C in an ice–water bath. The reaction mixture was diluted with acetonitrile and analyzed by ESI-MS.

3.4.9. ESI-MS analyses for investigation of chemical species generated by treatment of Ir-

a

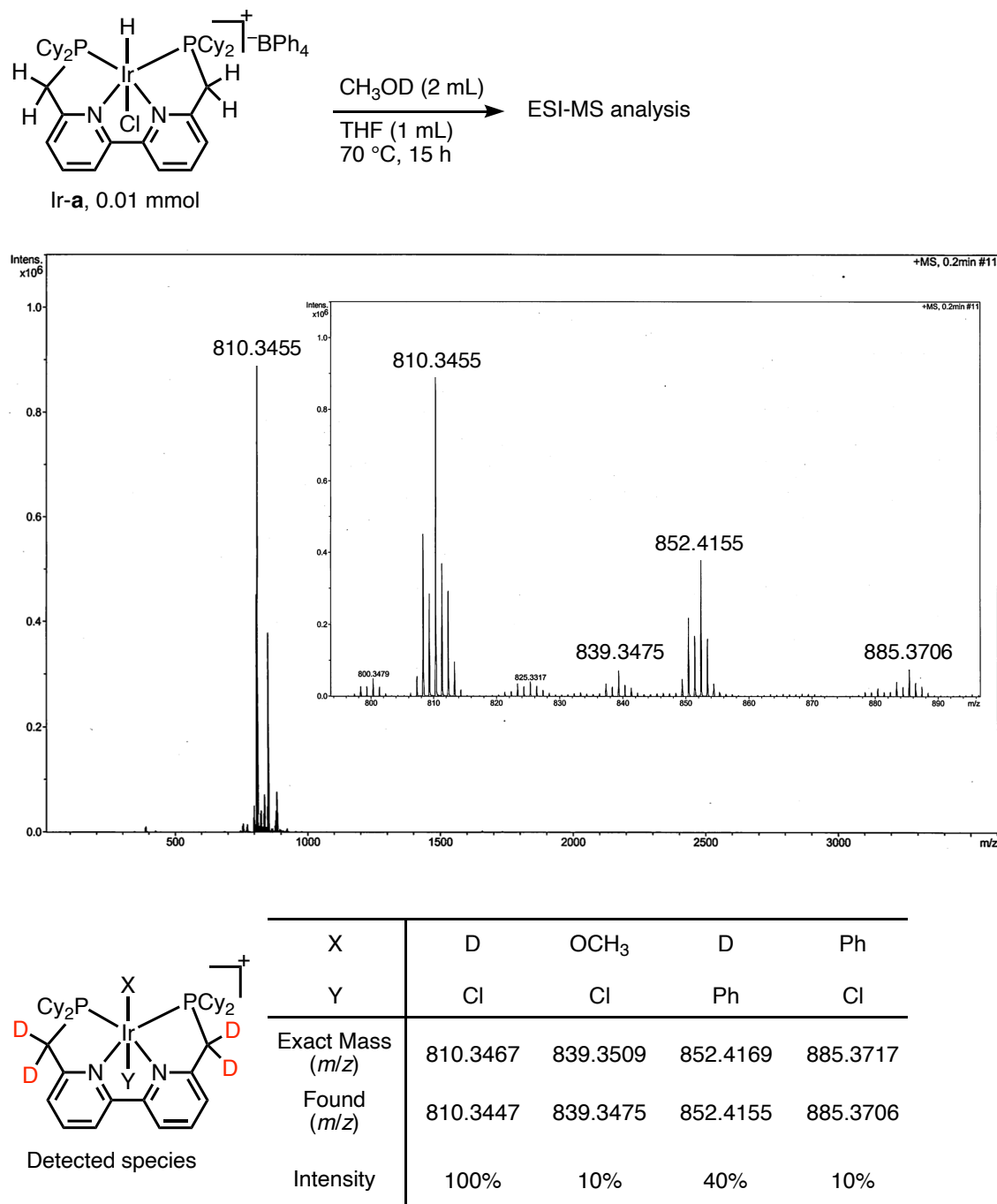


Figure S1.

ESI-MS spectrum of Ir species generated by treatment of Ir-a with CH₃OD ([Ir-a]₀ = 7.5 mM in THF and CH₃OD, T = 70 °C, and t = 15 h).

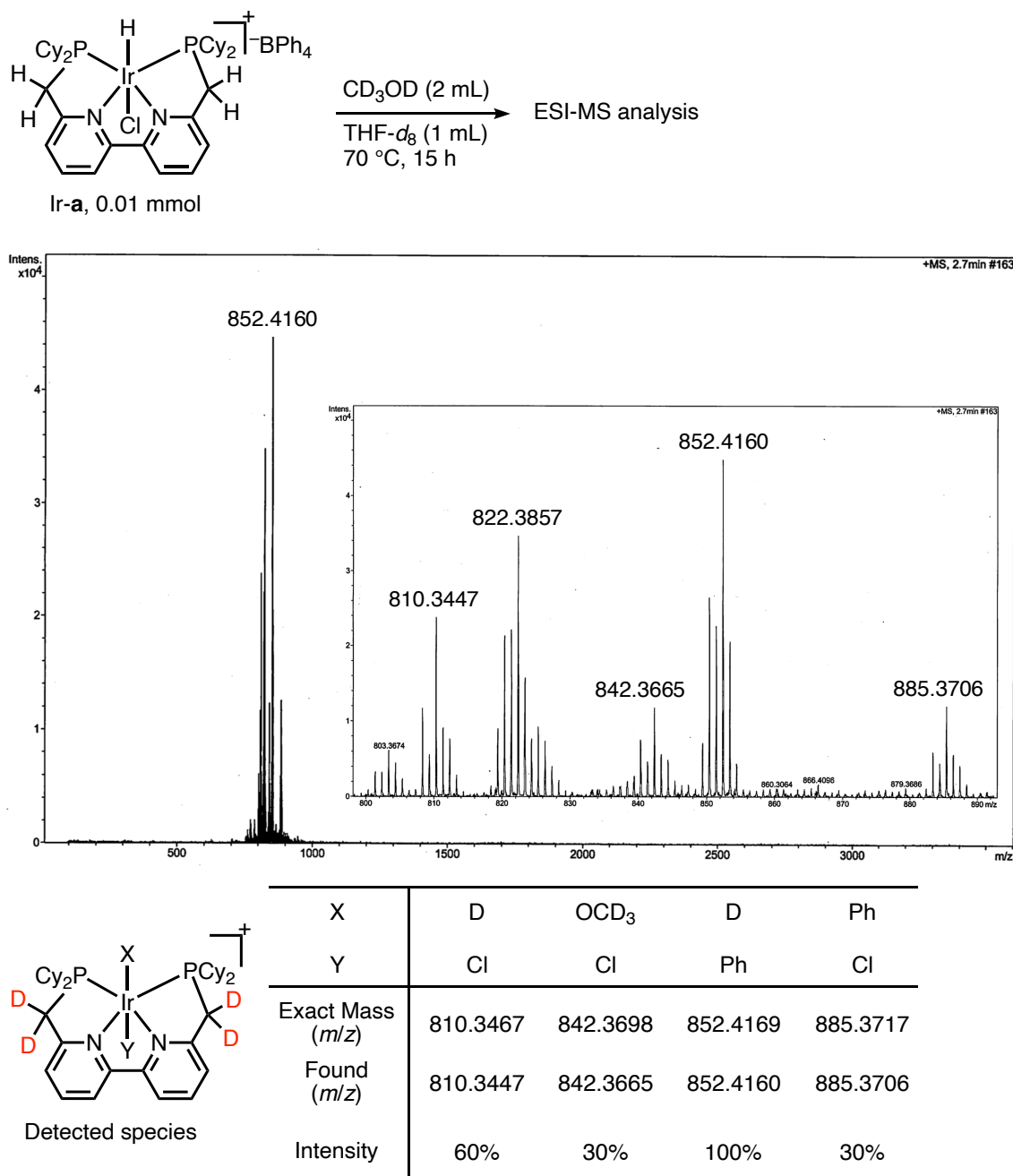


Figure S2.

ESI-MS spectrum of Ir species generated by treatment of Ir-a with CD_3OD ($[Ir-a]_0 = 7.5$ mM in $THF-d_8$, $T = 70\text{ }^\circ\text{C}$, and $t = 15$ h).

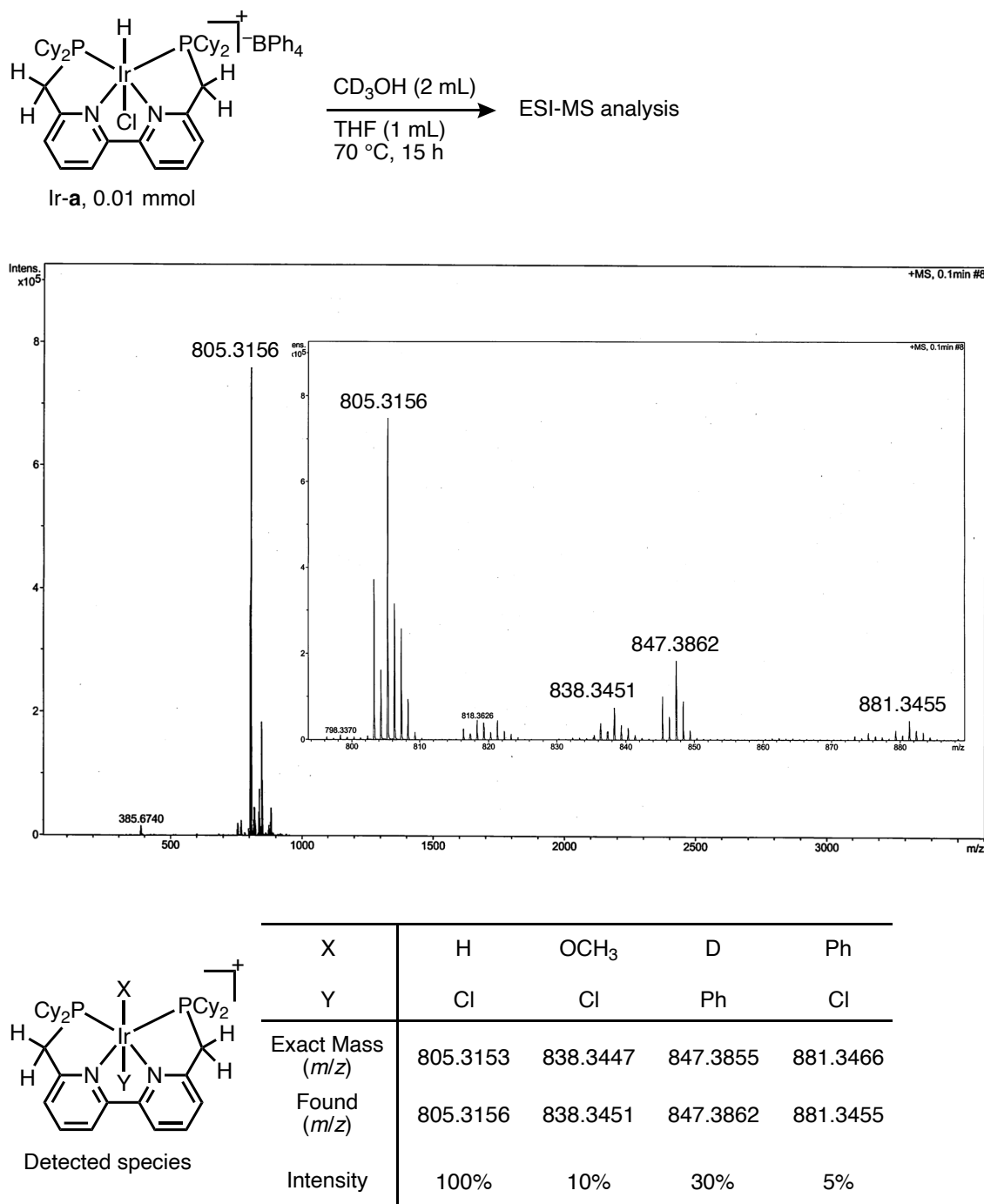


Figure S3.

ESI-MS spectrum of Ir species generated by treatment of Ir-a with CD₃OH ([Ir-a]₀ = 7.5 mM in THF and CD₃OH, T = 70 °C, and t = 15 h).

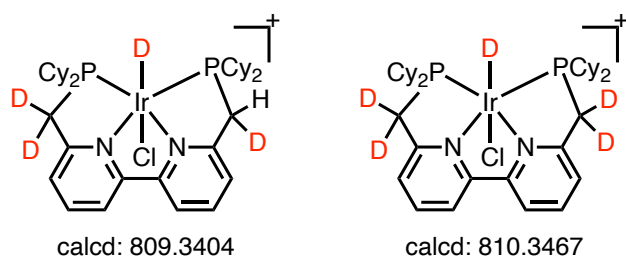
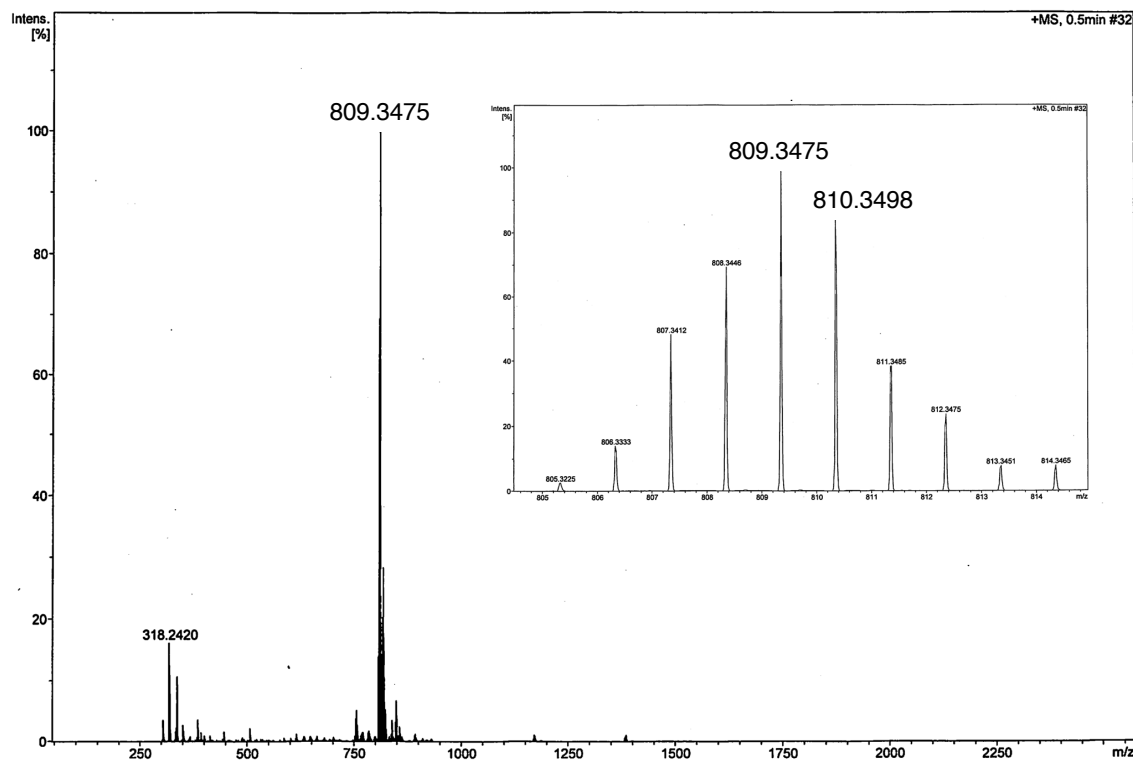
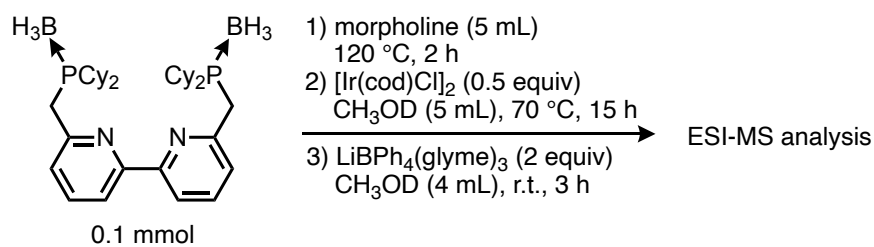


Figure S4.

ESI-MS spectrum of Ir-a synthesized from CH₃OD. ³¹P{¹H} NMR (243 MHz, DMSO-*d*₆) δ 19.5, 19.3. The synthetic procedure was modified from the procedure for the synthesis of Ir-**a** replacing the reaction solvent CH₃OH with CH₃OD.

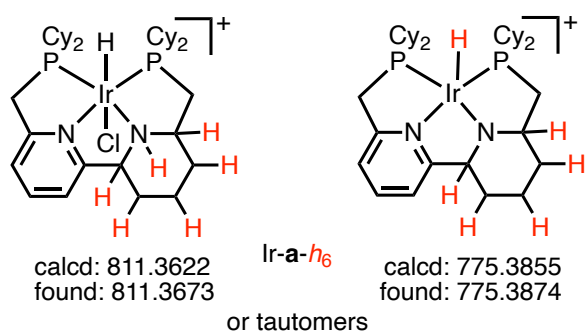
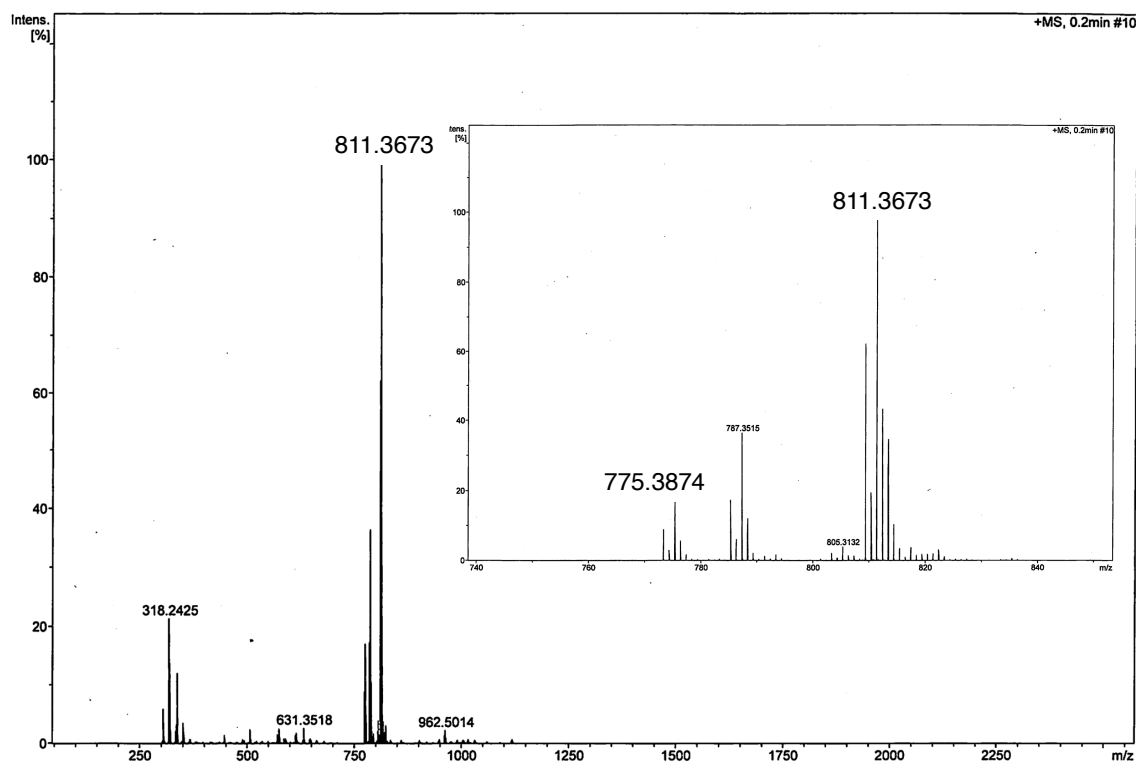
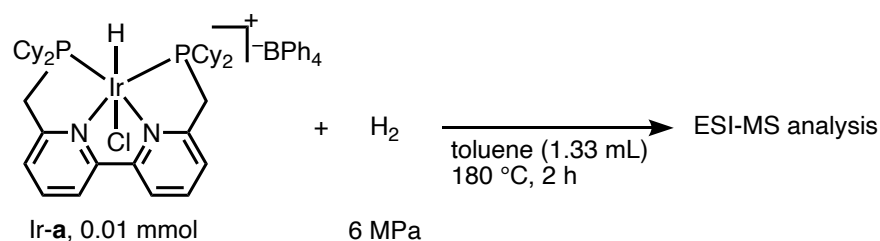


Figure S5.

ESI-MS spectrum of Ir species generated by treatment of Ir-a with H₂ ([Ir-a]₀ = 7.5 mM in toluene, P_{H₂} = 6 MPa, T = 180 °C, and t = 2 h).

¹H NMR (600 MHz, DMSO-*d*₆) δ -15.5 (d, *J* = 20.2 Hz), -16.4 (d, *J* = 17.7 Hz), -21.5 (t, *J* = 17.6 Hz), -21.8 (m); ³¹P{¹H} NMR (243 MHz, DMSO-*d*₆) δ 49.7, 33.7, 21.1, 17.1.

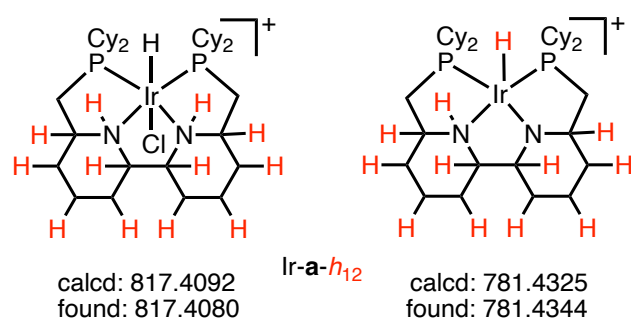
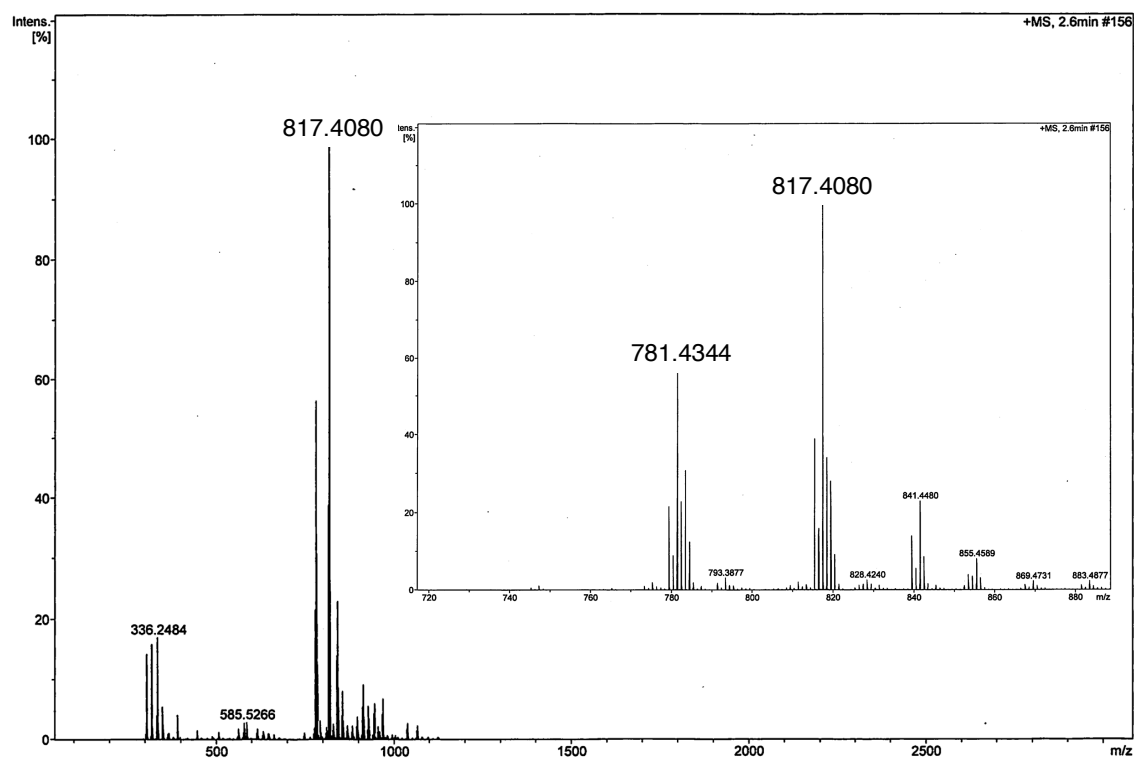
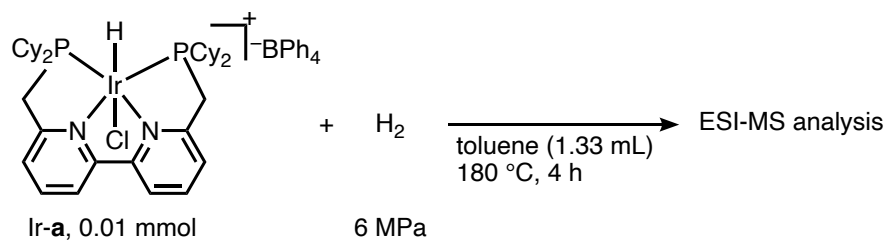


Figure S6.

ESI-MS spectrum of Ir species generated by treatment of Ir-a with H_2 ($[Ir-a]_0 = 7.5$ mM in toluene, $P_{H_2} = 6$ MPa, $T = 180$ °C, and $t = 4$ h).

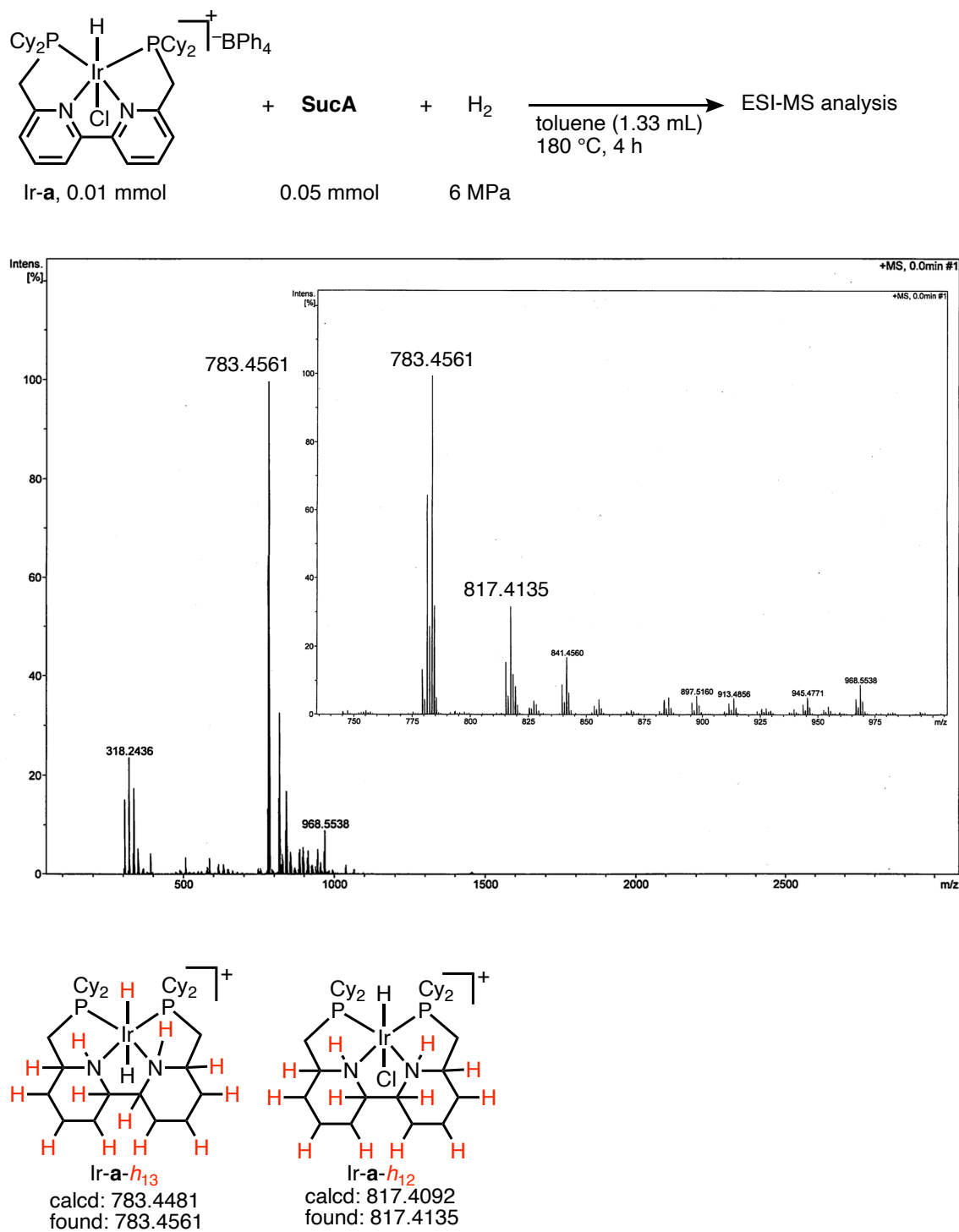


Figure S7.

ESI-MS spectrum of Ir species generated by treatment of Ir-a with H₂ in the presence of SucA ([Ir-a]₀ = 7.5 mM, [SucA]₀ = 37.5 mM in toluene, P_{H₂} = 6 MPa, T = 180 °C, and t = 4 h).

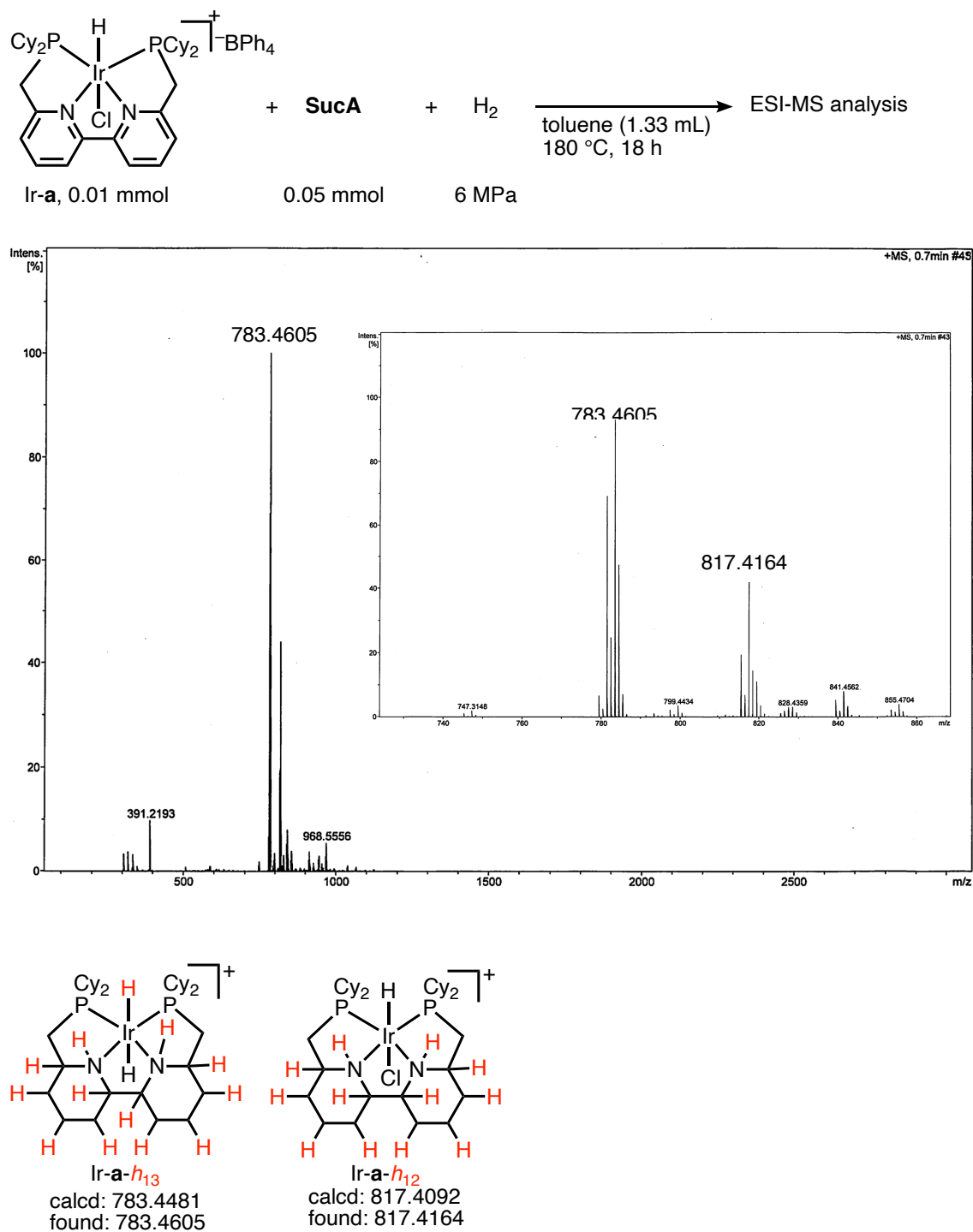


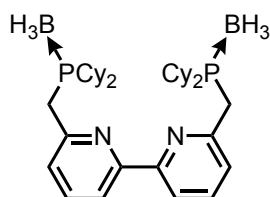
Figure S8.

ESI-MS spectrum of Ir species generated by treatment of Ir-a with H₂ in the presence of SucA ([Ir-a]₀ = 7.5 mM, [SucA]₀ = 37.5 mM in toluene, P_{H₂} = 6 MPa, T = 180 °C, and t = 18 h).

¹H NMR (600 MHz, DMSO-*d*₆) δ -9.29 (2H, t, *J* = 13.8 Hz, IrH₂), -23.1 (1H, t, *J* = 16.1 Hz, ClIrH); ³¹P{¹H} NMR (243 MHz, DMSO-*d*₆) δ 38.2, 31.7 (major), 30.4, 14.3.

3.4.10. Precatalyst preparation

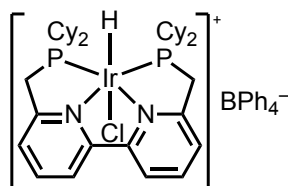
6,6'-Bis((dicyclohexylphosphino)methyl)-2,2'-bipyridine–diborane complex (see ref. 21)



6,6'-Bi-2-picoline (924.5 mg, 5 mmol), THF (25 mL), and a magnetic stirring bar were placed in a 500 mL three-way flask under argon atmosphere. The flask was immersed in an ice bath and stirred for 15 min at 0 °C. To the solution of 6,6'-bi-2-picoline in THF was added LDA [prepared by adding *n*-BuLi (1.5 M in hexane, 20 mL, 30 mmol) to a THF (15 mL) solution of diisopropylamine (4.2 mL, 30 mmol), and stirring for 10 min at 0 °C] at the same temperature. The reaction mixture was allowed to warm to room temperature and stirred for 1 h. To the solution was added chlorodicyclohexylphosphine (2.2 mL, 10 mmol) dropwise at 0 °C. The reaction mixture was allowed to warm to room temperature and stirred for 2.5 h. To the solution was added BH₃–THF (1 M in THF, 50 mL, 50 mmol) at 0 °C. After stirring for 18.5 h at room temperature, the reaction mixture was quenched with water (25 mL) at 0 °C, and the organic phase was removed under reduced pressure. The residue was dissolved into CH₂Cl₂ (50 mL), washed H₂O (50 mL), and extracted with CH₂Cl₂ (50 mL×2). The organic layer was dried over Na₂SO₄ and filtrated. The evaporation of the filtrate gave a yellow crude solid, which was purified by washing with 10 mL THF to afford target compound (1.67 g, 2.8 mmol, 55%) as a white solid. *R_f* = 0.33 (dichloromethane/hexane = 5/1).

¹H NMR (600 MHz, CDCl₃): δ 8.29 (d, 2H, *J* = 8.3 Hz, C₁₀H₆N₂), 7.75 (t, 2H, *J* = 7.9 Hz, C₁₀H₆N₂), 7.31 (d, 2H, *J* = 7.6 Hz, C₅H₄N), 3.31 (d, 4H, *J* = 11.0 Hz, PCH₂), 1.60–2.00 (m, 24H, C₆H₁₁), 1.11–1.50 (m, 20H, C₆H₁₁). ¹³C {¹H} NMR (151 MHz, CDCl₃): δ 155.2, 154.5 (d, ²*J*_{PC} = 7.2 Hz), 137.2, 125.0, 118.7, 31.5 (d, ¹*J*_{PC} = 30.3 Hz), 30.5 (d, ¹*J*_{PC} = 27.5 Hz), 27.0 (d, ²*J*_{PC} = 11.6 Hz), 26.9 (d, ²*J*_{PC} = 11.6 Hz), 26.7, 26.6, 26.0. ³¹P {¹H} NMR (243 MHz, CDCl₃): δ 28.6, HRMS (ESI, (M+H)⁺) calcd for C₃₆H₆₀B₂N₂P₂⁺: 605.4502. Found: 605.4502.

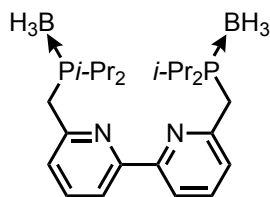
Chlorohydro(6,6'-bis((dicyclohexylphosphino)methyl)-2,2'-bipyridine)-iridium (III) tetraphenylborate (Ir-a)



6,6'-Bis((dicyclohexylphosphino)methyl)-2,2'-bipyridine–diborane complex (604.4 mg, 1.0 mmol), degassed morpholine (25 mL), and a magnetic stirring bar were placed in a vessel equipped with a Young's stopcock (75 mL) under Ar gas atmosphere. The mixture was stirred at 120 °C for 2 h and cooled to room temperature, before morpholine was removed *in vacuo* (ca. 0.1 mmHg, 50 °C). To the residue was added chloro(1,5-cyclooctadiene)iridium(I) dimer (335.8 mg, 0.50 mmol) and degassed methanol (30 mL). The resulting mixture was heated at 70 °C for 15 h, and then cooled down to room temperature. After the mixture was filtered through a pad of Celite® under Ar atmosphere, methanol (10 mL) solution of lithium tetraphenylborate tris(1,2-dimethoxyethane) (1193.0 mg, 2.00 mmol) was added to the filtrate to afford slightly yellowish beige precipitation. The suspension was stirred overnight at room temperature. The precipitate was collected by filtration, washed with methanol and diethyl ether, and then dried *in vacuo* to obtain slightly yellowish beige solid. The solid was dissolved in ca. 200 mL THF, and resulting solution was slowly concentrated using rotary evaporator (ca. 600 mmHg, 60 °C) to give slightly greenish yellow solid, which was collected by filtration, washed with methanol and diethyl ether, and then dried *in vacuo* to obtain Ir-a as a slightly greenish yellow solid (726.1 mg, 0.65 mmol, 65%).

1H NMR (600 MHz, DMSO- d_6): δ 8.45 (d, 2H, $J = 6.9$ Hz, $C_{10}H_6N_2$), 8.24 (t, 2H, $J = 8.1$ Hz, $C_{10}H_6N_2$), 7.95 (d, 2H, $J = 9.2$ Hz, $C_{10}H_6N_2$), 7.18 (br, 8H, $B(C_6H_5)_4$), 6.92, (t, 8H, $J = 8.1$ Hz, $B(C_6H_5)_4$), 6.78 (t, 4H, $J = 6.9$ Hz, $B(C_6H_5)_4$), 4.18 (m, 2H, PCH_2), 3.93 (m, 2H, PCH_2), 2.45 (br, 2H, C_6H_{11}), 2.25 (br, 2H, C_6H_{11}), 0.97–1.97 (m, 40H, C_6H_{11}), –21.6 (t, 1H, $J = 18.4$, IrH). $^{13}C\{^1H\}$ NMR (151 MHz, DMSO- d_6): δ 163.9, 163.5, 163.2, 162.9, 161.5, 155.8, 139.5, 135.5, 125.3, 124.5, 122.5, 121.5, 34.7 (t), 27.8, 27.3, 26.6, 25.6. $^{31}P\{^1H\}$ NMR (243 MHz, DMSO- d_6): δ 19.5 (s). HRMS (ESI, $(M-BPh_4)^+$) calcd for $C_{36}H_{55}ClN_2P_2Ir^+$: 805.3153. Found: 805.3127. Elemental analysis: calcd. C 64.08, H 6.72, N 2.49; found C 63.69, H 7.00, N 2.50.

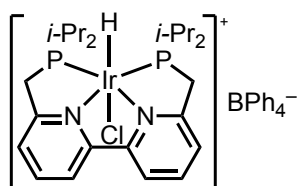
6,6'-Bis((diisopropylphosphino)methyl)-2,2'-bipyridine–diborane complex (see ref. 21)



6,6'-Bi-2-picoline (926.9 mg, 5 mmol), THF (25 mL), and a magnetic stirring bar were placed in a 500 mL three-way flask under argon atmosphere. The flask was immersed in an ice bath and stirred for 15 min at 0 °C. To the solution of 6,6'-bi-2-picoline in THF was added LDA [prepared by adding *n*-BuLi (1.5 M in hexane, 20 mL, 30 mmol) to a THF (15 mL) solution of diisopropylamine (4.2 mL, 30 mmol), and stirring for 10 min at 0 °C] at the same temperature. The reaction mixture was allowed to warm to room temperature and stirred for 1 h. To the solution was added chlorodiisopropylphosphine (1.7 mL, 10 mmol) dropwise at 0 °C. The reaction mixture was allowed to warm to room temperature and stirred for 2.5 h. To the solution was added BH₃–THF (1 M in THF, 50 mL, 50 mmol) at 0 °C. After stirring for 23 h at room temperature, the reaction mixture was quenched with water (25 mL), and the organic phase was removed under reduced pressure. The residue was dissolved into CH₂Cl₂ (50 mL), washed H₂O (50 mL), and extracted with (50 mL×2). The organic layer was dried over Na₂SO₄ and filtrated. The evaporation of the filtrate gave a yellow crude solid, which was purified by washing with 10 mL EtOAc to afford target compound (871.0 mg, 2.0 mmol, 39%) as a white solid.

¹H NMR (600 MHz, CDCl₃): δ 8.24 (d, 2H, *J* = 7.6 Hz, C₁₀H₆N₂), 7.76 (t, 2H, *J* = 7.9 Hz, C₁₀H₆N₂), 7.34 (d, 2H, *J* = 7.6 Hz, C₁₀H₆N₂), 3.33 (d, 4H, *J* = 11.0 Hz, PCH₂), 2.12–2.23 (m, 4H, CH(CH₃)₂), 1.17–1.27 (m, 24H, CH(CH₃)₂), 0.10–0.70 (br, 6H, BH₃). ¹³C {¹H} NMR (151 MHz, CDCl₃): δ 155.3, 154.2 (d, ²*J*_{PC} = 7.2 Hz), 137.3, 124.9, 118.8, 30.6 (d, ¹*J*_{PC} = 26.0 Hz), 21.8 (d, ¹*J*_{PC} = 31.8 Hz), 17.0 (d, ²*J*_{PC} = 5.8 Hz). ³¹P {¹H} NMR (243 MHz, CDCl₃): δ 36.0, 36.3, HRMS (ESI, (M+H)¹) calcd for C₂₄H₄₄B₂N₂P₂⁺: 445.3247. Found: 445.3247.

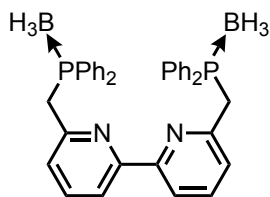
**Chlorohydro(6,6'-bis((diisopropylphosphino)methyl)-2,2'-bipyridine)-iridium
tetraphenylborate (Ir-b) (III)**



A degassed morpholine (10 mL) solution of 6,6'-bis((diisopropylphosphino)methyl)-2,2'-bipyridine–diborane complex (90.1 mg, 0.20 mmol) was heated at 120 °C for 8 h under Ar. The solution was cooled to room temperature and morpholine was removed *in vacuo* (ca. 0.1 mmHg, 50 °C). To the residue was added chloro(1,5-cyclooctadiene)iridium(I) dimer (95.0 mg, 0.14 mmol) and degassed methanol (10 mL). The resulting mixture was heated at 75 °C for 15 h under Ar, and then was cooled down to room temperature. The mixture was filtered through a pad of Celite®. To the solution was added methanol (5 mL) solution of lithium tetraphenylborate tris(1,2-dimethoxyethane) (193.0 mg, 0.32 mmol) to afford yellow suspension. The suspension was stirred at room temperature for 3 h. The precipitate was collected by filtration, washed with methanol and diethyl ether, and then dried *in vacuo* to obtain Ir-**b** as a yellow solid (103.0 mg, 0.11 mmol, 40%).

¹H NMR (600 MHz, DMSO-*d*₆): δ 8.49 (d, 2H, *J* = 6.9 Hz, C₁₀H₆N₂), 8.28 (t, 2H, *J* = 8.0 Hz, C₁₀H₆N₂), 8.00 (d, 2H, *J* = 6.9 Hz, C₁₀H₆N₂), 7.17 (br, 8H, B(C₆H₅)₄), 6.92, (t, 8H, *J* = 6.9 Hz, B(C₆H₅)₄), 6.79 (t, 4H, *J* = 6.9 Hz, B(C₆H₅)₄), 4.18 (m, 2H, PCH₂), 3.93 (m, 2H, PCH₂), 2.73 (m, 2H, CH(CH₃)₂), 2.26 (m, 2H, CH(CH₃)₂), 0.98–1.45 (m, 24H, CH(CH₃)₂), –21.31 (t, 1H, *J* = 18.4, IrH). ¹³C{¹H} NMR (151 MHz, DMSO-*d*₆): δ 163.8, 163.5, 163.2, 162.9, 161.5, 155.9, 139.6, 135.5, 125.3, 124.5, 122.6, 121.5, 25.9 (d), 25.1 (d), 18.2 (d), 17.8, 17.3. ³¹P{¹H} NMR (243 MHz, DMSO-*d*₆): δ 27.53, 27.47. HRMS (ESI, (M–BPh₄)⁺) calcd for C₂₄H₃₉ClN₂P₂Ir⁺: 645.1901. Found: 645.1878. Elemental analysis: calcd. C 59.78, H 6.17, N 2.90; found C 59.06, H 6.17, N 3.14.

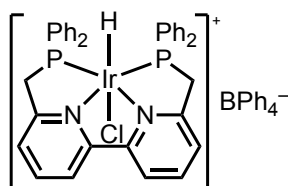
6,6'-bis((diphenylphosphino)methyl)-2,2'-bipyridine–diborane complex



6,6'-Bi-2-picoline (1.850 g, 10 mmol), THF (50 mL), and a magnetic stirring bar were placed in a 500 mL three-way flask under argon atmosphere. The flask was immersed in an ice bath and stirred for 15 min at 0 °C. To the solution of 6,6'-Bi-2-picoline in THF was added LDA [prepared by adding *n*-BuLi (1.5 M in hexane, 40 mL, 60 mmol) to a THF (30 mL) solution of diisopropylamine (8.4 mL, 60 mmol), and stirring for 10 min at 0 °C] at the same temperature. The reaction mixture was allowed to warm to room temperature and stirred for 1 h. To the solution was added chlorodiphenylphosphine (3.6 mL, 20 mmol) dropwise at room temperature. After stirring for 2.5 hours at room temperature, to the solution was added BH₃–THF (1 M in THF, 100 mL, 100 mmol). After stirring for 15 h at room temperature, another BH₃–THF (1 M in THF, 50 mL, 50 mmol) was added. After stirring for 10 hours at room temperature, the reaction mixture was quenched with water (40 mL), and the organic phase was removed *in vacuo*. The residue was dissolved into CH₂Cl₂ (50 mL), washed H₂O (50 mL), and extracted with (50 mL×2). The organic layer was dried over Na₂SO₄ and filtrated. The evaporation of the filtrate gave a yellow crude solid, which was purified by column chromatography (CH₂Cl₂/Hexane = 4/1) to afford target compound (2.353 mg, 4.0 mmol, 40%) as a white solid.

¹H NMR (600 MHz, CDCl₃): δ 7.74–7.38 (m, 24H, C₆H₅ C₁₀H₆N₂), 7.14 (d, 2H, *J* = 7.2 Hz, C₁₀H₆N₂), 3.86 (d, 4H, *J* = 11.4 Hz, PCH₂). ¹³C{¹H} NMR (151 MHz, CDCl₃): δ 155.1, 152.4 (d, *J* = 4.4 Hz), 136.8, 132.8 (d, *J* = 10.1 Hz), 131.1, 129.1, 128.7, 128.6 (d, *J* = 10.1 Hz), 125.0 (d, *J* = 4.4 Hz), 36.3 (d, *J* = 33.4 Hz). ³¹P{¹H} NMR (243 MHz, CDCl₃): δ 19.0. HRMS (ESI, (M+H)⁺) calcd for C₃₆H₃₇B₂N₂P₂⁺: 581.2624. Found: 581.2619.

**Chlorohydro(6,6'-bis((diphenylphosphino)methyl)-2,2'-bipyridine)-iridium
tetraphenylborate (Ir-c) (III)**



A degassed morpholine (6 mL) solution of 6,6'-bis((diphenylphosphino)methyl)-2,2'-bipyridine–diborane complex (120.0 mg, 0.21 mmol) was heated at 120 °C for 2 h under Ar. The solution was cooled to room temperature and morpholine was removed *in vacuo* (ca. 1 mmHg, room temperature). To the residue was added chloro(1,5-cyclooctadiene)iridium(I) dimer (70.0 mg, 0.10 mmol) and degassed methanol (8 mL). The resulting mixture was heated at 70 °C for 5 h under Ar, and then was cooled down to room temperature. The mixture was filtered through a pad of Celite. To the solution was added methanol (5 mL) solution of lithium tetraphenylborate tris(1,2-dimethoxyethane) (240.0 mg, 0.40 mmol) to afford yellow suspension. The suspension was stirred at room temperature for 3 h. The precipitate was collected by filtration, washed with methanol and diethyl ether, and then dried *in vacuo* to obtain Ir-c as a yellow solid (131.4 mg, 0.12 mmol, 58%).

¹H NMR (600 MHz, DMSO-*d*₆): δ 8.61 (d, 2H, *J* = 8.2 Hz, C₁₀H₆N₂), 8.36 (t, 2H, *J* = 7.6 Hz, C₁₀H₆N₂), 8.07 (d, 2H, *J* = 7.6 Hz, C₁₀H₆N₂), 7.66–7.28 (m, 20H, C₆H₅), 7.18 (br, 8H, B(C₆H₅)₄), 6.91 (t, 8H, *J* = 6.9 Hz, B(C₆H₅)₄), 6.78 (t, 4H, *J* = 6.9 Hz, B(C₆H₅)₄), 5.09 (m, 2H, PCH₂), 4.83 (m, 2H, PCH₂). ¹³C{¹H} NMR (151 MHz, DMSO-*d*₆): δ 163.8, 163.5, 163.2, 162.8, 160.8, 156.0, 140.0, 135.5, 133.3, 132.0, 131.4, 129.3, 128.9, 128.5, 128.3, 127.4, 126.7, 125.3, 123.2, 121.5, 115.2. ³¹P{¹H} NMR (243 MHz, DMSO-*d*₆): δ 5.2. HRMS (ESI, (M–BPh₄)⁺) calcd for C₃₆H₃₁ClN₂P₂Ir⁺: 781.1275. Found: 781.1303. ¹H NMR integral curves of the signals at 7.18, 6.91, and 6.78 were frequently over-measured differently from the theoretical values among separate batches of the synthesis of Ir-c.

References

- [1] T. Werpy, G. Petersen, “Top value added chemicals from biomass volume I—results of screening for potential candidates from sugars and synthesis gas” (U.S. Department of Energy, **2004**; <http://energy.gov/eere/bioenergy/downloads/top-value-added-chemicals-biomass-volume-i-results-screening-potential>).
- [2] L. Wu, T. Moteki, A. A. Gokhale, D. W. Flaherty, F. D. Toste, *Chem* **2016**, *1*, 32–58.
- [3] A. M. Ruppert, K. Weinberg, R. Palkovits, *Angew. Chem. Int. Ed.* **2012**, *51*, 2564–2601.
- [4] J. J. Bozell, G. R. Petersen, *Green Chem.* **2010**, *12*, 539–554.
- [5] C. Delhomme, D. Weuster-Botz, F. E. Kühn, *Green Chem.* **2009**, *11*, 13–26.
- [6] Biotechnology Innovation Organization, “Advancing the biobased economy: Renewable chemical biorefinery commercialization, progress, and market opportunities, 2016 and beyond” (**2016**; https://www.bio.org/sites/default/files/BIO_Advancing_the_Biobased_Economy_2016.pdf#search=%271%2C4BDO+is+among+the+most+versatile+synthetic+intermediates+and+is+an+important+commodity+chemical+used+to+manufacture+over+2.5+million+tons+annually+of+valuable+polymers+including+poly%28butylene%29+terephthalate+and+poly%28urethane%29s%27).
- [7] L. Rosi, M. Frediani, P. Frediani, Isotopomeric diols by “one-pot” Ru-catalyzed homogeneous hydrogenation of dicarboxylic acids. *J. Organomet. Chem.* **2010**, *695*, 1314–1322.
- [8] T. vom Stein, M. Meuresch, D. Limper, M. Schmitz, M. Hölscher, J. Coetzee, D. J. Cole-Hamilton, J. Klankermayer, W. Leitner, *J. Am. Chem. Soc.* **2014**, *136*, 13217–13225.
- [9] T. J. Korstanje, J. I. van der Vlugt, C. J. Elsevier, B. de Bruin, *Science* **2015**, *350*, 298–302.
- [10] S. D. Le, S. Nishimura, *ACS Sustainable Chem. Eng.* **2019**, *7*, 18483–18492.
- [11] V. Martin-Dominguez, J. Estevez, F. de Borja Ojembarrena, V. E. Santos, M. Ladero, *Fermentation* **2018**, *4*, 33.
- [12] T. P. West, *Fermentation* **2017**, *3*, 14.
- [13] G. A. Abdel-Tawab, E. Broda, G. Kellner, *Biochem. J.* **1959**, *72*, 619–623.
- [14] B. Beer, A. Pick, V. Sieber, *Metab. Eng.* **2017**, *40*, 5–13.
- [15] K. Kobayashi, J. Maruebi, K. Kirimura, *ChemistrySelect* **2016**, *1*, 1467–1471.
- [16] P. L. Show, K. O. Oladele, Q. Y. Siew, F. A. A. Zakry, J. C.-W. Lan, T. C. Ling, *Front. Life Sci.* **2015**, *8*, 271–283.
- [17] H. A. Krebs, W. A. Johnson, *Biochem. J.* **1937**, *31*, 645–660.
- [18] T. J. Korstanje, R. J. M. Klein Gebbink, *Top. Organomet. Chem.* **2012**, *39*, 129–174.

- [19] E. Furimsky, *Applied Catalysis A: General* **2000**, *199*, 147–190.
- [20] J. Pritchard, G. A. Filonenko, R. van Putten, E. J. M. Hensen, E. A. Pidko, *Chem. Soc. Rev.* **2015**, *44*, 3808–3833.
- [21] T. Miura, M. Naruto, K. Toda, T. Shimomura, S. Saito, *Sci. Rep.* **2017**, *7*, 1586.
- [22] T. Miura, I. E. Held, S. Oishi, M. Naruto, S. Saito, *Tetrahedron Lett.* **2013**, *54*, 2674–2678.
- [23] S. Yoshioka, S. Saito, *Chem. Commun.* **2018**, *54*, 13319–13330.
- [24] M. Naruto, S. Agrawal, K. Toda, S. Saito, *Sci. Rep.* **2017**, *7*, 3425.
- [25] M. Naruto, S. Saito, *Nat. Commun.* **2015**, *6*, 8140.
- [26] A. Saito, S. Yoshioka, M. Naruto, S. Saito, *Adv. Synth. Catal.* **2020**, *362*, 424–429.
- [27] Y. Takada, J. Caner, H. Naka, S. Saito, *Pure Appl. Chem.* **2018**, *90*, 167–174.
- [28] K. Kamada, J. Jung, T. Wakabayashi, K. Sekizawa, S. Sato, T. Morikawa, S. Fukuzumi, S. Saito, *J. Am. Chem. Soc.* **2020**, *142*, 10261–10266.
- [29] R. Crabtree, *Acc. Chem. Res.* **1979**, *12*, 331–337.
- [30] C. Gunanathan, D. Milstein, *Science* **2013**, *341*, 1229712.
- [31] C. Gunanathan, D. Milstein, *Acc. Chem. Res.* **2011**, *44*, 588–602.
- [32] J. Zhang, G. Leitus, Y. Ben-David, D. Milstein, *Angew. Chem. Int. Ed.* **2006**, *45*, 1113–1115.
- [33] D. Srimani, A. Mukherjee, A. F. G. Goldberg, G. Leitus, Y. Diskin-Posner, L. J. W. Shimon, Y. B. David, D. Milstein, *Angew. Chem. Int. Ed.* **2015**, *54*, 12357–12360.
- [34] G.N. Cohen, “The aspartic acid family of amino acids. Biosynthesis” in *Microbial Biochemistry* (Springer, Dordrecht, **2004**), pp. 139–149.
- [35] S. DeBolt, D. R. Cook, C. M. Ford, *Proc. Natl. Acad. Sci. U.S.A.* **2006**, *103*, 5608–5613.
- [36] J. W. Howard, W. A. Fraser, *Org. Synth.* **1925**, *4*, 63–64; **1941**, Coll. Vol. 1, 475–476.
- [37] M. Zhao, X. Lu, H. Zong, J. Li, B. Zhuge, *Biotechnol. Lett.* **2018**, *40*, 455–464.
- [38] S. P. Simeonov, M. A. Ravutsov, M. D. Mihovilovic, *ChemSusChem* **2019**, *12*, 2748–2754.
- [39] F. M. A. Geilen, B. Engendahl, A. Harwardt, W. Marquardt, J. Klankermayer, W. Leitner, *Angew. Chem. Int. Ed.* **2010**, *49*, 5510–5514.
- [40] M. Tang, S. Mao, X. Li, C. Chen, M. Li, Y. Wang, *Green Chem.* **2017**, *19*, 1766–1774.
- [41] H. T. Teunissen, C. J. Elsevier, *Chem. Commun.* **1998**, 1367–1368.
- [42] K. Yan, C. Jarvis, J. Gu, Y. Yan, *Renew. Sustain. Energy Rev.* **2015**, *51*, 986–997.
- [43] T. Abura, S. Ogo, Y. Watanabe, S. Fukuzumi, *J. Am. Chem. Soc.* **2003**, *125*, 4149–4154.
- [44] T. J. Schmeier, G. E. Dobereiner, R. H. Crabtree, N. Hazari, *J. Am. Chem. Soc.* **2011**, *133*, 9274–9277.
- [45] H. Li, X. Wang, F. Huang, G. Liu, J. Jiang, Z.-X. Wang, *Organometallics* **2011**, *30*, 5233–5247.

- [46] C. A. Sandoval, T. Ohkuma, K. Muñiz, R. Noyori, *J. Am. Chem. Soc.* **2003**, *125*, 13490–13503.
- [47] L. V. A. Hale, N. K. Szymczak, *ACS Catal.* **2018**, *8*, 6446–6461.
- [48] R. Tanaka, M. Yamashita, K. Nozaki, *J. Am. Chem. Soc.* **2009**, *131*, 14168–14169.
- [49] T. Toyao, S. M. A. H. Siddiki, A. S. Touchy, W. Onodera, K. Kon, Y. Morita, T. Kamachi, K. Yoshizawa, K. Shimizu, *Chem. Eur. J.* **2017**, *23*, 1001–1006.
- [50] T. Toyao, S. M. A. H. Siddiki, Y. Morita, T. Kamachi, A. S. Touchy, W. Onodera, K. Kon, S. Furukawa, H. Ariga, K. Asakura, K. Yoshizawa, K. Shimizu, *Chem. Eur. J.* **2017**, *23*, 14848–14859.
- [51] J. Ullrich, B. Breit, *ACS Catal.* **2018**, *8*, 785–789.
- [52] M. Shaul, Y. Cohen, *J. Org. Chem.* **1999**, *64*, 9358–9364.
- [53] H. Nishiyama, T. Kitajima, M. Matsumoto, K. Itoh, *J. Org. Chem.* **1984**, *49*, 2298–2300.
- [54] E. Zysman-Colman, N. Nevins, N. Eghball, J. P. Snyder, D. N. Harpp, *J. Am. Chem. Soc.* **2006**, *128*, 291–304.
- [55] T. Morimoto, M. Fujioka, K. Fuji, K. Tsutsumi, K. Kakiuchi, *J. Organomet. Chem.* **2007**, *692*, 625–634.
- [56] L. N. Dawe, M. Karimzadeh-Younjali, Z. Dai, E. Khaskin, D. G. Gusev, *J. Am. Chem. Soc.* **2020**, *142*, 19510–19522.

List of Publications

(副論文)

1. Catalytic Hydrogenation of Carboxylic Acids Using Low-valent and High-valent Metal Complexes
Shota Yoshioka, Susumu Saito
Chemical Communications **2018**, *54*, 13319–13330.
2. Development of Effective Bidentate Diphosphine Ligands of Ruthenium Catalysts toward Practical Hydrogenation of Carboxylic Acids
Shota Yoshioka, Ke Wen, Susumu Saito
Submitted
3. Catalytic Hydrogenation of N-protected α -Amino Acids Using Ruthenium Complexes with Monodentate Phosphine Ligands
Akari Saito, Shota Yoshioka, Masayuki Naruto, Susumu Saito
Advanced Synthesis & Catalysis **2020**, *362*, 424–429.
4. Reaction of H₂ with Mitochondria-relevant Metabolites Using a Multifunctional Molecular Catalyst
Shota Yoshioka, Sota Nimura, Masayuki Naruto, Susumu Saito
Science Advances **2020**, *6*, eabc0274.

(参考論文)

1. 高機能性金属錯体によるカルボン酸の水素化
Shota Yoshioka, Susumu Saito
CSJ Current Review: 『高機能性金属錯体が拓く触媒科学』 **2020**, *37*, 63–73.
2. PNNP 四座配位子をもつ精密金属錯体触媒を用いる再生可能炭素資源の還元法の開発
Shota Yoshioka, Jieun Jung, Susumu Saito
Journal of Synthetic Organic Chemistry, Japan **2020**, *78*, 856–866.